

EFFECT OF METAKAOLIN AND PROCESS PARAMETERS ON THE  
PYROLYSIS OF BIOMASS TO PRODUCE BIOCHAR FOR CARBON DIOXIDE  
SEQUESTRATION

BY

BELLO Alhassan  
PhD/SEET/2016/936

CHEMICAL ENGINEERING DEPARTMENT  
FEDERAL UNIVERSITY OF TECHNOLOGY  
MINNA

SEPTEMBER, 2023

## ABSTRACT

The increasing concentration of carbon dioxide in the atmosphere is one of the major environmental related issues confronting the world leading to global warming. These scenarios require research efforts to address this menace. Subsequently, biochar was identified as a viable option to sequester carbon in a stable carbon pool. The biochar is an important carbon-rich product that is generated from biomass sources through pyrolysis. This research work, was therefore, aimed at investigating the Effect of Metakaolin and Process Parameters on the Pyrolysis of Biomass to Produce Biochar for Carbon Dioxide Sequestration. Catalytic pyrolysis with kaolin was aimed to improving the biochar yield. In this work, biomass derived from sawdust and poultry waste were employed as potential low cost for biochar production. Accordingly, these wastes were employed as potential low-cost precursors for the biochar production. Biochars produced were activated chemically with  $H_2PO_4$  and NaOH to produce Activated Carbons which were used in adsorption study. About 20g of sample in the reactor were heated and pyrolyzed at different predetermined conditions. A range of set temperatures 300, 400, 450, 500, 550, and 600 °C, a series of residence time 10, 20, 30, 40, 50 and 60minutes, different volume of Nitrogen flow rates 0.5, 1.0, 1.5, 2.0, 2.5 and 3.0 L/min and a tested range of particle sizes 0.5, 1.0, 1.5, 2.0, 2.5 and 3.0mm were respectively investigated to ascertain both the effects of operating and non-operating pyrolysis conditions on biochar production. The process was optimized to ascertain the interactive effects of the process parameters. Results showed that moderate temperature of 400 °C which prevent secondary reaction of primary biochar favours biochar. Low nitrogen flow rate of 1.0 L/min, shorter residence time (10min), larger particle size of 3.0mm and low kaolin ratio (10g) were suitable for biochar production. Biochar yields were 39.2 and 50.3% from sawdust and poultry waste respectively. The content of volatile matter (VM) and fixed carbon (FC) for the generated biochars ranged from 50.16% to 53.21% and 18.67% to 25.44% for SBC and 50.66% to 47.06% and 21.64% to 26.54% for PBC, respectively. The C content for SBC increased from 51.2% to 56.06% and 59.7% to 61.86% for PBC, while the H and O contents decreased from 6.30% to 5.34% and 38.14% to 36.02% for SBC and 6.20% to 5.31%; 30.84% to 28.16% for PBC as the pyrolysis temperature increased from 400 to 600 °C respectively. These biochars were activated to produce array of activated carbons which were employed in adsorption study. The adsorption profiles show that there was a rapid and almost linear uptake of  $CO_2$  by all the adsorbents (SUMAC, PUMAC, SAMAC, PAMAC, SBMAC and PBMAC) as the contact time rises to 10 to 20 min for all adsorbent dosages with a corresponding rise in adsorption capacity of the adsorbent as the adsorbent dosage increases from 1 to 6 g. Beyond 20 min, the uptake was almost linear and constant without significant rise in adsorption capacity for all adsorbents. Thus, it can be concluded that the biomass amended with metakaolin increase biochar yield by 18.4 and 8.2 % while simultaneously increasing their carbon sequestration potentials by 10.1 and 33.2% for PKBC and SKBC respectively.

## TABLE OF CONTENTS

Content	Page
Cover Page	
Title Page	i
Declaration	ii
Certification	iii
Acknowledgements	iv
Abstract	v
Table of Contents	vi
List of Tables	xii
List of Figures	xiv
List of Plates	xvii
Abbreviation, Glossaries and Symbols	xviii
<b>CHAPTER ONE</b>	
1.0 INTRODUCTION	1
1.1 Background for the Study	1
1.2 Statement of the Research Problem	3
1.3 Aim and Objectives of the Study	5
1.4 Justification for the Study	6
1.5 Scope of the Study	8
<b>CHAPTER TWO</b>	
2.0 LITERATURE REVIEW	9
2.1 Concept of Biomass	9
2.2 Source of Biomass	10
2.3 Biomass Feedstocks	12
2.4 Biomass Resources in Nigeria	15
2.4.1 Sawdust	15
2.4.2 Poultry waste	16
2.5 Kaolin	17
2.5.1 Alumina	18
2.6 Biomass Energy Contents	20
2.6.1 Indicators of biomass energy contents	20
2.6.2 Higher and lower heating values	20
2.6.3 Heating values of various biomass	21
2.7 Availability of Biomass	22
2.7.1 Estimation of potential of waste biomass	23
2.7.2 Amount of waste biomass production	23
2.7.3 Energy potential of waste biomass	24
2.8 Biomass Categories	25

2.9 Biomass Composition	26
2.9.1 Cellulose	27
2.9.2 Hemicellulose	27
2.9.3 Lignin	28
2.9.4 Protein	29
2.9.5 Other components	29
2.10 Effect of Biomass Constituents	29
2.11 Physical and Chemical Characteristics of Biomass	32
2.12 Biochar Production Techniques	34
2.12.1 Combustion	35
2.12.2 Gasification	35
2.12.3 Pyrolysis	37
2.13 Comparison of Biochar Production Techniques	38
2.14 Concept of pyrolysis	40
2.14.1 History of pyrolysis	41
2.14.2 Evolution of pyrolysis	43
2.14.3 Principle of pyrolysis	43
2.14.4 Types of pyrolysis	44
2.15 Pyrolysis Products	46
2.16 Advantages of Pyrolysis	51
2.17 Effect of Pyrolysis Operating Conditions	52
2.18 Feedstock for Pyrolysis	67
2.19 Proximate Analysis of Feedstock	67
2.20 Pyrolysis of Biomass	68
2.21 Concept of Biochar	71
2.22 Components of Biochar	74
2.23 Characteristics of Biochar	77
2.24 Biochar and Climate Change Mitigation	80
2.24.1 Technologies for carbon dioxide capturing	81
2.25 Carbon Sequestration	83
2.25.1 Carbon sequestration potential of biochar	84
2.26 Adsorption Process	85
2.27 Factor Influencing on Adsorption Process	86
2.28 Adsorption Isotherms Theory	88
2.29 Activated Carbon	95
2.29.1 Preparation of activated carbon	97
2.30 Activation Processes	99
2.30.1 Physical activation process	99
2.30.2 Chemical activation process	101
2.30.3 Combination of physical and chemical processes	101
2.30.4 Advantages of chemical activation process	102
2.31 Adsorption by Activated Carbon	102
2.31.1 Potential of activated carbon as carbon sequester	103
2.31.2 Improving adsorptive capacity of activated carbon	104
2.32 Optimization in Chemical Engineering	107
2.32.1 Process simulators	107
2.32.1.1 Aspen plus	108
2.32.1.2 Design expert	109
2.33 Summary of Research Gap Identified	110

## CHAPTER THREE

3.0 RESEARCH METHODOLOGY	113
3.1 Equipment and Materials	113
3.2 Research Biomass	113
3.3 Experimental Design	114
3.4 Characterization of Biomass and Biochar	116
3.5 Preparation of $\gamma$ -Alumina from Kaolin	116
3.6 Evaluation of Effect of Process and Non-Process Parameters on Biochar	118
3.7 Characterization of Different Grades of Biochar Produced	120
3.8 Production of Activated Carbon from Biochar Produced	121
3.9 Adsorption Kinetic Studies	122
3.9.1 Intraparticle diffusion model	123
3.9.2 Elovich model	123
3.10 Optimization Software	124

## CHAPTER FOUR

4.0 RESULTS AND DISCUSSION	125
4.1 Characterization of Biomass and Kaolin	125
4.1.1 Proximate and Ultimate Analysis of Biomass	125
4.1.2 TGA Analysis of sawdust and poultry waste	126
4.1.3: XRF analysis of kaolin	127
4.1.4 XRD analysis of kaolin	128
4.2 Evaluation of the Effect of Process and Non-Process Parameters on Biochar	129
4.2.1 Effect of temperature on the product yields	129
4.2.2 Effect of nitrogen flow rate on product yields	132
4.2.3 Effect of feedstock particle size on pyrolysis product yields	134
4.2.4 Effect of residence time on pyrolysis product yields	136
4.2.5 Effect of kaolin mixing ratio on biochar formation	138
4.3 Production and Characterization of Different Grades of Biochar	140
4.3.1 Effect of temperature on the basic characteristic of biochars	141
4.3.2 Summary of effect of process parameters and kaolin on biochar yield	154
4.4 Evaluation of Potential of Biochar as Carbon Sequester	155
4.5 Adsorption of Carbon Dioxide by Activated Carbon	158
4.5.1 Effect of adsorption time and adsorbent dosage	158
4.5.2 Adsorption kinetic studies	163

4.6 Optimization Process	168
4.7 Optimization Outcomes	170
4.7.1 Optimization of sawdust pyrolysis	171
4.7.2 Optimization of poultry waste pyrolysis	183
CHAPTER FIVE	
5.0 CONCLUSION AND RECOMMENDATIONS	203
5.1 Conclusion	203
5.2 Recommendations	205
5.3 Contribution to Knowledge	205
References	207
Appendices	224

## LIST OF TABLES

Table	Page
-------	------

2.1: Biomass Resources and Estimated Quantities in Nigeria	15
2.2: Proximate and Ultimate Analysis of Sawdust in Different Compositions	16
2.3: Proximate and Ultimate Analysis of Poultry Waste	17
2.4: Chemical Composition of Marrand Kaolin	18
2.5: Typical Analysis and Heating Values of Biomass, Coal and Peat	22
2.6: Parameters Used for Estimating Waste Biomass Production	24
2.7: Biomass Species and Availability Ratio of Energy	25
2.8: Physical Characteristics of Selected Biomass Feedstock	33
2.9: Chemical Characteristic of Selected Biomass Materials	33
2.10: Comparisons of Biochar Production Techniques	38
2.11: Operating conditions for different types of pyrolysis	47
2.12: Summary of Pyrolysis Process Configuration and Parameters	66
2.13 Biochar Production at Different Pyrolysis Conditions	74
2.14: List of $q_{value}$ for Different Materials	94
3.1 List of Equipment and Materials	113
4.1: Proximate and Ultimate Analysis of Biomass	125
4.2 XRF of Kutigi Kaolin	128
4.3: Effect of Metakaolin on Biochar Yield	141
4.4: Proximate and Ultimate Results of Biochars	142
4.5 Surface Area and Pore Volumes	154
4.6 Data Used for Calculating Carbon Sequestration	155
4.7 Amount of CO <sub>2</sub> Removed by Biochars	156
4.8: Intra-particle Diffusion Model Parameters for Adsorption of CO <sub>2</sub>	164
4.9: Elovich Model Parameters for Adsorption of CO <sub>2</sub>	167
4.10: Preliminary Experiment on SD Pyrolysis	169
4.11: Preliminary Experiment on PW Pyrolysis	169
4.12: Fit Statistics for Sawdust Biochar	172
4.13: ANOVA for Bio-oil	176
4.14: Fit Statistics for Bio-oil	176
4.15: ANOVA for Biogas	180
4.16: ANOVA for Biochar	184
4.17: Fit Statistics for PW Biochar	185
4.18: ANOVA for PW Bio-oil	190
4.19: Fit Statistics for PW Bio-oil	190
4.20: ANOVA for PW Biogas	196
4.21: Fit Statistics for PW Biogas	196
4.22: Experimental and Predicted Values	201

## LIST OF FIGURES

Figure	Page
2.1: Biomass Categorization in terms of use and application	26
2.2: Conversion Techniques of Biomass	38
2.3: Illustration of the Pyrolysis Process	41
2.4: Simplified Reaction Model for Cellulose Decomposition	69

2.5 (a) and (b): Monolayer and Multilayer Adsorption	90
3.1 Flow Chart of Experimental Procedure	121
4.1: XRD of Kaolin	127
4.2: Effect of Temperature on Sawdust Pyrolysis	130
4.3: Effect of Temperature on Poultry Waste Pyrolysis	131
4.4: Effect of Sweeping Gas Flow Rate on Sawdust Pyrolysis	132
4.5: Effect of Sweeping Gas Flowrate on Poultry Waste Pyrolysis	134
4.6: Effect of Particle Size on Sawdust Pyrolysis	135
4.7: Effect of Particle Size on Poultry Waste Pyrolysis	136
4.8: Effect of Residence Time on Sawdust Pyrolysis	136
4.9: Effect of Residence Time on Poultry Waste Pyrolysis	137
4.10: Effect of Kaolin on Biochar Formation from Sawdust	138
4.11: Effect of Kaolin on Biochar Formation from Poultry Waste	140
4.12: Van Krevelen Diagram for SBC, PBC, SKBC and PKBC	144
4.13: HHV and LLV of Biochar Samples	145
4.14 FTIR Spectra of SBC400	146
4.15 FTIR Spectra of PBC400	147
4.16 FTIR Spectra of SKBC400	147
4.17 FTIR Spectra of PKBC400	148
4.18: XRD of PW, PBC400 and PBC@10%	150
4.19: XRD of SD, SBC400 and SBC@10%	150
4.20 SEM images of SD, SBC, SKBC, PW, PBC and PKBC	152
4.21: Effect of Contact Time and Adsorbent Dosage on CO <sub>2</sub> Removal by (a) SUMAC and (b) PUMAC Modified with Kaolin.	159
4.22: Effect of Contact Time and Adsorbent Dosage on CO <sub>2</sub> removal by (a) SBMAC and (b) PBMAC Modified with NaOH.	161
4.23: Effect of Contact Time and Adsorbent Dosage on CO <sub>2</sub> Removal by (a) SAMAC and (b) PAMAC Modified with H <sub>3</sub> PO <sub>4</sub> .	162
4.24 Normal Residual Plot for Biochar	173
4.25a: Contour Plot for Temperature and Particle size on Biochar yields	174
4.25b: 3D Plot for Temperature and Particle size on Biochar yields	174
4.26a: Contour Plot for Temperature and Residence time on Biochar yields	175
4.26b: 3D Plot for Temperature and Residence time on Biochar yields	175
4.27: Normal Residual Plot for Bio-oil	178
4.28a: Contour Plot for Temperature and Particle Sizes on Bio-oil yields	179
4.28b: 3D Plot for Temperature and Particle Sizes on Bio-oil yields	179
4.28c: Interaction Plot for Temperature and Particle Sizes on Bio-oil yields	180
4.29: Normal Residual Plot for SD Biooil	182
4.30a: Contour Plot for Temperature and Residence Time on Biogas yields	183
4.30b: 3D Plot for Temperature and Residence Time on Biogas yields	183
4.31: Normal Residual Plot for PW Biochar	186
4.32a: Single Effect of Temperature on PW Biochar	187
4.32b: Single Effect of Particle Size on PW Biochar	187
4.33a: Contour Plot for Temperature and Kaolin Ratio on PW Biochar yields	188
4.33b: Interaction Plot for Temperature and Kaolin Ratio on PW Biochar yield	189
4.34: Normal Residual Plot for PW Bio-oil	191

4.35a: Single Effect of Temperature on PW Bio-oil	192
4.35b: Single Effect of Particle Size on PW Bio-oil	193
4.36a: Contour Plot for Temperature and Kaolin Ratio on PW Bio-oil	194
4.36b: Interaction Plot for Temperature and Kaolin Ratio PW Bio-oil	195
4.37: Normal Residual Plot for PW Biogas	197
4.38a: Contour Plot for Temperature and Residence Time on PW Biogas	198
4.38b: Interaction Plot for Temperature and Residence Time on PW Biogas	199
4.35: Effect of Particle size and Kaolin Ratio on Biogas Formation	200

LIST OF PLATES

Plate	Page
I: Typical kiln Showing Production of Charcoal of Biochar	79
II: Structure	
III: Granular Activated Carbon	96
IV: Research Biomass and kaolin	114
V: Pyrolysis Experimental Set up	119
ABBREVIATIONS	
SD	Sawdust
PW	Poultry Waste
BC	Biochar
AC	Activated Carbon
SBC	Sawdust Biochar
PBC	Poultry Waste Biochar
SKBC	Sawdust Kaolin Biochar
PKBC	Poultry Waste Kaolin Biochar
SKBC10%	Sawdust Kaolin Biochar with 10% Kaolin Mixing Ratio
PKBC10%	Poultry Waste Kaolin Biochar with 10% Kaolin Mixing Ratio
SKBC400	Sawdust Kaolin Biochar obtained at 400 °C
PKBC400	Poultry Waste Kaolin Biochar obtained at 400 °C
SAMAC	Sawdust Acid Modified Activated Carbon
SBMAC	Sawdust Base Modified Activated Carbon
SUMAC	Sawdust Kaolin Modified Activated Carbon

PAMAC	Poultry Waste Acid Modified Activated Carbon
PBMAC	Poultry Waste Base Modified Activated Carbon
PUMAC	Poultry Waste Kaolin Modified Activated Carbon

## CHAPTER ONE

### 1.0

### INTRODUCTION

#### 1.1 Background to the Study

The use of biomass is an alternative to fossil fuels, as its regenerative capacity addresses the problem of non-renewable scarcity of conventional sources. Biomass can be employed as a renewable substitute of fossil fuels because it serves as the precursor of fossil feedstock (Neves et al., 2018). Energy is the life blood of technological and economic development, and countries' energy choices have effects on climate change (Azevedo et al., 2019). Governments of many countries have advocated biomass waste recycling and discouraged harvesting forests for charcoal production. However, by default, biomass residues are always in low calorific value, thus, it would be advantageous to convert the feedstock to a more dense and economical form for effective utilization. Productive use of sawdust and poultry waste by slow pyrolysis would not only prevent environmental pollution from biomass waste discharges, but also contribute to environment protection because the biochar can be used as soil remediator, carbon sequestrator or as charcoal briquette production to satisfy people's demand for solid fuel of high quality (Sharma et al., 2017).

The decrease trend of the fossil fuel source, their dispersed geographical distributions and major concerns for the environment has brought increasing attention to the renewable source. Biomass was identified as renewable energy source (Neves et al., 2018). In developing countries such as Nigeria, the contribution of biomass towards societal changes and environment is immense as people are directly associated with different forms of biomass. These forms of biomass may vary from forestry, small plants, trees

(woody plants), organic wastes, domestic wastes and agricultural wastes. The pyrolysis of biomass can produce three distinct phases of products, namely, solid, liquid and gaseous fuel (Lee et al., 2018). The proportion of each of these products depend on the feedstock and pyrolysis conditions including temperature, sweeping gas flow rate, vapour residence time, feedstock particle size, reactor type and heating rate (Wang et al., 2020). The characteristics of biomass-derived fuel depend on several biological and thermo chemical processes, and the pathway for their conversion. Out of these processes, pyrolysis is considered as the most popular and suitable method due to its eco-friendly, simplicity, inexpensive technology for managing wide varieties of feedstock and lower consumption of resources (Qiu et al., 2020). Pyrolysis of biomass is a complex process in which raw biomass undergoes thermochemical conversion under oxygen-limited conditions, resulting in different products (solid, liquid and gaseous).

According to the International Biochar Initiative (IBI, 2020), <http://www.biocharinternational.org/biochar>, biochar can be defined as a solid material obtained from the carbonization of biomass. The primary constituent of biochar is carbon, followed by hydrogen, oxygen, ash content and traces amount of nitrogen and Sulphur. The elemental compositions of biochar generally change with the nature of feedstock and pyrolytic conditions such as carrier gas flow rate, catalyst, heating rate, pressure, reactor bed height, particle size, residence time and temperature (Das et al., 2018). Owing to its intrinsic properties such as large surface area, porosity and surface functionality, biochar has wide application in several fields. It can be used as a precursor for activated carbon production or can be used as an adsorbent for the removal of various contaminants of water and wastewater. Biochar can potentially be used in a wide variety of ways such as soil carbon sequestration, pollutant removal and soil

amendment (Yang et al., 2019). In addition, high heating value and low emissions make biochar as the most suitable

substitute for solid fossil fuels.

The practice of co-pyrolysis of biomass feedstock is gaining more attention due to its potential in enhancing the performance and yield of pyrolysis products. Co-pyrolysis is the use of two or more components as feedstock. Bardalai and Mahanta (2020) observed an increase in biochar yield when the biomass was co-pyrolyzed with recycled bio-oil. These yields were further increased by air pre-treatment prior to co-pyrolysis. Likewise, Li et al. (2017) investigated the influence of mineral additives on biochar yields and concluded varying increments. Furthermore, Panda et al. (2018) observed considerable yields of biochar during co-pyrolysis of polypropylene with kaolin. This study, therefore, make use of our locally available kaolin (Kutigi kaolin) to obtain high porous biochar as prerequisite for activated carbon production and carbon dioxide sequestration. The objective of this research, apart from the use of kaolin, is to explore the appropriate reaction conditions to convert sawdust and poultry waste into biochar by slow pyrolysis, including the effects of pyrolysis temperature, sweeping gas flow rate, particle size and residence time as well as heating rate on physicochemical properties, calorific value, energy yield and the surface characteristics of biochar with and without kaolin addition. In addition, yield of other pyrolysis products, including biooil and biogas in different conditions, were illustrated, and the relationship between reaction conditions and the distribution of pyrolysis products was investigated to determine which combination of these factors could give the highest yield of biochar for activated carbon production and

CO<sub>2</sub> sequestration

## 1.2 Statement of the Research Problem

Air pollution poses dangerous threat to the quality of air by causing climatic change, smog, acid rain and toxic air. These are responsible for severe and irreversible damage to the earth. CO<sub>2</sub> is the primary cause of global warming and it is released into the atmosphere from thermal power plants. In 2020, about 79 % of Green House Gas (GHG) emission is CO<sub>2</sub> arising from the combustion of fossil fuel and industrial processes (Woolf et al., 2017). Growth in economy and population are also drivers for CO<sub>2</sub> emission. Frequent use of fossil fuels by the citizens added more of GHG. Effort must be undertaken to rectify this global issue. The use of solid adsorbent has been proven to be successful in reducing CO<sub>2</sub> emission to the atmosphere. One promising approach to reduce the CO<sub>2</sub> concentration is to convert biomass into biochar – a solid product from thermal decomposition of biomass under limited supply of oxygen. In recent years, the literature on biochar production has increased, with a number of studies evaluating the physical and chemical characteristics of biochar used as a soil amendment (Biederman and Harpole, 2018), soil remediator (Qiu et al., 2020), raw material for catalyst development (Dehkhoda and Ellis, 2017) and modifier agent in the controlled release formulations of nutrients (Gonzalez et al., 2018a) with little information on the production and evaluation of biochar for CO<sub>2</sub> sequestration.

Despite the types of feedstocks, the operating conditions during pyrolysis affect the resulting products. There has been much research on the properties of biochar generated under different pyrolysis conditions. The distribution of pyrolysis products and properties of biochar are strongly dependent on reaction conditions including highest treatment temperature (HTT), heating rate and retention time, particle size, gas flow rate, feed stock and catalyst addition. However, most of the previous research mainly focused on few parameters such as feedstock types and the HTT (Zhang et al., 2019), temperature and heating rate (Azevedo, 2019), particle size and feed stock (Sun et al., 2019) on the characteristics of biochar, with little concern on the combined effect of

these process parameters. In a null shell, these parameters have been studied separately or not systematically. Only Gonzalez et al., (2020) and Liu et al (2020) reported the effect of the residence time, highest treatment temperature (HTT), and carrier gas flow rate on the biochar yield from oat hull and sugar cane bagasse. Yet, there is no correlation between the biochar physicochemical properties, combined pyrolysis conditions and kaolin addition on the yield of biochar.

The objective of this study is to explore the appropriate reaction conditions alongside kaolin addition to convert sawdust and poultry waste into biochar by slow pyrolysis, including the effects of temperature, particle size, sweeping gas flow rate, residence time as well as feed stocks on the yields, physicochemical properties, adsorptive capacity, energy yield and the porosity characteristics of biochar. In addition, yield of other pyrolysis products, including oil and gas in different conditions, were illustrated, and the relationship between reaction conditions and the distribution of pyrolysis products was investigated to determine which combination of all these factors' levels could obtain the highest yield of biochar for activated carbon formation and CO<sub>2</sub> sequestration.

### 1.3 Aim and Objectives of the Study

The aim of this research is to investigate the Effect of Metakaolin and Process Parameters on the Pyrolysis of Biomass to Produce Biochar for Carbon Dioxide Sequestration.

In order to achieve the aim, the following objectives were proposed to be achieved:

- I. Characterization of biomass materials and raw kaolin
- II. Evaluation of the effect of process and non-process parameters such as temperature, sweeping gas flow rate, residence time, particle size and metakaolin on biochar yields using a prototype reactor

- III. Production and characterization of different grades of biochar from selected biomass at optimum operating conditions determined from stage II
- IV. Production and characterization of different activated carbons from biochar produced
- V. Testing for CO<sub>2</sub> sequestration potentials of the biochar and activated carbons through evaluation of carbon contents of biochar and adsorption capacity of activated carbon produced.

#### 1.4 Justification for the Study

Waste and residues are better converted to useful products. Wastes and residues from poultry farming and furniture production industries are valuable resources that can be used directly or indirectly for energy, including pyrolysis energy and biochar. In addition to providing energy and biochar, the pyrolysis process will decrease the amount and the weight of the waste material. In other words, many waste streams offer economic opportunities for energy recovery particularly when a significant reliable source of feedstock is generated at a specific location. Biochar as a waste management strategy decreases GHG emissions associated with traditional strategies.

The usual practice of land filling of organic waste results in the release of significant quantities of methane. Anaerobic digestions of animal wastes release methane and nitrous oxide, and these gases are 25 and 298 times, respectively, more potent as GHGs than CO<sub>2</sub> (Woolf et al., 2017). Management strategies that avoid these emissions can therefore contribute significantly to mitigation of climate change (Gaunt and Cowries 2019). The production of biochar rather than composting is more effective in locking up carbon. Carbon contained in compost will be released by microbial transformations within 10 to 20 years (Gaunt and Cowries 2019). In contrast, the carbon sequestered in

the pyrolyzed wastes would be stable in the soil, and also simultaneously prevent emissions of GHGs, such as methane (Mohan et al., 2021).

Biochar has the potential to provide enormous economic and environmental benefits in comparison to current conventional methods for the utilization of biomass and waste materials, such as combustion, land filling, and incineration in the case of wastes. Biochar should be seen as an integral approach to the efficient utilization of biomass and waste materials. Depending on the operational time and temperature considerations, three subclasses of pyrolysis can be identified. These are conventional slow pyrolysis, fast pyrolysis, and flash pyrolysis (Maschio et al., 2017). Yields of liquid products are maximized in conditions of low temperature, high heating rate, and a short gas residence time, whereas a high temperature, low heating rate and long gas residence time would maximize yields of fuel gas. Low operational temperatures and low heating rates give maximum yields of biochar. Hence, the choice of slow pyrolysis in this present study. The reaction conditions are one of the main determinants of the yield of biochar and its physical and chemical compositions. Much research is still required to fully characterize the effect of these parameters on biochar formation and characteristics. Utilization of locally available resource (Kaolin) was intended to improve biochar yield with sequestration property. With the current recognition of biochar as strategy to mitigate global warming, there is need to investigate and optimize its production conditions to ensure that:

- i. Waste and residues from poultry farming and furniture industries are efficiently utilized for energy and biochar production.
- ii. Biochar as waste management strategy decreases GHG emissions associated with traditional strategies
- iii. The production of biochar rather than composting is an effective way of locking up carbon (carbon sequestration).

- iv. Biochar when activated is a good adsorbent for carbon dioxide capture and storage.
- v. The results are likely to increase yields, stability and CO<sub>2</sub> sequestration ability.
- vi. The findings aid reproducibility.

### 1.5 Scope of the Study

The study is limited to the following scopes:

- i. Pyrolysis of sawdust and poultry waste biomass with and without kaolin
- ii. Characterization of sawdust biochar (SBC), sawdust-kaolin biochar (SKBC), poultry waste biochar (PBC), poultry waste- kaolin biochar (PKBC) and activated carbons
- iii. Calculation of the percentage conversion yield of biochar from the biomass
- iv. Production of activated carbons from biochar produced
- v. Evaluation of the CO<sub>2</sub> adsorption capacity of functionalized biochar and activated carbon.

### 2.1 Concept of Biomass

The term "Biomass" refers to organic matter that has stored energy through the process of photosynthesis. It exists in one form as plants and may be transferred through the food chain to animals' bodies and their wastes, all of which can be converted for everyday human use through processes such as combustion, which releases the carbon dioxide stored in the plant material (Liu et al., 2020). Most of the biomass fuels used today come in the form of wood related products such as dried vegetation, crop residues, and aquatic plants. Biomass has become one of the most commonly used renewable sources of energy in the recent time, which is next to hydropower in the generation of electricity. It is such a widely utilized source of energy, probably due to its low cost and indigenous nature, that it accounts for almost 15 % of the world's total energy supply and as much as 35 % in developing countries, mostly for cooking and heating (Liu et al., 2020).

Biomass, by nature, is a complex biological organic or non-organic solid product derived from living or recently living organisms and therefore available naturally. Various types of wastes such as animal manure, waste paper, sludge and many industrial wastes are also regarded as biomass because, like natural biomass, these waste materials also are in a mixture of organic and non-organic constituents and can be processed to obtain energy. Biomass is one of the most promising sources of alternative energy which can solve the problem of energy crisis in world up to some extent due to its potential availability. Besides, the use of biomass can also reduce the problem of global warming and pollution

(Vassilev et al., 2020). Biomass is the only renewable energy source which can be converted into three different forms: solid fuel, liquid fuel and gaseous fuel. As the new

technologies are involved renewable energy production is increasing rapidly. The worldwide renewable energy production has increased from 18 % in 2006 to 21 % in 2013 and is expected to reach 35 % by the year 2025 (Demirbas, 2018a). This was confirmed by Tripathi (2019) on a study evaluating the significant of renewable energy in the 21<sup>st</sup> century.

Many countries like Germany, Australia, United Kingdom, Finland and Turkey are using biomass for the generation of electricity (Motasemi and Afzal, 2021). The heat generation from the agricultural waste is very common in different developing countries. Besides these many other countries like Cuba, India, Brazil, and Columbia are using sugarcane waste to generate power (Bilgen et al., 2018). Sweden supplies more than 50% of its energy demand from biomass (Vassilev et al., 2020). Unfortunately, Nigeria still depends solidly on crude oil as source of energy for which the reserve is finite and yet the contributor of CO<sub>2</sub> available in the atmosphere.

## 2.2 Source of Biomass

Biomass is organic in nature which implies it is made of material that comes from living organisms, such animals and plants. The most common biomass materials used for energy generation are plant residues, wood and waste. According to report of ‘Imperial College Centre for Energy Policy and Technology’ total land area across the world is about 13 Gha. Approximately 1.5 Gha of this area is used to grow arable crops and 4 Gha is occupied by forests. Pasture covers about 3.5 Gha of land and the rest is used for other applications (Demirbas, 2018a). Biomass can be classified in different ways depending upon various parameters such as organic, inorganic and fluid or as primary, secondary and tertiary biomass (Vassilev et al., 2020). Vassilev et al. (2020) classified the biomass into natural and anthropogenic biomass. Natural biomass includes those with the natural origin while anthropogenic biomass is formed by the processing of

natural matter. In the same literature, authors classified biomass in five different groups depending upon the source from where it is obtained which include woody, agricultural, aquatic, human and animal waste and industrial waste biomass.

The majority of the biomass is woody biomass which involves stem, branch, leaves, bark, lumps, chips of different trees like pines, spruces, oaks, maples, redwoods and larches. Main source of the woody biomass are the forest trees. Agricultural biomass is the next source of biomass which envelops a wide range of different agricultural crops. Stalks, straw, shells of these crops are used as biomass. Agricultural biomass and woody biomass are widely utilized for the energy production in different parts of the world. Different kinds of microalgae, plants and microbes found in water forms another category of biomass called aquatic biomass. Blue algae, green algae, fungus and different kinds of water weeds are the examples of aquatic biomass. Animal and human waste biomass is the next category of the biomass. When these waste materials are treated and converted to useful energy products not only energy is being produced but the problem of disposing of these materials also is reduced to a certain extent.

Industrial waste involves waste from various industries like paper sludge from paper industry, sugarcane residue from sugar mill, waste from food processing industries and others. Animal and human waste biomass and industrial biomass are categorized differently because industrial biomass contains different types of toxic chemicals and harmful additives in it while animal and human waste is free of these types of harmful exposures. Moreover, biomass can be classified on the basis of cellulose and lignin content present in it.

Classification of the biomass on the basis of their sources can reveal an estimation of some of the elements present in it rather than classification on the basis of cellulose or lignin component or any other type of classification. For example, it is expected that industrial and animal waste biomass will contain more sulphur as compared to woody

and agriculture biomass. Prediction of elements can help in comparing the energy content in biomass which is highly important in selection of biomass for pyrolysis process. Classification on the basis of lignin and cellulose may change the product distribution. Hence classification based on the lignin and cellulose content is helpful only when a certain type of product is desirable after the pyrolysis. Biomass has been converted by partial-pyrolysis to charcoal for thousands of years. Charcoal, in turn has been for several applications such as forging metals and for light industry for millennia. Both wood and charcoal formed part of the backbone of the early Industrial Revolution (Northern England, Scotland and Ireland were deforested to produce charcoal) prior to the discovery of coal for energy production (Simeon et al., 2019)

### 2.3 Biomass Feedstock

Organic materials that are used for the production of energy are referred to as biomass. Subsequently, this energy production process from biomass is called bioenergy. For the production of such energy from biomass, the term feedstock is commonly used to refer to all type of organic materials that has potential to be converted to energy. Wood and waste biomass supplied about 31 % of world energy consumption of the renewable sources and generated about 1.6 % of America's electricity (Akwasi, 2020). Wood which makes up to about half of all biomass employed for energy, has been used by people for thousands of years to cook food and to keep warm in the required season. Grasses, agricultural residues (such as rice husks, corns, sugar cane), landfill waste and manure are other examples of biomass. Aquatic plants could also be considered as a raw material for biochar production. Similarly, saline or polluted water that is unsuitable for food crops may support the production of algae or salt tolerant plants, such as palms, reeds and mangroves for biochar feedstock. The mindset for shifting from fossil fuel-based economies to sustainable energy economies is alarming. The suitability of a particular biomass resource as a potential feedstock for biochar

production depends on various characteristics, such as moisture content, calorific value, fixed carbon, oxygen, hydrogen, nitrogen, volatiles, ash content and cellulose: lignin ratio. Certain feedstock properties, such as size or silica content, can limit the practicality of using it for biochar production (Hossaini et al., 2018). The significant abundance of lignocellulosic biomass worldwide and its suitability for biochar production makes it a widely considered feedstock for this application. Lignocellulosic biomass includes biomass such as agricultural residues (Corn Stover, crop straws and bagasse), herbaceous crops, woody plants, forestry residue, waste paper and other municipal green wastes that are composed mainly of cellulose, hemicelluloses and lignin. The composition and proportions of these constituents vary with the type of biomass (McHenry, 2020). Feedstock with a high lignin content produce the highest biochar yields when pyrolyzed at moderate temperatures (to the order of 500 °C) (Demirbas and Balat, 2019).

There are noted concerns that biochar feedstock production could compete with food production, and hence the decision to use biomass for this purpose needs to take into account the potential for leading to negative food security impacts (Demirbas 2019; Heidari et al., 2021; McHenry, 2020). This is particularly important in a developing country like Nigeria. Rather than negatively impacting on food production, biochar feedstock options should be chosen in such a way as to help prevent erosion, rehabilitate degraded land and/or improve the habitat for the conservation of wildlife (Mohan et al., 2021). For this research, environmental benefit of converting waste to useful products (biochar and others) was aimed. It is considered an alternative waste management strategy with production of value-added products.

The feedstock majorly known for offering the best chance of financial viability are often derived from biomass residues such as by-products from agriculture and forestry. In many cases, these residues already present waste management challenges, and

production of biochar can therefore be viewed as a potential solution, although it is possible that there may be competition for these feedstocks, for example, for composting or in biorefineries. The largest limitation to the suitability of a feedstock, however, is often the ability to procure it in large and continuous quantities and at low cost. This includes the costs of harvesting and transportation (Das et al., 2018).

Biomass energy has been identified as one of the earliest and now the third largest global source of energy, comprising up to 40 % to 50 % of energy usage in many developing countries that have large agriculture and forest areas for its cultivation (Vamvuka and Zografos, 2021). Biomass is used to meet variety of needs, including generating electricity, heating homes, producing biochar and bio-oil and providing process heat for industrial facilities. The solar energy driving photosynthesis is stored in the chemical bonds of the structural components of biomass which is a natural process. During combustion, biomass releases this energy in the form of heat. For that reason, biomass species are considered as renewable sources of energy which do not add carbon dioxide to the environment, in contrast to non-renewable sourced fossil fuels. In addition, the unique feature of biomass is that it is the only renewable energy source which can be converted into convenient solid, liquid and gaseous fuels (Tillman, 2021). The high heating value (HHV) of the raw biomass and pyrolysis products are calculated by means of the following Institute of Gas Technology (IGT) formula presented in Equation (2.1) (Fagbemi, et al., 2020). The amounts of the elements (C, H, O, N and ash) are expressed in mass percentages:

$$HHV = 354.68C + 1376H - 15.92Ash - 124.69(O + N) + 71.26 \quad (2.1)$$

#### 2.4 Biomass Resources in Nigeria

Biomass resources in Nigeria include Agricultural crops, wood, charcoal, grasses and shrubs, residues and wastes (agricultural, forestry, municipal and industrial), and

aquatic biomass. Total biomass potential in Nigeria, consisting of animal and agricultural waste, and wood residues, was estimated to be  $1.2 \times 10^{15}$  kg in 2017 (Ajueyitsi, 2018). In 2019, research revealed that bio-energy reserves/potential of Nigeria stood at: Fuel wood 13071,464 hectares, animal waste, 61 million tonnes per year, crop residues, 83 million tonnes (Agba et al., 2020).

Table 2.1: Biomass Resources and Estimated Quantities in Nigeria (2019)

Resources	Quantity (Million tonnes)	Energy Value ('000 MJ)
Fuel wood	39.1000	531.0000
Agro-waste	11.2444	147.7000
Sawdust	1.8000	31.4333
Municipal Solid Waste	4.0750	-

(Source: Agba et al., 2020)

#### 2.4.1 Sawdust

Nigeria being a fertile land support agricultural activity. This in turn results in production of waste which constitutes environmental problems. Utilization of wood for man uses in most cases resulted in the production of sawdust. Badejo (2017) stated that the quantity of wood waste generated in the saw mills is estimated at about 3.87 million  $m^3$  of which sawdust accounts for about 20 %. According to Hall (2018), about 42 tons of sawdust is generated from every 100 tons of timber produced with an average of about  $4.39 \times 10^6 m^3$  of log split and plywood processed annually in Nigeria. The potential for sawdust generated can therefore be estimated at 1.8 million tons annually. This type of bioenergy is presently not exploited and yet constitutes an environmental problem (Hall, 2018).

This is one of the reasons for the use of sawdust as one of the biomasses in this study.

Table 2.2: Proximate and Ultimate Analysis of Sawdust in Different Compositions

Proximate Analysis		Ultimate Analysis	
Property	wt %	Property	wt %
Moisture	6.4	Carbon	58.60
Ash	3.3	Hydrogen	4.89
Volatile Matter	74.3	Oxygen	36.01
Fixed Carbon	16.0	Nitrogen	0.32
Calorific Value (MJ/kg)	18.34	Sulphur	0.18

(Source: Hall, 2018)

#### 2.4.2 Poultry waste

Poultry is known as one of the most developed animals' industries in Nigeria. Historically, the growth of poultry industry began as a result of its high level of energy and protein, rapid turnover rate and short incubation period (that is, 21days) which are advantages of poultry over other livestock (Mokwunye, 2021). Poultry waste consists of droppings, wasted feed, broken eggs and feathers. It also includes dead birds and hatchery waste, all of which is high in protein and contain substantial amount of calcium and phosphorus due to high level of mineral supplement in their diet. Available statistics showed that there is a consistent increase in the population of chicken in Nigeria from 166 million in 2015 to 196 million in 2021 (FAO, 2022). The volume of waste certainly has increased due to increasing birds' population but appropriate waste management process has not been refined. Hence, pyrolysis of biomass to biochar can serve as effective waste management strategy to utilizing abundant waste arising from ever increasing population.

Table 2.3: Proximate and Ultimate Analysis of Poultry Waste Proximate Analysis Ultimate Analysis

Property	wt %	Property	wt %
----------	------	----------	------

Moisture	6.4	Carbon	48.98
Ash	3.3	Hydrogen	4.89
Volatile Matter	74.3	Oxygen	36.01
Fixed Carbon	16.0	Nitrogen	0.32
Calorific Value (MJ/kg)	18.34	Sulphur	0.18

(Source: Vamvuka and Zografos, 2021)

## 2.5 Kaolin

Kaolin is any of a group of fine clay minerals with the chemical composition of  $\text{Al}_2\text{O}_3 \cdot 2\text{SiO}_2 \cdot 2\text{H}_2\text{O}$  which means two-layer crystals (silicon-oxygen tetrahedral layer joined to alumina octahedral layer) exist alternately. Clay minerals include kaolinite, nacrite, dickite, illite, chlorite, attapulgite and anauxite. Chemical compositions of kaolin minerals vary from layers stacked on top of one another. Kaolinite is the principal constituent of kaolin. Its chemical structure is  $\text{Al}_2\text{Si}_2\text{O}_5(\text{OH})_4$  (theoretically 39.8 % alumina + 46.3 % silica + 13.9 % other elements) but elements are not diverted from this ideal composition. Kaolinite is a hydrous aluminium silicate produced by the chemical weathering of feldspar and decomposition of aluminium silicate rocks. It is a soft, earthy and white mineral but is coloured light orange to red by iron oxide. Kaolin minerals for long have been the basic raw materials used in the ceramic industry, especially in fine porcelains. They can be easily moulded, have a fine texture, and are white when fired. Large quantities of kaolin are used also in paper coating, filler, paint, plastics, fibre glass, catalysts, and other specialty applications.

Table 2.4: Chemical Composition of Marrand Kaolin

Materials	Weight Percentage
-----------	-------------------

SiO <sub>2</sub>	61.5
Al <sub>2</sub> O <sub>3</sub>	24.5
Fe <sub>2</sub> O <sub>3</sub>	0.55
CaO	1.55
Na <sub>2</sub> O	0.8
MgO	0.6
L.O.I	10

(Source: Hossein et al., 2019)

### 2.5.1 Alumina

Alumina is the technical name used for oxide of aluminium (Al<sub>2</sub>O<sub>3</sub>). It is also referred to as aloxide, alkoide or alundum, although these other names are not as commonly used as the famous name, alumina. Alumina exists in different thermodynamically stable phases depending on the method and/or extent of processing applied to its source material (Salaudeen et al., 2019). The thermodynamically stable transitional phases of alumina include gamma, delta, kappa, theta and alpha phase (Lee et al., 2020). When it exists in these phases, the material is referred as gamma-alumina, delta-alumina, kappa-alumina, theta-alumina and alpha-alumina respectively. Virtually in all its possible phases alumina possesses high economic viability owing to its versatile technological applications which cut across a wide range of fields. Some of these includes: high quality insulators (Chang et al., 2019), semiconductors (Lee et al., 2020) and microelectronics in electrical, electronic and computer engineering. It is used for the production of high strength materials (Lee et al., 2020) in the construction industry. It is used in the materials and metallurgy industry for the production of varieties of ceramics, alloys and refractories (Chang et al., 2019). Alumina is also used as a highly potent processing material and as a catalyst in biofuel and cell-fuel processing. Alumina remains a very important catalyst support for metal supported and zeolite catalysts used for processing petroleum, gas, and petrochemicals and for other applications in the chemical processing industries.

### 2.5.2 Kaolin deposit in Nigeria

Kaolin is found in large quantities in many parts of Nigeria. It deposits are found in the Abia, Anambra and Enugu state. Sokoto Basins. Katsina and Kaduna also recorded million tons reserve of kaolin. Others are the Benue Trough and the Niger Delta Basin. In the Northern part of the country, they are found in Bauchi, Borno, Gombe, Katsina, Kaduna, and Kebbi States respectively. In North central zone, kaolin is predominantly found Kutigi in Niger State, Ahoko in Kogi State and large deposit at Lafiagi, Kaima, Patigi in Kwara State. In the South west, kaolin is available in Ondo, Ogun, and Oyo States (Bello et al., 2017).

### 2.5.3 Composition of kaolin

Kaolin is commonly the product of weathering of naturally occurring hydrated aluminium silicates. It consists of the main mineral referred to as kaolinite. In frequent uses, the term kaolin basically includes the raw clay and refined commercial products (Ojo et al., 2017). it is dominated by kaolinite, a clay mineral that is composed mainly of  $\text{Al}_2\text{Si}_2\text{O}_5(\text{OH})_4$ . Ideally, kaolin has specific gravity that ranges from 2.58 to 2.63 with a refractive index of between 1.56 and 1.62. it has composition of 39.8 % alumina, 46.3 % silica and 13.9 % of other elements (Ojo et al., 2017).

### 2.5.4 Kaolin in biochar production

Biochars have been highlighted as a means of carbon sequestration, which is significant for achieving carbon neutrality. Kaolin was generally understood to be unreactive at room temperature. Because it is chemically unreactive under normal conditions, kaolin is in high demand as a raw material in the production of paper, ceramics, paint, chalk, cosmetics, pharmaceuticals and agrochemical industries (Mohan et al., 2021). In recent time, the utilization of calcined clay was presumed to enhance product selectivity in pyrolysis reaction (Lehmann, and Joseph, 2019). The addition of minerals promoted

the formation of a stable carbon structure in biochar. Hence the co-pyrolysis of biomass with kaolin and other materials with catalytic effects.

## 2.6 Biomass Energy Content

### 2.6.1 Indicators of energy content

For the establishment of biomass energy system, the content of each type of biomass feedstock should be firstly determined. Heating value is often used as an indicator of the energy that biomass contained. Heating value is the amount of heat generated when a substance undergoes complete combustion and is also called the heat of combustion. Heating value is determined by the ratio of components and the various kinds and ratios of elements (especially carbon content) in biomass.

### 2.6.2 Higher and lower heating value

Biomass comprises of organic substances which composed mostly of carbon, hydrogen, and oxygen and when completely combusted, it produces water and carbon dioxide. The generated water and water vapor contain latent heat that is given off during condensation.

The heating value which includes latent heat is the higher heating value (HHV) while that from which latent heat is subtracted is lower heating value (LHV). Heating Value  $Q_o$  is the amount of heat that arises from complete combustion per unit material under standard conditions. Although biomass contain much moisture and ash, which must be taken into consideration when energy is produced. Merely evaluating low heating value is inadequate as an indicator of whether biomass in its natural state will sustain combustion. The energy to raise ambient air to the temperature that maintains the fire and the endothermic energy of ash should also be taken into consideration. The heat amount that takes them into account is the available heat, and it is expressed with

Equation (2.2)

$$\text{Available Heat } (Q) = Q (1 - W) - 1000W - [FHA] - [AHA] \quad (2.2)$$

where  $w$  is the moisture content, FHA is the Flue heat absorption and AHA is Ash heat absorption.

### 2.6.3 Heating values of various type of biomass

Chemical compositions for various biomass were captured in Table 2.5 which gives the data for moisture content, organic matter content, ash content, and heating values of representative types of biomasses, coal and peat. These values are based on the geographical locations and type of biomass in consideration.

Table 2.5: Typical Analysis and Heating Values of Biomass, Coal and Peat

Category	Biomass	Moisture Content* [wt %]	Organic Matter [dry wt %]	Ash ** [wt%]	Higher heating value [MJ/drykg]
Waste	Cattle manure	20 – 70	76.5	23.5	13.4
	Activated biosolid	90 – 97	76.5	23.5	18.3
	Refuse derived fuel (RDF)	15 – 30	86.1	13.9	12.7
Herbaceous Plant	Sawdust	15 – 60	99.0	1.0	20.5
	Sweet Sorghum	20 – 70	91.0	9.0	17.6
	Switch grass	30 – 70	89.9	10.1	18.0

Aquatic Plant	Giant brown kelp	85 – 97	54.8	45.8	10.3
	Water hyacinth	85 – 97	77.3	22.7	16.0
Woody plant	Eucalyptus	30 – 60	97.6	2.4	18.7
	Hybrid poplar	30 – 60	99.0	1.0	19.5
	Sycamore	30 – 60	99.8	0.2	21.0
Derivatives	Paper	3 – 13	94.0	6.0	17.6
	Pine bark	5 – 30	97.1	2.9	20.1
	Rice straw	5 – 15	80.8	19.2	15.2
Coal	Illinois bituminous	5 – 10	91.3	8.7	28.3
Peat	Reed sedge	70 – 90	92.3	7.7	20.8

---

(Source: Ogi, 2022)

\*Moisture content is determined from the weight loss after drying for 105 °C under atmospheric pressure

\*\*Ash content is determined from the weight of residue (metal oxide) left after heating to about 120 °C.

## 2.7 Availability of Biomass

The earth has a large stock of biomass covering wide regions including forests and the oceans. The total biomass of the world is 1,800 billion tons on the earth and 4 billion tons in the ocean, and a comparative amount of biomass exists in the soil. The total biomass on the earth can provides 80 times or more of the annual energy consumption of the world (Ogi, 2022). However, some part of the biomass is used as food by living things including humans, and also for uses other than foods, which are necessary for human living.

### 2.7.1 Estimation of potential of waste biomass

Waste biomass includes waste and residues discharged from our living. Quantity of this production is now referred to as “waste biomass production”. Waste biomass has a variety of uses, not only for energy but also for feed or fertilizer. On the other

hand, biomass currently not being utilized but convertible to energy is referred to as “energy potential of biomass”

### 2.7.2 Amount of waste biomass production

It is important to know the waste biomass production to estimate current stock of waste biomass, but it is difficult to know the amount of waste biomass production in each country and region of the world. Therefore, the waste biomass production is often estimated typically by assuming the ratio of waste production relative to the biomass production as captured in Table 2.6. Note that these parameters are different for each region.

Table 2.6: Parameters Used for Estimating Waste Biomass Production and Amount of Resources

Biomass species	Ratio of waste production (t/t)	Coefficient of energy conversion (GJ/t)
Rice	1.4	16.3
Wheat	1.3	17.5
Maize (corn)	1.0	17.7
Roots and tubers	0.4	6.0
Sugarcane and residue (tops and leaves)	0.28	17.33
Cattle	1.10 (t/y/day)	15.0
Swine	0.22(t/y/day)	17.0
Poultry	0.037(t/y/day)	13.5
Horses	0.55(t/y/day)	14.9
Buffaloes and camels	1.46 (t/y/day)	14.9
Sheep and goats	0.18 (t/y/day)	17.8
Industrial logs	1.17	16.0
Fuel logs	0.67	16.0

Wood waste	0.784	16.0
------------	-------	------

\*Dung production rate, dry tons basis. (Source: Ogi, 2022)

### 2.7.3 Energy potential of waste biomass

Among the current stock of waste material, biomass has already been used for other applications, making it difficult to efficiently recover the complete mass, and to reuse it as an energy source even if it is reserved unused. For example, some of rice straw is used as feed for livestock at present. It may be almost impossible to collect dung of cattle in pasture, and it is not always possible to completely collect dung of cattle even if they are fed as being tried. Whenever current stock of biomass quantity is estimated, it is necessary to consider such availability, so that energy potential of waste biomass is given as a portion of the entire current stock as an energy source. Ratios proposed by Hall et al., (2018) are presented in Table 2.7

Table 2.7: Biomass Species and Availability Ratio of Energy

	Biomass species	Availability ratio of energy (%)
Agricultural waste	Rice, Wheat, Roots and tubers, Sugarcane (crop residue)	25
Livestock	Cattle, Sheep and Goats, Swine, Horses, Buffaloes and Camels, Poultry	12.5
Forestry waste	Industrial log	75
	Fuel log	25
	Wood waste	100

(Source: Hall et al., 2018)

### 2.8 Biomass Categories

There is no fundamental means of categorizing biomass; this is defined differently according to the field of study; categorization changes depending on the purpose and application. Generally, there are two ways of categorizing biomass: One is biological categorization which is based on types of existing biomass in nature (such categorization is according to ecology or type of vegetation), and the other is based on the use, application and resources. The latter is highly significant in terms of making effective use of biomass energy. An example of biomass categorization appears on Figure 2.1. In this categorization, biomass includes not only the conventional product and waste from agriculture, forestry, and fisheries but also plantation biomass. Categorization according to source is important for designing biomass usage system.

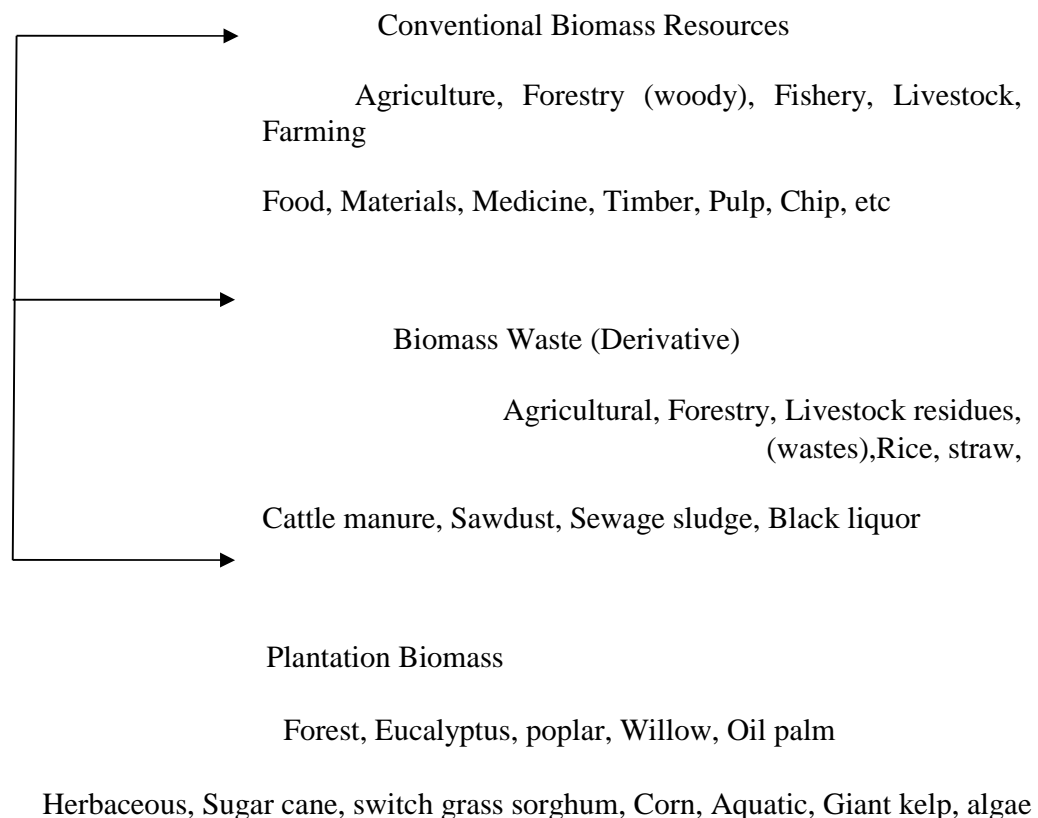


Figure 2.1: Biomass Categorization in terms of Use and Application

Moisture content is an important factor to be considered when using biomass especially as energy. Because moisture content is defined differently in each field. In the energy field, moisture content is often defined as follows:

$$\text{Moisture Content} = \text{—————} \times 100\% \quad (2.3)$$

$$\text{Total weight} = (\text{Biomass dry weight}) + (\text{Moisture weight}) \quad (2.4)$$

Using this definition, moisture content never exceeds 100%. In the forestry and ecology fields, moisture content is usually defined as follows:

$$\text{Moistur content} = \text{—————} \times 100\% \quad (2.5)$$

## 2.9 Biomass Composition

There are different kinds of biomass and compositions are also diverse. Some primary components of biomass are cellulose, hemicelluloses, lignin, starch, and proteins. Trees mainly consist of cellulose, hemicelluloses and lignin and so herbaceous plants, although the component percentages differ. Grains have much starch, while livestock waste has a lot of protein. Because these components have different chemical structures, their reactivity's are also different. Moreover, decomposition of each component depends on heating rate, temperature and the presence of contaminants due to different molecular structures (Yaman, 2017). In the process of pyrolysis, the three components are not decomposed at the same time. Hemicelluloses would be the easiest one to be pyrolyzed, followed by cellulose, while lignin would be most difficult one. Interestingly, both lignin and hemicelluloses could affect the pyrolysis characteristics of cellulose while they could not affect each other obviously in the pyrolysis process (Wang et al., 2018).

### 2.9.1 Cellulose

Cellulose is a glucose polymer consisting of linear chains of B (1,4) d-glucopyranose units. Its average molecular weight is close to 100,000 (Soltes and Elder 2020). Aggregation of these linear chains within the micro fibrils provides a crystalline structure that is highly inert and not accessible to chemical reagents. Cellulose component normally constitutes 45-50 % of the dry wood. Shafizadeh (2019) has studied the pyrolysis of cellulose as the temperature is increased. At temperatures less than 300 °C, the dominant process is the reduction in degree of polymerization. In the second step, at temperatures above 300 °C, there is formation of char, tar and gaseous products. The major component of tar is laevoglucose which vaporizes and subsequently decomposes with increasing temperature.

### 2.9.2 Hemicellulose

Hemicellulose is a combination of polysaccharides mainly composed of glucose, mannose, galactose, xylose, arabinose, 4-O methyl glucuronic acid and residues of galacturonic acid. Generally, it is of much lower molecular weight than cellulose and is amorphous in structure unlike cellulose. Its content varies from 20 to 40 %. According to Soltes and Elder (2020), hemicellulose is thermally most sensitive and decomposes in the temperature range 200 to 260 °C. This decomposition may occur in two steps; decomposition of the polymer into soluble fragments and conversion into monomer units that further decomposes into volatile products. As compared to cellulose, hemicelluloses give rise to more volatiles, less tar and char. The components of tar are organic acids such as acetic acid, formic acid and a few furfural derivatives.

### 2.9.3 Lignin

Lignin is amorphous in nature and a random polymer of substituted phenyl propane units that can be processed to yield aromatics. It is believed as the main binder for agglomeration of fibrous components. The lignin content in biomass varies between 17

and 30%. According to Soltes and Elder (2020), lignin decomposes when heated between 280 °C and 500 °C. Char is the more abundant constituent in the products of lignin pyrolysis with a yield of 55 %. A liquid product known as pyroligneous acid consists of 20 % aqueous components and 15 % tar residue on dry lignin basis. The aqueous part is composed of methanol, acetic acid, acetone and water. The tar residue consists mainly of homologous phenolic compounds. The gaseous products represent 10% of the lignin and are composed of methane, ethane and carbon monoxide. Like cellulose, starch is a polysaccharide whose constituent units are D-glucose, but they are linked by  $\alpha$ glycosidic bonds. Owing to the difference in the bond structures of biomass, cellulose is not water soluble while part of starch is soluble in hot water (amylase with a molecular weight of about 10,000 to 50,000, accounting for 10 % to 20 % of starch) and part is not soluble (amylopectin, with a molecular weight of about 50,000 to 100,000, accounting for 80 % to 90 % of starch). Starch is found in seeds, tubers (roots) and stems and invariably has a very high value as food (Brownsort, 2019).

#### 2.9.4 Protein

These are macromolecular compounds in which amino acids are polymerized to a high degree. Properties differ depending on the kinds and ratios of constituent amino acid, and the degree of polymerization. Proteins are not primary component of biomass and account for lower proportion than the previous three components (Brownsort, 2019).

#### 2.9.5 Other components (organic and inorganic)

The amount of the other organic components varies widely depending on specie, but there are also organic compounds with high value such as glycerides (representative examples includes rapeseed oil, palm oil, and other vegetable oil) and sucrose in sugarcane and sugar beets. Biomass comprises of organic macromolecular compounds, but it also contains inorganic substances (ash) in trace amounts. The primary metal

elements include Ca, K, P, Mg, Si, Al, Fe, and Na. substances and their amounts differ according to the feedstock type.

#### 2.10 Effect of Biomass Constituents

Lignin along with the cellulose is considered to be the main constituent of the biomass. Composition and type of the biomass influence the composition and nature of the pyrolysis products. Studies over the biomass structure revealed that cellulose, hemicellulose and lignin are the main ingredients of biomass which influence the product yield of pyrolysis. Generation of the char from lignin is the outcome of fracturing of relatively weak bonds and the consequent formation of more condensed solid structure

(Industries, 2018). Different quantities of lignin associated with various species of wood result in different rates of degradation. Coniferous lignin is found to be more stable than deciduous lignin and the former produces larger char (Brebun and Vasile, 2020). At relatively low temperature cellulose degrades to rather stable anhydrocellulose resulting in the production of high char but at high temperature the cellulose decomposes to produce volatile products (Demirbas, 2018b).

Cellulose contributes mainly to the production of tar which eventually is a mixture of discrete ketones, aldehydes, organic liquids and char while Lignin primarily produces char and small amount of water on pyrolysis. Cellulose and hemicellulose component in biomass are liable to the volatile products and lignin for the char yield (Yang et al., 2019). It has also been found that the structural difference in the biomass also produces compositional change in the pyrolysis product. Presence of oxygen is another factor which influences the reactivity of biomass during pyrolysis which consequently affects the final product yield and quality. Studies have suggested that more the presence of oxygen in the biomass more will be the reactivity (Gani and Naruse, 2017). Both

cellulose and lignin present in the biomass enhance the formation of biochar but the biochar production is higher in the biomass which has more lignin as compared to cellulose (Skoulou and Zabaniotou, 2017; Lathouwers and Bellan, 2020). Demirbas (2018a) during the pyrolysis of olive husk, corncob and tea waste showed that olive husk having the most lignin content produced the highest amount of char and corncob with least lignin content end up with least biochar yield. Similar findings were documented by Lv et al. (2017), rice husk containing most lignin as compared to other biomass has the highest char yield and sugarcane bagasse with the lowest lignin content produced lowest biochar.

Biomass always is associated with some amount of water/moisture content. This water inside a biomass can exist as water vapor, chemically bound water (adsorbed within the pores of biomass) and free liquid water (Bryden and Hagge, 2018). Biomass can have up to 60 % of water content in it. During pyrolysis, fraction of the heat energy supplied to the biomass is utilized in removing the moisture present in it and rest is used to increase its temperature. Very large amount of moisture reduces the heating rate resulting in more time in achieving the pyrolysis temperature (Janse et al., 2019). Biomass with more than 30 % moisture content is not suitable for use in pyrolysis (Demirbas, 2018a). For the biomass with 40 % moisture, more energy was needed for the pyrolysis as compared to dry wood which suggests that drying the biomass out before pyrolysing is very beneficial for high moisture containing biomass (Akhtar et al., 2017). Air drying and sun drying can reduce the moisture content of biomass up to a little extent.

During pyrolysis of wood with 5 % and 20 % moisture content, it was observed that lower moisture biomass leads to high amount of residue. The results were based on different heating rates (Fang et al., 2019). Demirbas (2018a) observed that increasing the moisture content of wood increases the bio-oil yield but the biochar yield gets

reduced. Xiong et al. (2018) observed during pyrolysis of sewage sludge that increase in water content decreases the biochar yield which is in accordance with the result obtained by other researchers (Huang et al. 2020; Dominguez et al., 2017). Low moisture supports the biochar production. Low moisture is advisable for the biochar production using pyrolysis because it not only reduces the heat energy required for the pyrolysis but it also lowers the time required for the process making it economically viable as compared to biomass with high moisture content (Dominguez et al., 2017).

### 2.11 Physical and Chemical Characteristics of Biomass

Having the knowledge of feedstock used for pyrolysis process is important. However, little is known about the optimal feedstock constituents for energy production. This is because the current commercial and research-scale pyrolysis plants are dedicated to specific waste streams, giving little attention to optimize the constituents. However, some recent studies have focused on a wide range of biomass feedstock in pyrolysis applications. Feed stocks with high lignin content produce the highest bio-char yields when pyrolyzed at moderate temperatures (500 °C). In addition, the ratios of volatile matter, fixed carbon, ash content and moisture are also indicators of pyrolysis product yields. In general, biomass with high volatile matter produces high quantities of bio-oil and syngas, whereas fixed carbon increases the bio-char production. Therefore, biomass such as walnut shell, olive husk and hazelnut shell are more favourable in bio-char production (which is related to lignin content). The elemental ratio of carbon, oxygen, hydrogen, nitrogen and ash content has an important effect on pyrolysis products. Friedl et al. (2017) found that feed stocks with low mineral and nitrogen contents are favoured for bio-oil and biogas production. These include wood and biomass from energy crops, woody plants high productivity grasses and low-cost

agricultural by-products including cereal straw. The basic characteristics of biomass in terms of physical and chemical attributes are shown on Tables 2.8 and 2.9 respectively.

Table 2.8: Physical Characteristics of Selected Biomass Feedstock

	Density (Kg/m <sup>3</sup> )	Moisture Content (%)	Ash Content (%)	Volatile Matter (%)	Fixed Carbon (%)
Wood	1186	20	0.4-1	82	17
Bituminuos coal		11	8-11	35	45
Hybrid poplar	150	45	0.5-2	-	-
Switchgrass	108	13-15	4.5-5.8	-	-
Miscanthus	70-100	11.5	1.5-4.5	66.8	15.9
Sugarcane baggage	1198		3.2-5.5	-	-
Barley straw	210	30	6	46	18
Wheat straw	1233	16	4	59	21
Danish pine		8	1.6	71.6	19
Rice straw	200	6	4.3	79	10.7
Fire wood	-	7.74	1.98	80.86	17.16
Grateloupiafilicina	-	4.93	22.37	55.93	17.01
Birch	125	18.9	0.004	-	20
Pine	124	17	0.03	-	16
Poplar	120	16.8	0.007	-	-

(Source: Wang et al., 2020)

Table 2.9: Chemical Characteristic of Selected Biomass Materials

Feedstock	Carbon (%)	Hydrogen (%)	Oxygen (%)	Nitrogen (%)	Ash (%)
Wood	51.6	6.3	41.5	0.1	1
Bituminuos coal	55	6.5	38.1	-	0.4
Hybrid poplar	66.9	9.2	21.9	2	-
Switchgrass	48.5	5.5	3.9	0.3	4
Miscanthus	45.7	6.1	38.3	0.4	6
Sugarcane baggage	73.1	5.5	8.7	1.4	9
Barley straw	56.4	6.3	-	0.1	0.09

Wheat straw	44	6.9	49	0.1	0.004
Danish pine	45.7	7	47	0.1	0.03
Rice straw	48.1	5.30	46.10	0.14	0.007
Fire wood	47.78	5.90	46.10	0.31	1.30
Grateloupiafilicina	44.77	5.79	49.13	0.31	4.30
Birch	45.96	5.81	48.49	0.34	5.10
Pine	42.96	5.70	49.44	1.90	7.50
Poplar	42.22	5.64	50.65	1.50	7.30

(Source: Wang et al., 2020)

## 2.12 Biochar Production Techniques

Bioenergy conversion technologies are those which are used to extract the energy out from the biomass. Various energy rich products can be obtained by the bioenergy conversion of the biomass. It is highly important to choose the appropriate method for the conversion of the biomass into energy and various value-added products so that the maximum energy can be obtained at the minimum expense keeping the environmental issues also in mind. Generally, bioenergy conversion techniques can be divided into two groups namely biochemical conversion and thermochemical conversion (Das et al., 2018). Biochemical conversion involves the biological catalysts and biological organism to produce the energy from biomass while thermochemical conversion involves heat and the chemical catalyst to produce energy from biomass. Fermentation is the main process involved in biochemical process, which is widely used to obtain methanol and biodiesel from the biomass while thermochemical conversion technique can further be divided into combustion, gasification and pyrolysis. However, biochemical conversion technology is less expensive and more environment friendly as compared to thermochemical conversion technique but the rate of hydrogen production and yield is quite low in biochemical conversion method (Das et al., 2018). Because of

this observed constraint, thermochemical conversion is more popular as compared to biochemical technique.

As the term implies, thermal conversion refers to the use of heat as the primary mechanism for converting biomass into another form. Combustion, pyrolysis, torrefaction, and gasification are the basic thermal conversion technologies either in use today or being developed for the future. In this work, pyrolysis is the primary source. The thermochemical process involves multiple stages. The first stage involves converting solid biomass into gases. In the second stage the gases are condensed into oils. In the third and final stage the oils are conditioned and synthesized to produce biogas.

#### 2.12.1 Combustion

Combustion is the oldest process known to utilize the biomass as energy producing material. Combustion is a process in which the chemical energy stored in the biomass is obtained in the form of heat by its direct burning in the presence of oxygen/air. Combustion ensures the complete oxidation of the biomass. Combustion of biomass takes place within the temperature range of 800 –1000 °C, recovering almost all the available chemical energy into thermal energy leaving no unconverted energy in flue gas and very low unconverted energy in ash (McHendry, 2020). Although combustion can be employed to any type of biomass, it is feasible only if the moisture content in the biomass is less than 50% (Goyal et al., 2018). In most of the situations direct combustion of the biomass is not very efficient. A pre-treatment of the biomass before combustion increases the efficiency of the combustion process (Mckendry, 2020). Although the pretreatment process increases the cost of the combustion, the increased efficiency after combustion covers the increased cost.

#### 2.12.2 Gasification

Gasification is a thermochemical process in which carbonaceous contents of the biomass are converted into the gaseous fuel in the presence of gaseous medium like oxygen, air, nitrogen, carbon dioxide, steam or some mixture of these gases at an elevated temperature ranging between 700 °C and 900 °C (Neves et al., 2018). Unlike combustion, it is partial oxidation of biomass which extracts out the energy present in the biomass and packages it into chemical bonds in the form of gaseous products. In this process, the intrinsic chemical energy of carbon present in the biomass is converted into combustible fuel gases which can be used more efficiently and easily than raw biomass (McHendry, 2020). The gas produced by the gasification is generally referred as bio syngas. This bio-syngas consists of mainly CO, CO<sub>2</sub>, H<sub>2</sub> and N<sub>2</sub>. The residue after gasification is char which is solid carbonaceous material, ash, tar and some component of oil (Morrin et al., 2020). Gasification is a very efficient method to produce H<sub>2</sub> from the biomass not only on the laboratory scale but for the large-scale hydrogen production also gasification is being widely used (Saxena et al., 2018). Most of the problems faced in the production of high energy containing biochar from biomass generally come from its composition itself. It is a well-known and established fact that O/C ratio is very important for high gasification efficiency.

Low O/C ratio biomass on gasification leads to high efficiency gasification. Torrefaction is a process which reduces the O/C ratio of biomass. Torrefaction can be considered to be a pre-treatment before conventional gasification for improved quality of product. It is a low temperature process which occurs in the temperature range from 200 to 300 °C and a heating rate of about 50 °C/min depending upon the composition and type of the biomass. Torrefaction can be employed effectively on solid waste and biomass to get fuel gases more efficiently and economically. Biomass in general is a low energy density hydrophilic material which absorbs moisture very easily but upon torrefaction it becomes a hydrophobic solid with improved calorific value. Solid

residue after the torrefaction contains approximately 30% more energy per unit mass as compared to regular biomass making the solid biochar more energy dense material (Mubarak et al., 2017). Porosity of the biochar formed after torrefaction is reasonably also high as compared to conventional gasification.

### 2.12.3 Pyrolysis

Pyrolysis is one of the most effective and efficient processes to obtain energy in the form of char from biomass. Other than charcoal, pyrolysis also produces different bio-oil and other value-added products (Tripathi et al., 2019; Mubarak et al., 2017). Pyrolysis is a thermochemical process in which biomass is thermally degraded in its chemical constituents under inert or very low stoichiometric oxygen atmosphere. Along with the efficiency pyrolysis also offers less pollution as compared to combustion. Xiao et al. (2020) observed that most of the oxygenated components of the biomass were present in derived bio-oil from pyrolysis, so it required to undergo for upgrading catalysts resulting in an increase in the energy density. The pyrolysis process occurs in the temperature range of 400 to 1200 °C. Although the product yield depends upon various operating parameters but generally low temperature and high residence time favours the char production. Figure 2.2 summarized the pictorial representation of the biomass sources, their thermal conversion techniques and the final products obtained by these conversions. Classification of biomass into five groups has been taken from Vassilev et al. (2020). It is clear from Figure 2.2 that pyrolysis is the only technique which provides a wide range of products including liquid (bio-oil), solid (biochar) and gas (bio-syngas) in significant amount. No other conversion method produces such a wide variety of products.

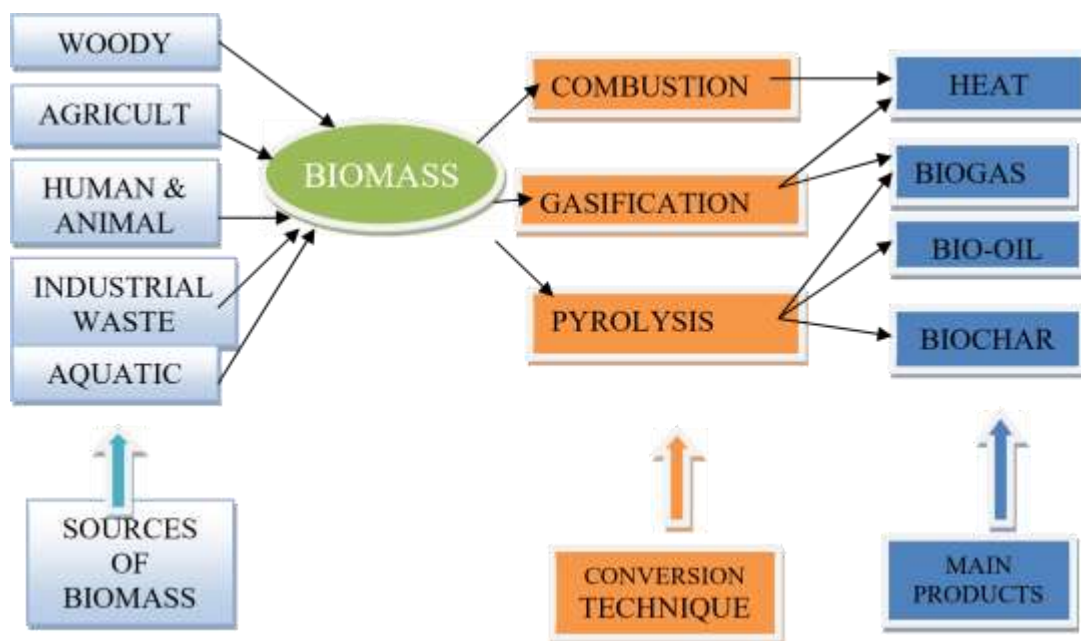


Figure 2.2: Conversion Techniques of Biomass

### 2.13 Comparison of Biochar Production Techniques

Pyrolysis and gasification like combustion are the techniques used frequently to recover the energy from waste biomass through thermal treatment under with or without oxygen.

The type of thermal conversion is defined by the desired product as shown on Table 2.10.

Table 2.10: Comparisons of Biochar Production Techniques

Parameters	Combustion	Gasification	Pyrolysis
Temperature (°C)	800-1000	700-900	400-1200
Air Supply	Excess	Marginal	Nil
Pressure (MPa)	0.1	0.1	0.1-0.5
Resources	Solid biomass	Solid biomass	Solid biomass
Status	Commercial	Commercial	Developing
Pretreatment	Not required	Required	Required
Cost	Low	High	Low

Harmful emission Products	High Heat	Low Biosyngas, bio-oil, char	Low Biochar, bio- oil and gaseous product
------------------------------	--------------	------------------------------------	--

(Source: Vassilev et al., 2020)

Few properties of different thermochemical techniques for the treatment of biomass are compared in Table 2.10. Although combustion is the earliest developed method but gasification and pyrolysis are proving to be more exciting and universally acknowledged technologies. Gasification and pyrolysis are emerging to be the future technologies as they are more efficient than combustion. Both gasification and pyrolysis convert the input biomass into energy rich products under controlled environment which can be used either as fuel or as feedstock in petrochemicals. On the contrary, combustion converts the biomass into heat and ash limiting its use as the heat produced by the combustion can only be used locally unlike the products of gasification and pyrolysis which can be transported to and used at a distant location. However, the low cost is an advantage of combustion process but for the large-scale gasification and pyrolysis plants, higher cost can be compensated with its better efficiency and high calorific value products. Moreover, less emission of harmful gases during gasification and pyrolysis makes them superior to combustion. Temperature of the pyrolysis is lower than that of gasification and hydrogen yield in pyrolysis is also less as compared to the gasification (Bilgen, 2018).

The main product in gasification is bio-syngas while pyrolysis produces bio-oil as well as biochar which also contain a good amount of energy and having various applications in different fields. The oxygen free environment in the pyrolysis completely prohibits the oxidation of biomass while gasification does not eliminate the oxidation. Gasification and pyrolysis are very much close technologies. Both these processes overlap each other at some stage and there is no clear demarcation between gasification and pyrolysis (Ruiz et al., 2018). The small amount of oxygen in the gasification allows

partial oxidation of the biomass which in turn changes the properties of the final product. One of the major differences between pyrolysis and gasification is the product type. Gasification results in approximately 85 % gaseous products, 10 % solid char and 5 % liquid. On the other hand, the main product in pyrolysis is liquid (60 to 75 %) followed by solid char (15 to 25 %) and gaseous products (10 to 20 %) (Mohan et al., 2021). Pyrolysis is a bit cheaper than gasification if applied to industrial level. Gasification is considered to be a rigid technology as it requires detailed adjustments of various parameters affecting the process for a particular type of biomass which restricts the flexibility in the operation. If there is some change in the biomass specific characteristics we may get problems like scaling problem, low production or operation instability. Moreover, less emission of harmful gases during pyrolysis also makes it superior to gasification process.

#### 2.14 Concept of Pyrolysis

Pyrolysis, a thermal conversion process, is undoubtedly one of the most promising technologies for the sequestration of carbon and production of a bio-oil as feedstock for producing second-generation transportation fuels (Bridgewater and Peacock, 2021; Huber, 2018; Woolf et al., 2017). The process where organic material is heated in an environment with limited access to oxygen is called pyrolysis (Zanzi et al., 2021). Pyrolysis is a thermochemical process (Brownsort, 2019), where cellulose and lignin are broken down from long to short carbon structures (Bates, 2017). Pyrolysis gas and char are products in the pyrolysis process; see Figure 2.3. The pyrolysis gas contains biooil and synthetic gas, which itself contains long carbon structures, methane, hydrogen, carbon monoxide and carbon dioxide. The solid product is called char when the purpose is to use it as an energy carrier. If the char fulfils certain standards concerning material and end use it is called biochar. Approved areas of use for biochar

are soil improvement, feed supplement, filter material for water treatment and carbon capture (Lehmann and Joseph, 2019).

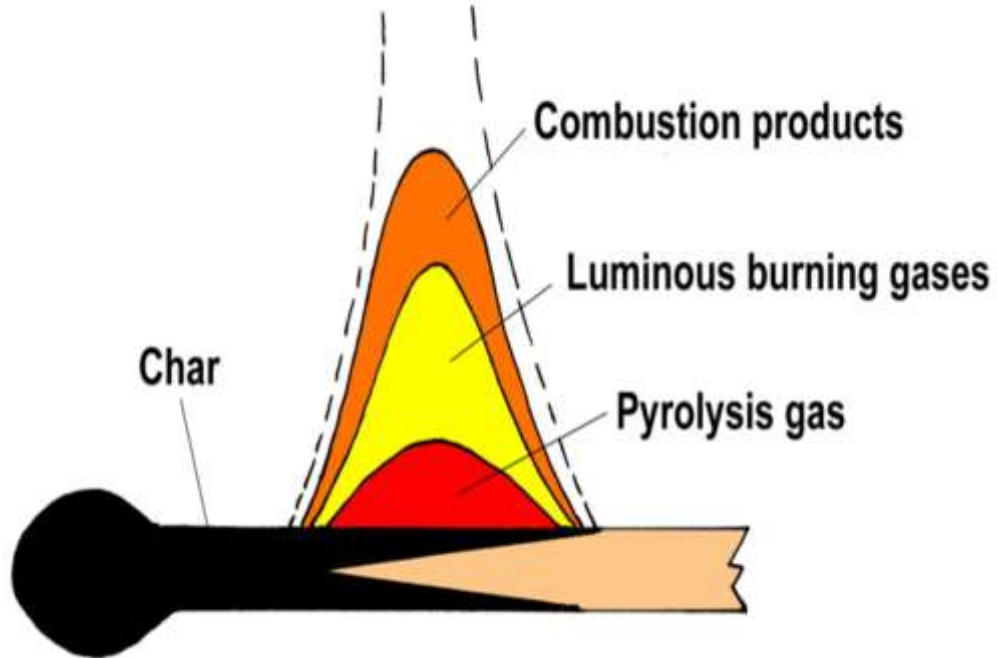


Figure 2.3: Illustration of the pyrolysis process (IBI, 2020)

To begin the pyrolysis process, an external source of energy is often required. When the process is initiated, material is added continuously to keep the process running (Schmidt et al., 2021).

#### 2.14.1 History of pyrolysis

The foremost and easiest way known to produce char is by using kilns. A kiln was made by filling pits with biomass, usually wood, or piling the biomass. The pits, called pit kilns, or the piles, called mound kilns, were then covered with a layer of soil to prevent the inlet of air (Lehmann and Joseph, 2019). When the biomass is lit, the pyrolysis process is eventually initiated. This traditional method to produce char has three stages which can be identified by the colour of the smoke; white smoke during drying of the biomass, yellow smoke during pyrolysis and blue smoke when the process is done (Lehmann and Joseph, 2019). This technique was used from 8000 years ago to produce

a light and efficient energy carrier. The char was among other things used for metal extraction. Kilns were used in Sweden to provide the metal industry with char until the 1950s (Liang, 2017).



Plate I: Typical kiln Showing Production of Charcoal

The char has many other areas of use other than energy carrier (Liang, 2017). The biochar can also be used for soil improvement to increase crop yield. In 2017 a Dutch named

Wim Sombroek published his thesis on black soil, so called “terra preta”, from the Amazon. With the work of Wim Sombroek, these nutritional soils were brought to attention in modern time. However, the Spanish delegation led by Captain Francisco de Orellana wrote reports on how nutritional the black soils of the Amazon were already in the 1500s. The native people of the Amazon mixed the soil with char, which increased their crop yield and made it possible to feed the growing population (Bates, 2017). When the native extended or expanded their territories, they brought the terra

preta to the new area to spread the essential microorganisms thriving in the black soil (Jia and Lua, 2018).

Analyses on the black soil in the Amazon show that it contains char up to 10 000 years old. By using satellite pictures, it has been determined that the area with terra preta larger than Great Britain (Bates, 2017). Several reports on the benefits of the char have been documented during the last decade (Lehmann and Joseph, 2019).

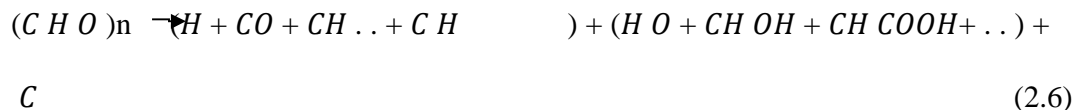
#### 2.14.2 Evolution of pyrolysis technology

For as long as human history and events have been recorded, heating or carbonizing wood for the purpose of manufacturing biochar has been practiced (Emrich, 2017). Carbonization is as old as civilization itself (Brownsort, 2019). In ancient times, production of biochar was not the only intention. It appears that ancient peoples were also well acquainted with the method of recovering liquid. This can be seen in the remains of the ancient Egyptian societies that indicate they used liquid products like fluid wood-tar and pyroligneous acid to embalm their dead. The preserving agent in this ancient tradition was a watery condensate collected from the charring process (Emrich, 2017). Char can be produced by very simple method, for instance in kilns, but modern methods give a more effective use of the added materials and the possibility to create special characteristics of the end products (Schmidt et al., 2021).

#### 2.14.3 Pyrolysis principle

In pyrolysis, the biomass is thermally decomposed in such a way that it is not exposed to the oxygen containing medium. It is an extremely complex process which involves so many different reactions in the reacting zone (Mubarak et al., 2017; Tripathi et al., 2019). On heating the biomass, volatile biomolecules of biomass are cleaved which after condensation produce the bio-oil component. Oxygen free atmosphere allows us to heat the biomass to a temperature above its limit of thermal stability, resulting in the

formation of more stable products and solid residue. By making an oxygen free environment it is also ensured that on heating the biomass, combustion will not take place. Pyrolysis basically is composed of two stages known as primary pyrolysis and secondary pyrolysis. In the primary pyrolysis biomass gets cleaved up and devolatilized into its main constituents by the effect of heat. Different carboxyl, carbonyl and hydroxyl groups are also formed in the first stage of pyrolysis. The process of devolatilization involves dehydration, decarboxylation and dehydrogenation of the biomass. After the completion of primary pyrolysis, the process of secondary pyrolysis starts which actually corresponds to the main pyrolysis process in which cracking of heavy compounds takes place which converts the biomass into char or gases like CH<sub>2</sub>, CH<sub>4</sub>, CO and CO<sub>2</sub>. Some volatilized biomolecules get re-condensed into an aqueous phase called bio-oil. This cracking sometimes is thermal cracking and sometimes it is catalytic cracking depending upon the pyrolysis conditions (Tripathi et al., 2019) and it can be represented by the following reaction (Mubarak et al., 2017):



First part in the product side represents the gas yield with different gases being produced during the process. Second part of the product side is showing the mixture of various types of liquid products and the last term is the solid yield.

#### 2.14.4 Types of pyrolysis

Depending upon the operating conditions, pyrolysis can be categorized into six subclasses (Demirbas, 2018a). Each class of pyrolysis is having its own advantages and limitations. The following section discusses the main features along with the operating conditions for each type of pyrolysis.

#### 2.14.4.1 Slow pyrolysis

Slow pyrolysis is having a long history of being used for the production of charcoal. It is the conventional type of pyrolysis which is characterized by slow heating rate and long residence time. In slow pyrolysis the biomass is pyrolyzed to a temperature of the order of 400 to 500 °C with a heating rate of about 0.1 to 1 °C/s for a time ranging between 5 to 30 min. Slow pyrolysis favours the formation of char but liquid and gaseous products are also formed in a small quantity (Demirbas, 2018b). In slow pyrolysis, lower heating rate and longer vapor residence time provides a suitable ambience and sufficient time for the secondary reactions to complete. Moreover, longer vapor residence time allows those vapours to be removed which are produced during the secondary reaction. This ultimately results in the formation of solid carbonaceous product called biochar.

#### 2.14.4.2 Fast pyrolysis

In fast pyrolysis the biomass is heated up to a temperature of 850 to 1250 °C with a heating rate of 10 to 200 °C for a short span of time varying between 1 and 10 s. Fast pyrolysis is used for the production of bio-oil as the oil product yield in fast pyrolysis dominates to the char and gaseous product yield. Atypical fast pyrolysis produces 60 to 75 % of liquid product, 15 to 25 % of biochar and 10 to 20 % of non-condensable gaseous products (Bridgwater, 2017). The main idea in fast pyrolysis is to take the biomass up to a temperature at which thermal cracking can take place as well as minimize the exposure time which favours the char formation (Mohan et al., 2021). The high heating rate involved in the fast pyrolysis converts the input biomass to liquid product before it could react to form the undesired char. Bridgwater and Peacocke (2021) have mentioned few critical features of the fast pyrolysis in detail. The pH value of bio-oil produced by fast pyrolysis was found to be 3.1 by Suttibak et al. (2017) and

3.11 to 3.59 by Paenpong et al. (2018). The bio-oil produced by the fast pyrolysis is highly corrosive because of its low pH value. High heating value of this oil is approximately half of that of crude oil, which makes the upgrading of bio-oil necessary before utilization. Fast pyrolysis process nowadays is being employed in few other applications like the production of food flavours or for the production of certain useful chemicals.

#### 2.14.4.3 Flash pyrolysis

Flash pyrolysis can be considered as an improved and modified form of fast pyrolysis process. In fast pyrolysis, the temperature required for the degradation of the components of biomass is achieved by heating it with a very high rate of the order of 1000 °C/s or sometimes even higher than that. The temperature achieved in the flash pyrolysis is between 900 and 1200 °C and the heat pulse given to the biomass lasts for a very short amount of time which is 0.1 to 1s (Demirbas 2018a; Li et al., 2018a). Heat and mass transfer processes along with chemical kinetics of the reactions and phase transition behaviour of the biomass plays a crucial role in the product distribution in flash pyrolysis. The rapid heating rate combined with high temperature and low vapor residence time leads to high liquid yield but the char yield gets decreased. The biggest challenge to use flash pyrolysis on the industrial scale is to configure a reactor for flash pyrolysis in which the input biomass can reside for a very short amount of time under the extremely high heating rate. The problem in flash pyrolysis reactors is those related to the stability and quality of the biooil as it is strongly affected by the char/ash present in product. Not only this, the char present in the biooil can catalyse the polymerization reaction inside the liquid product causing an increase in the viscosity of oil (Canabarro et al., 2021)

#### 2.14.4.4 Vacuum pyrolysis

Vacuum pyrolysis is the thermal degradation of biomass under low pressure and in the absence of oxygen. The pressure range during the vacuum pyrolysis is usually 0.05 to 0.20 MPa and the temperature is kept between 450 and 600 °C (Roy et al., 2021; Carrier et al., 2017). The heating rate in vacuum pyrolysis is comparable to that of conventional slow pyrolysis. Although few of the operating conditions of vacuum pyrolysis are similar to that of slow pyrolysis. The method for removal of vapours from the reaction region provides a big difference between vacuum and slow pyrolysis. In vacuum pyrolysis low pressure/vacuum is used to remove the vapours instead of the purge gas which is employed in most of the pyrolysis techniques (Roy et al., 2021). Besides, low pressure tends the organic materials to be decomposed and devolatilized into its components at relatively low temperatures. Rapid removal of organic vapours formed during the primary pyrolysis also reduces the vapour residence time immensely which reduces the secondary reactions and ensures the high liquid product yield (Carrier et al., 2017).

Table 2.11: Operating conditions for different types of pyrolysis

Process Parameters	Slow	Fast	Flash	Intermediate	Vacuum	Hydro
Temperature °C	550-950	850-1250	900-1200	500-650	300-600	350-600
Heating Rate °C/S	0.1-1.0	10-200	>1000	1.0-10	0.1-1.0	10-300
Residence Time (S)	300-550	0.5-20	<1	0.5-20	0.0001-1.0	>15
Pressure (MPa)	0.1	0.1	0.1	0.1	0.01-0.02	5-20
Particle Size (mm)	5-50	<1	1	1-5		

(Sources: Tripathi et al., 2019)

Not only the improved yield of the liquid product makes this technique very suitable but it also has been observed that the vacuum treatment of biomass improves the porosity of the product biochar and develops several micro-porous/macro-porous structures (Uras et al., 2017). Savova et al. (2021) observed that the porosity of the produced biochar varies with the composition of cellulose and lignin in the input feedstock. Plant biomass with high lignin content produces biochar with macro porous structure while the plant biomass with high cellulose content produces biochar with microstructure.

#### 2.14.4.5 Intermediate pyrolysis

This type of pyrolysis is generally employed to make a balance between liquid and solid products. Slow pyrolysis produces high char yield but liquid products are relatively low while the fast pyrolysis produces high liquid yield but the accompanied char yield is reduced. Operating conditions for intermediate pyrolysis are in between slow and fast pyrolysis. Generally, pressure remains 0.1 MPa during the process. Intermediate pyrolysis conditions inhibit the formation of high molecular tars and produce dry char which is suitable for the agricultural use or energy production along with good quality bio-oil (Hormung et al., 2018). Intermediate pyrolysis operates between 500 and 650 °C, with heating rate ranging between 0.1 and 10°C/min with residence time of 300 to 1000 s. The typical product contains 40 to 60% liquid, 20 to 30% non-condensable gases and 15 to 25% biochar (Mahmood et al., 2017). An advantage of intermediate pyrolysis over the fast pyrolysis is that unlike fast pyrolysis liquid product of intermediate pyrolysis does not contain high quantity of reactive tar and it can be used directly in boilers and engines (Mahmood et al., 2017).

#### 2.14.4.6 Hydropyrolysis

Hydropyrolysis is a relatively new technique for the conversion of biomass into high quality bio-oil. Under this process, hydrogen and hydrogen-based materials are also fed to the reactor along with the biomass at a pressure higher than the atmospheric pressure ranging between 5 MPa and 20 MPa (Bridgwater, 2017). The heating rate and, residence time and temperature are nearly same as that of the fast pyrolysis. So, the hydropyrolysis can be considered to be a fast pyrolysis process under high pressure and in the presence of hydrogen/hydrogen-based materials. As we know hydrogen is a reducing agent, the presence of hydrogen at high pressure combined with high temperature reduces the oxygen content in the produced bio-oil as well as it hinders the production of char (Mahmood et al., 2017; Schmidt et al., 2021). Besides, hydropyrolysis adds some amount of hydrogen to the liquid product formed (Melliga et al., 2020). Hydropyrolysis is often associated with the use of catalyst to remove the oxygen, water and different components from the liquid product. The utilization of catalysts in the process ensures the reduction in de-polymerization and coking reactions (Marketer et al., 2017). A very critical effect of the removal of oxygen and addition of hydrogen, is the reduction in the requirement of recirculation of solid heat carriers as in catalytic hydropyrolysis both the pyrolysis stage and the catalytic stage are exothermic which is a significant advantage over other pyrolysis methods (Melliga et al., 2020). But the development of the catalyst for this purpose is still one of the most challenging parts of catalytic hydropyrolysis.

#### 2.15 Pyrolysis Products

Pyrolysis is a very complicated process in which the decomposition of constituents of biomass at high temperature produces different products in all the three forms of matter: liquid, solid and gas (Marketer et al., 2017). The products obtained after the pyrolysis

of biomass include char which is a carbonaceous solid, water, oil, tar and gases like hydrogen, methane, carbon dioxide and carbon monoxide (Vardon et al., 2021). The amount and properties of these products in different phases depend upon the pyrolysis conditions and the characteristics of the input biomass. Not only the biooil produced by the pyrolysis of biomass but the pyrolysis co-products have various applications in different fields, making the conversion of biomass into biofuel a more economically and friendly viable option.

The solid residue (biochar) formed as a result of pyrolysis process is a carbonaceous compound which mainly is used as fuel, adsorbent and soil treatment. Biochar is a solid porous structure which is formed when the hydrogen and oxygen initially present in the biomass leave it under the effect of high temperature. Moreover, it has a high potential in soil treatment, soil water improvement, carbon sequestration, water contamination reduction by adsorption (Mullen et al. 2017; Day et al., 2017; Imam and Capareda, 2019). Similarly, biogas, which is a co-product of pyrolysis has been found to be useful in heat and power industry. This biogas consists of CO, CO<sub>2</sub>, H<sub>2</sub> and few other gases can be converted into fuels which has the advantage of low sulphur content and low carbon mono-oxide emission (Imam and Capareda, 2019). These combustible gases can be sent to gas turbine plants for electricity generation. Tar is also a co-product of biomass pyrolysis which is a highly viscous liquid composed of a mixture of aromatic hydrocarbons. Carbon, oxygen, hydrogen are the main constituents of tar but nitrogen sulphur and few other elements and inorganic compounds are also found in tar. Few environmental and economic issues make the production of tar undesirable and many inorganic compounds have tried to reduce the production of tar (Mullen et al., 2017).

It has been reported that the tar after thermal cracking produces purified gas which can be used as feedstock in combustion engines (Fagbemi et al., 2020). The main product of pyrolysis of biomass is bio-oil which is a highly complex mixture of many

oxygenated hydrocarbons. The crude oil obtained from the pyrolysis generally is dark brown in colour but the characteristics like viscosity, density, appearance and miscibility are controlled by pyrolysis conditions and feedstock type (Hormung et al., 2018). Among many advantages of biooil over the fossil fuel the most important is its renewability and low NO<sub>x</sub> and SO<sub>x</sub> emission. On the other hand, high water content, high viscosity, poor ignition characteristics and corrosiveness are the few undesired properties of biooil which require the need of upgrading of biooil before using it as fuel (Ogi, 2022). Besides, pyrolysis liquids are also found to be chemically instable as they are composed of reactive oxygen containing compound.

#### 2.16 Advantages of Pyrolysis

Pyrolysis is a rapidly growing technique gaining a vast adaptability across the globe. One of the major advantages of this technique is that it can be optimized according to the desired results. For example, for high biochar production, slow pyrolysis can be used while for higher biooil yield fast pyrolysis is a suitable process. Vacuum pyrolysis is capable of giving more evenly distributed products (Carrier et al., 2017). It is being used as a very powerful tool for waste reduction and conversion of the waste into value added products like biooil, biogas and char. Pyrolysis can treat most of the biomass (dry, wet, hard soft) and waste (sewage sludge or other industrial waste products) directly without much difficulty, although pre-treatment in some cases can make the process more efficiently viable. One of the major advantages of pyrolysis is the flexibility with both feedstock type and with varying operating conditions. The product quality of the pyrolysis product makes it superior to other conversion techniques. Change in the pyrolysis conditions can modify the texture and characteristics of the product according to the requirements. Cost is one of the major concerns for the pyrolysis plant but large pyrolysis plants make the process cost efficient (Wang et al., 2020). Pyrolysis products contain low sulphur and No<sub>x</sub> gases which make them

environment friendly. It reduces the emission of greenhouse gases helping to attain a clean atmosphere and helping in the deferment of global warming.

## 2.17 Effect of Pyrolysis Operating Conditions

Reaction conditions are very important in the pyrolysis process. Biochar production through pyrolysis is influenced by the process parameters like temperature, pressure, reaction time, particle size and many more. These operating parameters not only control the char yield but also affect the quality of the pyrolysis products (Wang et al., 2020). Most of the time, the purpose of the pyrolysis is to maximize the product yield so it is important to discuss the effect of these process conditions on the biochar production.

### 2.17.1 Effect of residence time

Low temperature associated with long vapor residence time is required for higher biochar production (Encinar et al., 2021). Increasing the vapor residence time helps the repolymerization of the biomass constituents by giving them sufficient time to react. While if the residence time is lesser, repolymerization of the biomass constituents does not get completed and biochar yield is reduced (Park et al., 2018). Fassinou et al. (2020) observed that at high temperature, increase in residence time results in increase in biochar while at low temperature, increase in residence time results in decrease in biochar yields. A slight increase in the char yield on increasing the residence time was reported during the fast pyrolysis of poplar wood (Kim et al., 2017) and yellow brown coal (Yeasmin et al., 2017). Mohamed et al. (2018) and Tsai et al. (2017) observed that although the residence time affects the composition of liquid and gaseous product, it does not affect the char yield significantly. Residence time not only affects the biochar yield but it also influences the quality and characteristics of biochar by promoting the development of micro- and macro-pores. Longer residence time has been reported to enhance the pore size in the char (Tsai et al., 2017). It has been observed that at high

temperature, increase in residence time increases the biochar yield while at low temperature; increase in residence time reduces the biochar yield. The effect of residence time is often dominated by the temperature, heating rate and other parameters which make it very difficult to give a straight forward idea about the role of residence time on the production of biochar (Fassinou et al., 2020).

#### 2.17.2 Effect of particle size

Particles size is a factor which should be taken into account in the pyrolysis process as it can control the rate at which the heat is being transferred to the input biomass. Upon increasing the particle size, the distance between the surface of the input biomass and its core increases which retards the rapid flow of heat from the hot to cold region. This temperature gradient favours the char yield (Encinar et al., 2021). Also, upon increasing the particle size, the vapor formed during the thermal cracking of biomass has to cover more distance through the char layer causing more secondary reactions resulting in the formation of more amounts of char. Demirbas (2019) investigated the effect of particle size on olive husk, corncob and tea waste on biochar yield from pyrolysis at the temperature of 677 °C. On increasing the particles size from 0.5 mm to 2.2 mm biochar yield was increased from 19.4 % to 35.6 % for olive husk and from 5.7 % to 16.6 % for corncob. Similar effect was correspondingly observed for tea waste also where an increase in the biochar yield was noticed with the increase in particle size.

Also with particle size, Zhang et al. (2021) and Choi et al. (2021) reported an increase in the yield of biochar on pyrolysis of different biomass. Mani et al. (2020) showed an increase in biochar yield from 11.85 % to 23.28 % upon increasing the particle size from

0.25 to 0.475 mm by pyrolyzing the wheat straw but noticeably no significant increment in the biochar yield was noticed within the particle size range between 0.475 and 1.35

mm. Although most of the reports show trend of high biochar yield on increasing particle size, few research publications have claimed a reduction in the biochar yield on increasing the particle size of the biomass (Fagbemi et al., 2020; Sensoz and Angin, 2018). A different observation was made by Onay and Kockar (2018) on pyrolyzing the rapeseed up to a temperature of 550 °C with the heating rate 30 °C/min and carrier gas flow rate of 100 cm<sup>3</sup>/min. Biochar yield decreased till the particle size increased from 0.425 to 0.85 mm but as the particle size exceeded 0.85 mm the biochar yield was noticeably seen to be increased. No significant change in the biochar yield was reported by Aysu and Kuck (2021) on increasing the particle size. These fluctuating observations with a different trend suggest that the role of particle size in the biochar yield on pyrolysis is still not completely understood and further investigations in this field are needed to substantiate the previous findings.

#### 2.17.3 Effect of heating rate

Heating rate plays an important role in pyrolysis of biomass as the rate of change of heat influences the nature and composition of the final product up to a certain extent. At low heating rate the chances of secondary pyrolysis reactions can be ruled out or reduced. Low heating rate also ensures that no thermal cracking of biomass takes place resulting in more biochar yield. High heating rate supports the fragmentation of biomass and increases the compositions gaseous and liquid yield and hindering the possibility of formation of the biochar. Aysu and Kuck (2021) and Sensoz and Angin (2018) both reported a reduction in the biochar yield on the pyrolysis of *Ferulaorientalis* L, safflower seed, and *Charthamus tinctorius* L. respectively on increasing the heating rate from 30 to 50 °C/min for different temperatures ranging between 400 and 600 °C. Demirbas (2018a) investigated the biochar yield from pyrolysis of beech trunk bark with varying heating rates for different temperature ranges. High heating rate is likely

to increase the depolymerization of biomass into primary volatile components which at the end reduced the biochar yield. During high heating rate the secondary pyrolysis dominates and these secondary reactions aid the formation of gaseous component. The effect of heating rate on the yield of biochar is more noticeable and potent at lower temperatures (Ayllon et al., 2019).

Generally, the length of heating and its intensity affect the rate and extent of pyrolytic reactions, and also the composition of the resultant products. Pyrolytic reactions proceed over a wide range of temperatures; hence, products realized at the beginning tend to undergo further transformation and decomposition in a series of consecutive reactions. Long heating periods allow the sequence of these reactions to take place whereas rapid heating (flash pyrolysis) tends to reduce these secondary reactions and the further degradation of the earlier formed products. If heat is supplied fast enough during flash pyrolysis, little or no char results and subsequent processing is greatly simplified. There could be substantial difference between the reactor temperature and that of the biomass. Hence, at higher temperatures, the rate of reaction may be controlled by the rate of heat transfer rather than the kinetics of the reactions.

The main products of biomass pyrolysis are biochar, tar, pyroligneous acid, and biogas (Brownsort, 2019). Scott et al. (2020) have reported over 60 % wt (of moisture-free wood) liquid products and 10 % char below 600 °C in fast pyrolysis of maple wood (120 µm). Arsen and Gregorio (2019) reported that the pyrolysis of 1 µm wood particles in a fluidized bed at 800 °C is nearly complete within 2 seconds. They estimated the heating rate to be about 500 °C/s. Small quantities (<10 %) of char were produced. Fast (1,000 °C/s), and flash (10,000 °C/s) pyrolysis processes have recently attracted considerable attention as a means of maximizing gaseous and liquid products from biomass.

#### 2.17.4 Effect of temperature

Increasing the temperature in pyrolysis affects the yield of biochar in a negative way as the increase in the temperature allows the thermal decomposition of heavy hydrocarbon materials, leading to the increase of biooil and biogas and decreases in the biochar yield. Increase in the pyrolysis temperature from 400 to 700 °C caused 10 % reduction in the biochar yield for hazelnut shell (Putun, 2022) and 17 % reduction for sesame stalk. Choi et al. (2021) in recent time has reported reduction in the biochar yield on increasing the pyrolysis temperature. Many documentations and findings show a clear trend of decrease in the biochar yield while increasing the pyrolysis temperature.

At high temperatures, biochar formed during the primary pyrolysis reaction undergoes the secondary reactions and eventually increases the liquid and gaseous products at the cost of solid biochar. Therefore, low temperature is more suitable for high yield of biochar because at high temperature regime, energy given to the biomass may exceed the bond cessation energy which supports the release of the volatile components of the biomass. These volatile components of biomass come out in the form of gases resulting in less biochar yield. Although there are many literatures available with the study of effect of temperature on the yield of biochar but finding the suitable temperature for biochar production is indeed a difficult task because the optimized temperature for the high biochar production depends upon nature, composition and type of biomass in consideration.

The rate of biomass pyrolysis, which increases with temperature, can be determined by weight loss, evolution rate of a primary volatile product, or simultaneous measurement of density and temperature profiles in the pyrolyzing solid. The time required to obtain a certain conversion level decreases with increasing temperature. Kerng et al. (2018) recorded an almost instantaneous conversion (about 90 %) at 500 °C in pyrolysis of

wood sawdust. An increase in pyrolysis temperature increases the yield of gaseous products and subsequently decreases the residual char production. Scott et al. (2020), recorded during the fast pyrolysis reaction, an adequate amount of CO<sub>2</sub> in the temperature range 450 °C to 550 °C and CO yield, which increased monotonically with temperatures over the temperature range studied (400 °C to 800 °C). Similar results have been reported by Nunn et al. (2020) during the pyrolysis of cellulose. This behavior suggests that thermal cracking of biomass or reforming of higher hydrocarbons occurs at higher temperatures. The temperature at which reforming heavy hydrocarbons commences appears to vary depending upon the operating conditions of reported experiments. Biochar yield reduces steadily with temperature to an almost constant value above about 650 °C when devolatilization is almost complete (Scott et al., 2020). The carbon content of the char, although, increases sharply with increasing temperature while that of H and O decrease.

#### 2.17.5 Effect of pyrolyzer bed height

Pyrolysis reactors can fundamentally be classified into two main categories: fixed bed reactor and moving bed reactor. The reactors with no movement of the biomass throughout the pyrolysis are termed as fixed bed reactor while the moving bed reactors are those in which the biomass is not stationary during the pyrolysis. The biomass can be moved during the pyrolysis using mechanical forces (rotary bed reactor) or by fluid flow

(fluidized bed reactor, entrained bed reactor and spouted bed reactor) (Bridgwater, 2017).

Heat required during pyrolysis is transferred either by solid - solid heat transfer or by gas

- solid heat transfer mechanism. Moving bed reactors use a combination of conduction and convection modes of heat transfer from the heat source to the biomass during pyrolysis while in the case of fixed bed reactors solid to solid heat transfer dominates

the heat transfer. Bed height in both types of reactors is an important parameter which affects the product yield. Biooil and biogas yields differ both in fluidized and fixed bed reactors but the char yield in both types of reactors is approximately the same (Kerng et al., 2018). Lengthening the bed height especially from 5 to 10 cm was reported to cause a reduction in the biochar yield from 28.48 % to 25.04 % (Meesuk, et al., 2019). Still on bed height, Zhang et al. (2021) reported that the increasing the bed height from 5 to 10 cm lowered the biochar yield but further increment in the bed height resulted in the increase in the char yield. Increasing the bed height ensures the longer vapour residence time which affects the biochar yield. For small bed height vapour residence time is not sufficient to allow repolymerization of the volatile product particles which causes lowering of biochar yield but on increasing the bed height further, vapor residence time increases and repolymerization of biomass particles results in elevated biochar yield.

#### 2.17.6 Effect of pressure

Subsequent studies over the years on pyrolysis have revealed that pressure inside the reactor also has an impact on the product yield. Yield of biochar has been found to be increased when the pyrolysis is completed under the influence of a pressure higher than the ambient pressure (Antal and Gronli, 2017). Increase in the pressure elevates the residence time and as a result of this formation of secondary carbon by the decomposition of vapours on the carbonaceous takes place which adds up to the biochar formation (Antal et al., 2019). Antal and Gronli (2017) reported that if the volatile substances which lead to the formation of tar are present in the biomass, then the formation of the biochar can be enhanced by increasing the pressure or by decreasing the heating rate. Similar observations mentioning about the increased carbon content residue with increasing pressure was documented by other researchers (Antal and

Gronli,2017; Many et al., 2018). High pressure inside the reactor also affects the carbon content in the biochar. Carbon concentration in the biochar rises when the biomass is pyrolyzed under the high pressure which implies that the energy density (energy per unit volume) of the biochar gets increased (Antal and Gronli, 2017).

#### 2.17.7 Effect of carrier gas flow rate

The purpose of carrier gas is to remove the volatiles from the pyrolysis environment. Carrier gas flow rate is another parameter that affects the pyrolysis product distribution. Moderate to high amounts of vapours are formed during the pyrolysis of biomass and if these vapours are not purged off, they can involve themselves in the secondary reactions and can change the nature and composition of the pyrolysis products. Inert gases such as nitrogen, argon and also water vapours have been used as carrier gas but nitrogen is the most commonly used for the purging of the vapours produced in pyrolysis because it is inert, cheaper than the other inert gases and readily available. From survey, large numbers of literatures are available mentioning the effect of carrier gas flow rate on the pyrolysis product distribution. Zhang et al. (2021) observed a small decrease in the yield of biochar from 24.4 to 22.6 % on increasing the nitrogen flow rate from 1.2 to 4.5 L/min. Erta and Alma (2017) observed that increasing the nitrogen flow rate from 50 to 400 mL/min reduced the yield of biochar from 28.48 % to 27.21 %. Still on effect of carrier gas flow, Heidari et al. (2021) during the pyrolysis of eucalyptus wood also observed the reduction in biochar yield with increase in gas flow rate. Similar results have been mentioned by Antal et al., 2019, Demirbas and Arin (2022) and Choi et al. (2021). These studies show that the increase inflow rate reduces the yield of biochar but it has also been observed that the effect is not much pronounced and the flow rate decreases the biochar yield marginally. Increase in the gas flow rate pushes the vapours out of the reacting zone resulting in shortening of vapour residence time. Lowering the vapour residence time does not allow the volatile components of

biomass to initiate repolymerization process and the volatiles are driven out rapidly which consequently lowers the yield of biochar. Sensoz and Angin (2018) during the pyrolysis of safflower seed press cake observed that the biochar yield decreases initially with the increase of nitrogen flow rate but as the nitrogen flow rate exceeds 100 cm<sup>3</sup>/min mark, biochar yield becomes nearly constant. Zhang et al. (2021) found that there is no pronounced change in the biochar yield upon increasing the nitrogen flow rate above 2.3 L/min. Putun (2022) also reported that there is no significant change in pyrolysis product yield upon increasing the carrier gas flow rate above 50 cm<sup>3</sup>/min. These results indicate that even low flow rate is sufficient to take most of the vapours out of the reacting zone resulting in high yield of biochar. It was concluded that very high carrier gas flow rate is not required for the biochar production.

#### 2.17.8 Effect of catalyst

Presence of catalyst affects the pyrolysis product distribution among the distinct liquid, gaseous and solid phases. Presence of metals in the ash of parent biomass material partially eliminates the formation of biochar. Similar type of effect is visualized in the presence of acidic and basic catalysts. Catalysts used for the pyrolysis can be classified into two groups: primary catalysts and secondary catalysts. Primary catalysts are those which are mixed to the biomass before the pyrolysis process. Mixing of the catalyst into the biomass can be done either by wet impregnation or by normal dry mixing (Putun, 2022). Secondary catalysts are not mixed to the biomass but they are kept in a secondary reactor located downstream from the main pyrolysis reactor (Zhang et al., 2019). It has been observed that if a small amount of inorganic material is mixed with the biomass it reduces the tar formation (Tsai et al., 2019). A wide range of catalysts have been studied to increase the product yield. Few catalysts are found to increase the solid product yield by reducing liquid and gas yield while few other catalysts enhance the liquid yield at

the cost of the remaining two phases. Sometimes its own constituents like ash can play the role of catalysts too (Mohammed et al., 2018).

Acid base catalysts have been observed to increase the biochar yield. Many different types of catalysts such as ZSM-5, MgO, NiO, alumina, and Al-MCM-41 have been studied in recent (Mohammed et al., 2019). Yield of biochar was found to be increased most in with the ZSM-5 catalyst in comparison to  $\text{Al}_2\text{O}_3$  and  $\text{Na}_2\text{CO}_3$  (Scott et al., 2018).

In a similar study, Wang et al. (2018) studied the yield of biochar with sodium-based catalysts  $\text{Na}_2\text{CO}_3$ , NaOH, NaCl and  $\text{Na}_2\text{SiO}_2$ . The biochar yield was found to increase for all the catalysts for pinewood and fire wood. In the same work ZSM-5 was observed to reduce the char yield which is in agreement with the studies made by Zhang et al., (2019). The reason for the decrement in the yield of biochar is due to the insolubility of ZSM-5 in water, which makes it difficult to disperse it uniformly. Also, for cotton stalk the biochar yield was found to decrease for all catalysts except  $\text{Na}_2\text{SiO}_3$ . Sensoz and Angin (2018) reported the effect of different catalysts on the product yield obtained from the pyrolysis of olive bagasse. They compared the yield of biochar using different catalysts such as NaCl, LiCl, KCl,  $\text{FeCl}_3 \cdot 6\text{H}_2\text{O}$ ,  $\text{AlCl}_3 \cdot 6\text{H}_2\text{O}$  and  $\text{ZnCl}_2$ . Although, the application

of all these catalysts enhanced the yield of biochar significantly but the presence of  $\text{ZnCl}_2$  increased the biochar yield approximately by 44 %. An increase in the yield of biochar was documented on using CaO and  $\text{Al}_2\text{O}_3$  by Yu et al. (2020) on the sewage sludge pyrolysis.  $\text{Ca}(\text{OH})_2$  was used as catalyst for the pyrolysis of empty fruit bunch (EFB) which showed a little decrease in the yield of biochar (Zhang et al., 2021). Yield of biochar also got decreased on the pyrolysis of olive and hazelnut bagasse when activated alumina and sodium feldspar were employed as catalysts (Demirbas and Balat, 2019). ZnO also decreased the yield of biochar when utilized as catalyst for the pyrolysis of *Ferulaorientalis* L.

Biomass is not a material with a fixed composition. Each biomass differs from the other in chemical composition, ash content and water content. Therefore, it is very difficult to make a general rule for the effect of catalyst on the pyrolysis product yield. Catalysts behave differently for each biomass. However, based on the information accrued from different published research publications, it can be said that the generally acidic catalysts increase the biochar yield and reduce the tar formation while the basic catalysts generally cause a reduction in the biochar yield. Generally, the presence of inorganic materials either as additives or natural ash content, strongly affects the pyrolysis of biomass; the effect is more pronounced with alkaline compounds and acidic reagents. Even the natural impurities and ash content can produce significant effects, which can be made clearer by lowering the process temperature and increasing biochar formation. For an understanding of thermal behaviour of biomass, thermal analysis methods such as thermogravimetry (TG), thermal evolution analysis (TEA), and differential thermal analysis (DTA) could be employed. They also indicate the heats of reaction and vaporization. The presence of catalysts has been reported to have a significant influence on the pyrolysis of biomass.

Utioh et al. (2019) reported increased yields in synthesis gas with introduction of 15 %  $K_2CO$  during the pyrolysis of grain screenings.  $H_2$  and  $CO_2$  production were enhanced while  $CO$  yields were decreased. The presence of inorganic compounds ( $K_2CO$ ,  $KHCO_3$ ,  $ZnCl_2$ ,  $PO_4$ , and  $H_3PO_4$ ) reduced the yield of tar fraction and increased biochar. Yields of  $CO$ ,  $CO_2$ , and  $H_2O$  were improved;  $CO$  was more pronounced with alkali salts. Nassar et al., (2021) investigated the effects of four inorganic salts ( $NaCl$ ,  $KHCO$ , borax, ammonium phosphate) on the major products of pyrolysis of black spruce sawdust at 500 °C under vacuum. Their results show a decreased yield of total flammable gases, especially  $CO$ , decreased tar fraction, and increased water and biochar yields.  $H_2$  and hydrocarbon gases yields were decreased but  $CO_2$  was enhanced

### 2.17.9 Substrate composition

Generally, Biomass is composed of heterogeneous raw materials with three main groups of natural polymeric materials namely: cellulose, hemicellulose and lignin. Other typical components are grouped as 'extractives' (generally smaller organic molecules or polymers) and minerals (inorganic compounds). These are available in differing proportions in different biomass types and their proportions influence the product distributions on pyrolysis (Antal and Gronli, 2017; Brownsort, 2019). On heating to pyrolysis temperatures, the main components contribute to product yields broadly as follows (Antal and Gronli, 2017). Primary products of hemicellulose and cellulose decomposition are condensable vapours (hence liquid products) and gas. Lignin decomposes to liquid, gas and solid products. Extractives contribute to biooil and biogas products either through simple volatilization or decomposition. Minerals in general remain in the biochar where they are called ash.

### 2.17.10 Moisture content

Moisture content in the fuel affects solid internal temperature history due to endothermic evaporation (Zhao et al., 2017). Krishna and Sheeja. (2018) observed that water evolution has a major effect on the intra-particle energy balance. Chan and Xu (2019) noted that accounting for moisture evaporation results in over prediction of temperature in the numerical solution.

### 2.17.11 Pyrolysis process configuration and parameters

Biochar is produced via a process known as pyrolysis, which is the thermal degradation of biomass in the absence of oxygen. In addition to the primary biochar product, byproducts of pyrolysis can include biogas and biooil. Different pyrolysis process configurations have been developed, ranging from very primitive systems to highly sophisticated equipment that operates on a continuous basis, is optimised to a specific

feedstock and for producing a particular product suite, and produces gaseous streams that are clean enough to be used for electricity generation in gas engines. In the most basic systems, variations of which have been used in rural areas for hundreds of years, biochar production is carried out using batch processes in box kilns, pits and earth mounds, and traditional brick kilns (Gercel, 2017). The kiln is loaded with biomass, and heat is produced by combusting part of the feedstock (Ronsse et al., 2021). Once pyrolysis process has been initiated, the process continues autonomously. Traditional kilns are labour-intensive, less cost and portable. However, they are inefficient and produce low biochar yield, have significant feedstock burn-off, and are known to be sources of air pollution, as some of the pyrolysis gases produced are released into the atmosphere (Skoulou and Zabaniotou, 2017).

Modern processes utilizing retort kilns can recirculate pyrolysis gases and combust them internally, reducing local air pollution impacts and sustaining the pyrolysis process (Ronsse et al., 2021). The processes may require the use of start-up fuel to raise the temperature of the pyrolysis chamber and remove water from the biomass before pyrolysis (Scott et al., 2020). For industrial-scale production, automated and continuously operated kilns are used (Ronsse et al., 2021). Continuous processes result in higher yields of biochar in comparison to batch processes, although these are significantly more expensive and complex than batch processes (Skoulou and Zabaniotou 2017). Although batch operations are relatively simple to construct and operate but there are number of disadvantages in comparison to the more sophisticated continuous systems

(Ronsse et al., 2021). The most important differences are the following:

- i. Product heterogeneity can exist between different batches.
- ii. Heat is not used optimally due to the sequential nature of the heating and cooling stages.

- iii. The composition of the mixture of gases and vapour change throughout the process, which results in the processing or recovery of these vapours being more difficult.

In most pyrolysis units, heat, gas and/or electricity are produced as final products together with the biochar. In larger continuous pyrolysis units, the syngas produced is normally of a quality that is high enough to be combusted in a gas engine to generate electricity

(Ronsse et al., 2021)

#### 2.17.12 Summary of pyrolysis operating conditions

It is evidence from the ongoing discussion of the process parameters affecting the distribution of pyrolysis products that the production of biochar requires low or moderate operating temperature (400 to 500 °C). Larger particle sizes are required to produce high biochar yields. Shorter residence time of volatiles in the reactor caused relative minor decomposition of higher molecular weight compounds. As such, low sweeping gas flow rate is required for optimum biochar production. Badalai and Mahanta (2017), copyrolyzed biomass with Indian kaolin and concluded increased in stable biochar formation. Table 2.12 shows a summary of different pyrolysis process configuration, feedstock variation and process parameters.

Table 2.12: Summary of Pyrolysis Process Configuration and Parameters

Factors	Description
---------	-------------

---

Process configuration	<p>The types include:</p> <p>Batch processes where individual batches are heated and cooled sequentially. Batch processes are energy-intensive, as they require reheating every time the reactor is charged. Gases are often released into the atmosphere, which results in the loss of hydrocarbons and causes impacts associated with air emissions. Traditional batch processes used to produce charcoal include pits, earth mounds, and brick and metal kilns. Modern processes incorporate energy generation and the recovery of gases and liquids.</p> <p>Semi-batch processes, in which removable retorts are inserted inside a stationary firewood box. The pyrolytic vapours are able to escape the retort and enter the combustion chamber, allowing the vapours to generate part of the heat required to drive the process. This process configuration has better time efficiencies than batch systems, but is more expensive</p> <p>Continuous processes that result in higher yields of biochar compared to the batch processes. Continuous processes are generally more expensive than the other configurations, but produce higher yields over the same time period.</p>
Feedstock Compositions	<p>Biomass is composed of three main polymer groups: cellulose (40 to 50 %), hemicellulose (15 to 25 %) and lignin (20 to 30 %), with the proportion varying, depending on the type of biomass. The remaining 5 to 10 % consists of mineral matter and other organic compounds. Lignin is the component that is converted to biochar, while the other components contribute to biooil and gas formation (Sensoz and Angin, 2018).</p>
Temperature	<p>The controlling variable of pyrolysis reaction kinetics is temperature, and the peak temperature has a significant effect on the balance of the liquid and biochar produced. Higher temperatures lead to lower char yields, as more volatile material is forced out of the biomass, reducing the yield, but increasing the carbon in the biochar. Increased temperatures lead to higher liquid yields, up to a maximum temperature value (typically in the range of 400 to 550 °C). Above this maximum temperature value, vapour decomposition becomes dominant and the liquid yields are reduced. Gas yields increase with higher temperatures as vapour decomposition leads to gas production.</p>
Residence time, gas flows and	<p>Long vapour residence times and low gas flow rates are required to maximise biochar production.</p> <p>High gas flow rates and short vapour residence allow minimal contact time between vapours and biochar, thereby inhibiting secondary char formation and promoting bio-oil formation.</p>

---

(Source: Ronsse et al., 2021)

## 2.18 Feedstock for Pyrolysis

Various feedstocks are available for pyrolysis process. In fact, many sources of organic matter can be used as feedstocks for pyrolysis (Klark and Rule, 2021; Cantrell et. al., 2017). Sources from plant include sawdust, nut shells, straw, cotton trash, rice hulls, and switchgrass. Animal sources include waste streams, such as chicken manure, poultry litter, swine manure, beef feedlot manure and dairy manure. In the pyrolysis process, moisture content, ash levels, and chemical components of the feedstock will have a strong impact on the conversion of biomass to biogas, biooil or biochar. Almost any form of organic material can be pyrolyzed; however, both energy conversion efficiency and the quality of the resulting products are dependent on the nature of the feedstock. In order to reduce energy loss, pyrolysis reactors should be fed with materials that has low moisture content (<10 percent moisture by mass). Lignocellulosic feedstocks with high content of alkaline (Na, K, Mg, Ca) typically result in high yields of biochar and relatively low yields of poor-quality bio-oil (Lehmann and Joseph, 2019). Feedstock with high cellulose content produce bio-oils rich in pyrolytic sugars, low molecular weight organic acids and water; whereas feedstock high in lignin produce higher energy bio-oils enriched with mono-and oligo-phenols. The wide range of feedstocks which can be processed by pyrolysis and the large number of design variables make it difficult to identify the optimum pyrolysis technology for a given situation.

#### 2.19 Proximate Analysis of Feedstock

Under proximate analysis, volatile matter is an expression of the amounts of gases, oils and tars given off when biomass is heated above 300 °C and is determined by American Society for Testing Materials procedure (Kim et al., 2017). Ash is the mineral matter left after complete combustion of the biomass has occurred. These high ash levels in animal manures results in less biooil and biogas per unit (volume or mass) of dry solids

being pyrolyzed. In addition, animal waste may also contain soil, which increases the ash content of the feedstock. Because ash generally contains alkali salts, in particular potassium. Thermochemical conversion of these materials may lead to surface fouling and corrosion of metals in pyrolysis reactor systems. This will shorten the useful life of equipment, reduce system performance, and increase maintenance costs. On a positive note, certain elements in ash are catalytic to the thermal decomposition process and at low levels may improve overall efficiency for producing a specific product (Cantrell et al., 2017). Fixed carbon is created in the pyrolysis process. It is obtained by subtracting out the percentage of water, volatile solids, and ash from the starting mass. In standard laboratory analysis of manures, fixed carbon is included in the solid measurement.

## 2.20 Pyrolysis of Biomass

Cellulose, hemicellulose, and lignin, the major components of biomass, have different reaction kinetics. Hemicellulose is the most reactive constituent and lignin the least (Lehmann, 2017). Pyrolysis of whole biomass can be described in terms of the behaviour of these components which are discussed separately in the following sections. The reaction rates, products, and other thermal behaviour of biomass pyrolysis are considered a combination of the behaviour of its principal components. Each component contributes to the behaviour to an extent proportional to its weight percent contribution to the composition of the raw biomass. This is true in the absence of secondary reactions (Huber, 2018).

### 2.20.1 Pyrolysis of cellulose

Among the principal components of biomass, cellulose is the most widely studied. This is mainly because it is the major component of most biomass (43 %). In addition, it is the least complicated and well-defined component of biomass. Cellulose is the major source of the combustible volatiles that fuels flaming combustion. Cellulose also

appears naturally almost in its pure state (for example, cotton). Numerous studies of pyrolytic thermal degradation of cellulose under various conditions have been reported and a simplified, two-pathway mechanism of its decomposition has been proposed in literature and presented in Figure 2.4

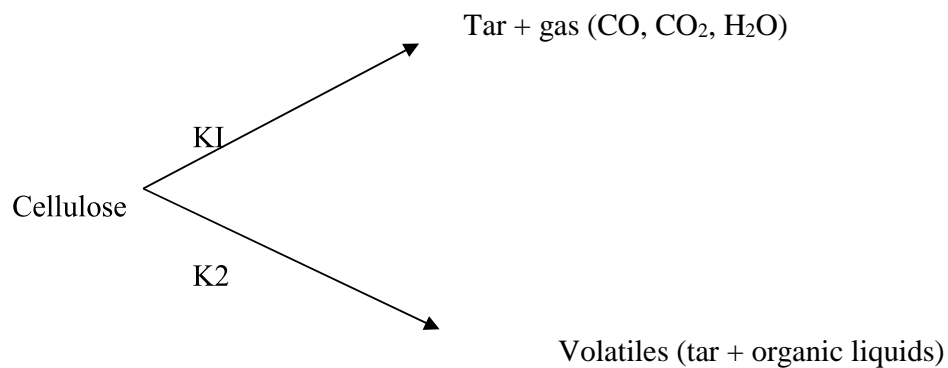


Figure 2.4: Reaction Model for Cellulose Decomposition (Lehmann, 2017)

Reaction 1 dominates at low temperatures while reaction 2 dominates at high temperatures. The existence of the two pathways is demonstrated by studies of the rates of weight loss of cellulose in nitrogen; the transition is found to occur at about 300 °C. Below this temperature, the following chemical reactions may take place: reduction of molecular weight, the appearance of free radicals, oxidation, dehydration, decarboxylation, and decarbonylation. The products are mainly CO, CO<sub>2</sub>, H<sub>2</sub>O, and a char residue.

The second pathway occurs at temperatures above 300 °C which involves decomposition of cellulose to tarry pyrolyzate containing levoglucosan as the major component (22-50 %), which vaporizes and then decomposes with increasing temperature. As the temperature is increased from 300 °C to 500 °C, the amounts of tarry products increases while the proportion of char component reduces and the yields of levoglucosan remain

almost constant. The major products of pyrolysis of cellulose below 500 °C are biochar, tar (mainly levoglucosan), water, CO<sub>2</sub> and CO (Funakuzuri et al., 2021). The yield of light hydrocarbons, that is, C1 to C4, is negligible below 500 °C but becomes considerable at high temperatures (Scott et al., 2020). Tar yield begins to drop as pyrolysis temperature is raised above 600 °C (Lehmann, 2017). A rapid increase in total yield of biogas was recorded at almost the same temperature at which the tar yield begins to drop. This is an indication that primary tar cracking contributes to the total gas production at elevated temperatures. Pyrolysis of cellulose is essentially complete above 600 °C (Funazukuri et al., 2021) and thermal breakdown of tar and some liquid fractions begin, resulting in a considerable increase in gaseous products.

#### 2.20.2 Pyrolysis of hemicellulose

Glucuronoxylans (commonly referred to as xylene) are the most important hemicelluloses of hardwoods, and glucomannan is the predominant hemicellulose in softwoods. Xylene has been utilised in several studies (Kerng et al., 2018) to model the pyrolysis of hemicelluloses. Hemicelluloses are the most reactive major component of wood decomposing in the temperature range 200 °C to 260 °C. The thermal instability of hemicelluloses is probably due to their lack of crystalline. Decomposition of hemicellulose under pyrolytic conditions is postulated to occur in two steps (Soltes and Elder, 2020). First is the decomposition of polymer into water soluble fragments followed by conversion to monomer units, and finally is the decomposition of these units to volatiles. Hemicelluloses produce more gases and less tar than cellulose, and no levoglucosan. They also produce more methanol and acetic acid than cellulose.

#### 2.20.3 Pyrolysis of lignin

Lignin, the third principal component of woody biomass, is a highly linked (3-D network polymer), amorphous, high molecular weight phenol compound. Lignin serves

as cement between the wood fibres and as a stiffening agent within them. Lignin is the least reactive component of biomass; higher temperatures are necessary for the pyrolysis of most lignin. The time required for complete pyrolysis of woody biomass at a given temperature is controlled by the pyrolysis rate of lignin at the operating conditions. Thermal decomposition of lignin occurs in the temperature range 280 °C to 500 °C, although some physical or chemical changes (depolymerization, loss of some methanol) may occur at lower temperatures (Kerng, et al., 2018). Lehmann (2017) observed that at a slow heating rate, lignin loses only about 50 % of its weight when the pyrolysis is stopped at 800°C. Soltes and Elder (2020) have reported a product composition of 51 - 66 % biochar, 14 – 15 % tar, 13 – 28 % pyrolygneous acid and about 12 % gaseous products (consisting majorly CO, CH<sub>4</sub> and C<sub>2</sub>H<sub>6</sub>). The tar residue is a Pyrolysis mixture of phenol compounds while the aqueous distillate contains, among other compounds, methanol, water, acetic acid and acetone.

## 2.21 Concept of Biochar

Biochar is a new word for many, but the technology is a traditional one in several regions of the world. Biochar refers to a kind of charcoal made from biomass. Unlike charcoal made for fuel, biochar has properties which make it a valuable soil amendment. Before exploring biochar materials in more detail, it is useful to understand where the recent interest for the study and use of biochar as a soil amendment comes from.

### 2.21.1 Terra preta de Indio, “black soil of the Indians

Soils in the Amazon Basin are largely represented by Oxisols and Ultisols (Bryden and Hagge, 2018), which are acidic and highly weathered. High temperatures and rainfall throughout the year, coupled to the low ability of these soils to retain positively charged

plant nutrients result in highly leached, nutrient poor soils (Van Wambeke, 2018). When natural vegetation is cleared and its complex biological networks destroyed, the soil is of low value for agriculture. Partly because of this, for a long time it was believed that large settlements of organized societies did not exist in the Amazon in pre-Columbian times. The “re-discovery” of Terra preta soils starting about 40 years ago (Lehmann, 2017) sheds a doubt on such theories: Terra preta soils were most likely formed in the kitchen middens of indigenous people, by the accumulation of charcoal and nutrient-rich food and bone wastes among others (Lehmann, 2017). The resulting soils are up to 2 m deep and cover areas ranging from several hundred square meters to several hectares, indicating large amounts of people living at these locations for long periods of time, until contact with Europeans. It is difficult to estimate the total area covered by these anthropogenic soils, since the majority of them are currently covered by vegetation. However, it is the fact that these soils remain fertile to date (McLaughlin et al., 2019), centuries to millennia after they were formed (Liang et al., 2017). This motivated researchers to learn from Terra preta with the goal of improving soil fertility in other regions of the world. Indeed, charcoal or biochar, which makes these soils black has been shown to be a beneficial soil amendment.

#### 2.21.2 Production of biochar

Biochar is made by “baking” biomass in the presence of little or no oxygen. This differs from actually burning biomass because in an open fire, plenty of oxygen is available to fully oxidize the C in the biomass to CO<sub>2</sub>, thus practically all the C leaves as CO<sub>2</sub> and only ashes and small amounts of C are left behind. Restricting oxygen availability results in a greater retention of C in the biomass. However, the efficiency of the process in terms of C is usually 50 % or less (Lehmann, 2017), that is only half the C in the feedstock or less remains in the biochar. This is because not only biochar results from

the pyrolysis process: combustible gases and volatile compounds also escape from the pyrolyzing biomass.

When biomass is heated up from ambient temperatures, it begins to dry. First, moisture in the biomass must be driven off and this requires the supply of energy because the heat capacity of water is high: large amounts of energy are required to vaporize water (Taylor and Mason, 2021). This has consequences for the use of wet feedstock to make biochar: they should ideally be passively dried (for example, in the sun) to 10 to 15 % moisture before being subjected to pyrolysis. Once the biomass is dry, the torrefaction process begins. During torrefaction, the biomass is “roasted”, and becomes darker in colour as chemical changes occur and some gases and volatile compounds exit the biomass. As the biomass is further heated and reaches approximately 300 °C, true pyrolysis begins and the process becomes exothermic. The biomass completely rearranges itself into solid biochar, combustible gases and volatile compounds (Taylor and Mason, 2021). Overall, pyrolysis produces heat as well as fuels which can be burned at once to produce more energy in the form of heat and potentially electricity, or gases and volatiles can be refined and used as fuels in other applications. Thus, the pyrolysis process by which biochar is made produces renewable energy which can be used to displace fossil fuels. Table 2.13 shows the review of pyrolysis processes at different operating conditions.

Table 2.13: Biochar Production at Different Pyrolysis Conditions

Source	Biomass	Pyrolysis	Reactor	Catalyst	Temperature	Product	Remark
Mani et al 2020	Pine sawdust	Flash 10min	8- Spouted Bed	HZSM-5	400-500	Liquid, Char	Char yield was low
Kim et al 2017	India sawdust	Conventional	Fixed bed	Y-Zeolite	375-475	Biochar, Biogas	Low temp favoured Biocoal

Sharrif et al 2017	Pine at sawdust	Fast	Induction Heater	H-ZSM5	500-700	Biooil	Fast pyrolysis favoured Biooil
Mani et al 2020	Waste Furniture	Conventional	Fixed Bed	ZSM-5 H-Y MCM-4	400-550	Biooil	Increased Biooil functional groups
Taylor and Mason 2021	Orange Peel residue	Slow	Fixed Bed	-	300700	Biochar	Biochar for waste Mgt
Manya et al 2018	Halzenu t al ell, Grape seed	Conventional	Fixed bed	-	477550	Biochar , Biooil	Different yields from biomass
Gonzalez et al 2018b	Municipal waste	Slow 1-2mm	Fixed Bed	-	400450	Biochar , Biooil	Different grades of biochar emerged
Woolf et al 2017	Chest nut shell	Fast	Tubular	H-Y	500700	Biooil, Biochar	Catalyst favoured Biooil yield
Schmist 2018	Rice husk	Slow	Fixed	-	300500	Biochar , Biooil	Biochar is favoured

## 2.22 Components of Biochar

Generally speaking, biochar can be understood to contain four important fractions: moisture, ash, stable and unstable matter (McLaughlin et al., 2019). The words “stable” and “unstable” have not been widely adopted, but the fractions they represent as explained in the following subsection, are generally considered to be key determinants of the effect of biochar in the soil.

### 2.22.1 Moisture contents

The moisture content of biochar does not have an impact on its usefulness as a soil amendment, but does have serious implications for the purchasing, handling and application of biochar to soil. When it exits the pyrolysis unit, the reaction of air with biochar can cause it to spontaneously ignite (Blackwell et al., 2019). Trucks transporting biochar are known to have caught fire in transit, and it is considered a dangerous material for shipping. A simple way of avoiding spontaneous combustion is to spray the biochar with water as soon as it exits the pyrolysis unit. However, this is undesirable to the extent that it makes the biochar heavy for transportation. Biochar can hold up to three times its own weight in moisture (McLaughlin et al., 2019), and it can contain a large percentage of moisture without looking like it does.

#### 2.22.2 Ash

The different feedstocks used to make biochar contain various amounts of ash, and this ash is mostly maintained in the biochar. However, it represents a greater proportion of the overall material since component of carbon; hydrogen and oxygen are lost during pyrolysis. Wood contains less ash (< 1 %) than straws and other crop residues (up to 24 %), which also contain more silica (Lehmann & Joseph, 2019), thus for instance, wood biochar contains less ash than straw biochar made under similar conditions. Manures produce what are known as “high-ash biochar”, with ash contents up to 45 % (Lehmann, 2017). The ash content of biochar is measured by heating it to high temperatures in the presence of air: all of the non-mineral matter is combusted and the ash left behind.

Standard methods developed for determining the ash content of fuel charcoal can be used for biochar.

Biochar ash consists mainly of calcium (Ca), iron (Fe), magnesium (Mg), sodium (Na), potassium (K), phosphorus (P), silica (Si) and aluminum (Al) (Lehmann and Joseph,

2019). The ash of biochar made from plant parts generally contains very small amounts of nitrogen (N). With the exception of Al these elements are plant nutrients, thus applying them to soil with biochar may alleviate deficiencies and improve crop growth.

### 2.22.3 Unstable matter

Literally, unstable matter refers to the fraction of biochar which is decomposed by soil microorganisms in the days and months following soil application. This fraction is important because its decomposition has the potential to lead to N immobilization, if insufficient N is available in the soil during decomposition. Indeed, some authors observed reductions in plant yield with biochar application, and attributed this effect to potential N immobilization by biochar (Asai et al., 2019; Blackwell et al., 2019; McLaughlin et al., 2019). Also, since it decomposes on a short time frame, it is important to know the size of this fraction of biochar in order to assess the C sequestration potential of a biochar material. Total C analysis alone does not fully indicate the C sequestration potential of biochar. It is necessary to know the amounts of unstable and stable matter (and C) it contains. Finding rapid and cheap laboratory tests that provide data relating to the fractions of biochar which decompose in soil in the short to medium term would be ideal. To date, members of workgroups on biochar characterization around the world have proposed heating the biochar to temperatures around 450 °C, under an oxygen-free atmosphere, and quantifying the amount of “unstable” matter as the difference in mass before and after heating (McLaughlin et al., 2019). This is economical and quick, but more data is needed in order to relate information provided by this test to biochar decomposition in soil by biotic and abiotic factors.

### 2.22.4 Stable matter

The recalcitrant fraction of biochar, which persists in soil over the long term, can be termed “stable matter”. This fraction of biochar includes domains which are chemically recalcitrant to biotic and abiotic decomposition in soil. However, size of the stable and unstable biochar fractions in the soil varies.

### 2.23 Characteristics of Biochar

The char yield as well as, the chemical and physical characteristics of biochar depends on the nature of the feedstock used (woody vs. herbaceous) and operating conditions and environment of the pyrolysis unit (low vs. high temperature, residence time; slow vs. fast pyrolysis, heating rate and feedstock preparation). The wide range of process parameters leads to the formation of biochar products that vary considerably in their elemental and ash composition, density, porosity, pore size distribution, surface area, surface chemical properties, water and ion adsorption and release, pH and uniformity of biochar physical structure (Antal and Gronli, 2017; Downie et al., 2019; Chan and Xu, 2019)

#### 2.23.1 Chemical characteristics

Some of the quantification techniques may also be relevant to the characterization and comparison of various samples of biochar produced. The purpose here is to assessing variation in properties of black carbon between samples, and to document the process of aging in contrasting soils and environments. Elemental ratios of O: C, O:H and C:H have been found to provide a reliable measure of both the extent of pyrolysis and the level of oxidative alteration of biochar in the soil, and are relatively straightforward to determine.

Diffuse reflectance infrared Fourier transform spectroscopy (FTIR), X-ray photoelectron spectroscopy (XPS), energy dispersive X-ray spectroscopy (EDX), near-edge X-ray absorption fine structure (NEXAFS) spectroscopy have been used to

examine surface chemistry of biochar in more detail (Brownsort, 2019). These analyses provide qualitative information that may enable the mechanisms behind aging and functionalization of biochar to be elucidated. The solid product contains between 60 and 90 % carbon (Brownsort, 2019). Some carbon is fixed and some is volatile. The inorganic material in the char is called ash which consists of different mineral compounds (Lehmann and Joseph, 2019). If the char is produced from wood material it contains approximately 6.8 g phosphorus per kg char (Lehmann and Joseph, 2019). The carbon atoms in the char are strongly bound to each other like graphite. Different type of biomass produces different strong bonds to each other. Scientists have shown that the half-life of biochar is about 6 000 years. The half-life depends on the choice of biomass, the soil quality, the temperature in the soil and the size of the biochar. The density of biochar is approximately 2 g/cm<sup>3</sup> (Lehmann and Joseph, 2019). The biochar is full of microscopic holes as can be seen in Plate II that among other things absorb moisture and nutrients throughout their lifetime (Lehmann and Joseph, 2019).

### 2.23.2 Physical characteristics

Pyrolysis temperature and feedstock composition have a significant influence on the physical characteristics related to pore structure, surface area and adsorption properties (Antal and Gronli, 2017; Downie et al., 2019; Joseph et al., 2020). As pyrolysis temperatures increase, volatile compounds in the feedstock matrix are lost, surface area and ash increase but surface functional groups that provide exchange sites decrease (Goyal et al., 2018). Ligno-cellulose degradation begins at approximately 120 °C, hemicelluloses are lost at 200 to 260 °C, cellulose between 240 and 350 °C and lignin is degraded at 280 to 350 °C. The proportions of these fractions remaining along with the ash content influence the level of reactivity of the biochar and the development of shifts in physical structure that define the biochars' attributes (Downie et al., 2019).

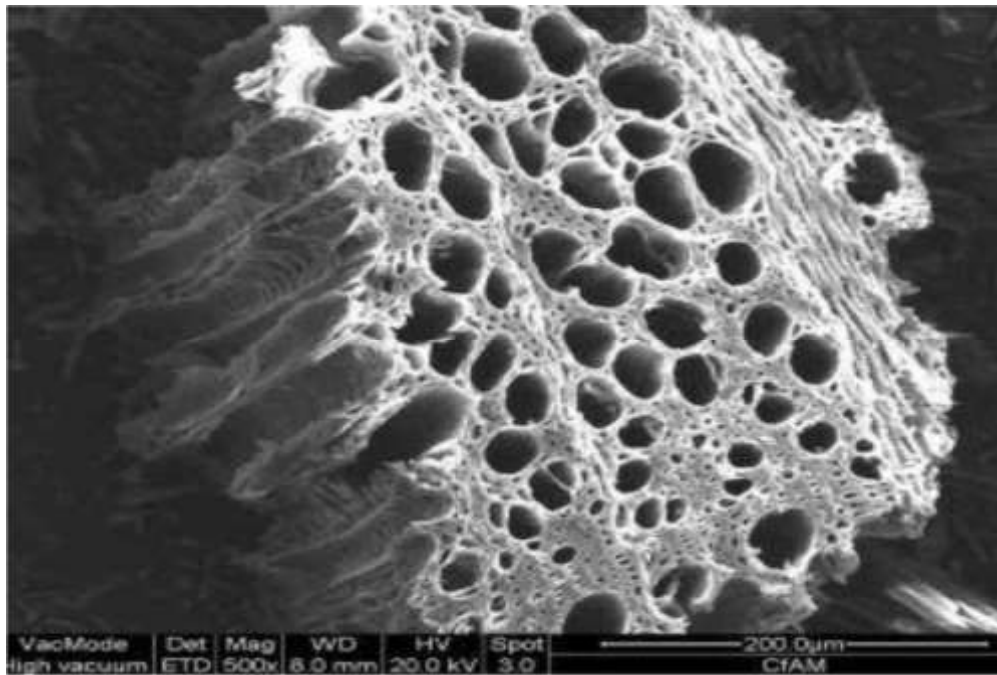


Plate II: Structure of Biochar (IBI, 2020)

As pyrolysis temperatures increase the poly-condensation of C into aromatic rings provides a structure that enhances pore development and surface area of the biochar. Biochars with large amounts C in these condensed structures formed at high temperatures (400 -700 °C) generally have lower functional groups for generating surface charge and ion exchange due to decarboxylation, where low temperature chars contain significantly more C=O and C-H functional groups that promote nutrient retention (Glaser et al., 2022; Biedemann et al., 2018).

#### 2.24 Biochar and Climate Change Mitigation

Climate change has become one of the most important environmental and energy policy issues in the 21<sup>st</sup> century and continuous demand of fossil fuel has caused the rising of greenhouse gases (GHG) emission (Nurrokhmah et al., 2018). As widely believed, carbon dioxide CO<sub>2</sub> is considered the chief culprit contributor to the global warming through anthropogenic emission from power plant generation, transportation and industrial sector. In 2017, the CO<sub>2</sub> concentrations in ambient air approached 400 parts

per million (ppm) and it increased by 120 ppm from CO<sub>2</sub> concentrations in the preindustrial time (Hileman, 2018). These GHG block the sun's energy from escaping to the space and eventually the atmosphere gets warmed and resulted in global warming. By forecast, in 2035, CO<sub>2</sub> concentrations were estimated to reach about 550 ppm and results in temperature rise of 2 °C which will threaten 15 to 40 species with extinction (Hileman, 2018). Thus, urgent action is required to decrease CO<sub>2</sub> concentrations in the atmosphere. Some of these reduction strategies includes enhancement in combustion and energy efficiency, reduction in the use of fossil fuel, switch to non-carbon emitting resources, that is, renewable energy and to capture and sequester CO<sub>2</sub> (CCS) permanently (Nurrokhmah et al., 2018).

Currently, CCS is considered the best viable option since it provides ample time for the development of low-cost renewable energies and cleaner usage of fossil fuels resources during the transition period. At present, chemical absorption using amine-based solvent is the most matured technology used in industries. However, it was reported that amine consumptions have some limitations such as low CO<sub>2</sub> absorption capacity, high energy penalty during absorbent regeneration, amine degradation and potential of corrosion (Plaza, 2019). As against these shortcomings, solid adsorbents are proposed. Solid adsorption is one of the plausible technologies for CO<sub>2</sub> capture due to low energy requirement, low capital and operating cost, together with limited secondary waste generation (Plaza, 2019). Carbon materials such as activated carbon is recently gaining attraction as solid adsorbent due to its availability, high thermal stability, low cost and low sensitivity to moisture. Generally, for good climate mitigation strategy, cost effective means and processes of CO<sub>2</sub> sequestration are essential to meet reasonable reduction in CO<sub>2</sub> concentrations available in the atmosphere.

## 2.24.1 Technologies for capturing carbon

According to Olajire (2017) capturing CO<sub>2</sub> from flue gas streams is an essential parameter for the carbon management particularly for sequestration of CO<sub>2</sub> from our environment. Iron et al. (2017) revealed three methods of capturing CO<sub>2</sub> from power generation as post-combustion, pre-combustion and oxyfuel combustion. The concentration of CO<sub>2</sub> in the gas stream, the pressure of the gas stream and fuel type (solid or gas) are important factors in selecting the capturing system (Olajire, 2017).

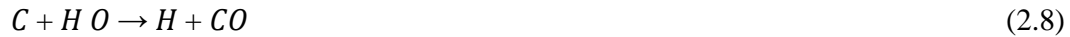
### 2.24.1.1 post-combustion process

Separation of CO<sub>2</sub> from flue gas stream produced through the burning of fuel is termed Post-Combustion Separation. Post-combustion capture is a downstream process and in many respects is analogue to flue gas desulphurization (FGD), which is widely used to capture SO<sub>2</sub> from flue gas in coal and oil-fired power plants (Olajire, 2017). This method requires separating the CO<sub>2</sub> from other flue gases because sequestration of combustion gases is not feasible due in part to the cost of gas compression and storage. Although, Post combustion capturing is capital intensive due to large equipment requirement for capturing CO<sub>2</sub> with low concentration (4 to 14 %) and high temperature of flue gases which posed design problem (Olajire, 2017). Regeneration of the solvents used to release the CO<sub>2</sub> and costly chemical utilized are added disadvantages of this process.

### 2.24.1.2 Pre-combustion process

This referred to reaction between fuel and oxygen or air or steam to produce mainly carbon monoxide and hydrogen (Iron et al., 2017). This is also known as gasification, partial oxidation or reforming process. The mixture of mainly CO and H<sub>2</sub> is mainly passed through a catalytic reactor called shift converter where the CO reacts with steam

to give CO<sub>2</sub> and more H<sub>2</sub>. The CO<sub>2</sub> is separated and H<sub>2</sub> is used as fuel in a gas turbine cycle plant (Olajire, 2017). This is mostly used for coal gasification, although, it is also applicable for liquid and gaseous fuel. Typical reactions for this process are shown below



Gas mixture from the shift converter was then cooled and a Selexol acid gas removal unit separates CO<sub>2</sub> and sulphur compound streams (Iron et al., 2017). The profit of precombustion capture is based on transformation of carbon fuel to carbonless fuel. Gasification process uses chemical energy of carbon and transforms it to chemical energy of hydrogen (Olajire, 2017). With high concentration of CO<sub>2</sub> in this process compared to post combustion, little energy penalty applied for solvent regeneration and minimal equipment size is required. Although, high total capital cost of generating facility is disadvantageous.

#### 2.24.1.3 Oxyfuel combustion process

As a modified form of post combustion capturing process, fuel is reacted and burnt with pure oxygen instead of air resulting in high concentration of CO<sub>2</sub> in the flue gases. When fuel is burnt in pure oxygen, noticeably, the flame temperature is excessively high, so some CO<sub>2</sub>-rich flue gas would be recycled to the combustor to make the flame temperature similar to that in normal air-blown combustor (Olajire, 2017). With high concentration of CO<sub>2</sub> (over 80%) only simple CO<sub>2</sub> purification may be required. Desulphurization is avoided and the process relies mainly on physical separation

processes for O<sub>2</sub> production and CO<sub>2</sub> capturing thereby avoiding the use of reagent and/or solvents that contribute to operating costs and environmental disposal of any related solid or liquid waste (Olajire, 2017). The only disadvantage of this process is large quantity of oxygen requirement.

#### 2.24.1.4 Geotechnical solution

Due to the fundamental disadvantages of the combustion processes, geotechnical process was recently recommended to provide efficient and cost-effective methods of reducing carbon dioxide concentrations in the atmosphere (Olajire, 2017). This method required the use of solid adsorbent to capturing and sequestering CO<sub>2</sub> in the environment.

#### 2.25 Carbon Sequestration

Carbon Sequestration is the process of capture and long-term storage of atmospheric carbon dioxide (Roger et al., 2022). It describes long term storage of carbon dioxide or other forms of carbon to either mitigate or defer global warming and avoid dangerous climate change. It has been proposed as a way to slow the atmospheric and marine accumulation of greenhouse gases which are released by burning fossil fuel. It is generally accepted that reducing atmospheric concentrations of CO<sub>2</sub> by permanently sequestering C in the soil could reduce the impact of climate-related damage. Increasing soil organic carbon (SOC) storage by conventional soil management practices such as conservation tillage, no-till, and perennial cropping systems can take many years and there is uncertainty about the C sequestration potential of these systems (Bates, 2017; Drag et al., 2017). By contrast, application of biochar to agricultural soils is an immediate and easily quantifiable means of sequestering C and is rapidly emerging as a new management option that may merit high value C credits (Glaser at al., 2022). During pyrolysis, the biomass, feedstock's molecules are rearranged. Gas and volatile

compounds are formed and escape the biomass, and the solid fraction, biochar, remains in the pyrolysis chamber. The changes which occur during pyrolysis include a condensation of the carbon in the feedstock, where the aromaticity increases.

#### 2.25.1 Carbon sequestration potential of biochar

The potential of biochar as a carbon sequestration agent depends upon both the amount and the rate that carbon dioxide could be removed from the atmosphere and stored as carbonaceous solid in soils. The amount that could be removed is enormous. To reduce CO<sub>2</sub> levels in the atmosphere to pre-industrial levels, every hectare of arable land (about 6% of the Earth's surface) would have to incorporate about 90 metric tons of biochar, a large but not inconceivable quantity. (For comparison, biochar for agronomic purposes is often applied at rates of 50 metric tons per hectare (Cantrell, et al., 2017). This provides a need for an inexpensive means of capturing or removing carbon from the atmosphere. Biochar, produced from biomass which is in abundance, fills this void while being a form of waste disposal and recycling (Cao et al., 2018). By an adaptation of the current biological carbon cycle, the biochar is produced from biomass and half is returned to the soil as charcoal and the other half is return to commercialization for an organic fuel.

The efforts to reduce the world's carbon dioxide emissions and reduce the amount of carbon dioxide that already exists in the atmosphere are on-going (Zornoza et al., 2019). Sweden has so far focused on the controversial method of carbon capture and storage, CCS, (Zornoza et al., 2019) which means that carbon dioxide is pumped down and trapped in rooms in the ground (Velez et al., 2019). Necessary equations suggested by Lehman et al 2019 for the calculation of biochar production, total potential C sequestration and amount of CO<sub>2</sub> removed are described below

$$\text{Biochar Production} = \text{Biomass Production} \times \% \text{ Conversion} \quad (2.10)$$

$$\text{Biochar Production interms of C Content} = \text{Total Potential C Sequestration} \quad (2.11)$$

$$\text{Total Potential C Sequestration interms of 80\% C stabilty} = \text{CO}_2 \text{ Reduction} \quad (2.12)$$

## 2.26 Adsorption Process

Adsorption can be defined as a phenomenon in which material (adsorbate) travels from a gas or liquid phase and forms a superficial monomolecular layer on a solid or liquid condensed phase called substrate (Cao, et al., 2018). This process involves the removal and subsequent accumulation of a substance of interest onto the surface of adsorbent. Being a surface phenomenon, the extent to which adsorption takes place is dependent upon the nature of both adsorbing agent and the substances adsorbed. The greater the surface of the adsorbing agent, the greater is the adsorption. However, the attractive forces on the surface are limited to distances one molecule deep. Usually, it is reversible and the reverse process is called desorption. It is responsible not only for a subtraction of substances but also for release after been adsorbed. Adsorption is a mass transfer process that is a phenomenon of sorption of gases or solutes by solid or liquid surfaces. The adsorption on the solid surface occurs when the molecules or atoms on the solid surface have residual surface energy due to unbalanced forces.

When some substances collide with the solid surface, they are attracted by these unbalanced forces and stay on the solid surface. According to the different adsorption forces, the adsorption process can be divided into two categories: physical adsorption and chemical adsorption. Physical adsorption is produced by the interaction of intermolecular forces (i.e., Van der Waals forces), for example, the adsorption of gas on activated carbon. Physical adsorption is generally carried out at a low temperature, and fast adsorption rate, low adsorption heat, and non-selective. As the effect of

intermolecular attraction is weak, the structure of the adsorbate molecules hardly changes, the adsorption energy is small, and the adsorbed substance is easily separated again. The adsorption due to the action of chemical bonds is chemical adsorption.

Chemical adsorption process includes the formation and destruction of chemical bonds. The absorption or release of adsorption heat is larger, and the activation energy required is also larger. Physical adsorption and chemical adsorption are not isolated and often occur together.

## 2.27 Factor Influencing Adsorption Process

### 2.27.1 pH Effect

The solution pH is one of the fundamental factors affecting the adsorption and ionic exchange processes in clay minerals (George and Betzy, 2018). However, in case of surfaces containing polarized or charged location, the amount of adsorption increases if the surface acquires a charge that exceeds the charge of the minutes absorbed by the effect of acidity. Conversely, the amount of adsorption decreases if the surface and the evaporated minutes acquire a similar charge (George and Betzy, 2018). For low solution pH, the adsorption levels may decrease because of the competition shown by the protons for the active sites in the soil granules and the amount of adsorption of the elements from the aqueous solutions increases by increasing the pH. Angin (2018) showed that the lead ions in the water solution turned into  $PbOH$  at  $pH = 5.9$  and  $Pb(OH)_2$  at  $pH = 7.9$  and  $Pb(OH)_3$  at  $pH = 9.5$ .

### 2.27.2 Temperature

From the fundamental, adsorption is known to be a heat-generating process (Exothermic) while absorption is a heat-absorbing process (Endothermic). Adsorption is through adsorption, which is often accompanied by energy emission (Angin, 2018). As it is evident, the increase in temperature caused a decrease in adsorption due to

increased desorption. While the adsorption process, which is accompanied by the process of absorption or spread of molecules inside the pores, is absorbent to the heat and thus the kinetic energy of the molecules absorbed increases the ability to enter the pores of the steel phase and increase the speed of spread in it, so increase the adsorption process by increasing the temperature (Hall, 2018). Chen et al. (2021) showed that the percentage of nickel removal from the water solution increased by increasing the temperature of the solution due to the absorption process associated with adsorption. The adsorption speed increases exponentially with the absolute temperature while the absorption process increases with the speed of absorption.

#### 2.27.3 Initial concentration

One of the primary factors that affect adsorption process is concentration of the adsorbent material because the largest number of ions or absorbable molecules is exposed to the active sites in the adsorbent at the high concentration, which increases the adsorption speed while the percentage of adsorption equally increased.

#### 2.27.4 Nature of adsorbate

The size of the ion plays an important role in the adsorption process, affecting the amount of adsorption of certain ion on the surface of the adsorbent with the presence of more than one ion of different size in the solution. Angin (2018) has shown that under certain conditions lead ion is twice as dense as the ion of cadmium because of the large lead ion volume. The solubility of the adsorbent in the solvent also has an effect on the adsorption process where the amount of the adsorbent is reduced by increasing its solubility in the solvent Angin (2018).

#### 2.27.5 Surface area

Adsorption is significantly affected by the rate of granularity of the adsorbent material because adsorption occurs mainly on the outside of the granules and slightly inside the granules because only a few of the internal effective sites allow the element ion to propagate within. Therefore, the decrease in grain size increases the surface area of adsorption, which increases the availability of suitable sites for adsorption (Chen et al., 2021).

## 2.28 Adsorption Isotherms Theory

Isotherm is defined as the relationship between the amount of adsorbent adsorbed on a surface and the equilibrium concentration of the substance absorbed in the solution at a constant temperature. It can also be defined as a description of the relationship between the amount of adsorbate on the surface of adsorbent and the primary concentration of the solution at a constant temperature Chen et al. (2021). The reliability of the isotherm depends on the temperature in extracting useful information about the nature of the adsorption process because it provides important information in describing the nature of adsorption and its conditions. Adsorption also helps to obtain thermodynamic amounts of adsorption (Hall, 2018).

### 2.28.1 Langmuir isotherm

According to Langmuir (1918) cited in Rashidi and Yusup (2016), Langmuir isotherm defines that the maximum adsorbent capacity occurs due to the presence of a single layer (monolayer) of adsorbate on the adsorbent surface. There are four assumptions in this type of isotherm, namely:

- a. The molecules are adsorbed by a fixed site (the reaction site at the adsorbent surface).
- b. Each site can "hold" one adsorbate molecule.
- c. All sites have the same energy.

d. There is no interaction between the adsorbed molecules and the surrounding sites.

Adsorption process form monolayer. Illustration of monolayer formation during adsorption is shown in Figure 2.5 (a). Langmuir isotherm model is represented by Equation (2.13):

$$Q_e = \frac{Q_{max} C_e}{1 + K_L C_e} \quad (2.13a)$$

Where  $Q_e$  is the amount of adsorbed adsorbate molecule per gram of adsorbent (mg/g),  $Q_{max}$  is the capacity of the adsorbent monolayer (mg/g),  $C_e$  is the adsorbate equilibrium concentration (mg/L), and  $K_L$  is the Langmuir adsorption constant. Based on the Langmuir postulation, the important parameter is the dimensionless constant otherwise known as separation factor represented by the following relationship

$$R_L = \frac{K_L C_e}{1 + K_L C_e} \quad (2.13b)$$

This dimensionless constant according to Langmuir has the following values:

- i  $R_L > 1$ , unfavorable adsorption process (allows the adsorption process to occur, most desorption processes occur).
  - ii  $R_L = 1$ , linear adsorption process (depending on the amount adsorbed and the concentration adsorbed).
  - iii  $R_L = 0$ , Irreversible adsorption process (strong adsorption).
- $0 < R_L < 1$ , Favourable adsorption process (normal adsorption).

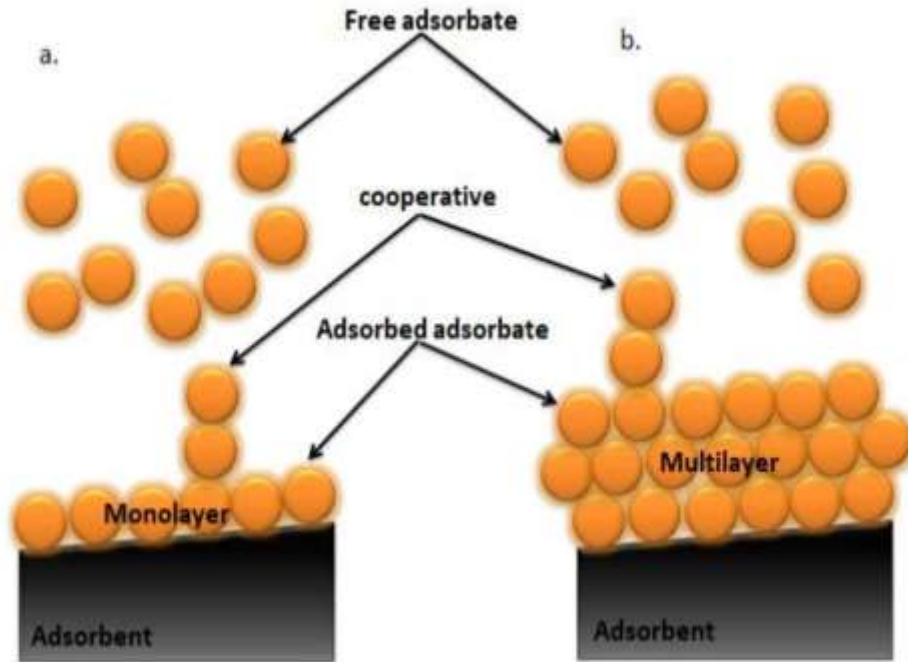


Figure 2.5 (a) and (b): Monolayer and Multilayer Adsorption (Simeon et al., 2019)

### 2.28.2 Freundlich isotherm

Freundlich isotherm emphasizes a physical form of adsorption in which the adsorption occurs in several layers and the bonds between adsorbate and adsorbent are not strong (multilayer). Multilayer formation is illustrated in Figure 2.5(b). According to Drag et al., (2017), Freundlich isotherm also assumes that the sites of adsorption are heterogeneous and not homogeneous as obtainable in Langmuir predictions. The empirical relationship for expressing Freundlich isotherm is represented in Equation (2.14):

$$\ln Q_e = \ln K_f + \frac{1}{n} \ln C_e \quad (2.14)$$

From the Freundlich expression,  $K_f$  is Freundlich constant,  $C_e$  is the concentration of adsorbate under equilibrium conditions (mg/L),  $Q_e$  is the amount of adsorbate absorbed per unit of adsorbent (mg/g), and  $n$  is the value indicating the degree of linearity between the adsorbate solution and the adsorption process (Drag et al., 2017). The value of  $n$  is described as follows:

i  $n=1$ , linear adsorption. ii  $n<1$ , adsorption

process with chemical interaction. iii  $n>1$ , adsorption

process with physical interaction.

iv Favorable adsorption process is declared when  $0 < 1/n < 1$ , and a cooperative adsorption process occurs when  $1/n > 1$ .

### 2.28.3 Temkin isotherm

Three postulations were assumed according to Temkin isotherm which includes: the adsorption heat decreases linearly with increasing surface adsorbent coverage, the adsorption process assumes a uniform binding energy distribution on the adsorbent surface, and lastly, the adsorption interaction involves the interaction between adsorbateadsorbent (Romero et al., 2018). Temkin isotherm is expressed according to Equation (2.15):

$$Q = B \ln A + B \ln Ce \quad (2.15)$$

Where  $B$  is the adsorption heat constant (if the  $B < 8$  kJ/mol, the adsorption process occurs physically),  $A$  is the binding equilibrium constant, and  $T$  is the absolute temperature.

### 2.28.4 Dubinin-Radushkevich isotherm

This isotherm assumes adsorption process takes place on filling of micropores volume of adsorbent (Romero et al., 2018). Dubinin-Radushkevich isotherm expresses the adsorption process on the adsorbent which has a pore structure or adsorbent which has a heterogeneous surface and expresses the adsorption free energy. Dubinin-Radushkevich isotherm is given in Equation (2.16):

$$\ln Qe = \ln Qs - (\beta\epsilon^2) \quad (2.16)$$

Based on Equation (2.16),  $\beta$  is the Dubinin-Radushkevich isotherm constant,  $Q_s$  represents the saturation capacity of theoretical isotherms, and  $\mathcal{E}$  is the Polanyi potential (J/mol) which is calculated with following Equation (2.17):

$$\mathcal{E} = RT \ln[1 + \frac{Q_s}{Q_e}] \quad (2.17)$$

The calculation of the free energy of adsorption per adsorbate molecule can be achieved using Equation (2.18):

$$E = \sqrt{\frac{RT}{2}} \quad (2.18)$$

According to Dubinin-Radushkevich expressions,  $C_e$  is the equilibrium concentration of solute and  $E$  is the adsorbate energy per molecule as the energy needed to remove molecules from the surface. The two basic forms of adsorption are described by the following values of  $E$ :

- (i)  $E < 8$  kJ/mol, physical adsorption.
- (ii)  $8 < E < 168$  kJ/mol, chemical adsorption.

#### 2.28.5 Jovanovic isotherm

Jovanovic isotherm is based on the restrictions of some of the assumptions found in the Langmuir model. It does not allow some mechanical contact between the adsorbate and the adsorbent (Cao, et al., 2018). The linear correlation of the Jovanovic model is represented by the Equation (2.19):

$$\ln Q_e = \ln Q_{max} - K_j C_e \quad (2.19)$$

Where  $Q_e$  is the amount of adsorbate in the adsorbent at equilibrium (mg/g),  $Q_{max}$  is the maximum uptake of adsorbate, and  $K_j$  is the Jovanovic constant.

#### 2.28.6 Halsey isotherm

According to Drag et al. (2017), Halsey isotherm evaluates a multilayer adsorption system. The Halsey model is written according to Equation (2.20):

$$Q_e = \frac{1}{K} - \frac{1}{C_e} \quad (2.20)$$

For the expression in Equation (2.20), KH and n are the Halsey model constants.

### 2.28.7 Harkin-Jura isotherm

Harkin-Jura Isotherm opines that the adsorbent has a heterogeneous pore distribution which implies that adsorption occurring on the surface is multilayer adsorption. The expression of the model is represented in Equation (2.21)

$$\frac{1}{C} = - \beta \log C \quad (2.21)$$

Where the value of  $\beta$  is related to the specific surface area of the adsorbent and  $A$  are the Harkin-Jura constant. The modification to the Harkin Jura model is used to determine the surface area of the adsorbent. The modified form is represented in Equation (2.22)

$$\beta = \frac{q}{S} \quad (2.22)$$

Where  $q$  is the constant which is independent of the nature of adsorbent,  $S$  denotes the specific surface area ( $\text{m}^2/\text{g}$ ),  $R$  represents the universal gas constant given as  $8.314 \text{ J/molK}$ ,  $T$  is the absolute temperature  $298\text{K}$  and  $N$  is the Avogadro's number.

From equation (2.22), the surface area can be calculated as

$$S = - \frac{q}{\beta} \quad (2.23)$$

Table 2.14: List of  $q_{\text{value}}$  for Different Materials

Material	T(K)	$q(\text{m}^2/\text{g})$
Carbon	298	$1.053 \times 10^{21}$
	308	$1.760 \times 10^{21}$
	313	$1.727 \times 10^{21}$
	323	$1.677 \times 10^{21}$
	325	$1.662 \times 10^{21}$
Titanium Oxide	328	$1.664 \times 10^{21}$
	308	$1.011 \times 10^{24}$
	313	$6.631 \times 10^{23}$
	323	$4.552 \times 10^{23}$

	325	4.553X10 <sup>23</sup>
	328	2.633X10 <sup>23</sup>
Silica	298	3.436X10 <sup>22</sup>
Tungsten Trioxide (WO <sub>3</sub> )	298	1.141X10 <sup>24</sup>

(Source: Drag et al., 2017)

#### 2.28.8 Elovich model

The model assumes that the rate of adsorption of solute decreases exponentially as the amount of adsorbed solute increase. As the system approaches equilibrium,  $t \gg 1/\alpha\beta$ , the linearized form of

Elovich model is expressed according to Equation (2.24)

$$q = - \ln(\alpha\beta) + - \ln(t) \quad (2.24) \text{ The}$$

graph of  $qt$  vs  $\ln(t)$  helps to determine the nature of adsorption on the heterogeneous surface of the adsorbent, whether chemisorption or not, and a number of gases have been reported to follow the Elovich kinetics model.

where  $\alpha$  = the initial adsorption rate (mg/g.min), and  $\beta$  = desorption constant.  $t$  = time (min),  $qt$  = the amount of adsorbate adsorbed in mg/g at equilibrium and at time  $t$ .

#### 2.29 Activated Carbon

Activated carbon otherwise called activated charcoal is a form of carbon that has been processed with oxygen to create substantial numbers of tiny pores between the carbon atoms. Commercial activated carbons have internal surface area ranging from 500 to 1500 m<sup>2</sup>/g (Foroutan et al., 2018). Joan (2020) defined it as “any porous material formed in the major part of carbon and characterized by a well- developed porosity”. Activated carbon is a generic term used to describe a family of amorphous and highly carbonaceous materials none of which can be characterized by a structural formula (Joan, 2020). Activated carbon, a recently discovered adsorbent utilized in industrial

processes, is composed of a microporous, homogenous structure with high surface area and exhibits thermal stability. The process for producing high-efficiency activated carbon is not completely investigated in developing countries (George and Betzy, 2018). Because of the problems with the regeneration of used activated carbon, there is a great interest in finding inexpensive and effective alternatives to the existing commercial activated carbon. The cost of activated carbon prepared from biomaterials is very low compared to the cost of commercial activated carbon (George and Betzy, 2018). Activated carbon can be prepared from feed stock with high carbon and low inorganic content. The most common feed stocks used for the production of activated carbon are wood, coconut shell, bituminous coal, peat etc. The chars obtained from them could be activated easily to produce reasonably high-quality activated carbons. During the process of activation, the expected internal pores were created, which provides the activated carbon its fundamental adsorptive properties. Carbon is known to occur in three main forms; these are; powder, granular and pellet. Nonetheless, the most frequently used are granular and powdered AC (Dabrowski et al., 2018). Figure. 2.6 shows a pile of granular AC



Plate III: Granular Activated Carbon (Foroutan et al., 2018)

Based on intrinsic high surface area, the AC is understood to be useful in removing many contaminants from both potable water and wastewater (Erta and Alma, 2017). Activated carbons have a number of unique peculiarities such as large internal surface area, chemical properties and good accessibility of internal pores (Rashidi and Yusup, 2016).

According to IUPAC definitions three groups of pores can be identified.

- i. Macropores (above 50nm diameter)
- ii. Mesopores (2-50 nm diameter) iii.
- Micropores (Under 2 nm diameter)

Micropores generally contribute to a major part of the internal surface area. Macro and micropores are generally classified as the highways into the carbon particle, and are crucial for (Simeon et al., 2019). The desirable pore structure of an activated carbon product is achieved by combining the right raw material and suitable activation procedure. The AC adsorption characteristics persuaded most researchers to use AC in almost every field of chemistry, basically due to its simplicity of design and operation, selectivity towards certain substances as well as complete removal of pollutants even from dilute solutions (Foroutan et al., 2018). This, in no small measure, has resulted in more hands for the production of AC for various domestic and industrial purposes. The most common feed stocks used for the production of activated carbon are wood, coconut shell, bituminous coal, peat, wastes etc. The chars obtained from them could be activated easily to produce reasonably high-quality activated carbons. During the activation process, the unique internal pore structure is created, which provides the activated carbon its outstanding adsorptive properties. Activated carbons have a number of unique characteristics such as large internal surface area, chemical properties and good accessibility of internal pores.

#### 2.29.1 Activated carbon preparation

Virtually all carbonaceous substances can be transformed into activated carbon; although, the final properties of the resulting carbon will depend significantly on the nature of the starting material and activation conditions. A large number of processes for making activated carbons have been postulated and developed over the past century. However, most of the processes involve the pyrolysis of the starting material, which is accompanied by a stage of controlled oxidation or vice versa. The main purpose of the oxidation stage is to activate the carbon (Simeon et al., 2019). Preparations of AC have been reported by many researchers which were basically classified into four main processes which includes: pyrolysis process, physical and chemical activation process and carbonization and steam/thermal activation (Anex et al., 2020; Zhao et al., 2017; Cao et al., 2018). The production of AC involves the following steps: pretreatment of the precursor, impregnation of the precursor with the activator, carbonization of the impregnated precursor, and removal of the activator.

#### 2.29.2 Material pretreatment

In most cases, raw materials undergo a few preliminary stages before the actual production of AC, such as crushing, milling, and sieving to the appropriate particle size. Particle size is an important factor for the subsequent use of the raw materials, such as in mixing with a catalyst or impregnating with precursor; although, particle size was observed to affect the properties of the resulting AC. Most researchers documented the use of materials with sizes in the range of 1 mm to 2 mm (Emam, 2018; Demirbas,

#### 2019). 2.29.3 Pyrolysis process

Pyrolysis step (or also called as Carbonization) involves heating the source materials to temperatures ranging between 400 to 900 °C in the absence of air (Lehmann, 2017). Thermo-chemical conversion of organic materials into three distinctive phases (biochar, bio-oil and biogas) at elevated temperature in the absence of oxygen is termed

as pyrolysis. Pyrolysis is a simultaneous process that changes both the chemical composition and physical phase of the parent materials and it is irreversible (Foroutan et al., 2018). Pyrolysis process is mostly understood to occur when materials are exposed to a reasonable temperature regime. Some factors affecting pyrolysis such as temperature has the most significant effect and this is followed by retention time, heating rate and nitrogen flow rate. Usually, when the reaction temperature was increased, AC and char production reduced, while at the same time increasing the pyrolysis temperature leads to a drop off of solid yield and an increase in both gases and liquid percentages yield. On the other hand, increasing the temperature leads to an increased ash and AC percentage, whereas the volatile matter gets reduced. Therefore, high quality AC is obtained at a higher temperature (Foroutan et al., 2018).

Generally, pyrolysis process is undertaken to eliminate most of the non-carbon elements such as hydrogen, nitrogen, oxygen and Sulphur as volatile gaseous products. Volatiles with low molecular weight are first released, accompanied by light aromatics and finally the hydrogen gas. The resultant solid product, being rich in fixed carbon, is called biochar. These residual carbon atoms are grouped into condensed sheets of aromatic ring with a cross-linked structure in a random manner. The mutual and irregular arrangement of these aromatic sheets leaves free interstices between the sheets, which are mostly filled with the tarry materials.

To evacuate these tarry materials, activation process is necessitated. More so, it also enlarges the diameters of the pores, which were earlier created during the carbonization process and creating new porosity (Cao, et al., 2018).

### 2.30 Activation Processes

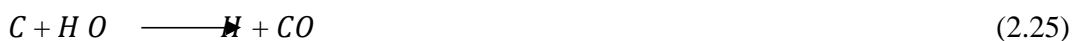
The fundamental characteristics of a carbon are established during the pyrolysis process, and the required oxidation step must be undertaken to complement the pyrolysis step. During activation process, the oxidizing agent aggressively erodes the

internal surfaces of the carbon, develops an extensive and fine network of pores in the carbon, and changes the atoms lying on the surface to specific chemical forms which may have selective adsorption capabilities. This activation step can be carried by two basic methods called physical activation and chemical activation.

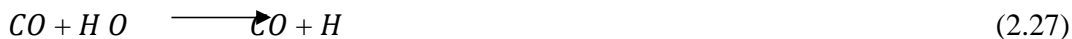
### 2.30.1 Physical activation process

Physical activation is a two-stage process. Carbonization of carbonaceous materials comes first, and then activation of the resulting biochar at high temperatures using CO<sub>2</sub> or steam or mixture of the two as oxidizing gases. Because of easy way of handling, cleaning and processing at low reaction rate and around 800 °C temperature, CO<sub>2</sub> is frequently used as it facilitates the control of activation process. A temperature range of 400 °C and 850 °C was found to be the carbonization temperature, though it may sometimes reach up to 1000 °C while activation temperature between 600 °C and 900 °C (Foroutan et al., 2018).

Gasification of the carbonaceous material with steam and CO<sub>2</sub> occurs by the following endothermic reactions:



The reaction of C with steam is followed by the water gas formation reaction, which is catalyzed by the carbon surface (Foroutan et al., 2018) as represented in Equation (2.27),



Since the reaction of carbon with steam and with carbon dioxide is both endothermic, external heating is required to drive the reactions and to maintain the reaction temperature. The activation process can be manipulated to produce products of desired characteristics. Activation temperature, steam and CO<sub>2</sub> flow rates control the pore

development, which in turn affect pore size distributions and the level of activity of the activated carbon. This carbonization process consists of four main steps namely: (i) the first stage that is at temperature lower than 200 °C refers to a dehydration process wherein moistures from the waste structure are removed, (ii) the second stage is where the biomass starts to decompose while light tar and organic acid is discharged, and this takes place at temperature range of 170 to 270 °C, (iii) the third stage which is at 270 to 350 °C is where the biomass are decomposed and significant amount of liquid and gas is evolved in producing bio-char, and (iv) at the final stage (temperature > 350 °C), an acceleration in carbon content occurs by removing the remaining volatiles (Rashidi and Yusup, 2016).

### 2.30.2 Chemical activation process

Chemical activation process in practice involves one step taking place with the use of dehydrating chemicals. Impregnation and carbonization at moderate temperature with the chemical activating agents mixing with the precursor, as oxidants and dehydrates (Foroutan et al., 2018). Activation with dehydrating agents and carbonization simultaneously during the chemical activation process at lower temperature results in having better porous structures of AC. Chemical activation requires impregnation of the material with the desired chemical either in solid or liquid form. Impregnation process can take up to 24 hours depending on the chemical used, the parent material, and the further processes required. The chemical agents assist in developing porosity through dehydration and degradation processes. The impregnated precursor is then heated at a maximum of 500 °C. The adoption of a lower temperature compared with that of physical activation is compensated by the interaction between the chemicals and the carbon skeleton (Waqas et al., 2021). In order to remove residual chemicals from the material, the material is washed with either distilled water or a mild acid. The major

advantages of Chemical activation include its high yield, low temperature of activation (less energy cost), less activation time, and generally, high porosity development. The disadvantages include the high costs of the activating agents and the need for an additional washing stage to remove the chemical agent (Waqas et al., 2021).

### 2.30.3 Combination of physical and chemical activation

A combination of physical and chemical activation can be used to prepare granular activated carbons with a very high surface area and porosity adequate for certain specific applications such as gasoline vapour control and gas storage. Activated carbons of this types have been reported using lignocellulosic precursors chemically activated with phosphoric acid and zinc chloride and later activated under a flow of carbon dioxide. Uniform, medium-size microporosity and surface areas above 3600 m<sup>2</sup>/g are obtained with this mixed procedure (Gonzalez et al., 2018a).

### 2.30.4 Advantages of chemical activation over physical activation

An important advantage of chemical activation is that the process normally takes place at a lower temperature and for a shorter time than those used in physical activation. In addition, very high surface area activated carbons can be obtained with the yields of carbon in chemical activation being usually higher than those in physical activation because the chemical agents used are substances with dehydrogenation properties that inhibit the formation of tar and reduce the production of other volatile products. The activation of wood using H<sub>3</sub>PO<sub>4</sub> could be carried out at temperature less than 500 °C (Cao et al., 2018), while ZnCl<sub>2</sub> activation was carried at between 600 °C to 709 °C. The carbonization step generates the porosity, which becomes accessible when the chemical is removed by washing (Cao et al., 2018). Consequently, the modification of chemical/precursor ratio permits the adjustment of the porosity in the final activated

carbon. However, the most important disadvantage of chemical activation is the incorporation of impurities, coming from the activating agent, which may affect the chemical properties of the activated carbon. Another disadvantage is the investment needed for the unit for recovering chemical used for impregnation (Downie et al., 2019).

### 2.31 Adsorption by Activated Carbon

Activated carbons have well developed micro and meso-porosities which are applied in wide range of industrial and technological processes (Arenillas et al., 2017). The surface chemistry of activated carbons is governed by the presence of heteroatoms, such as oxygen and nitrogen. These heteroatoms exist in the form of acidic, basic or neutral organic functional groups (Arenillas et al., 2017). The adsorption capacity of activated carbons to adsorb CO<sub>2</sub>, which is based on physical adsorption, can be increased by introducing nitrogen functional groups into their structure (Drag et al., 2017). However, Pevida et al. (2018) advised on systematic modification of commercial activated carbon with nitrogen so as to promote CO<sub>2</sub> adsorption without altering textural properties of the parent carbon. Rashidi and Yusup (2016) studied CO<sub>2</sub> adsorption by activated carbon prepared from coconut shell at 25 °C and 1bar and observed maximum adsorption capacity to be 49.75 and 70.42 cm<sup>3</sup>/g for both synthesized and commercial activated carbons.

#### 2.31.1 Potential of activated carbon as CO<sub>2</sub> separator

It's widely acknowledged that activated carbon has great potential in separating CO<sub>2</sub> from gas streams, particularly in capturing CO<sub>2</sub> in post combustion conditions, which is moderate temperatures and atmospheric pressure (Rashidi and Yusup, 2016). Any carbonaceous materials with low ash content, significant volatile matters that would escape during heating and resulting in more pores and low moisture content are good candidates for making activated carbon. Aside that raw precursors must be easily

activated and to have a lower degradation rate in order to preserve their physiochemical characteristics. Thus, proximate and ultimate analyses should be considered as prerequisite for activated carbon formation. Apart from the origin and nature of precursors, operating conditions for the production are essential for developing suitable activated carbon for gas phase application (Rashidi and Yusup, 2016).

### 2.31.2 Improving adsorptive capacity of activated carbon

In order to enhance the adsorptive capacity of activated carbon- specific interaction between the activated and CO<sub>2</sub>, surface modification is important. The surface chemistry of the activated carbon is governed by the heteroatoms such as nitrogen and oxygen, controlled by the nature of raw precursors as well as the activation conditions (Rashidi and Yusup, 2016). These functional groups can be manipulated either by thermal or chemical treatment in order to produce the adsorbent that serve specific applications (Cao et al., 2018). Generally, the surface modification step is performed after the activation process, and the modification technique can be classified into physical (heat treatment), chemical (acidic, basic, impregnation), and biological modification. Since CO<sub>2</sub> is a Lewis acid, affinity of activated carbon towards CO<sub>2</sub> can be achieved by chemical treatment via increasing their basicity properties through neutralization of acidic functional group, or to replace acidic group to basic functionalities. As such, Sun et al. (2021) reported that chemistry of the activated carbon can be altered by introducing basic groups such as sulphur, nitrogen, and metallic atoms.

### 2.31.3 Modification by nitrogen

Nitrogen modification is usually carried out through heat treatment with ammonia (NH<sub>3</sub>) or impregnation with amine groups (Pevida et al., 2018). The thermal treatment

with  $\text{NH}_3$  gases otherwise called animation process, involves heating the pristine activated carbons to elevated temperature (200 to 1000 °C) in  $\text{NH}_3$  atmosphere for certain period of time prior to cooling to ambient temperature under  $\text{N}_2$  flow (Pevida et al., 2018). During the heating period,  $\text{NH}_3$  decomposes to free radicals such as  $\text{NH}_2$ ,  $\text{NH}$ , atomic hydrogen, and nitrogen, which will react with carbon surfaces to form nitrogen functionalities such  $-\text{NH}_2$ -,  $-\text{CN}$ , pyridinic, pyrrolic and quaternary  $\text{N}_2$  (Pevida et al., 2018). Plaza et al. (2020) reported that upon the animation process, the composition of Nitrogen on the synthesized activated carbon will be increased from 0.7 to 1.0 wt% up to 4.5 wt%. However, since the surface of activated carbon is said to be non-reactive towards  $\text{NH}_3$  gas, pre-oxidation before animation process is proposed (Shafeeyan et al., 2022). Thus, the carbon samples will be pre-heated with air until preferred temperature is reached, then only purified  $\text{NH}_3$  is introduced into the reactor (Shafeeyan et al., 2022). It was reported that using oxygen functional group prior to animation may act as anchoring sites to react with the free radicals from  $\text{NH}_3$  decomposition process.

#### 2.31.4 Modification by metal oxides

Apart from nitrogen modification, metal oxide modification also exists for  $\text{CO}_2$  uptake from flue gases. Metal elements impregnation onto carbon matrix can be justified in terms of chemical reaction between metal oxide and  $\text{CO}_2$  molecules, especially at elevated temperature. The presence of copper oxide onto the carbon material can enhance the adsorption capacity of acidic molecules, since metal oxides are classified as electron donors (Hosseini et al., 2019). The importance of metal doping technique that includes the utilization of alkaline earth metals (such as, Mg, Ca) and transition metals (such as Cu, Co, Ni, Fe, Cr) is elucidated in terms of possible enhancement of  $\text{CO}_2$  adsorption due to high affinity of elements toward  $\text{CO}_2$  molecules, mainly at

elevated temperatures. Thus, introduction of alkaline metals (Ca, Mg) onto the activated carbon will produce a basic surface that has strong affinity towards CO<sub>2</sub> molecules (Yong et al., 2019).

Hosseini et al. (2019) who studied the performance of CO<sub>2</sub> adsorption onto Cu/Zn modified activated carbon suggested that the catalytic surfaces provide active sites to adsorb a single CO<sub>2</sub> molecule. The oxygen atoms in CO<sub>2</sub> molecules will attract and chemisorbed onto the cationic Cu<sup>2+</sup> and Zn<sup>2+</sup> on the carbon support, and shorter distance between the cations and CO<sub>2</sub> adsorbates will favour the adsorption process due to lesser adsorption energy (Hosseini et al., 2019). The practice of metal impregnation is otherwise called wet impregnation, which involves a mixing process of activated carbon with inorganic salt that contain specified metal, and followed by calcination process at high temperature (Yong et al., 2019). Aside from wet impregnation, solid-solid mixing of carbon materials with metal-based precursors for direct pyrolysis has been proposed lately (Haro et al., 2022). The purpose is to develop porous adsorbent at the same contain active chemical for an efficient gas separation. Furthermore, this one-step is promising as it prevents multi-stage process that involves carbonization, activation and subsequent modification. As such, Przepiorski et al. (2018) studied one-stage pyrolysis of the mixture of PET waste with either dolomite or limestone at high temperature of 800 to 1000 °C under inert environment. During the process, dolomite and limestone decomposes to form CaO and MgO while releasing CO<sub>2</sub>, and PET waste will be converted to biochar.

#### 2.31.5 Advantages of phosphoric acid over zinc chloride

The classical chemical used on a large scale for chemical activation was zinc chloride due to its efficiency and simplicity of the process. However, its use is on the decline,

because of the problems of corrosion, ineffective chemical recovery and environmental disadvantages associated with zinc chloride. This process produces activated carbons with large porosity, although the pore size distribution is determined for a given precursor mainly by the degree of impregnation, that is, the larger the degree of impregnation, the larger the average pore size of the final carbon. The activated carbon obtained using zinc chloride however, requires much of its concentrations to attained well developed pore activated carbon and also cannot be used in pharmaceutical and food industries as it may contaminate the products (Gonzalez et al., 2020). Hence, there have been many studies reporting the activation of carbon using phosphoric acid, because of the disadvantages associated with zinc chloride, phosphoric acid is used largely in industry to impregnate lignocellulosic materials, mainly wood.

Also, phosphoric acid includes important changes in the pyrolytic decomposition of the lignocellulosic materials since it promotes depolymerization, dehydration and redistribution of constituent biopolymers, favouring the conversion of aliphatic to aromatic compounds at temperatures lower than when heating in the absence of an additive, thus increasing the yield. One of the reasons why activation with phosphoric acid has become popular is because of the environmental consideration and its cost effectiveness. It also resulted in the product that does not require washing or little.

### 2.32 Optimization in Chemical Engineering

The field of chemical engineering is in constant change, confronted with series of challenges. Available calculation tools and software packages are constantly evolving to meet up with the engineering tasks. In fast everyday life, it is a considerable challenge for a chemical engineer to know which tool can serve best for solving a certain problem. However, different packages can be applied to solve typical problems in mass and energy balance, fluid mechanics, heat and mass transfer, unit operations,

reactor engineering, and process and equipment design and process performance evaluation (Lathouwers and Bellan., 2020).

### 2.32.1 Process simulators

The simulation, design, and optimization of a chemical process plant, which encompasses several processing units interconnected by process streams, are the core activities in process engineering. These challenges require performing material and energy balancing, sizing of equipment, and calculation of cost requirement. A computer package that can accomplish these duties is known as a computer-aided process design package or simply a process simulator. The process simulation market underwent severe transformations in recent times. Relatively few systems have survived and they are still invoked: CHEMCAD, Aspen Plus, Aspen HYSYS, and Design Expert.

#### 2.32.1.1 Aspen plus and hysys

These are two similar software packages with essential functionalities that are used as process simulator and most widespread among chemical engineers. AspenTech has a wide array of modelling tools, among them are Aspen Hysys and Aspen Plus. Aspen HYSYS (or simply HYSYS) is a chemical process simulator used to mathematically model chemical processes, from unit operations to full chemical plants and refineries. HYSYS is able to perform many of the core calculations of chemical engineering, including those concerned with mass balance, energy balance, vapor-liquid equilibrium, heat transfer, mass transfer, chemical kinetics, fractionation, and pressure drop. HYSYS is used extensively in industry and academia for steady-state and dynamic simulation, process design, performance modelling, and optimization of process. Aspen Plus is a process modelling tool for conceptual design, optimization, and performance monitoring for the chemical, polymer, specialty chemical, metals and

minerals, and coal power industries. It can also be used for mass and energy balances, physical chemistry, thermodynamics, chemical reaction engineering, unit operations, process design and process control.

#### 2.32.1.2 Design expert

Design Expert is a piece of software designed to help with the design and interpretation of multi-factor experiments. It offers the latest technology for multi-factorial data analysis and design of experiments in a very user-friendly environment. This software walks you through the classic stages of the screening, optimization (RSM) and validation and equally provides the flexibility to map complex tasks in a “simple” experimental design. Thus, it allows you to save time and costs of developing new products while achieving the best process conditions (Ajueyitsi, 2018).

Design-Expert provides the rotatable 3D plot. It helps you to visualize so-called response surfaces. The optimum is reached via the numerical optimization function. Therefore, the optimal factor settings are determined simultaneously. The optimization platform controls multivariate optimization to allow, for example, multiple target values being simultaneously optimized. According to Lathouwers and Bellan, (2020), argument for design expert software includes:

- i. Rotatable 3D graphics, interactive contour diagrams (isolines), best ternary representation,
- ii. classical experimental designs, d-optimal for screening and i-optimal for RSM,
- iii. Latest split-plot designs and definitive screening designs,
- iv. Best optimizing function (multiple target variables and optimizing with respect to factor settings),

v. Fitted function exported as a formula to Excel vi. Error

propagation (propagation of error) helps you to find robust settings vii.

Indispensable for formulation optimizing

#### 2.32.1.3 MS Excel

It is a known fact that Microsoft Office Excel is a spreadsheet application that features calculation, graphing tools, tables, and a macro programming language - Visual Basic. The main advantage of Excel is that it is available and is widely used in industry and academia (Ajueyitsi, 2018). Thus, it is a perfect tool or interface not only to perform calculations but also to connect different software so that the end user can interact with Excel, and behind the scenes, other software such as MATLAB is running and reporting the results back to Excel.

#### 2.32.2.4 Matlab

MATLAB is a programming language. Its operation is based on the use of .m files that can be divided in two classes, scripts and functions. A script is basically a number of operations that we want to perform in a certain sequence. Functions are a particular type of scripts that must begin with the word “function” at the top of them. Functions can be user-defined or typical operations such as equation solving or differential equations. Within MATLAB, we have all the algebraic, statistical functions predefined along with plotting capabilities.

### 2.33 Summary and Research Gap Identified

The concept of biochar was implemented by pre-Columbian Amazonian tribes all over the amazon basin. The soil, called ‘Terra Preta’, was found to be rich in mineral residue and decomposed organic material which made it fertile enough to sustain continuous crop yields. Biochar has been popularised as a mechanism to aid improve fertility of

soil, as well as reduce the effects of climate change by acting as a tool for carbon sequestration in soil. A review of the existing applications of biochar showed that it had basic applications in both agricultural and environmental areas of research.

A review of the various production methods provided some insight into the cost effectiveness, time consumption, advantages, and disadvantages of the different techniques. Slow pyrolysis was found to require very few resources and be the most cost effective, but studies have shown that fast pyrolysis can optimise the yield of useful byproducts such as bio-oil and syngas, which can act as alternative fuel sources. Comparing the research on biochar production methods shows the need to optimise a production method that provides the greatest quantity of effective biochar, while also producing usable by-products to ensure the product is as sustainable as possible. It was concluded that although few data exist, repeatability of the results are needed to affirm the effectiveness of slow pyrolysis conditions for biochar production.

Biochar publications have increased rapidly in the recent years following its applications in many areas of human endeavours. Some of these studies include evaluating the physical and chemical characteristics of biochar used as a soil amendment (Biederman and Harpole 2018), soil remediator (Qiu et al., 2020; Waqas et al., 2021), raw material for catalyst development (Dehkhoda and Ellis 2017), modifier agent in the controlled release formulations of nutrients ((Gonzalez et al., 2020), and immobilization support (Gonzalez et al., 2018b). Little is known about the production of biochar as basis for activated carbon formation, except recently, where activated carbon was produced from risk husk derived biochar (Park, 2018) and used for removal of dye.

The physicochemical properties of biochar such as pore diameter, size distribution, total surface area, and nutrient content are closely related to the pyrolysis conditions and the original biomass feedstock (Cheng et al., 2017). Undoubtedly, pyrolysis temperature

causes chemical and physical changes to the feedstock such as decreasing the H/C and O/C ratios. For instance, during pyrolysis, high temperature increases the specific surface area (Devi and Saroha, 2019) but decrease the amount of biochar produced, and they cause demethylation and decarboxylation reactions that result in high amounts of carbonized and aromatic structures (Chen et al., 2021; Devi and Saroha, 2019).

There are few studies on the interaction among the pyrolysis conditions on biochar production for carbon dioxide sequestration. Presently in literature, some of the studies addressing the effect of pyrolysis temperature, residence time and raw material include: Allyson 2017, Simeon et al., 2019 and Dominguez et al., 2017. However, these parameters have been studied separately and not in collaboration. Few studies of joint significance study of pyrolysis conditions include the recent work of Gonzalez et al., (2020) using oat hull. This project will aim to provide substantial analysis of the characteristics involved (optimization of process conditions and kaolin addition) in producing effective biochar in terms of high yield as prerequisite for activated carbon production. Furthermore, one step production of activated carbon was considered suitable as it eliminates cost of carbonization, activation and subsequent modification.

## CHAPTER THREE

### 3.1 Equipment and Materials

Table 3.1 lists the material, equipment and reagents used in carrying out the pyrolysis and characterization of this research report. While some are imported, some are locally sourced.

Table 3.1 List of Equipment and Materials

Equipment			Materials		
Equipment	Manufacturer	Model	Materials	Manufacturer	Model
Furnance	England	SAR-210-X	Kaolin	Kutigi	Raw
Eye Shield	England	GERHADT	Sawdust	Belad Furniture	Raw
Spatula	England	BS410	Poultry Waste	Amasco Farm	Raw
Sieve	England	SCOUT			98.9
		PRO	HCL	England	purity
		BNB-			97.8
Weighing	England	380600ml	KOH	England	purity
					97.8
Beaker	England	C31860/9	ZnCl <sub>2</sub>	England	purity
Petric			Nitrogen		99.9
Dishes	England	PYREX	gas	Lagos	purity
Pyrolyser	SEDI				

### 3.2 Research Biomass

Poultry waste was obtained at Amasco Poultry Farm in Ilorin, while Sawdust was procured at Belad Furniture workshop in Ilorin, Kwara State. Kaolin was sourced from abundant kaolin area at Kutigi, in Lavun Local Government Area of Niger State. Biomass from woody and agricultural wastes which are sawdust and poultry waste were used as the feedstock to produced biochar in conjunction with locally sourced Kutigi kaolin via slow pyrolysis. 10 kg each of the biomass procured were prepared as follows. The samples were air-dried as received prior to division and utilization in the experiment. The feedstock had undergone the sun drying and later Subsequently, the collected biomass was thoroughly washed with clean water to get rid of sand, dried at

80 °C for 6 hours in oven and then ground to powder using mortar and pestle. After that, the grounded sample were sieved through different mesh sizes ranged from 0.5 – 3.0 mm. Proximate analysis and Ultimate analysis were done at National Cereal Research Institute in Bida while

Thermo gravimetric analysis was done at Step B, Bosso Campus, Federal University of Technology, Minna. The prepared samples were used in the pyrolysis

The choice of sawdust and poultry waste was as a result of their abundant availability in the environment mostly as wastes and their respective properties as revealed by proximate and ultimate analysis coupled with information from literature. Their pyrolysis with kaolin was aimed at enhancing biochar yield, carbon retention and stability in the biochar produced. Sawdust and poultry waste are representative of the woody and agricultural waste biomass.



Kaolin



Poultry waste



Sawdust

Plate IV: Research Biomass and kaolin

### 3.3 Experimental Design

To evaluate the effect of process parameters such as temperature, flow rate, particle size and residence time with kaolin ratio on the yields of pyrolysis products, an Un-replicated 2 level Factorial Design was adopted. In order to generate the experimental design results and perform the appropriate statistical analysis, the Design Expert 12.0 (Stat Ease,

Incorporated Minneapolis, MN, USA) was used for the computational program. Each range of factor was coded to a computer language, says, -1, 0, +1 interval to represent low, middle and high levels of each parameter selected in this research.

Table 3.2: Experimental Conditions for Biochar Production

Parameters	Experimental conditions
Biomass/impregnated material	Sawdust and Poultry Waste / kaolin
Pyrolysis temperatures	300, 350, 400, 450, 500 550 and 600 °C
Particle sizes	0.5, 1.0, 1.5, 2.0, 2.5 and 3.0 mm
Residence times	10, 20, 30, 40, 50 and 60 mins
Carrier gas flow rates	0.5, 1.0, 1.5, 2.0, 2.5 and 3.0 L/min
Carrier gas	Nitrogen
Heating rate	10 °C/min

For each of the experiments, the production of biochar, bio-oil and the gaseous products obtained during the pyrolysis reaction were determined on weight basis according to the following equations:

The biochar yield equation

$$\text{Biochar yield (\%)} = \frac{(\text{ })}{(\text{ })} \times 100\% \quad (3.1)$$

The biooil yield equation

$$\text{Bio-oil yield (\%)} = \frac{(\text{ })}{(\text{ })} \times 100\% \quad (3.2)$$

The biogas yield equation

$$\text{Biogas yield (\%)} = 100\% - \text{Biochar yield} - \text{Bio-oil yield} \quad (3.3)$$

### 3.4 Characterization of Biomass and Biochar Composition

Biomass composition can be expressed on the basis of as-received, air dried or dry and ash-free (Alhassan et al., 2017). For this research work, the composition of biomass was expressed as as-received (ar) basis and thus the result of proximate and ultimate analysis can be expressed according to the below equations.

$$\text{Ultimate Analysis: } C + H + O + S + N = 100\% \quad (3.4)$$

$$\text{Proximate Analysis: } VM + FC + MC + ASH = 100\% \quad (3.5)$$

Where H, C, N, O, and S represent weight percentage in hydrogen, carbon, nitrogen, oxygen and sulphur content of biomass as received. While VM, FC, and ASH represent weight percentage of volatile matter, fixed carbon and ash content of biomass as measured from proximate analysis.

### 3.5 Preparation of Y-Alumina from Kaolin

#### 3.5.1 Clay beneficiation

The raw Kaolin clay sample was sourced from high mountain rock in Kutigi town, Niger State. The clay sample was ground using wooden pestle and mortar. The ground clay sample was wet beneficiated using 100 g/L clay to water ratio (Salahudeen et al., 2019) and allowed to settle overnight. The fine kaolin slurry was dewatered until a solid clay cake was obtained, then sieved with continuous manual shacking. The oversize was further ground followed by sieving on the same sieve. The procedures were repeated till the entire clay sample passed through the sieve of 3 mm. Subsequently, 200 g, 300 g and 400 g samples were wet beneficiated and that with highest yield was used.

### 3.5.2 Metakaolinization

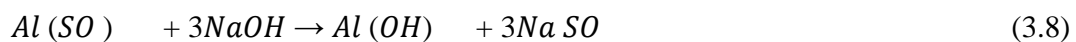
Ground clay sample was subjected to calcinations. A muffle furnace with a wide temperature range was used. The heating was carried out at 700 °C for 1 h to activate the clay before acid treatment, which is reported in some previous work to be the recommended conditions for activation (Panda et al., 2020). The endothermic dehydration resulted in the formation of metakaolin and water

### 3.5.3 Acid leaching

Convictional activation approach was adopted in this research. This involved contacting the calcined clay with strong acid and then calcining at 500 °C using liquid to solid ratio of 10 ml/g (Panda et al., 2020). To this effect, 1M H<sub>2</sub>SO<sub>4</sub> solution was prepared, from which 500ml was carefully added to 50 g of kaolin. The resulting mixture was stirred with the aid of magnetic stirrer at 100 °C for 5 hrs. During the leaching of metakaolin in H<sub>2</sub>SO<sub>4</sub> the alumina in metakaolin is extracted and dissolved in H<sub>2</sub>SO<sub>4</sub> which leads to formation of aluminium sulphate.

### 3.5.4 Precipitation

This involves the addition of caustic soda to the solution of aluminium sulphate to precipitates aluminium hydroxide. Then the mixture was cooled and excess acid first removed through several washing with distilled water. This was followed by calcination at 700 °C for 1hr which produces  $\gamma$ -alumina. Cooled and sieved for use.



### 3.6 Evaluation of the Effect of Process and Non-Process Parameters on Biochar

## Production Using a Prototype Reactor

The slow pyrolysis of sawdust (Maple) and poultry waste (litter) were carried out in a fixed bed reactor in a poor oxygen environment as shown in Plate V. The sample was fed into a pyrolyzer with an inner diameter of 50 mm and 800 mm long. The biomass pyrolysis reactor was connected to an electrical power source which can be regulated with on/off controller. Water cooling device and separation apparatus of pyrolysis vapours were improvised to collect bio-oil and to separate non-condensable gas. About 20 g of sample in the reactor were heated and pyrolyzed at different set temperatures. After reaching the desired set temperature, they were maintained for a sufficient period for complete pyrolysis process to be attained. A range of set temperature 300, 400, 450, 500, 550, and 600 °C, a series of residence time 10, 20, 30, 40, 50 and 60 mins, different volume of Nitrogen flow rates 0.5, 1.0, 1.5, 2.0, 2.5 and 3.0 L/min and a tested range of particle sizes 0.5, 1.0, 1.5, 2.0, 2.5 and 3.0 mm were respectively investigated to ascertain both the effects of operating and non-operating pyrolysis conditions on biochar production. The feeding with biomass was carried out manually. For measurement, rectangular crucibles have been used.

The set up for the horizontal fixed bed reactor for the pyrolysis of sawdust and poultry waste impregnated with kaolin was shown in Plate V. The design was based on the actualization of pyrolysis products but the keen interest is biochar. Pyrolyser was designed and constructed at the Scientific Equipment Development Institute, Minna, Niger State. Analytical grade Nitrogen gas was purchased in Lagos.



Plate V: Pyrolysis Experimental Set up

- 1- Flow Meter 2- Gas Cylinder, 3.-Gas inlet point, 4-pyrolyser containing biochar, 5-Temperature regulator, 6-Bio-oil collector, 7- Gas outlet, 8- Bench, 9- Condenser.

Every sample of biomass was placed on the crucible and introduced into the reactor. Each test experiment was carried out with 20g of sample by varying a particular operating parameter while keeping others constant. The biochar in the reactor was naturally cooled down to the room temperature by switching off the reactor. The produced biochars were weighed and packaged in a sealed transparent plastic container to prevent it from absorbing moisture from the environment. The bio-oil was equally weighed while the gas produced in the process was calculated by subtracting both the mass of biochar and bio-oil yields from the mass of the feedstock charged to the reactor. Since the biomass (sawdust and poultry waste) was pyrolyzed in a sealed reactor, it is expected that the water vapor and CO<sub>2</sub> produced in dry and pre-pyrolysis processes would drive away the initial oxygen inside the reactor. There would be no air into the reactor during process of pyrolysis. As such, the effect of air oxidation of carbon on the characteristics of biochar could be ignored. Temperature being a major driven force in

pyrolysis was varied within the range of 300 °C to 600 °C to ascertain maximum yields. It was at the range of maximum yield temperature and other parameters that different concentrations of Kaolin were impregnated into biomass and pyrolyzed to enhance yield, carbon retention and stability in biochar.

### 3.7 Characterization of Different Grades of Biochar Produced

After carrying out the slow pyrolysis of sawdust and poultry waste in a batch fixed bed reactor, the following characterization were performed on the resulting charred product

- i. Proximate analysis was conducted to determine moisture content, ash, fixed carbon and volatile matter of produced biochar
- ii. Elemental analysis (C, H, O, N, S) was performed using a Flash 2000 Elemental Analyser (Thermo Fisher Scientific, Waltham, MA). Oxygen content was not determined directly but calculated by difference.
- iii. HHV (higher heating value) of biochars and feedstock materials were determined using an established empirical relationship as a function of process temperature
- iv. BET surface area was measured using nitrogen gas adsorption accordingly to determine the surface area and pore volume of the biochars
- v. SEM analysis was carried out to visualize the morphological structures of the biochars
- vi. FTIR analysis was aimed to determine the functional groups present in the original feedstock and the produced biochar

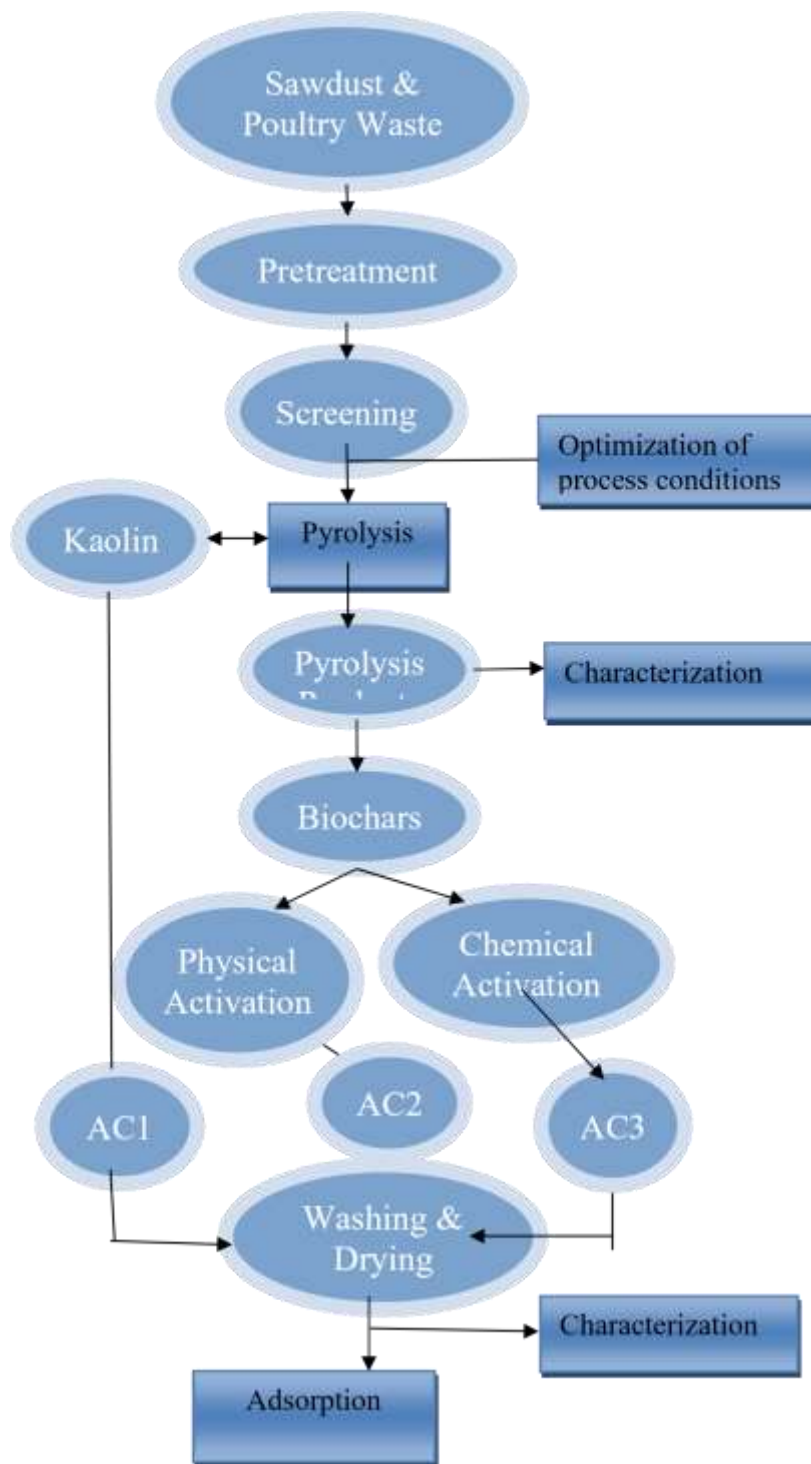


Figure 3.1 Flow Chart of Experimental Procedures

### 3.8 Production of Activated Carbon from Biochar Produced

In order to produce and activate the biochar, 100 g each of sawdust and poultry waste (SBC and PBC) was suspended in 1M  $H_3PO_4$  solution, continuously stirred on a magnetic

stirrer (at 60 °C for 5 hrs) and then filtered. The resulting biochar residues were thereafter washed several times with deionized water the solution pH attained almost a neutral value. Finally, the washed samples were dried at 110 °C overnight in an oven and the resulting samples were named Sawdust Acid Modified Activated Carbon (SAMAC) and Poultry Waste Acid Modified Activated Carbon (PAMAC) respectively. The same procedures were undertaken with the use of 1M NaOH solution with Sawdust and Poultry wastes biochars to obtain Sawdust Base Modified Activated carbon (SBMAC) and Poultry waste Base Modified Activated Carbon (PBMAC). While the Sawdust Unmodified Activated Carbon and Poultry waste Unmodified Activated Carbon were obtained from direct catalytic pyrolysis of SBC and PBC with metakaolin to obtain SUMAC and PUMAC respectively.

#### 3.8.1 Characterization of metakaolin and Activated carbon produced

To ascertain the desired properties of activated carbon produced, BET analytical technique was employed to measure and provide data on the specific surface area which relate to the reactive surface of the activated carbon, including the pore size distribution. Mineral compositions and crystallinity nature of metakaolin was obtained with the use XRF and XRD analysis. The measured peak position and intensities showed a particular crystalline phase present in metakaolin. Identification was accomplished by comparing the measured patterns with the entries in reference data base using a search-match algorithm.

#### 3.9 Adsorption Kinetics Studies

Adsorption kinetics involves the study of the experimental conditions that influences the rate of an adsorbate into an adsorbent. Pseudo-first-order, pseudo-second-order,

intraparticle diffusion and Elovich model are the majorly examine adsorption kinetic model use to described the mechanism of adsorbate uptake into an adsorbent (Moradi et al., 2019). This study examines intra-particle diffusion and Elovich models to describe the experimental data.

### 3.9.1 Intra-particle diffusion model

The intra-particle diffusion model according to Ho et al. (2020) is expressed by Equation 3.10. Accordingly, the adsorption process obeys the intra-particle diffusion model if a straight linear plot that passes through the origin was observed (Romero et al., 2018).

$$q = k_{id} t^{1/2} + C$$

(3.10) where,  $q_t$  = amount of the adsorbate adsorbed in mg/g at time  $t$ ,  $k_{id}$  = the intra-particle rate constant (mg/g.min<sup>1/2</sup>),  $C_i$  = intra-particle diffusion constant (mg/g)  $t$  = contact time (min<sup>1/2</sup>).

### 3.9.2 Elovich model

The model assumes that the rate of adsorption of solute decreases exponentially as the amount of adsorbed solute increase. As the system approaches equilibrium,  $t \gg 1/\alpha\beta$ , the linearized form of

Elovich model is expressed according to Equation (3.11)

$$q = -\ln(\alpha\beta) + \alpha \ln(t) \tag{3.11}$$

The graph of  $q_t$  vs  $\ln(t)$  helps to determine the nature of adsorption on the heterogeneous surface of the adsorbent, whether chemisorption or not, and a number of gases have been reported to follow the Elovich kinetics model.

where  $\alpha$  = the initial adsorption rate (mg/g.min), and  $\beta$  = desorption constant.  $t$  = time (min),  $q_t$  = the amount of adsorbate adsorbed in mg/g at equilibrium and at time  $t$ .

### 3.10 Optimization Software

Optimization is the discipline of adjusting pyrolysis process so as to optimize (make the best or most effective use of) some specified set of parameters without violating some constraints. This is considered one of the best quantitative tools in decision making during pyrolysis experiment. The goal is to maximize the biochar production while keeping all others within their constraints (bio-oil and biogas to be minimized). The functional relationships between the responses (biochar, bio-oil and biogas) and the independent variables (temperature, flow rate, particle size, residence time and kaolin ratio) were quantified by means of estimated parameters of the regression model. The computational software (Design Expert version 12.0) adopted for the optimization purpose divided the coded factor into low, mid and upper points corresponding to -1, 0 and +1 languages understood by computer. Temperature had its points as 300, 450 and 600 °C, flow rate 0.5, 1.75 and 3 L/min, particle size 0.5, 1.75 and 3 mm, residence time 10, 35 and 60 min and kaolin 5, 17.5 and 30 g.

## 4.1 Characterization of the Biomass and Kaolin

## 4.1.1 Proximate and ultimate analysis of biomass

Table 4.1 shows the Proximate and Ultimate constituents of the sawdust and poultry waste to determine their compositions. Usually, the proximate analysis gives the moisture content, ash content, fixed carbon content and volatile matters, while ultimate analysis aims to provide carbon, hydrogen, oxygen, nitrogen and sulphur content of biomass under consideration.

Table 4.1: Proximate and Ultimate Analysis of Biomass

Properties	Sawdust (%)		Poultry Waste (%)	
	Present Study	Erta and Alma (2017)	Present Study	Vamvuka and Zografos (2021)
Moisture Content	3.56	-	1.4	-
Ash Content	1.49	0.03	15.0	17.7
Volatile Matter	66.63	88.4	32.0	26.7
Fixed Carbon	28.32	11.6	51.6	55.6
Carbon	72.32	50.5	64.72	55.9
Hydrogen	14.36	6.7	13.82	8.2
Nitrogen	3.19	0.03	4.82	10.6
Oxygen	9.94	42.8	16.43	6.2
Sulphur	0.19	0.17	0.21	1.1

The proximate analysis of the sawdust shows that it contains moisture Content of 3.56 %

(dry basis), Volatiles matters (66.63 %wt), hydrogen (14.36 %wt) and Oxygen (9.94 %wt). The difference in the values reported in literature (Erta and Alma., 2017), could be affiliated to either as received, dry ash free basis and origin of the feedstock. 28.32

% fixed carbon content and 60.6 % volatiles provide measure of the ease with which the biomass can be ignited or oxidized. The values of sulphur and nitrogen are small and thus the sawdust can be accepted to be the future source of sustainable green energy because it contains less sulphur and nitrogen (Tripathi et al., 2019). Similarly, the properties of Poultry waste were listed in Table 4.1. The proximate and ultimate analysis shows that Poultry waste have volatile content (32.0 % wt), carbon (64.72 % wt), and hydrogen (13.82 % wt). The presence of sulphur and chlorine in biomass is not desirable in combustion properties. Chlorine and sulphur are the major contributing factor to ash formation as they facilitate the mobility of inorganic compounds from the fuel to surfaces where they form corrosive compounds (Wang et al., 2020). The ash content of sawdust (woody biomass) as might be expected is significantly lower than that of poultry waste (15.0 %) which is also consistent with previous study (George and Betzy, 2018).

#### 4.1.2 Thermogravimetric analysis of biomass

Thermogravimetric degradation of sawdust and poultry waste samples was carried out in order to know the thermal properties of the samples. Figure 4.1(a) shows the normalised weight loss for the sawdust and poultry waste as a function of temperature. The degradation started from 29 °C to 887 °C. The first mass loss ( $29 < T \leq 100$  °C) is due to moisture and some extractive compound evaporation. The second one ( $100 < T \leq 400$  °C) is mainly related to hemicelluloses and cellulose thermal degradation. Lignin is a more stable component presenting a large range of thermal degradation (from 250 °C to 500 °C or even higher temperature depending on biomass) and in this way the third degradation step ( $400 < T \leq 600$  °C) is attributed to lignin degradation.

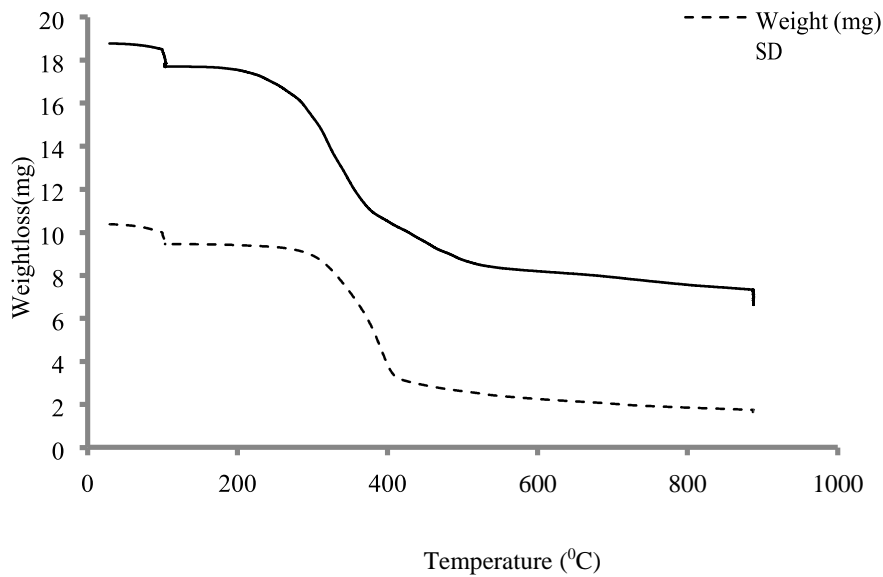


Figure 4.1(a): TGA of Sawdust and Poultry Waste

#### 4.1.2: X-ray fluorescence analysis of the kaolin

The chemical analysis of the Kutigi kaolin as shown in Table 4.2 indicates that it contains alumina, silica, iron and calcium in major quantities and other elements in minor quantities. Result as presented shows that percentage of SiO<sub>2</sub> is 42.67 % while that of Al<sub>2</sub>O<sub>3</sub> is 34.0 %. The metal oxide compositions of Kutigi kaolin as presented is close to the reported literature value (Anex et al., 2020). The little variation could be attributed to different geographical and geological formation of kaolin. They reported that kaolin<sub>3</sub> has approximately 45 % SiO<sub>2</sub> and 37 % Al<sub>2</sub>O<sub>3</sub>. Also, in their report are 0.29 % Fe<sub>2</sub>O<sub>3</sub>, 0.17 % CaO, 0.96% Na<sub>2</sub>O, 0.50 % K<sub>2</sub>O, and 0.95 % MgO. The presence of these essential compounds in Kutigi kaolin are believed to enhanced pyrolysis product distribution with much regard to biochar production. Just like in some biomass, when Al<sub>2</sub>O<sub>3</sub> and CaO were added, the weight changed positively which indicated the presence of this mineral matter.

Table 4.2: XRF of Kutigi Kaolin

Compounds	Values (wt%)

SiO <sub>2</sub>	42.67
Al <sub>2</sub> O <sub>3</sub>	34.0
Fe <sub>2</sub> O <sub>3</sub>	1.925
CaO	4.075
Mn <sub>2</sub> O <sub>3</sub>	0.004
TiO <sub>2</sub>	3.141
LSF	2.783
CaCO <sub>3</sub>	7.843
L.O.I	3.57

#### 4.1.4 X-ray diffraction analysis of the kaolin

The structural transformations that took place in the raw Kutigi kaolin clay material due to acid treatment were studied using X-ray diffraction analysis. Figure 4.1(b) shows the XRD diffractograms of the untreated and acid modified kaolin. The raw clay shows welldefined reflections at  $2\theta$  value of  $29^\circ$  and  $43^\circ$  which are typical characteristic peaks of kaolinite. Upon acid treatment the peak intensity of kaolin was observed to decrease progressively. This is due to the structural disorder that occurred owing to the acid treatment, which affects the crystalline character of the clay. The narrowing of the peak may be related to the increase of crystallite size (Downie et al., 2019).

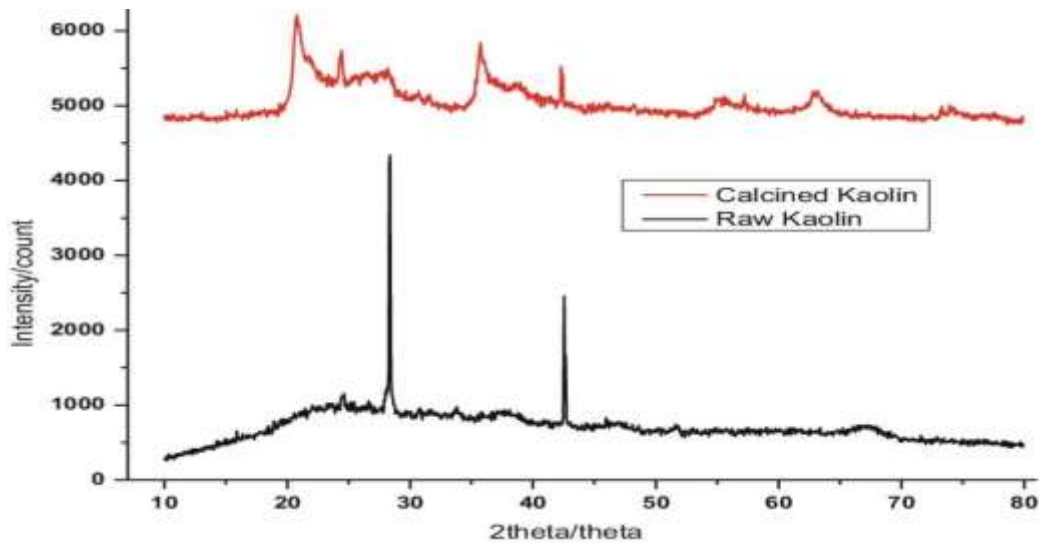


Figure 4.1(b): XRD of Kaolin and Metakaolin

## 4.2 Evaluation of the Effect of Process and Non-Process on Parameters on the Production of Biochar

### 4.2.1 Effect of temperature on the product yields

Conventionally in pyrolysis process, three phases are produced during the thermal transformation of biomass under an inert atmosphere which includes biochar (solid), biooil (tar, condensable vapours etc) and biogas ( $\text{CO}_2$ ,  $\text{CO}$ ,  $\text{CH}_4$  and non-condensable gases).

One of the key factors that affect the distribution among the three products is temperature. Higher biochar yields are typically generated at low temperature or low heating rate (Alhassan et al., 2017) while under higher temperature or fast heating rates, the process produces high yields of either liquid or gas (Bouraoui et al., 2017). To determine the effect of pyrolysis temperature on the biochar yield, final temperature of 300, 400, 450, 500, 550 and 600 °C were examined under nitrogen flow rate of 1.0 L/min, residence time of 10 min, heating rate of 10 °C/min and particle size of 3.0 mm. Figure 4.2 shows the effect of temperature on the product yields. The yield of biochar

in pyrolysis experiment decreased from 39.2 % to 20.1 % corresponding to 400 to 600 °C.

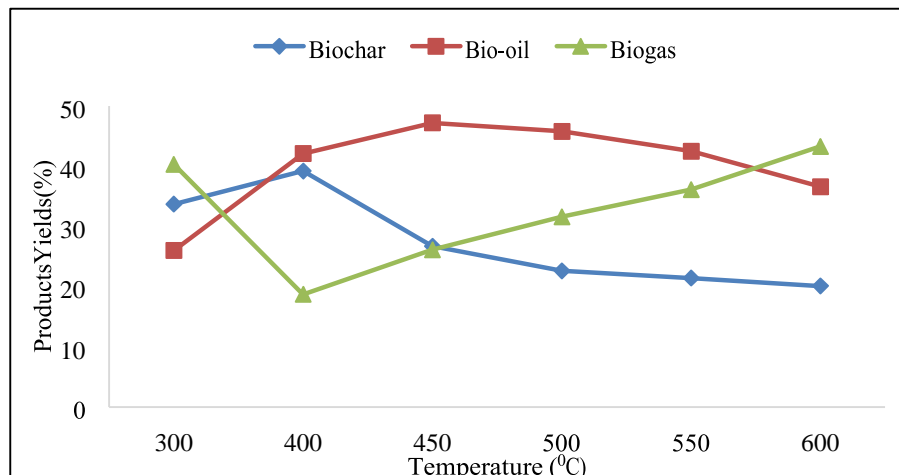


Figure 4.2: Effect of Temperature on Sawdust Pyrolysis

It was observed from Figure 4.2 that the yield of biochar decreases (39.2 to 21.4 %) as the temperature increased from 400 to 550 °C. The decrease is in agreement with the reported literature values (Shariff et al., 2017). This was probably due to decomposition of the lignocellulosic material at this temperature range (Intani et al., 2018). When the pyrolysis temperature further increased from 550 to 600 °C, the biochar yields only decreased from 21.4 % to 20.1 %. This result indicated that most of the volatile fraction had been earlier removed at lower temperatures.

Previous study on the biomass pyrolysis have shown that the increased temperature leads to decreased biochar yield, primarily due to gasification reaction occurring at the higher temperature (Encinar et al., 2021). The higher pyrolysis temperature also resulted in more liquid cracking, resulting in more production of gaseous product and lower yield of tar and/or biochar (Zanzi et al., 2021). The initial increase in the bio-oil yield from 26.0 % to 45.8 % corresponding to 300 to 500 °C could be as a result of degradation of lignin content of sawdust which usually occurs at such a high

temperature. Further increase in temperature to 600 °C led to reduction of bio-oil yield to the tune of 36.6 %.

This can be attributed to the secondary reaction of pyrolysis vapours at elevated temperature (Jung et al., 2020). The yield of non-condensable gases increased with increasing reaction temperature. This trend, particularly at higher temperatures (500 to 600 °C) could be due to further cracking of the vapor and more decomposition of biochar.

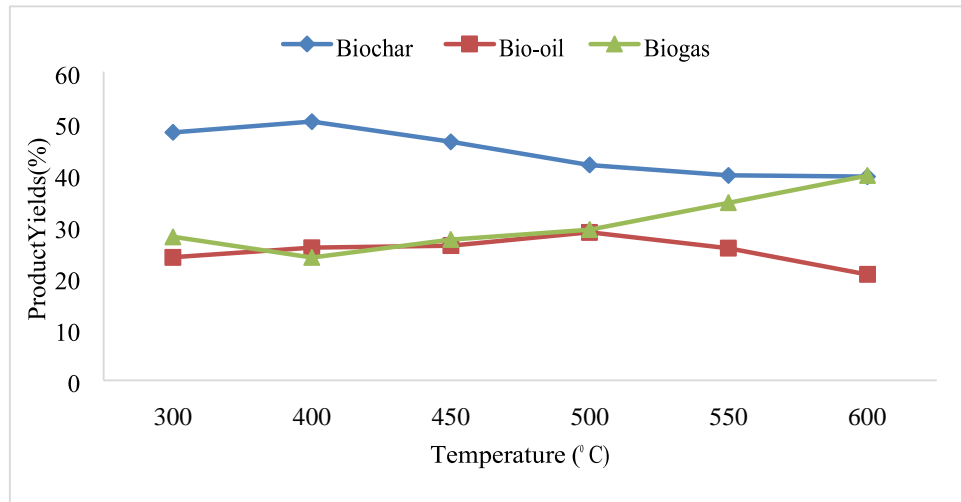


Figure 4.3: Effect of Temperature on Poultry Waste Pyrolysis

Figure 4.3 shows the product yield distribution on the pyrolysis of poultry waste under the same conditions of sawdust. Similar to that of sawdust, the results shows that biochar yields decrease with increasing pyrolysis temperature and tend to stabilize at higher temperatures. This observation is in conformity with the conclusions of Hossaini et al. (2018) on sludge biochar and Keiluweit et al. (2019) on risk husk. Poultry waste yielded biochar of 50.3 % as compared to optimum of 39.2 % obtained for sawdust derived biochar. This is not surprising as alkali metals contained in the poultry waste are known to catalyse pyrolysis reactions which enhance more char formation whereas the yield of bio-oil is low. Co-incidentally, at 600 °C, close marks of 39.6 % and 39.8 % were respectively obtained for biochar and biogas at the expense of 20.6 % bio-oil yield. Generally, biochar product yield decreased with increasing pyrolysis

temperature. This is not surprising since the devolatilization of organic materials progresses with increasing temperature.

#### 4.2.2 Effect of nitrogen flow rate on product yields

The purpose of the carrier gas (purging or sweeping gas) is to remove the volatiles from the pyrolysis environment during the biomass pyrolysis process. In other word, to avert secondary reaction of the primary biochar with the released volatiles in the reaction zone.

Usually, inert gases like Nitrogen, Argon, H<sub>2</sub> and CO<sub>2</sub> are commonly used. Kerng et al. (2018) reported that the use of H<sub>2</sub> during pyrolysis increases the yield of tar and may change the char's morphology significantly hence the choice of nitrogen. To investigate the effect of the Nitrogen flow rate on the biochar yield, the pyrolysis experiments were carried out at 400 °C, heating rate of 10 °C/min, residence time of 10 min, particle size 3.0 mm with different Nitrogen flow rates of 0.5, 1.0, 1.5, 2.0, 2.5 and 3.0 L/min. The biochar yield of 30.7 % was achieved when the nitrogen flow rate was set at 0.5 L/min.

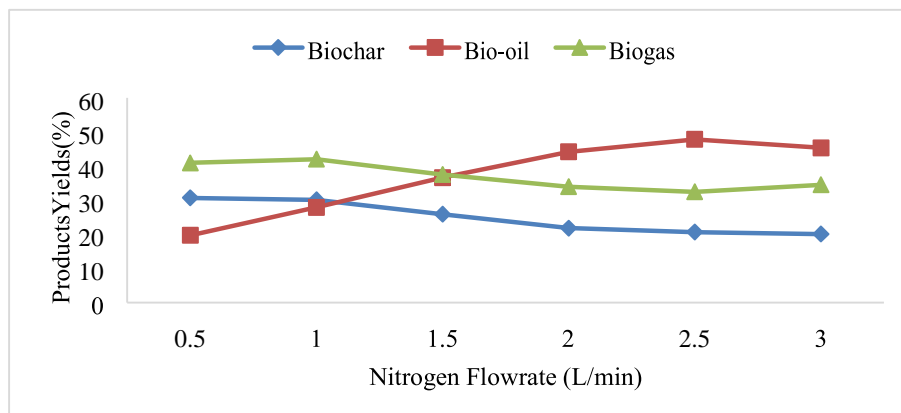


Figure 4.4: Effect of sweeping gas flow rate on sawdust pyrolysis

A close value of 30.9 % of biochar was also achieved at flow rate of 1.0 L/min and subsequent increase of Nitrogen flow rates from 1.5 L/min to 3.0 L/min drastically reduced the yield of biochar from 25.9 % to 20.1 %. It would be reasonable to suggest that at lower nitrogen flow rate, the velocity of the sweeping gas was slightly lower to

transfer the hot vapours into the condensation section, hence, more yield of biochar. The yield of bio-oil increases from 19.7 % to 47.8 % corresponding with increasing Nitrogen flow rate from 0.5 to 2.5 L/min. Fassinou et al. (2020) suggested that the sweeping Nitrogen gas had removed the hot vapour quickly and reduced the residence time of hot vapours. As such, it had contributed to the higher mass of bio-oil obtained. Gerçel (2017) had reported that the minimization on the secondary reaction was achieved by higher velocity of the sweeping gas that transferred the hot vapours into the condensed bio-oil. However, the bio-oil seemed reduced when the Nitrogen flow rate was increased from 2.5 to 3.0 L/min. This could be due to insufficient condensation of the hot vapours by the cooling apparatus improvised to the system. Erta and Alma (2017) support the assertion. The decreased trend of bio-oil over increasing flow rates (2.5 to 3.0 L/min) seemed to increase the production of biogas. It could also be suggested that certain volume of condensable gases had transferred and escaped the condensation due high velocity of the sweeping gas.

For the case of poultry waste, as shown in Figure 4.5, the maximum biochar yield was 50.1 % at a low flow rate of 1.0 L/min. This decreases to 33.1 % as the flow rate attain 3.0 L/min. Putun et al. (2020) affected by the flow rate of the sweeping gas. In summary, biochar yield decreased with increasing flow rate due to rapid removal of the pyrolysis vapours from the reaction zone. In this study, low Nitrogen flow rate of 1.0 L/min gave the optimum yield of biochar and this condition was used in the subsequent experiments.

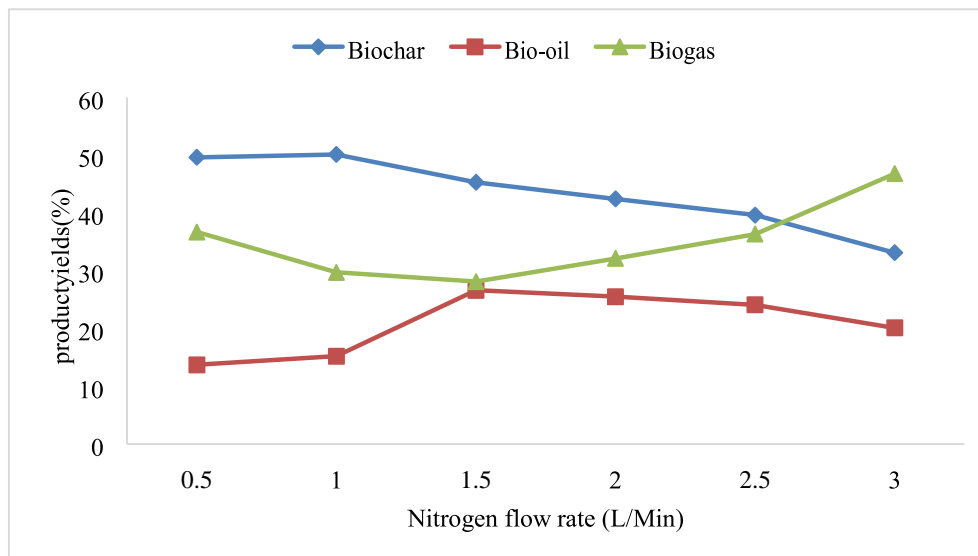


Figure 4.5: Effect of Sweeping gas flowrate on poultry waste pyrolysis

#### 4.2.3 Effect of feedstock particle size on pyrolysis product yield

Feed particle size is another factor that influences pyrolysis product distribution. As shown in Figure 4.6 the yield of biochar increases from 21.5 % to 27.5 % corresponding to 400 to 650 °C and 0.5 to 3.0 mm particle sizes. The increasing trend of biochar results was influenced by heat transfer mechanism between the biomass particles. Because as the particle size was increased, heat transfer between the particles was decreased and thus enhancing the yield of biochar and reducing bio-oil yields (36.6 to 27.9 %). The increasing and decreasing trends of biochar and bio-oil are respectively depicted in Figure 4.6. Larger particles require more time to heat by intra-particle conduction (Uzun et al., 2017) and thus eventually lead to slower heating rate and incomplete thermal decomposition which favours biochar yields (Park, 2018). As can be seen from Figure

4.6, the yield of biogas increases with progressing particle sizes. Maximum yield of 44.6 % was obtained at 3.0 mm particle size. Obviously from the Figure 4.6, at the last particle size consideration, optimum yield of biochar (27.5 %) closely corresponds to minimum yield of bio-oil (27.9 %).

Considering the carbonization of poultry waste, particle size also plays a key role as it controls the rate of heat transfer to the biomass. On increasing the particle size from 0.5 to 3.0 mm, the biochar yields correspondingly increased from 44.8 % to 52.3 %. Over the same range of particle size, bio-oil yield decreases from 28.4 % to 15.9 % while biogas production slightly increased from 26.8 % to 31.8 %. On increasing the particle size, the distance between the surface of the biomass (poultry waste) and its core increases which retards the rapid heat flow from the hot to cold region. This temperature gradient favours the biochar yield (Encinar et al., 2021). This increment trend of biochar also conformed to the conclusions of Demirbas (2018a) and Mani et al. (2020) on (5.7 to 16.6 %) and (11.8 to 23.3 %). The difference in the values could be attributed to different feedstock used.

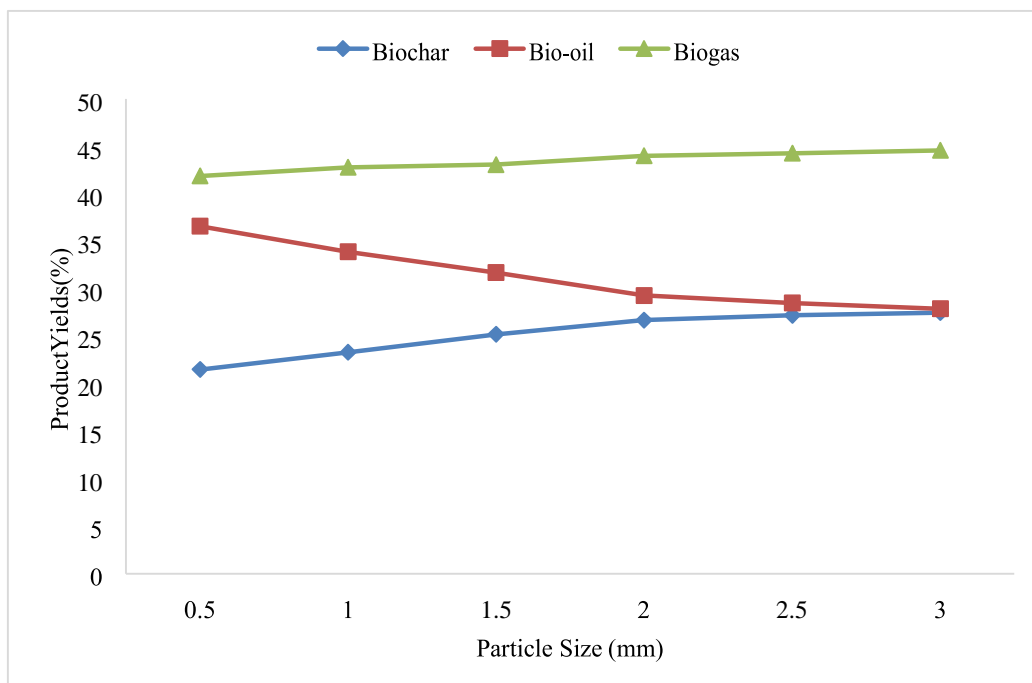


Figure 4.6: Effect of Particle size on sawdust pyrolysis

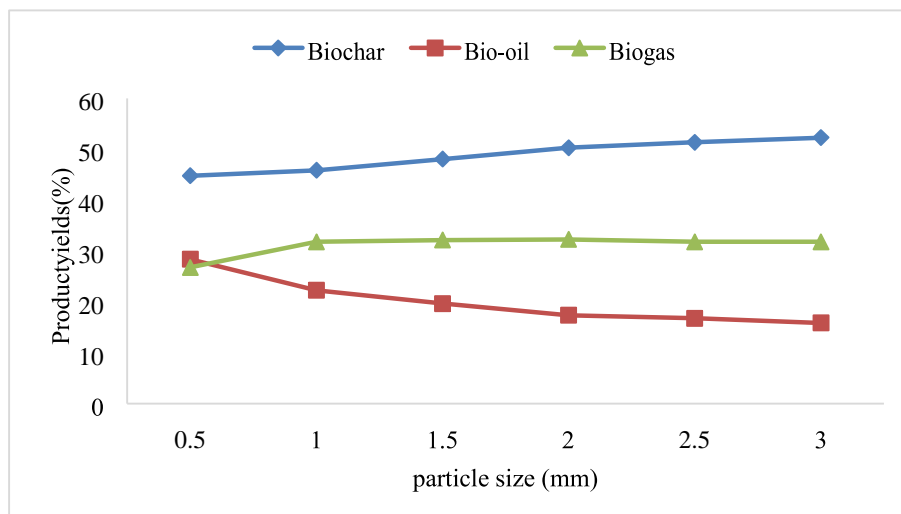


Figure 4.7: Effect of Particle size on poultry waste pyrolysis

#### 4.2.4 Effect of residence time on pyrolysis product yields

To investigate the effect of residence time on the pyrolysis of maple sawdust, a slow pyrolysis was conducted at optimum conditions of other parameters: temperature 400 °C, particle size 3.0 mm, nitrogen flow rate 1.0 L/min, heating rate 10 °C/min and 10, 20, 30, 40, 50 and 60 min residence times. Figure 4.8 shows the percentage of pyrolysis products obtained from varying residence times on sawdust pyrolysis

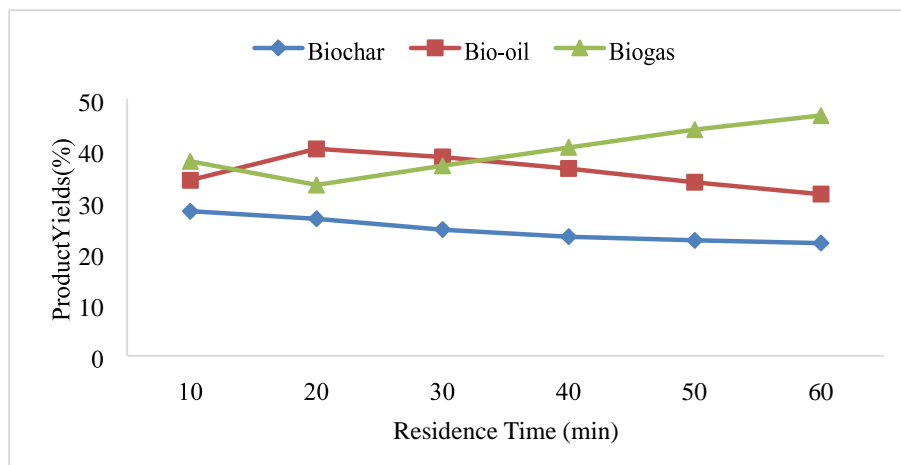


Figure 4.8: Effect of residence time on sawdust pyrolysis

The yield of biochar, as can be seen from the graph, portrayed a negative correlation as the residence time increases. In other words, biochar yields decrease (28.1 to 21.9 %) with increasing residence time (10 to 60 mins). With the negative trend, it is logical to state that greater mass would be volatilized during longer pyrolysis conditions (Zhao et al., 2017). However, the close value of biochar yields at 50 min (22.4 %) and 60 min (21.9 %) suggests the constant value of biochar yield trend for subsequent pyrolysis beyond this research value. The shorter residence time of the volatiles in the reactor caused relatively minor decomposition of higher molecular weight products (Sensoz and Angin, 2018).

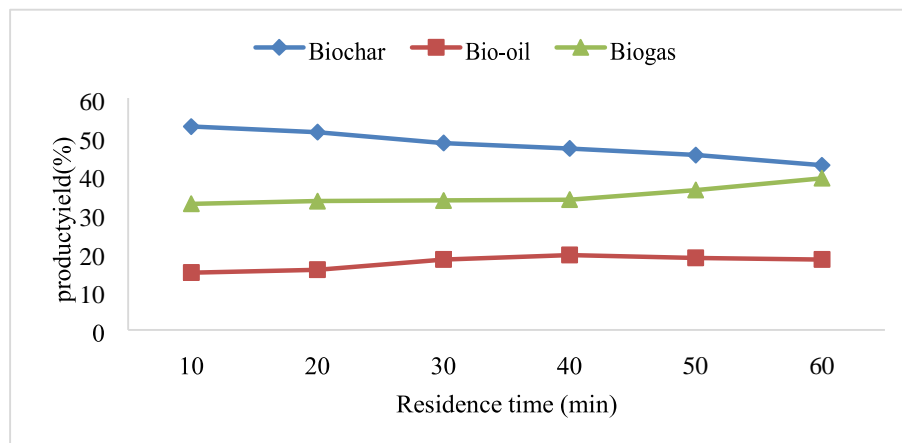


Figure 4.9: Effect of Residence time on poultry waste pyrolysis

Likewise for poultry waste pyrolysis, as depicted in Figure 4.9, a decreasing trend of biochar yield was observed from 52.6 % down to 42.6 % while the increasing trend of biogas ranges from 32.6 % to 39.2 % both corresponding to 10 to 60 min residence time. Fassinou et al. (2020) observed that at high temperature, increase in residence time results in increase in biochar while at low temperature, increase in residence time results in decrease in biochar yields. This goes in line with the trend for yield of biochar for this research findings.

#### 4.2.5 Effect of metakaolin mixing ratio on biochar formation

To evaluate the effect of Kaolin on the pyrolysis product distribution, a slow pyrolysis of maple sawdust was studied in a fixed bed reactor operating at 400 °C, 1.0 L/min, 10 °C/min and a particle size of 3 mm was used. Kaolin was added to sawdust feed stock at ratios of 5 %, 10 %, 15 %, 20 %, 25 % and 30 % (w/w) for biochar formation. It is observed from Figure 4.10 that the yield of biochar was optimum at 10 % kaolin mixing ratio. It could be reasonable to suggest that at lower percentage of kaolin (5 %) the metakaolin arising from calcination of kaolin is insufficient to combine with the generated ethanol volume from decomposition of sawdust to form double bond aromatic compound. However, beyond 10 % mixing ratio, the yields of biochar reduce drastically. Reduction in biochar yield at increasing mixing ratios (25 % and beyond) was earlier concluded by Bello et al. (2017). Li et al. (2017) investigated the addition of mineral additives including kaolin to rice straw feed stock and concluded an increasing carbon retention, moderate biochar yields alongside strengthening biochar stabilization.

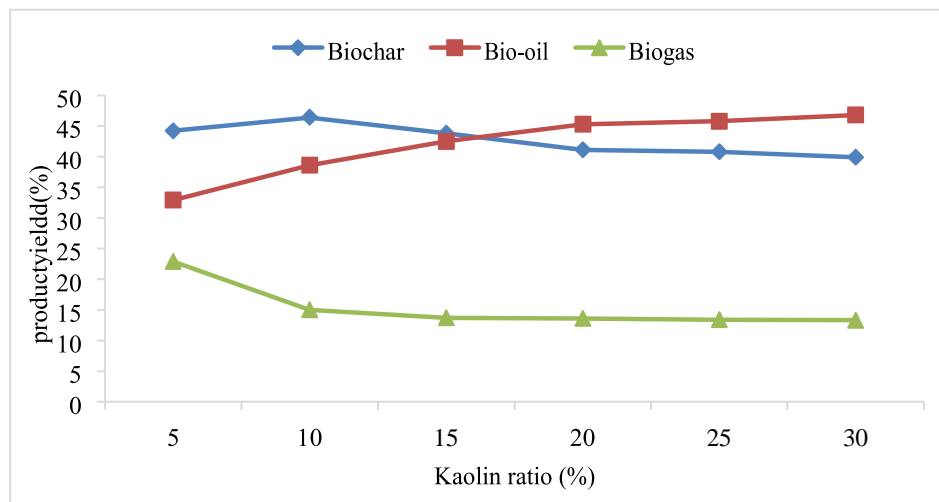


Figure 4.10: Effect of metakaolin on biochar formation from sawdust

Compare to untreated biomass, the yield of bio-oil progressively increases from 32.9 % to 46.8 % corresponding to 5 to 30 % kaolin mixing ratio. Bio-oil yields increase with rising catalyst ratio which is in conformity with the report of Onay (2018), who says pyrolysis oil yield increase with the use of catalyst. Bardalai and Mahanta (2020)

reported that when sawdust is mixed with catalyst  $\text{Al}_2\text{O}_3$ , there's drastically positive change in the weight of products. Traditionally, maximizing the production of biochar relative to the mass of initial feedstock is always at the expense of bio-oil and biogas. Thus, the findings demonstrated the dual function of Kutigi kaolin in enhancing both the yields of biochar and bio-oil at the expense of biogas production. Similarly increment of biochar yield was observed in poultry waste carbonization (Figure 4.11) as maximum yield of 54.4 % was obtained as compared to 50.3 % obtained in un-catalyzed condition.

This could be due to  $\text{CaO}$  and  $\text{Al}_2\text{O}_3$  present in kaolin. In support of this outcome, Alhassan (2017) co-pyrolyzed biomass with bone matter and concluded an increment in biochar yield. Contrary to increasing rate of bio-oil yield in sawdust pyrolysis, the biooil for poultry waste decreases from 22.1 % to 17.3 % while biogas yield slightly increase in the order of increasing mixing ratio. Decrease in bio-oil yield could be due to initial alkali metal presence in the poultry waste and  $\text{Al}_2\text{O}_3$  from kaolin which favour char formation. Ineffectiveness of the condensing medium may also contribute to low biooil yield.

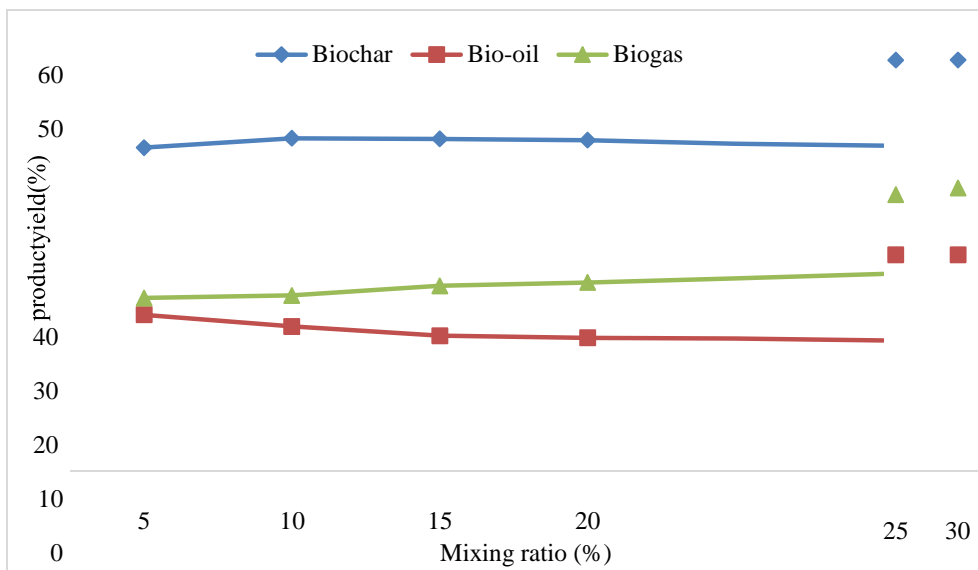


Figure 4.11: Effect of Metakaolin on Biochar from Poultry waste

### 4.3 Production and Characterization of Different Grades of Biochar

The yield for the production of biochar at optimum operating conditions were shown on

Table 4.3. This reflects the different grades of biochar namely: biochar obtained 400 °C (SBC400), biochar obtained at 500 °C (SBC500), biochar obtained at 600 °C (SBC600) and biochar obtained at 400 °C catalysed with 10 % kaolin ratio (SKBC400). Similarly, PBC400, PBC500, PBC600 and PKBC400 were obtained for poultry waste. The percentage increment when metakaolin was added at 10 % ratio shows 18.4 and 8.2 % increment for sawdust and poultry waste as compared to values obtained for SBC400 and PBC400.

Table 4.3: Effect of metakaolin on biochar yields

Biochar Grades	Biochar Yields (%)	Biochar Grades	Biochar Yields (%)
SBC400	39.2	PBC400	50.3
SBC500	22.6	PBC500	41.9
SBC600	20.1	PBC600	39.6
SKBC400	46.4	PKBC400	46.4
Kaolin Effect	18.4		8.2

### 4.3.1 Effect of temperature on the basic characteristic of biochars

#### 4.3.1.1 Proximate analysis

Table 4.4 presents the results of proximate analyses as a function of pyrolysis temperature. The content of volatile matter (VM) and fixed carbon (FC) for the generated biochars ranged from 50.16 to 53.21 % and 18.67 to 25.44 % for SBC and 50.66 to 47.06 % and 21.64 to 26.54 % for PBC, respectively. An increase in the pyrolysis temperature decreased the content of VM in both SBC and PBC, showing a similar trend with the yield of biochar, while an opposite trend was found for the content of fixed carbon. This might due to the fact that the increasing temperature resulted in the further cracking of the volatiles fractions into low molecular weight liquids and gases instead of biochar (Ronsse et al., 2021). Meanwhile, the dehydration of hydroxyl groups and thermal degradation of cellulose and lignin might also occur with the increasing temperature (Zhang et al., 2021). These results confirmed that the increase in temperature enhanced the stability of biochar for the loss of volatile fractions (Zornoza et al., 2019). It was observed that the ash content of SBC remarkably increased from 24.08% to 28.42% with an increase in the pyrolysis temperature from 400 to 600 °C while that of PBC increased from 23.76 to 26.36 % corresponding to 400 to 500 °C. The increase in the content of ash resulted from progressive concentration of inorganic constituents (Chen et al., 2021). A reduction of ash content of PBC at 600 °C (26.06 %) could be as a result of volatilization of inorganic materials into gas and liquid constituents (Zhang et al., 2021).

Table 4.4: Proximate and Ultimate Results of Biochars

Biochars Proximate (%)	SD			PW				
	SBC 400	SBC 500	SBC 600	SKBC 400		PWB500	PWB600	PKBC
MC	1.23	1.19	0.32	0.88	3.64	0.34	0.21	0.33

ASH	24.08	26.19	28.42	31.16	23.76	26.36	26.06	32.52
VM	53.21	51.71	50.16	29.16	50.66	49.36	47.06	43.14
FC	18.67	18.92	25.44	28.8	21.64	22.77	26.54	24.01
Ultimate (%)								
C	51.2	52.62	56.06	57.5	59.7	61.86	60.77	60.78
H	6.3	6.06	5.34	7.18	6.2	5.56	5.31	7
O	38.14	37.96	36.02	31.74	30.84	29.66	28.16	28.06
N	3	2.02	1.84	2.44	2.22	1.92	1.74	2.3
S	1.36	1.31	0.74	1.14	1.04	1	0.22	0.96

#### 4.3.1.2 Elemental analysis

The elemental compositions for the generated biochars of Sawdust Biochar (SBC) and Poultry Waste Biochar (PBC) changed with pyrolysis temperature as shown in Table 4.4.

The C content for SBC increased from 51.2 % to 56.06 % and 59.7 % to 61.86 % for PBC, while the H and O contents decreased from 6.30 % to 5.34 % and 38.14 % to 36.02% for SBC and 6.20 % to 5.31 %; 30.84 % to 28.16 % for PBC as the pyrolysis temperature increased from 400 to 600 °C, respectively. These results were consistent with previous result (Wang et al., 2020). The decrease in the contents of H and O at higher temperature was likely due to the decomposition of the oxygenated bonds and release of low molecular weight byproducts containing H and O (Bouraoui et al., 2017). Subsequently, the ratios of H/C (the degree of aromaticity) and O/C (the degree of polarity) (Wang et al., 2018) varied as a function of pyrolysis temperature. In this study, the H/C and O/C ratios of SBC and PBC were significantly decreased from 1.48 to 1.14 and 0.55 to 0.48 and 1.25 to 1.05 and 0.39 to 0.36 with the

increasing temperature, respectively. The gradually reduced in the H/C and O/C atomic ratios with the increasing pyrolysis temperature was mainly contributed to the dehydration reactions (Li et al., 2018b), which could be well described by the Van Krevelen diagram (Figure 4.12). In addition, the H/C and O/C ratios also indicated that the structural transformations have occurred (Wang et al., 2018). The higher extent of carbonization resulted in loss of functional groups containing O and H (such as hydroxyl, carboxyl,). The higher temperature resulted in the lower ratios of H/C and O/C, indicating that the surface of biochar was more aromatic and less hydrophilic (Keiluweit et al., 2019). More interestingly, Sawdust Kaolin Biochar (SKBC) and Poultry Waste Kaolin Biochar (PKBC) had O/C ratios of 0.41 and 0.35 which show that kaolin enhanced the polarity of the produced biochars as compared to SBC and PBC. This property is believed to support adsorption of CO<sub>2</sub> by biochar.

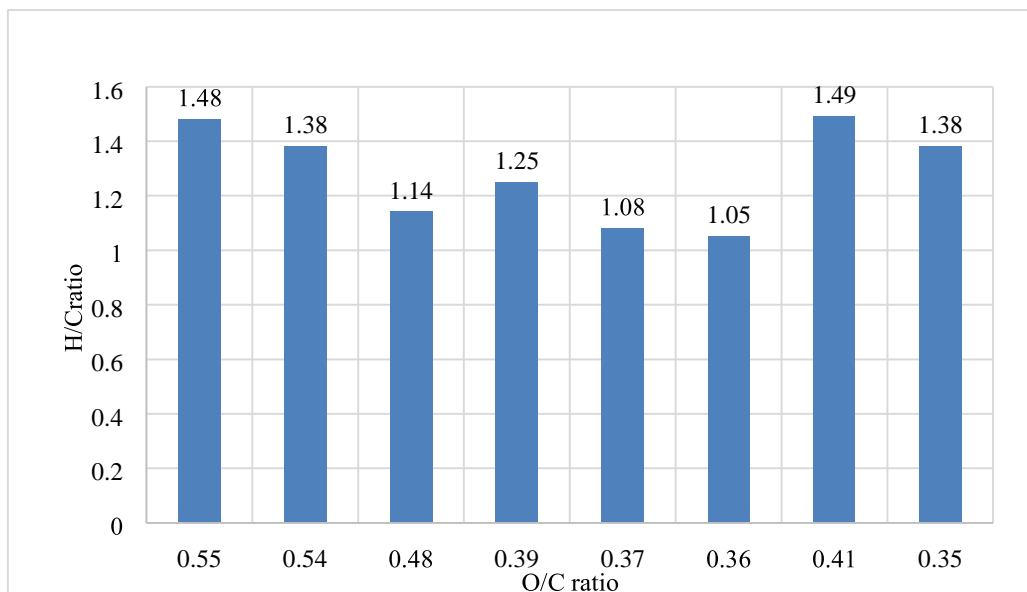


Figure 4.12: Van Krevelen Diagram for SBC, PBC, SKBC and PKBC

#### 4.3.1.3 Higher heating value

The higher heating values (HHV) of the biochars increased with an increase in the pyrolysis temperature. This agrees with the increase in fixed carbon content or biochar

quality. Higher heating values indicate the biochar's potential to be used as fuel. As shown on Figure 4.13, the higher heating value of the biochars obtained at 400, 500 and 600 °C for SBC (21.32, 21.67, 22.20 MJ kg<sup>-1</sup>) and (25.21, 25.31, 24.4) are much higher than other solid fuel such as lignite (20 MJkg<sup>-1</sup>) (Claoston et al., 2017). The higher heating values of the biochars were similar in comparison with that of other biochars such as those derived from sewage sludge and cherry stones (Chen et al., 2021; Gonzalez et al., 2018b). The HHV values of SKBC and PKBC (25.56 and 26.85 MJ kg<sup>-1</sup>) are higher than those of SBC and PBC which implies another positive effect of catalytic pyrolysis of biomass with kaolin at moderate ratio (10 %)

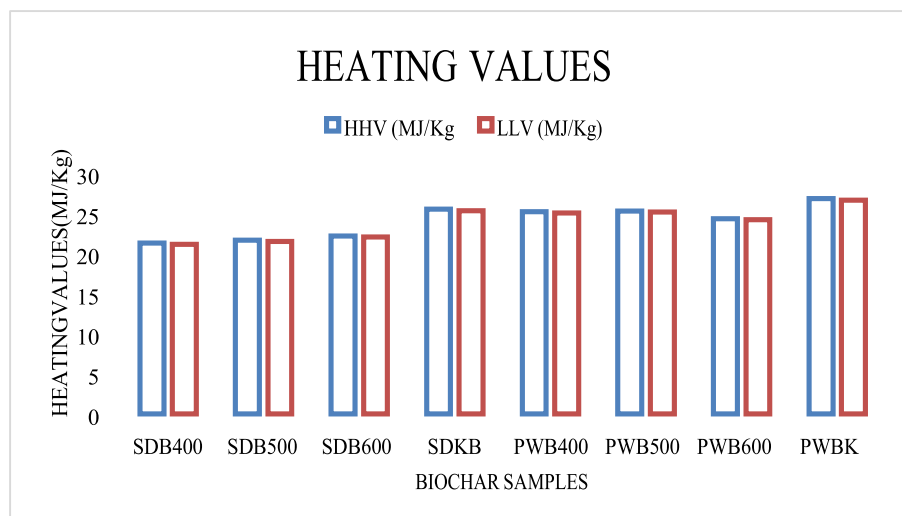


Figure 4.13: HHV and LLV of Biochar Samples

#### 4.3.1.4 Fourier transform infrared spectroscopy

Fourier Transform Infrared Spectroscopy (FTIR) is frequently used to identify and qualitatively track changes in functional groups in biochar. Figure 4.14 shows the peaks and functional groups of SBC400. The distinct peaks of SBC400 includes: peak at 3400 cm<sup>-1</sup> corresponding to NH stretching alcohol groups, peaks at 2900 and 2300 cm<sup>-1</sup>

correspond to C-H aldehyde and COOH groups, peaks at 1500 - 1700  $\text{cm}^{-1}$  are indicative of C=H alkene groups.

Figure 4.15 revealed the functional groups associated with PBC400. At 500  $\text{cm}^{-1}$ , C-S prevailed. This could be due to heterogenous nature of poultry waste, comprising of charred elements of digested foods and alkaline metals. Single bond hydrocarbon C-H occurs around 500 - 700  $\text{cm}^{-1}$ . Double bond compound =CH features around 1000  $\text{cm}^{-1}$  band. This was followed by C=C and NH groups above 1500 and 3000  $\text{cm}^{-1}$  respectively. Some of the differences in the spectra are as a result of organic matter combustion and the concentration of the mineral components that were changed when heated. To observed the effect of metakaolin on the produced biochar, the functional group analysis

of SKBC and PKBC were carried out. FTIR data graphs reveals number of similarities amongst the functional groups present for these special biochars shown on Figure 4,16 and 4.17. Alkene C=C group is associated with the biochars. The broad peak in the spectrum at the range 1000 - 1500 $\text{cm}^{-1}$  can be assigned to the existence of C-H alkyl stretch in all biochars at different areas. Aliphatic amines (NH) stretch amines are common stretch of SKBC and PKBC. These parameters are known to alter the sequestration ability of biochar (Lehmann, 2017). Noticeably from the spectra of SKPC and PKBC are functional groups like ketone stretching, primary and secondary amines, and hydroxyl which suggest that this biochar could have possibility to be used as potential adsorbent (Nunn et al., 2020).

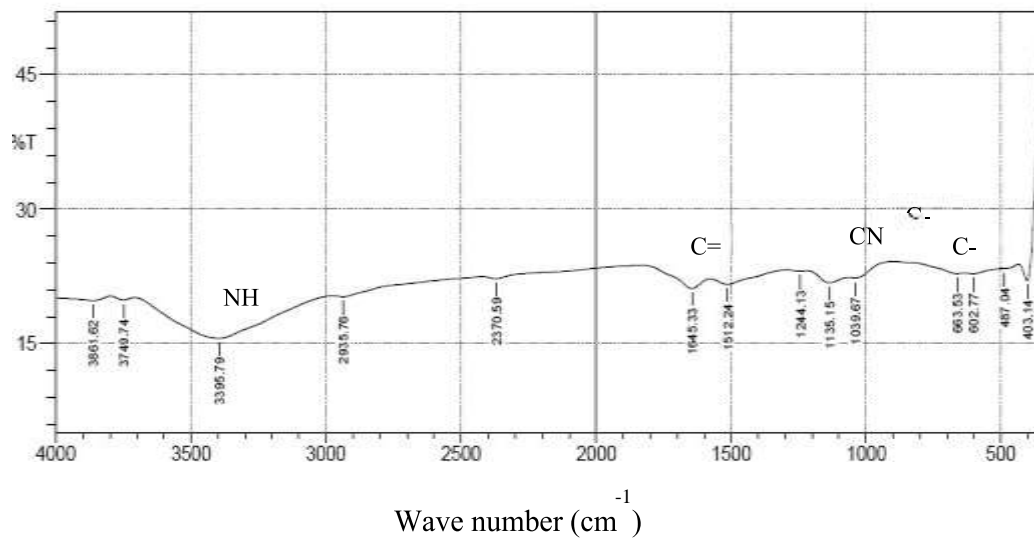


Figure 4.14: FTIR of SBC400

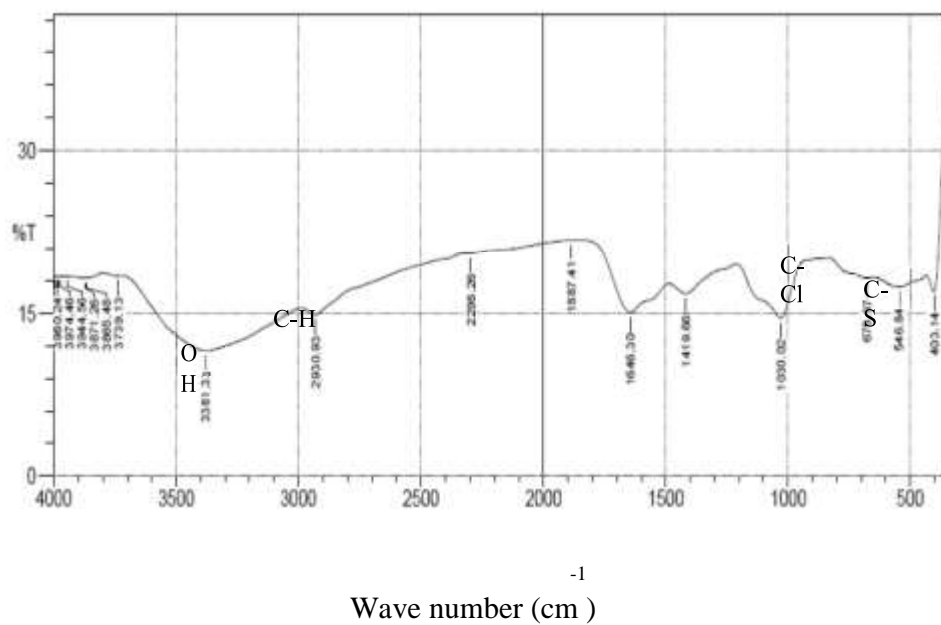


Figure 4.15: FTIR of PBC400

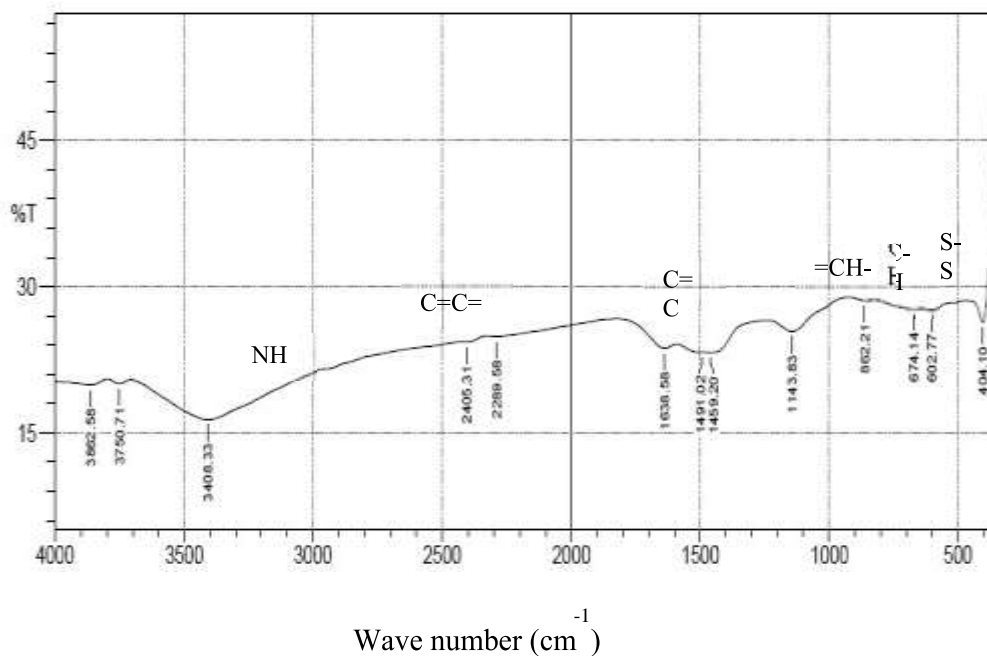


Figure 4.16: FTIR of SKBC400

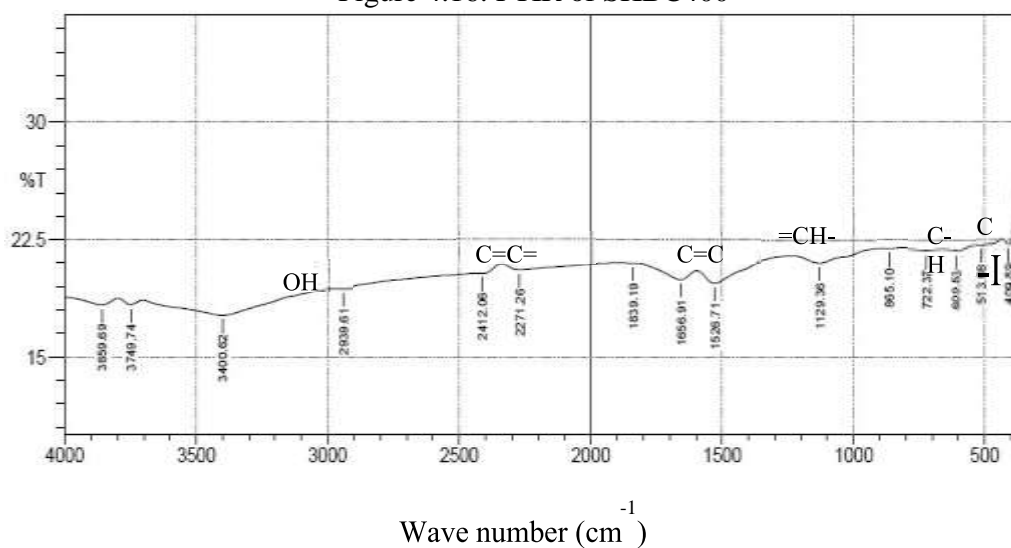


Figure 4.17: FTIR of PKBC

#### 4.3.1.5 X-Ray diffraction analysis

The analyses by X-Ray Diffraction show that the analysed samples of PW constituted Quartz, Calcite, Graphite and Potassium Aluminium Silicate. In Figure 4.18, PW, PBC400 and PKBC show similar trends with appearance of quartz peak at  $2\theta = 26.5^\circ$ . When pyrolyzed at 400 °C graphite and potassium aluminium silicate disappeared

while microcline and aluminium oxalate appeared in addition to Quartz and calcite. Thus, the biochars are good candidates for glass and ceramic production and with potential use in agricultural soil treatment (Mohammed et al., 2019). Subsequent pyrolysis with kaolin at 10% ratio, changed the constituents to kaolinite, quartz, sylvite, anorthite and sodian. Presence of kaolinite is a contributive factor of kaolin. With this, PKBC can be considered as a filler or paint and rubber formation. Similarly, in Figure 4.19, the raw sawdust contains whewellite and native cellulose. Whewellite is an important mineral used in metal speciation, physiology and biogeochemical processes (Li et al., 2018b). When pyrolyzed at 400 °C, the whewellite remained while graphite appeared. This is also a good non-metal that conduct electricity. Co-pyrolysis with kaolin resulted in the existence of quartz, calcite and muscovite. XRD search and match revealed biochar of poultry waste were predominantly made up of quartz as whewellite is to sawdust. Presence of native cellulose in sawdust is a characteristic of woody biomass. Treatment with kaolin produces quartz and calcite in both samples.

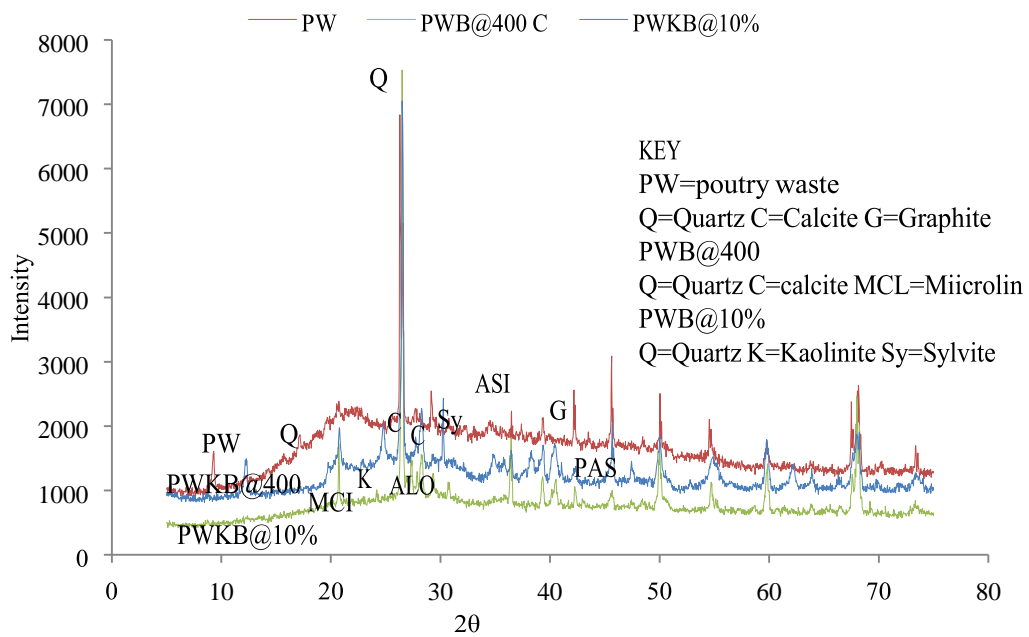


Figure 4.18: XRD of PW, PBC400 and PBC@10%

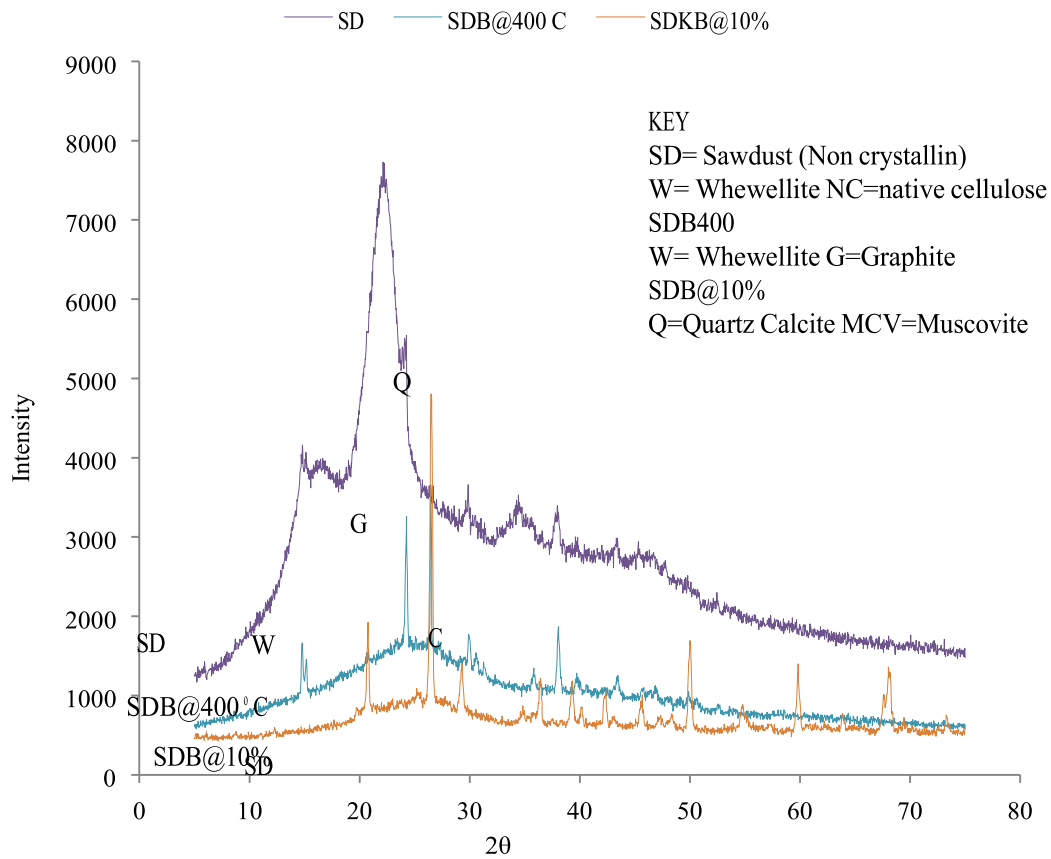


Figure 4.19: XRD of SD, SBC400 and SBC@10%

#### 4.3.1.6 Morphological analysis

SEM images of the feedstocks (SD, PW), the resulting biochars (SBC, PBC) and treated biochars (SKBC, PKBC) produced at the optimum temperature of 400 °C were shown in Figure 4.20. PW exhibited a complex morphology probably due to the heterogeneous components consisting of charred remnants of seeds, hairs, digested foods and bedding materials (Suleiman et al., 2018) and minerals such as S, K and P. when compared with PBC400, the image showed that the biomass had swollen, softened, melted and fused into a mass of vesicles. PKBC was observed to retain the fibrous structure of raw material (PW). The surface has some pores with white dots which signified the presence of silicon (Sharma et al., 2017). Due to dehydration and volatilization of raw materials, pores of different sizes emerged.

Similarly, SD displayed longitudinal fibrous structure arising from the cellulosic structure of sawdust that can be grouped into fibrous and spherical shapes (Joseph et al., 2020). The morphology of SBC400 had changed as revealed by the irregular surface. It became more complex due to the aggregation of mineral compound. SKBC inherited the longitudinal structure of sawdust with pores of different sizes. The micrograph of SKBC show many pores formed over the surface. According to Dominguez et al. (2017), properly arranged pore structure of biochars possess high adsorptive capacity.

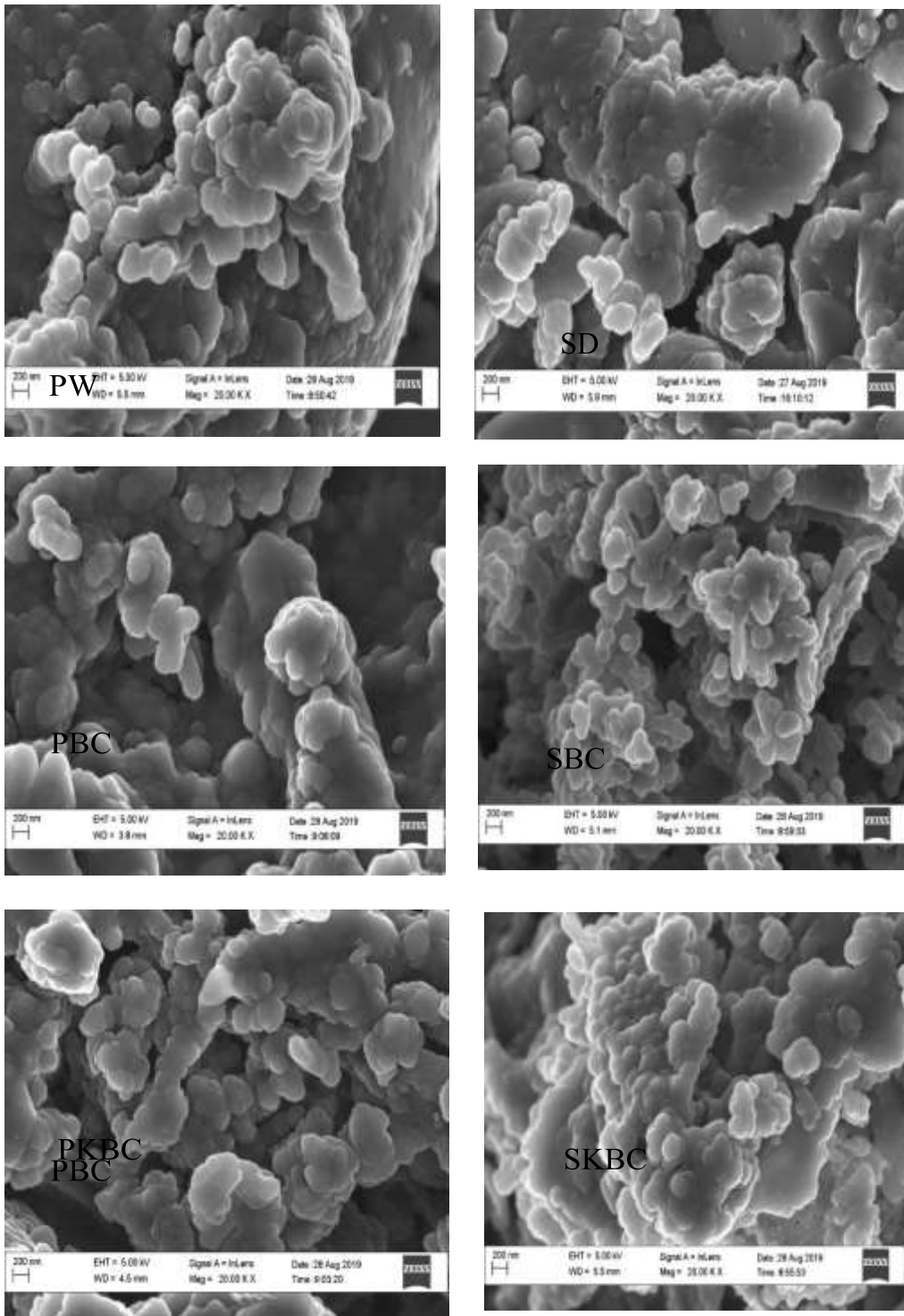


Figure 4.20: SEM images of SD, SBC, SKBC, PW, PBC and PKBC

#### 4.3.1.7 Production of activated carbon from biochars

After the initial porous structures (SBC and PBC) were created by pyrolysis, the residual carbon atoms were grouped into a condensed sheet of aromatic ring. The mutual arrangement of these sheets is regular and leaves a free interstice which may be by tarry materials (Romero et al., 2018). To remove these materials, activation was initiated. As such, SBC and PBC were reacted with a molar solution of phosphoric acid. Mixture was kneaded thoroughly to initiate the degradation of the feedstock which resulted in the formation of SAMAC and PAMAC respectively. The use of sodium hydroxide with SBC and PBC gave rise to the production of SBMAC and PBMAC. Direct impregnation of SD and PW with metakaolin resulted in the formation of SUMAC and PUMAC. These activators were characterized and subsequently employed in the adsorption study.

#### 4.3.1.8 The surface area and pore volume of biochars and activated carbon

The surface areas and pore volumes of produced biochars and activated carbons obtained by N<sub>2</sub> adsorption were shown on the Table 4.5. The specific surface area (BET) of SAMAC, SBMAC and SUMAC were 429.1, 298.6 and 414.2 m<sup>2</sup>/g with corresponding pore volumes of 0.1764, 0.1052 and 0.1188 cm<sup>3</sup>/g. Similarly, those of PAMAC, PBMAC and PUMAC were 427.6, 302.5 and 366.7m<sup>2</sup>/g with pore volumes of 0.1212, 0.0900 and 0.1011 cm<sup>3</sup>/g. This evolution is somewhat similar to that reported in the literature (Biederman and Harpole, 2018). The increase in the surface area and pore volume might be due to progressive degradation of organic materials (hemicellulose, cellulose and lignin) and appearance of channel structures during the pyrolysis process. The surface area of sawdust derived biochar is maximum when compared to others. This might be due to high VM content of sawdust as evidenced by proximate analysis. Also,

SUMACkaolin and PUMAC-kaolin show appreciable surface areas and pore volumes when compared with acid and base treated ACs. This might be due to the reactivity of metakaolin which aids more decomposition of organic compound at high temperature.

Table 4.5: Surface Area and Pore Volumes

Samples	Surface Area (m <sup>2</sup> /g)	Pore Volume (cm <sup>3</sup> /g)
SAMAC	429.1	0.1764
PAMAC	427.6	0.1212
SBMAC	298.6	0.1052
PBMAC	302.5	0.0900
SUMAC	414.2	0.1188
PUMAC	366.7	0.1011

#### 4.3.2 Summary of effect of process parameters and kaolin

Pyrolysis of biomass has recently gained interest due to its wide-ranging potential to produce biochar, bio-oil and biogas products in a single step conversion technology. However, various parameters affect the product yield, properties and compositions of pyrolysis products. These parameters include temperature, rate of biomass heating, vapor residence time, particle sizes, sweeping gas flow rate, proximate and elemental compositions of feedstock. As such, the effect of pyrolysis conditions in terms of temperature (400 to 650 °C), residence time (10 to 60 mins), nitrogen flow rate (0.5 to 3.0 L/min) and particle size (0.5 to 3.0mm) on the yield and physicochemical properties of biochar from sawdust and poultry waste were studied. The yield of biochar decreased with increasing pyrolysis temperature and optimum yield of biochar was attained at 400 °C in both samples. Increasing the nitrogen flow rate from 0.5 to 3.0 L/min decreases the yield of biochar. 1.0 L/min nitrogen flow rate resulted in optimum biochar yield and this was used in all other experiments. Larger particles, particularly at 3.00 mm,

were observed to favour biochar yield because of slow heating rate initiated and subsequent temperature gradient established. Residence time connote negative correlation with the biochar yield which implies that yield of biochars was decreasing with increasing residence time.

#### 4.4 Evaluation of Potential of Biochar as Carbon Sequester

Biochar as a solid product from the pyrolysis of biomass was identified as a means of sequestering carbon for over one thousand years (Lehmann, 2017). Thus, the potential of biochar as a carbon sequestration agent depends upon both the amount and the rate that carbon dioxide could be removed from the atmosphere and stored as carbonaceous solid in soils (Cantrell et al., 2017). In calculating the carbon sequestration potential of biochar, it is important to make valid assumptions as contained in the literature and utilisation of Equation 2.11, 2.12 and 2.13 as proposed by Alhassan et al. (2017). Some of the assumptions made in the calculation include:

- i. 100 million tonnes of biomass to be pyrolyzed
- ii. 80% Carbon contain in biochar is stable and can be sequestered

Table 4.6a: Sawdust Data Used in Calculating Carbon Sequestration

Parameters	SBC400	SBC500	SBC600	SKBC400
Biochar Yield (wt %)	39.2	22.6	20.1	46.4
Carbon (wt %)	51.2	52.62	56.06	57.50

Table 4.6b: Poultry waste Data Used in Calculating Carbon Sequestration

Parameters	PBC400	PBC500	PBC600	PKBC400
Biochar Yield (wt %)	50.3	41.9	39.6	54.4
Carbon (wt %)	59.7	61.86	60.77	60.78

Table 4.6a shows the data used for calculation of carbon sequestration potentials of sawdust derived biochars while Table 4.6b similarly shows the sequestration potentials of poultry waste derived biochars. Thus, for every 100 million tonnes of SBC pyrolyzed at 400 °C, approximately 39.2 % of it is converted to biochar. Similarly, 22.6 %, 20.1 % and 59.0 % were obtained for pyrolysis of SBC500, SBC600 and SKBC400 respectively. Amount of biochar produced, its carbon sequestration potential as well as amount of carbon dioxide removed from atmosphere is presented in Table 4.7a and b and detail calculation were shown in appendix C.

Table 4.7a: Amount of Carbon dioxide Removed by Sawdust Biochars

Biochar Grades	Biochar Produced (Mt)	Carbon Content (%)	Sequestration Potential of Biochar (Mt)	CO <sub>2</sub> Removed (Mt)
SBC400	39.2	51.2	20.07	16.05
SBC500	22.6	52.62	11.89	9.51
SBC600	20.1	56.06	11.26	9.01
SKBC400	46.4	57.50	26.68	21.34

Basis: 100 million tonnes of biomass

Table 4.7a shows the amount of Carbon dioxide that has the potential to be sequestered if the sawdust were thermally and catalytically pyrolyzed with metakaolin. Catalytic conversion of sawdust with metakaolin at 10 % mixing ratio yields the best conversion of total potential carbon and thus the largest amount of carbon dioxide capturing (21.34 %). This is followed by SBC400 (16.05 %), SBC500 (9.51 %) and SBC600 (9.01 %). It is evident from the result that pyrolysis of sawdust with metakaolin aiming to removed CO<sub>2</sub> is more significant compared to value obtained for their thermal degradation. It would be reasonable to suggests that biomass (sawdust) pyrolyzed with

metakaolin has potential to differ global warming through reasonable removal of carbon dioxide present in the atmosphere. Similarly, Table 4.7b presents the potential of poultry waste derived biochars as carbon dioxide sequesters.

Table 4.7b: Amount of Carbon dioxide Removed by Poultry waste Biochars

Biochar Grades	Biochar Produced (Mt)	Carbon Content (%)	Sequestration Potential of Biochar (Mt)	CO <sub>2</sub> Removed (Mt)
PBC400	50.3	59.7	30.3	24.02
PBC500	41.9	61.86	25.92	10.86
PBC600	39.6	60.77	24.06	19.24
PKBC400	54.4	60.78	33.06	26.45

Conversion of poultry waste biomass with metakaolin at 10% mixing ratio yields the best conversion of total potential carbon and by extension the largest amount of carbon dioxide capturing (26.45 %). This is followed by PBC400 (24.02 %), PBC500 (20.74 %) and PBC600 (19.24 %). It was observed from the result that pyrolysis of poultry waste with metakaolin aiming to removed CO<sub>2</sub> is more significant compared to value obtained for their thermal degradation. It would be reasonable to states that biomass (poultry waste) pyrolyzed with metakaolin has potential for the mitigation of global warming through reasonable removal of carbon dioxide that trapped heat and increase earth's temperature

#### 4.5 Adsorption of Carbon Dioxide by Activated Carbon

##### 4.5.1 Effect of adsorption time and adsorbent dosage

This assesses the effect of variation in contact time from 0 to 60 min on adsorption

capacity of SUMAC-kaolin, PUMAC-kaolin, SBMAC-NaOH, PBMAC-NaOH, SAMAC-H<sub>3</sub>PO<sub>4</sub> and PAMAC-H<sub>3</sub>PO<sub>4</sub> adsorbent at different adsorbent dosage of 1 to 6 g. Figure 4.21 (a) and (b) present effect of contact time and adsorbent dosage on CO<sub>2</sub> removal by SUMAC and PUMAC modified with metakaolin. The adsorption profiles show that there was a rapid and almost linear uptake of CO<sub>2</sub> by the two adsorbents (SUMAC and PUMAC modified with metakaolin) as the contact time rises to 15 min for all adsorbent dosage with a corresponding rise in adsorption capacity of the adsorbent as the adsorbent dosage increases from 1 g to 6 g. The rapid initial uptake of the CO<sub>2</sub> by the adsorbents and the rise in adsorption capacity with increase in adsorbent dosage can be attributed to the presence of a large number of adsorption sites available on the adsorbents for the retention of adsorbate molecules, as well as the availability of high number of adsorption sites available per unit mass of adsorbents (Emam, 2018, Parolo et al., 2021, El-Zahhar and Al-Hazmi, 2019; Foroutan et al., 2018, Hokkanen et al., 2018, Momina et al., 2018).

However, as the contact time increases beyond 15 min, the rate of CO<sub>2</sub> uptake by both adsorbent (SUMAC and PUMAC modified with metakaolin) remain almost constant without significant rise in adsorption capacity for all adsorbent dosage. This is attributed to the facts that as the CO<sub>2</sub> molecules are adsorbed onto the adsorption sites of the adsorbents particles, the number of available adsorption sites decreases, making the slope to flattens as the adsorption rate decreases for all adsorbent dosage (El-Zahhar and AlHazmi, 2019; Uduakobong and Augustine, 2020). Hence, the initial rate of adsorption of CO<sub>2</sub> in to SUMAC and PUMAC adsorbents modified with metakaolin increases rapidly with increases in time until equilibrium is reached in which no significant rises in adsorption capacity was observed while adsorption capacity increases with increase in adsorbent dosage for both adsorbent. Beyond 45 min, the adsorption becomes almost linear and eventually constant at 55 min.

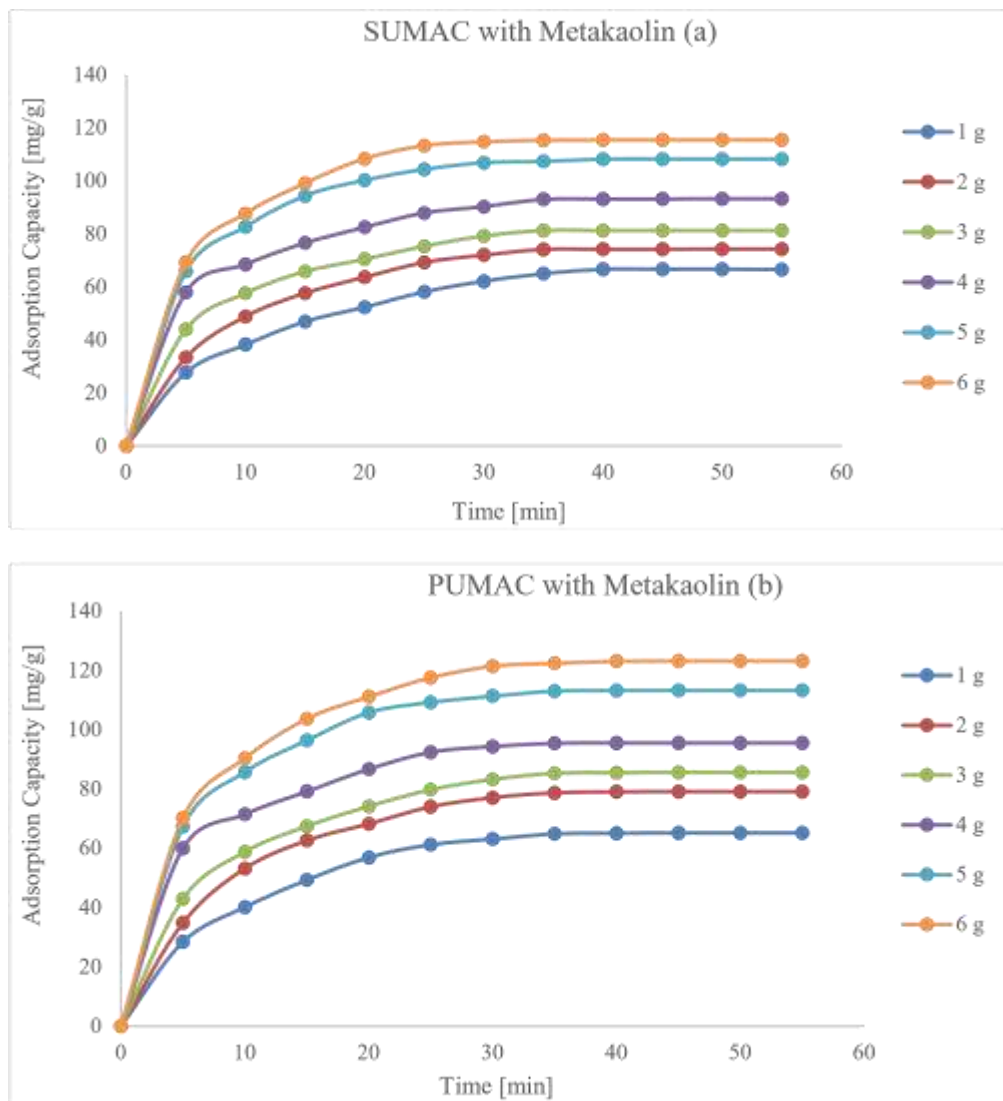


Figure 4.21: Effect of contact time and adsorbent dosage on CO<sub>2</sub> removal by (a) SUMAC and (b) PUMAC modified with metakaolin.

Figure 4.22 (a) and (b) also present effect of contact time and adsorbent dosage on CO<sub>2</sub> uptake by SBMAC and PBMAC modified with NaOH. Similarly, the adsorption profiles show that there was a rapid and almost linear uptake of CO<sub>2</sub> by the two adsorbents (SBMAC and PBMAC modified with NaOH) as the contact time rises to 10 min for all adsorbent dosage with a corresponding rise in adsorption capacity of the adsorbent as the adsorbent dosage increases from 1 g to 6 g. As usual, the rapid initial uptake of the CO<sub>2</sub> and increase in adsorption capacity with increase in adsorbent dosage is also attributed to the presence of high number of adsorption sites available on the

adsorbents for the retention of more molecules of the adsorbate due to high number of adsorption sites per unit mass of adsorbents (Emam, 2018, Parolo et al., 2021, El-Zahhar and Al-Hazmi, 2019; Foroutan et al., 2018, Hokkanen et al., 2018, Momina et al., 2018).

Whereas, increase in contact time beyond 10 min show an almost constant uptake of CO<sub>2</sub> by both adsorbent (SBMAC and PBMAC modified with NaOH) without significant rise in adsorption capacity for all adsorbent dosage. This is ascribed to the facts that continuous increase in CO<sub>2</sub> molecules uptake by the adsorbent result in a decrease in adsorption site available until equilibrium is reached in whereby there no further CO<sub>2</sub> molecule can be accommodated by the adsorbent, making the slope to flattens as the adsorption rate decreases for all adsorbent dosage (El-Zahhar and Al-Hazmi, 2019;

Uduakobong and Augustine, 2020). Hence, the initial rate of adsorption of CO<sub>2</sub> in to SBMAC and PBMAC adsorbents modified with NaOH increases rapidly with increases in time until equilibrium is reached in which no significant rises in adsorption capacity was observed while adsorption capacity increases with increase in adsorbent dosage for both adsorbent. The profiles were completely constant at 50 min of adsorption for all dosages in considerations.

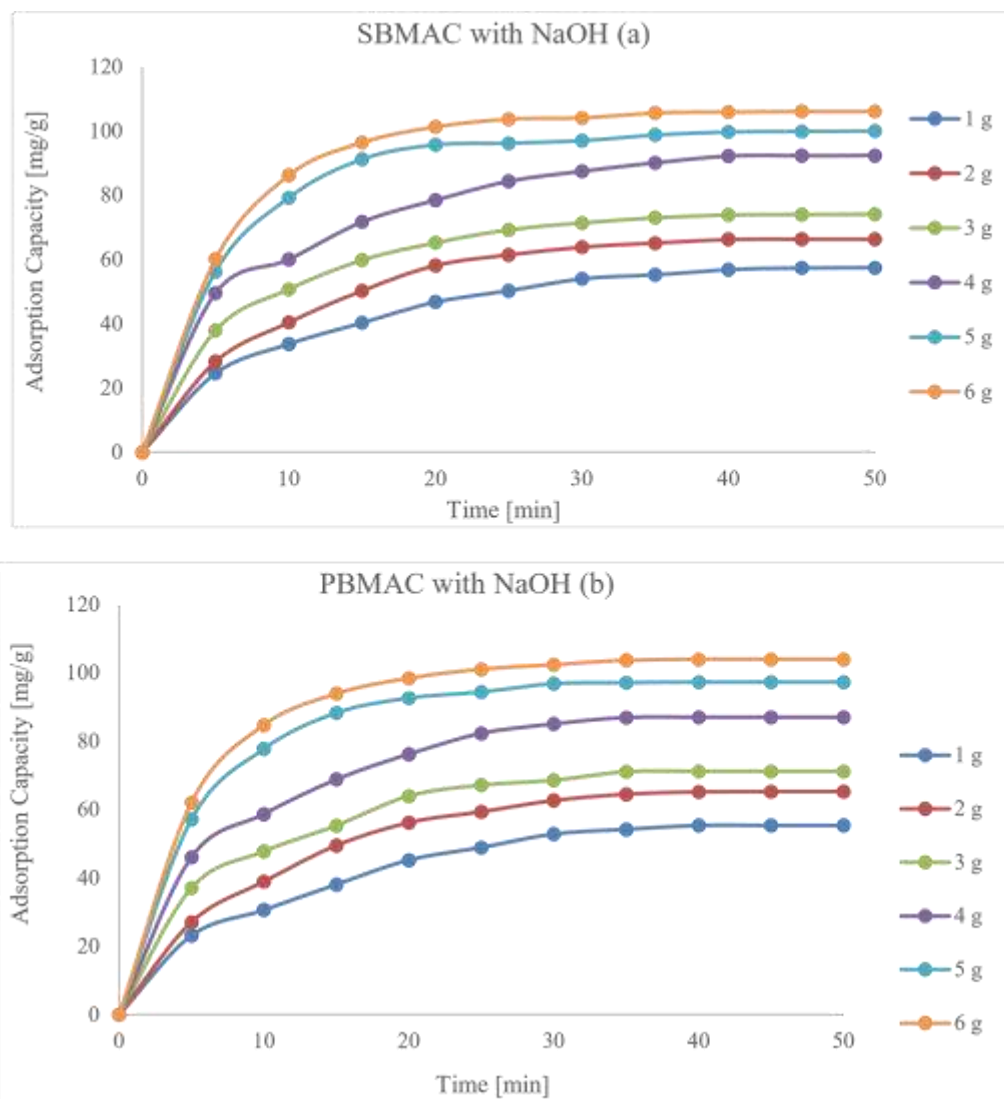


Figure 4.22: Effect of contact time and adsorbent dosage on CO<sub>2</sub> removal by (a) SBMAC and (b) PBMAC modified with NaOH

More so, Figure 4.23 also represents effect of contact time and adsorbent dosage on CO<sub>2</sub> uptake by SAMAC and PAMAC modified with H<sub>3</sub>PO<sub>4</sub>. Likewise, the adsorption profile shows that there was a rapid and almost linear uptake of CO<sub>2</sub> by the two adsorbents (SAMAC and PAMAC modified with H<sub>3</sub>PO<sub>4</sub>) as the contact time rises to 10 min for all adsorbent dosage with a corresponding rise in adsorption capacity of the adsorbent as the adsorbent dosage increases from 1 g to 6 g. The rapid initial uptake of the CO<sub>2</sub> and increase in adsorption capacity with increase in adsorbent dosage is also attributed to the presence of high number of adsorption sites available on the adsorbents

for the retention of more molecules of the adsorbate due to high number of adsorption sites per unit mass of adsorbents (Emam, 2018, Parolo et al., 2021, El-Zahhar and Al-Hazmi, 2019; Foroutan et al., 2018, Hokkanen et al., 2018, Momina et al., 2018).

However, increase in contact time beyond 20 min shows an almost constant uptake of CO<sub>2</sub> by both adsorbent (SAMAC and PAMAC modified with H<sub>3</sub>PO<sub>4</sub>) without significant rise in adsorption capacity for all adsorbent dosage. This is ascribed to the facts that continuous increase in CO<sub>2</sub> molecules uptake by the adsorbent result in a decrease in adsorption site available until equilibrium is reached in whereby there no further CO<sub>2</sub> molecule can be accommodated by the adsorbent, making the slope to flattens as the adsorption rate decreases for all adsorbent dosage (El-Zahhar and Al-Hazmi, 2019;

Uduakobong and Augustine, 2020). Hence, the initial rate of adsorption of CO<sub>2</sub> in to SBMAC and PBMAC adsorbents modified with NaOH increases rapidly with increases in time until equilibrium is reached in which no significant rises in adsorption capacity was observed while adsorption capacity increases with increase in adsorbent dosage for both adsorbent.

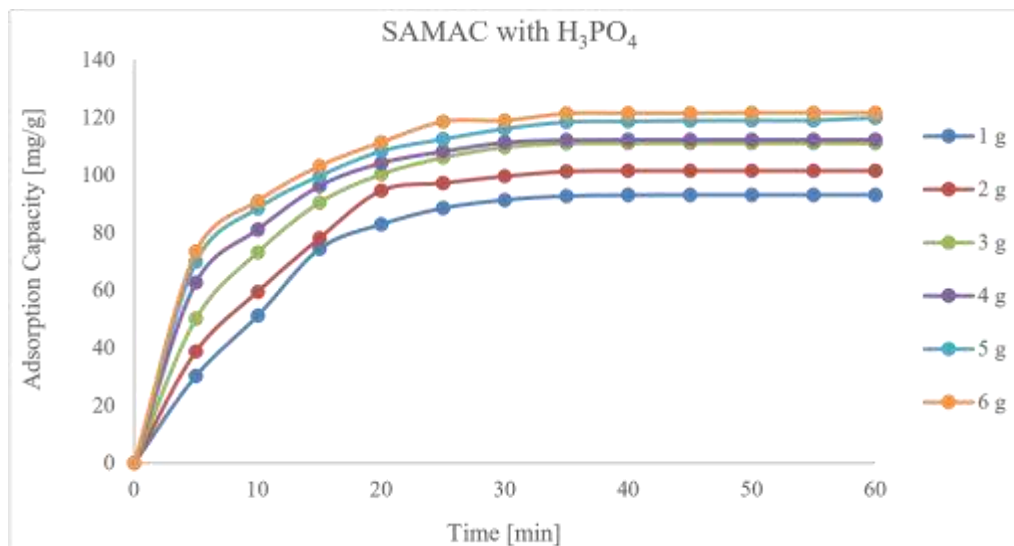


Figure 4.23a: Effect of contact time and adsorbent dosage on CO<sub>2</sub> removal by (a) SAMAC

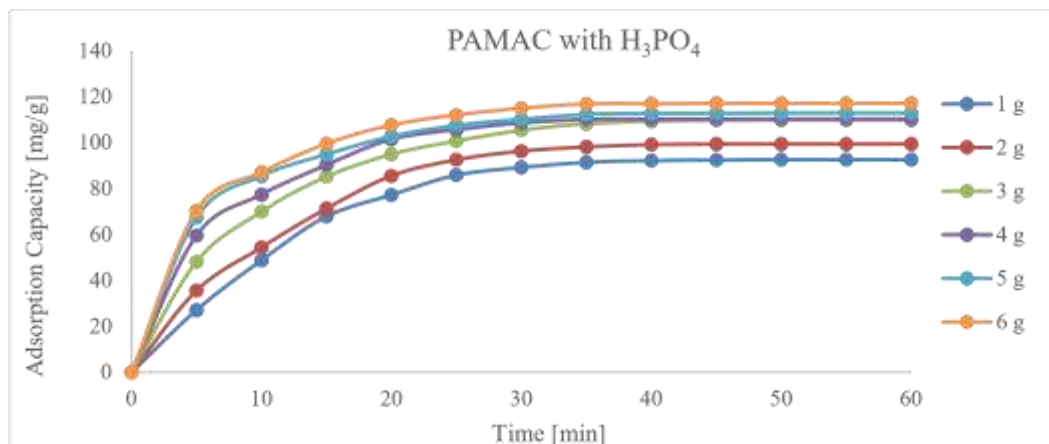


Figure 4.23b: Effect of contact time and adsorbent dosage on CO<sub>2</sub> removal by PAMAC

Overall, the rate of CO<sub>2</sub> adsorption increases rapidly in the early stage of the adsorption process and then slowly until equilibrium is reached when there is no further uptake of CO<sub>2</sub> due to unavailability of adsorption site for CO<sub>2</sub> molecule uptake while adsorption capacity increases with increase in adsorbent dosage for all adsorbents.

#### 4.5.2 Adsorption kinetics studies

The section examines the adsorption mechanism of the adsorbents using intra-particle diffusion and Elovich model.

##### 4.5.2.1 Intra-particle diffusion model

Intra-particle diffusion model was utilized to assess the adsorption kinetics of the adsorbents. Intra-particle diffusion model provides an insight of the mechanism in adsorption process and according to the model, different mechanisms are involved in this process of adsorption. Intra-particle diffusion process is described in basically three steps which are; superficial external adsorption, intra-particle diffusion corresponding to the limiting step and the final equilibrium, which is very fast (Mani et al., 2020; Alhassan et al, 2017; Romero et al., 2018). Hence, if the plot of the experimental data exhibit multilinear plots, two or more steps influences the adsorption process. Table 4.8

presents the adsorption kinetics studies of the adsorbents using Intra-particle diffusion model.

Details of the linear plots of the adsorption kinetic are presented in the Appendix. D

Table 4.8: Intra-particle diffusion model parameters for adsorption of CO<sub>2</sub>

Adsorbent Type		Adsorbent Dosage					
	Parameter	1 g	2 g	3 g	4 g	5 g	6 g
SUMAC-Kaolin	$k_{id1}$ , mg/g. min <sup>1/2</sup>	9.6403	13.4731	13.3964	13.4596	21.5135	22.4808
	$k_{id2}$ , mg/g. min <sup>1/2</sup>	7.1922	5.7417	6.1742	9.0138	1.2978	2.7771
	Ci	1.3436	1.3225	4.9357	6.6520	10.6880	11.4683
	$k_{id}$ , mg/g. min <sup>1/2</sup>	9.9173	12.1034	13.2040	15.9028	18.2053	19.4764
	R <sup>2</sup>	0.9959	0.9910	0.9723	0.9706	0.9234	0.9247
PUMAC-Kaolin	$k_{id1}$ , mg/g. min <sup>1/2</sup>	9.0750	13.6567	11.1621	13.8883	19.1772	19.6792
	$k_{id2}$ , mg/g. min <sup>1/2</sup>	7.5909	6.4593	4.6625	8.8729	4.2033	3.9273
	Ci	0.4974	1.0878	4.5379	5.7430	10.7816	12.3455
	$k_{id}$ , mg/g. min <sup>1/2</sup>	9.7247	11.8236	12.7331	15.5751	17.8314	18.8500
	R <sup>2</sup>	0.9981	0.9919	0.9750	0.9765	0.9292	0.9198
SBMAC-NaOH	$k_{id1}$ , mg/g. min <sup>1/2</sup>	11.7422	14.9372	13.4253	11.3927	17.4916	18.2827
	$k_{id2}$ , mg/g. min <sup>1/2</sup>	9.7820	8.3975	8.7530	7.8047	6.5672	6.4287
	Ci	1.2732	2.7594	6.5275	10.5189	11.9978	11.9142
	$k_{id}$ , mg/g. min <sup>1/2</sup>	11.4137	13.4317	14.3091	16.0961	19.4121	21.0118
	R <sup>2</sup>	0.9971	0.9874	0.9643	0.9345	0.9361	0.9453
PBMAC-NaOH	$k_{id1}$ , mg/g. min <sup>1/2</sup>	12.7739	17.1149	15.0990	11.7316	17.8915	20.4725
	$k_{id2}$ , mg/g. min <sup>1/2</sup>	6.2041	8.8622	9.0638	7.6280	5.4993	10.2708
	Ci	1.4556	2.9047	5.2179	10.6559	11.7800	11.3238
	$k_{id}$ , mg/g. min <sup>1/2</sup>	11.9291	14.4359	15.2681	16.9057	20.3694	22.0912
	R <sup>2</sup>	0.9921	0.9845	0.9777	0.9385	0.9426	0.9550
SAMAC-H <sub>3</sub> PO <sub>4</sub>	$k_{id1}$ , mg/g. min <sup>1/2</sup>	26.6990	23.9900	24.6702	20.4727	18.2702	18.2301
	$k_{id2}$ , mg/g. min <sup>1/2</sup>	8.4962	4.9145	9.3610	7.1344	7.7633	7.6683
	Ci	-2.7096	-0.6860	3.8019	9.4363	12.1310	12.8255
	$k_{id}$ , mg/g. min <sup>1/2</sup>	18.0716	19.5123	20.7796	20.5463	21.0590	21.7563
	R <sup>2</sup>	0.9760	0.9830	0.9844	0.9596	0.9448	0.9425
PAMAC-H <sub>3</sub> PO <sub>4</sub>	$k_{id1}$ , mg/g. min <sup>1/2</sup>	24.8442	21.7347	22.7246	18.8353	16.8946	17.7956
	$k_{id2}$ , mg/g. min <sup>1/2</sup>	12.0271	10.7701	10.4678	7.0872	7.4210	7.2803
	Ci	-3.9195	-1.8973	3.5975	8.0604	12.1098	12.3249
	$k_{id}$ , mg/g. min <sup>1/2</sup>	17.4907	18.5458	19.7908	20.0951	19.9652	20.8774
	R <sup>2</sup>	0.9811	0.9917	0.9873	0.9691	0.9397	0.9426

Table 4.8 shows that adsorption of CO<sub>2</sub> into all the adsorbents (SUMAC- Kaolin,

PUMAC- Kaolin, SBMAC-NaOH, PBMAC-NaOH, SAMAC-H<sub>3</sub>PO<sub>4</sub> and PAMAC-H<sub>3</sub>PO<sub>4</sub>) exhibit multilinear plots with two adsorption rate constants,  $k_{id1}$  and  $k_{id2}$ , which indicates that intra-particle diffusion is not the only rate-limiting step in the uptake of CO<sub>2</sub> adsorption process and the negative intercept ( $C_i$ ) obtained for some of the adsorbent's dosage indicate a complex adsorption process was for the specific adsorbent dosage. Also, the coefficient of determinant,  $R^2$  value of the intraparticle diffusion model for the adsorption of CO<sub>2</sub> at adsorbent dosage of 1g to 3 g are between 0.97 to 0.9981 (Table 4.8) which show that the adsorption process fitted well with the intraparticle diffusion model for 1 g to 3 g for all adsorbent while for adsorbent dosage of 4 g to 6 g, the  $R^2$  value is in the range of 0.91 to 0.96. This indicates that the experimental data fits well with intra-particle diffusion at adsorbent dosage of 1 to 3 g for all adsorbent type. The initial steeper region observed from the plots (Appendix D) with adsorption rate constant  $k_{id1}$  for all adsorbent type and dosage can be attributed to surface sorption while the second region can be attributed to intra-particle diffusion, indicating that the adsorption process followed two steps for CO<sub>2</sub> as the gradient did not pass through the origin (Nethaji et al., 2018; Kajjumba et al., 2018). Hence, the rate of adsorption of CO<sub>2</sub> into all adsorbent (SUMAC- kaolin, PUMAC-kaolin, SBMAC-NaOH, PBMAC-NaOH, SAMAC-H<sub>3</sub>PO<sub>4</sub> and PAMAC-H<sub>3</sub>PO<sub>4</sub>) can be said to be influence by external or surface adsorption (film diffusion) and intra-particle diffusion.

Also, Table 4.8 shows that the rate of adsorption of CO<sub>2</sub> by all adsorbent at all dosage is highest at the initial stage of surface sorption due to the availability of sufficient adsorption site (Emam, 2018, Parolo et al., 2021, El-Zahhar and Al-Hazmi, 2019; Foroutan et al., 2018, Hokkanen et al., 2018, Momina et al., 2018). Where the rate of adsorption of CO<sub>2</sub> by all adsorbent at all dosage reduces in subsequent region where intra-particle diffusion prevails. This is seen from Table 4.8 in which initial adsorption rate constant,  $k_{id1}$  is greater than the subsequent stage adsorption rate constant,  $k_{id2}$  for

all adsorbent type and at all adsorbent dosage. This further corroborates the rapid rate of adsorption of CO<sub>2</sub> observed at initial stage of the adsorption process.

The obtained values of  $k_{id\ 1} > k_{id\ 2}$ , indicates a faster sorption rate due to the availability of sufficient adsorption site at the initial stage while the rate of intra-particle diffusion reduces in subsequent region as adsorption time rises. This justified the high adsorption capacity recorded at the initial stage of the adsorption process for all adsorbent type at all dosage and indicates that the intra-particle diffusion is carried out in the micro and meson pores which results in the very high adsorption rate (Yong et al., 2019; Romero et al., 2018). Likewise, the rate of adsorption in the order,  $k_{id\ 1} > k_{id\ 2}$  (Table 4.12) for CO<sub>2</sub> adsorbed into all adsorbent and at all adsorbent dosage signifies a decrease in sorption rate as time increases which justify the high initial adsorption capacity observed at the initial stage of the adsorption process which could be attributed to availability of sufficient adsorption site in the adsorbent.

Therefore, the rate of adsorption of CO<sub>2</sub> by all adsorbent at 1 to 3 g adsorbent dosage is mainly influenced by surface adsorption and intra-particle diffusion while at 4 to 6g adsorbent dosage is mainly influenced by surface adsorption. Overall, the intraparticle diffusion model shows that the rate of adsorption of CO<sub>2</sub> adsorption into all the adsorbent is influence by surface adsorption and intra-particle diffusion.

#### 4.4.2.3 Elovich model

In order to further understand the chemisorption nature of adsorption of the adsorbents type and dosage effect, Elovich kinetic model was utilized to evaluate the adsorption mechanism of the adsorbents. This enables the prediction of the mass and surface diffusion, activation and deactivation energy of a system of an adsorption mechanism commonly applied in gaseous systems and wastewater processes. The equation was developed initially to describe the mechanism of chemisorption of gas onto solids

(Hamdaoui and Naffrechoux, 2017). The model assumes that the rate of adsorption of solute decreases exponentially as the amount of adsorbate increase. Table 4.9 presents the adsorption kinetics parameters of the adsorbents using Elovich model. Details of the linear plots of the adsorption kinetic are presented in the Appendix D.

Table 4.9: Elovich model parameters for adsorption of CO<sub>2</sub>

Adsorbent Type	Parameter	Adsorbent Dosage					
		1 g	2 g	3 g	4 g	5 g	6 g
SUMAC-Kaolin	$\beta$ , g/mg	0.0637	0.0521	0.0473	0.0393	0.0338	0.0316
	$\alpha$ , mg/g.min	14.093	16.418	25.125	32.495	44.092	47.339
	$R^2$	0.9963	0.9954	0.9964	0.9916	0.9726	0.9736
		5	5	3	5	7	4
PUMAC-Kaolin	$\beta$ , g/mg	0.0653	0.0534	0.0492	0.0402	0.0346	0.0327
	$\alpha$ , mg/g.min	12.473	15.684	23.876	29.776	44.610	50.146
	$R^2$	0.9887	0.9949	0.9946	0.9955	0.9757	0.9698
		4	2	7	5	5	7
SBMAC-NaOH	$\beta$ , g/mg	0.0554	0.0468	0.0436	0.0385	0.0319	0.0295
	$\alpha$ , mg/g.min	15.727	20.596	30.384	44.213	50.183	51.067
	$R^2$	0.9956	0.9997	0.9921	0.9716	0.9773	0.9823
		2	2	0	5	2	6
PBMAC-NaOH	$\beta$ , g/mg	0.0529	0.0435	0.0410	0.0367	0.0304	0.0281
	$\alpha$ , mg/g.min	16.499	21.895	27.990	45.118	50.114	50.207
	$R^2$	0.9960	0.9989	0.9980	0.9740	0.9812	0.9879
		1	1	8	6	5	6
SAMAC-H <sub>3</sub> PO <sub>4</sub>	$\beta$ , g/mg	0.0351	0.0324	0.0302	0.0303	0.0294	0.0285
	$\alpha$ , mg/g.min	17.241	21.773	30.774	43.463	51.831	54.556
	$R^2$	0.9677	0.9801	0.9977	0.9907	0.9819	0.9797
		6	6	9	0	9	7
PAMAC-H <sub>3</sub> PO <sub>4</sub>	$\beta$ , g/mg	0.0365	0.0343	0.0318	0.0311	0.0310	0.0297
	$\alpha$ , mg/g.min	15.228	19.154	29.371	39.678	51.048	52.383
	$R^2$	0.9963	0.9954	0.9964	0.9916	0.9726	0.9736
		7	6	3	2	8	6

Table 4.9 presents the Elovich model parameter,  $\alpha$  (initial adsorption rate) and  $\beta$  (desorption constant) which are related to the extent of surface coverage for chemisorptions for all adsorbent type (SUMAC- Kaolin, PUMAC- Kaolin, SBMACNaOH, PBMAC-NaOH, SAMAC- H<sub>3</sub>PO<sub>4</sub> and PAMAC-H<sub>3</sub>PO<sub>4</sub>) and at all dosage (1 to 6 g). Table 4.9 shows that the value of the initial adsorption rate ( $\alpha$ ) increases with increase in adsorbent dosage for all adsorbent types, which is due to the availability of high number of adsorption sites available per unit mass of adsorbents (Emam, 2018, ElZahhar and Al-Hazmi, 2019). However, the study showed that the desorption constant ( $\beta$ ) decreases with increase in adsorbent dosage for all adsorbent type (Table 4.9), which further confirms that CO<sub>2</sub> adsorption process by all the adsorbents and at all dosage is predominantly diffusionally in nature (Kajjumba et al., 2018). Therefore, it is suggested that CO<sub>2</sub> adsorption on all adsorbents type is attributed to both chemisorptions and physisorption.

Also, coefficient of determination, R<sup>2</sup> value is in the range of 0.9600 to 0.9997 for the Elovich model for all adsorbent type and at all dosage fits well with the experimental data which further signifies that diffusional rate limiting is predominant in the sorption of CO<sub>2</sub> by all adsorbents. Comparatively, the order of kinetic model capabilities to fit well with the experimental adsorption data of CO<sub>2</sub> uptake on all adsorbent type and at all dosage is Elovich is greater than intraparticle diffusion. Hence, the experimental data of the adsorption of CO<sub>2</sub> onto all adsorbent and at all dosage was highly fitted to the Elovich model in describing the absorption kinetics of CO<sub>2</sub>.

#### 4.6 Optimization Process

##### 4.6.1 Preliminary experiments

Table 4.10 and 4.11 show the preliminary experiments conducted for the pyrolysis of sawdust and poultry waste respectively at the chosen values of independent variables. The process parameters selected for the experiment include: temperature, flow rate, particle size, residence time and kaolin ratio. The range of each factor selected were shown in each Table 4.10 and 4.11 alongside the yields of pyrolysis products.

Table 4.10: Preliminary Experiment on SD Pyrolysis

Temp Biogas (° c) (mins)	Process Parameters				Product yields		
	Flowrate (g)	Particle size (g)	Residence time (mins)	Kaolin ratio	Biochar oil (g)	Bio- (mm)	Bio-
300	0.5	0.5	10	5	32.1	33.1	34.8
400	1	1	20	10	35.7	36.4	28.5
450	1.5	1.5	30	15	34.2	42.9	22.9
500	2	2	40	20	27.2	42.2	30.6
550	2.5	2.5	50	25	23.5	41.5	34
600	3	3	60	30	21.7	38.6	50.3

Table 4.11: Preliminary Experiment on PW Pyrolysis

Process parameters					Product yields		
Temp (° c)	Flowrate (l/min)	Particle size (mm)	Residence time (mins)	Kaolin ratio (g)	Biochar (g)	Bio- oil (g)	Biogas (g)
300	0.5	0.5	10	5	43.1	31.2	25.7
400	1	1	20	10	45.8	28.4	25.8
450	1.5	1.5	30	15	43.7	30.1	26.2
500	2	2	40	20	41.1	28.5	30.4
550	2.5	2.5	50	25	38.1	24.3	37.6
600	3	3	60	30	36	22.9	41.1

The temperature in a pyrolysis process is the most significant operating parameter (Devi and Saroha, 2019). At 300 °C, the yield of biochar and bio-oil were 32.1 and 33.1 % for SD and 43.1 and 32.2 % for PW. As the reaction temperature increases the biochar

and liquid product yields increases but further increase in temperature (above 500 °C) shows decrease in their yields. The reason for the lower yield of biochar and bio-oil at lower temperature may be due to the fact that the reaction temperature becomes too low to complete pyrolysis process. On the other hand, upon increasing the temperature, secondary reactions of the high molecular weight compounds in the pyrolysis vapours or between the vapours and primary biochar dominated, resulting in a decrease of the biooil yield and an increase of the biogas yield (Park et al., 2018). The interaction of the hot pyrolysis vapours with surrounding solid environment led to the formation of biochar. As thought of, the yield of biochar decreases in both scenario of SD and PW as flow rate increases. Thus, low flow rate favour biochar formation. Low flow rate of 0.5 L/min create more time for hot pyrolytic vapour to reside inside the reactor and thus maximizes the secondary reactions like thermal cracking, re-polymerization and recondensation which favours biochar product yield (Uzun et al., 2017). Larger particle sizes are expected to favour biochar production because of temperature gradient established between the particle core and its outer surface. However, the preliminary study shows decreases in biochar and bio-oil yields as particles sizes increase. This could be because of other conditions under which the process takes place. However, in case of slow pyrolysis, particle size does not show any significant influence on product yield (Beaumont and Schwob, 2021). Also from the preliminary studies, residence time was varied from 10 to 60mins and the yields of biochar and bio-oil correspond to 32.1 to 21.7 % and 31.1 to 38.6 % respectively. Fassinou et al. (2020) showed an interactive effect of temperature and residence time, wherein increased temperature and residence times resulted in increase in the biochar yield, whereas lower temperature and increase in contact time reduced the yield of biochar. It is therefore difficult to make conclusion regarding the relationship between the production of biochar and the residence times. The distribution of pyrolytic products can be affected by the presence of catalyst.

Kaolin addition shows changes in the yield of pyrolysis product. Yields of biochar were optimum at low kaolin addition. Several catalysts such as alumina, Al-MCM-41, oxides of magnesium, oxides of nickel and ZSM-5 showed positive effects on the yield of biochar (Stefanidis et al., 2017).

#### 4.7 Optimization Outcomes

Optimization is the discipline of adjusting pyrolysis process so as to optimize (make the best or most effective use of) some specified set of parameters without violating some constraints. This is considered one of the best quantitative tools in decision making during pyrolysis experiment. The goal is to maximize the biochar production while keeping all others within their constraints (bio-oil and biogas to be minimized).

##### 4.7.1 Optimization of SD pyrolysis

The pyrolysis results under the different operational conditions of temperature, flow rate, particle sizes, residence time and kaolin ratio on sawdust pyrolysis were shown on a Table attached at appendix D. The functional relationships between the responses (biochar, bio-oil and biogas) and the independent variables (temperature, flow rate, particle size, residence time and kaolin ratio) were quantified by means of estimated parameters of the regression model. As shown on the Table (appendix D), the computational software (Design Expert version 12.0) adopted for the optimization purpose divided the coded factor into low, mid and upper points corresponding to -1, 0 and +1 languages understood by computer. Temperature had its points as 300, 450 and 600 °C, flow rate 0.5, 1.75 and 3 L/mins, particle size 0.5, 1.75 and 3 mm, residence time 10, 35 and 60 min and kaolin 5, 17.5 and 30 g. After 46 runs, the results of the responses were tabulated in a Table shown in appendix D. Obviously, the yields of the biochar and bio-oil were optimum around 450 °C. Biogas productions were optimum at higher temperature regime.

#### 4.7.1.1 ANOVA for quadratic model of response 1: biochar

The fit statistics for response 1 coded as biochar is shown in Table 4.12. Upon computation, the Predicted R<sup>2</sup> of 0.8725 is in reasonable agreement with the Adjusted R<sup>2</sup> of 0.9380; that is, the difference is less than 0.2. Adequate Precision measures the signal to noise ratio. Fundamentally, a ratio greater than 4 is desirable. Thus, the ratio of 17.703 indicates an adequate signal. This model can be used to navigate the design space or adopted as basis in design.

Table 4.12: Fit Statistics for Sawdust Biochar

Fit Statistics			
Std. Dev.	1.98	R <sup>2</sup> 0.9656	Mean 31.70
C.V. %	6.25	Adjusted R <sup>2</sup>	0.9380
		Predicted R <sup>2</sup>	0.8725
		Adeq Precision	17.7027

#### Final Equation in Terms of Actual Factors

Equation 4.1 represents the final equation for the biochar response in terms of actual factors that are significant either as single factor or in interactive effect. Interestingly, temperature and kaolin had single effect on biochar production.

$$\text{Biochar} = -125.26108 + 0.658067 * \text{Temp} + 0.672467 * \text{Kaolin} + 0.012800 * \text{Temp} * \text{Particle Size} - 0.000580 \text{Temp} * \text{Residence Time} - 0.000688 * \text{Temp}^2 - 1.13467 * \text{Flow Rate}^2 \quad (4.1)$$

This equation in terms of actual factors can be used to make predictions about the response for given levels of each factor. Here, the levels were specified in the original units for each factor. This general equation cannot be used to determine the relative impact of each factor rather in combination because the coefficients are scaled to accommodate the units of each factor.

#### Model Validation for Biochar

## Normal Residual Plot

As the regression was ran, the Design Expert automatically calculates and plots the residual plot (Figure 4.24) to validate the model. Since the points in the residual plot are randomly distributed on the vertical axis, a nonlinear (quadratic) is appropriate for the data and model prediction can be considered accurate.

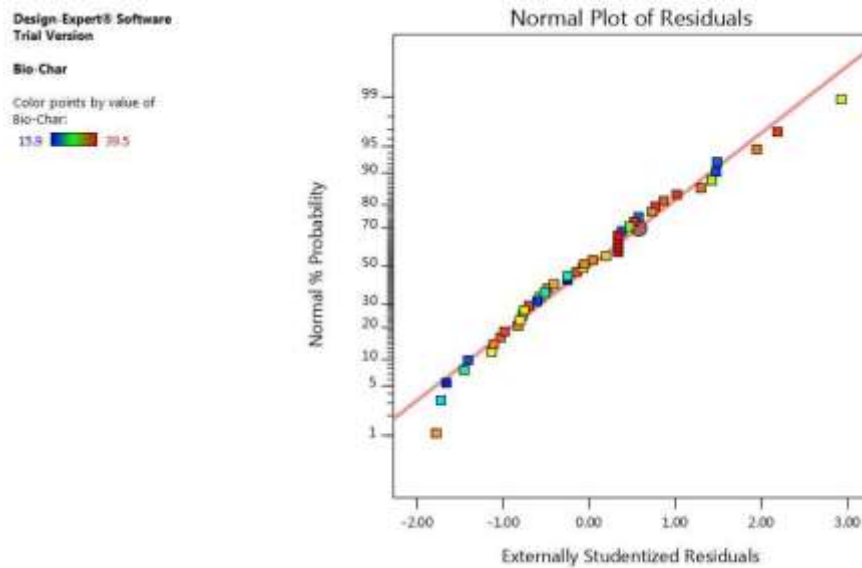


Figure 4.24: Normal Residual Plot for Biochar

## Contour and 3D Plots for SD Biochar

The four plots (Contour and 3D) represented on Figure 4.25a and 4.25b (for temperature and particle size) and Figure 4.26a and 4.26b (for temperature and residence time) were presented to visualize the response (biochar) yields as a function of two separate independent variables that are significant and had interactive effect on biochar production. For contour plot, the yields were represented on the contour line while temperature and particle sizes were represented on horizontal and vertical axis. For 3D plot, yields of biochar, temperature and residence time were represented on y, x and z planes.

Design-Expert® Software  
 Trial Version  
 Factor Coding: Actual

**Bio-Char ((g))**  
 ● Design Points  
 15.9 39.5

X1 = A: Temp  
 X2 = C: Particle Size

**Actual Factors**  
 B: Flow Rate = 1.75  
 D: Residence Time = 35  
 E: Kaolin = 17.5

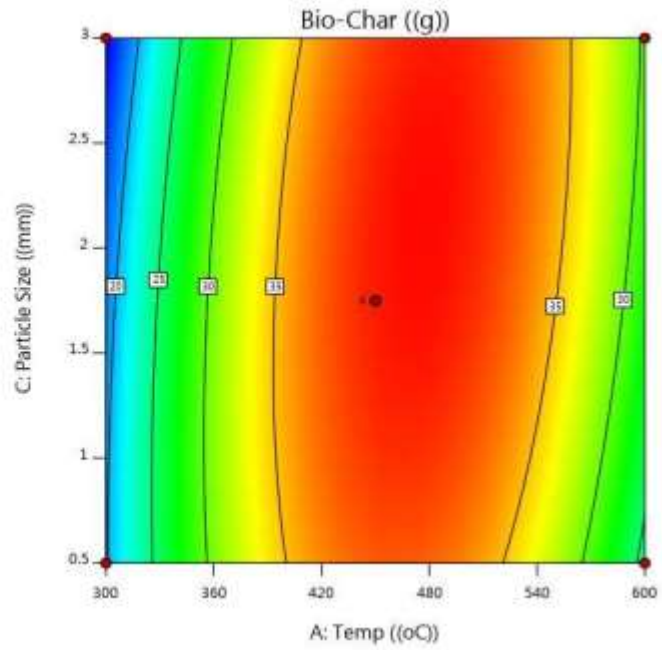


Figure 4.25a: Contour Plot for Temperature and Particle size on Biochar yields

Design-Expert® Software  
 Trial Version  
 Factor Coding: Actual

**Bio-Char ((g))**  
 ● Design points above predicted value  
 ○ Design points below predicted value  
 15.9 39.5

X1 = A: Temp  
 X2 = C: Particle Size

**Actual Factors**  
 B: Flow Rate = 1.75  
 D: Residence Time = 35  
 E: Kaolin = 17.5

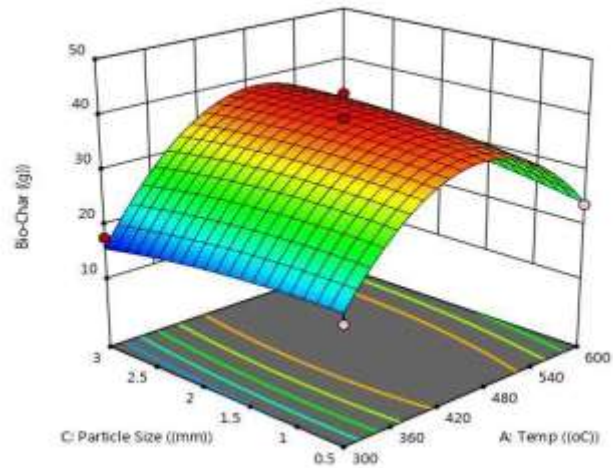


Figure 4.25b: 3D Plot for Temperature and Particle size on Biochar yields

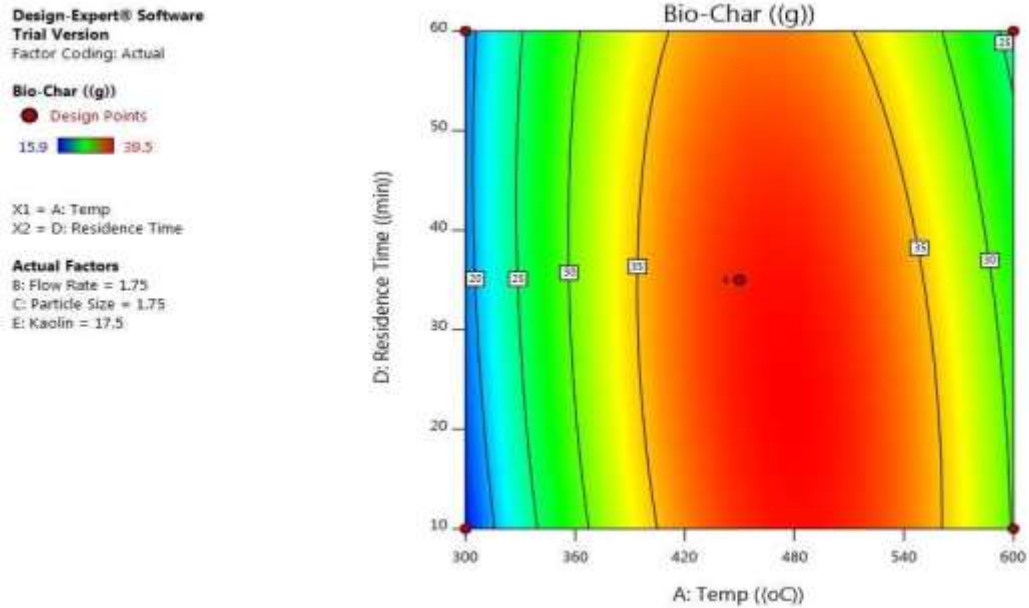


Figure 4.26a: Contour Plot for Temperature and Residence time on Biochar yields

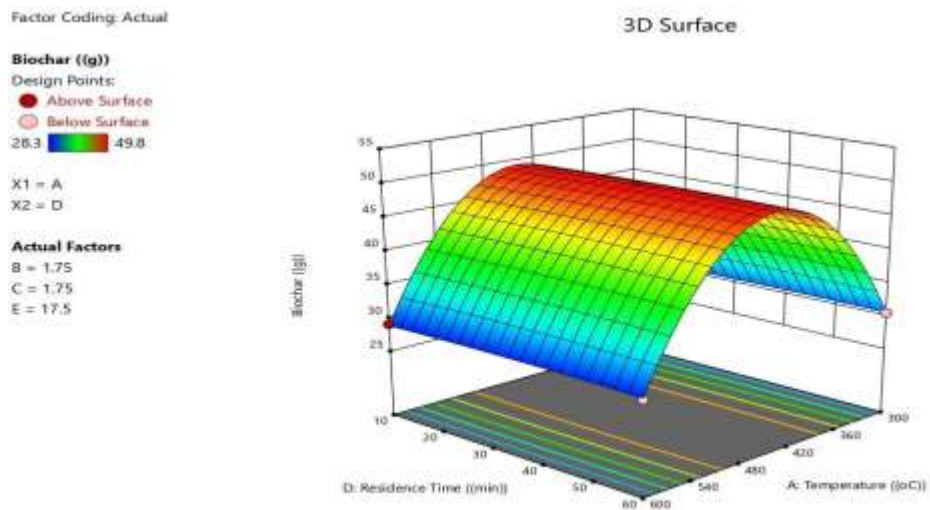


Figure 4.26b: 3D Plot for Temperature and Residence time on Biochar yields

#### 4.7.1.2 ANOVA for quadratic model of response 2: bio-oil

Analysis of variance for response 2 coded as bio-oil is presented in Table 4.13 and 4.14 respectively. The Model F-value of 6.14 implies the model is significant. There is only a 0.01% chance that an F-value this large could occur due to noise. P-values less than 0.0500 indicate model terms are significant. In this case A, D, AC, A<sup>2</sup>, D<sup>2</sup> are significant

model terms. Values greater than 0.1000 indicate the model terms are not significant. If there are many insignificant model terms (not counting those required to support hierarchy), model reduction may improve your model. The Lack of Fit F-value of 1.20 implies the Lack of Fit is not significant relative to the pure error. There is a 46.01 % chance that a Lack of Fit F-value this large could occur due to noise. Non-significant lack of fit is good -- we want the model to fit.

Table 4.13: ANOVA for Bio-oil

Source	Sum of Squares	df	Mean Square	Fvalue	p-value	
Model	1825.41	20	91.27	6.14	< 0.0001	Significant
A-Temp	93.61	1	93.61	6.30	0.0189	
D-Residence Time	74.39	1	74.39	5.01	0.0344	
AC	66.42	1	66.42	4.47	0.0446	
A <sup>2</sup>	1258.04	1	1258.04	84.66	< 0.0001	
D <sup>2</sup>	148.35		148.35	9.98	0.0041	
Residual	371.51	$\frac{1}{25}$	14.86			
Lack of Fit	307.31	20	15.37	1.20	0.4601	not significant
Pure Error	64.20	5	12.84			
Cor Total	2196.93	45				

Table 4.14: Fit Statistics for Bio-oil

Fit Statistics			
Std. Dev.	3.85	R <sup>2</sup> 0.8309	Mean 29.06
		Adjusted R <sup>2</sup> 0.6956	
C.V. %	13.26	Predicted R <sup>2</sup>	0.3984
		Adeq Precision	9.8222

The Predicted R<sup>2</sup> of 0.3984 is not as close to the Adjusted R<sup>2</sup> of 0.6956 as one might normally expect; i.e., the difference is more than 0.2. This may indicate a large block effect or a possible problem with the model. Adequate Precision measures the signal to noise ratio. A ratio greater than 4 is desirable. Thus, the ratio of 9.822 indicates an adequate signal. This model can be used to navigate the design space or design purpose.

### Final Equation in Terms of Actual Factors

$$\text{Bio-oil} = + 124.96725 - 0.439675 * \text{Temp} + 0.045483 * \text{Residence Time} - 0.021733 \\ \text{Temp} * \text{Particle Size} + 0.000534 * \text{Temp}^2 + 0.006597 * \text{Residence Time}^2 \quad (4.2)$$

The equation in terms of actual factors can be used to make predictions about the response for given levels of each factor. Here, the levels are specified in the original units for each factor. This equation cannot be used to determine the relative impact of each factor because the coefficients are scaled to accommodate the units of each factor.

### Model Validation for Bio-oil

#### Normal Residual Plot

In the same manner, as the regression was run, the Design Expert automatically calculates and plots the residual plot for bio-oil (Figure 4.27) to validate the model. Since the points in the residual plot are randomly distributed on the vertical axis, a nonlinear (quadratic) is appropriate for the data and model prediction can be considered accurate.

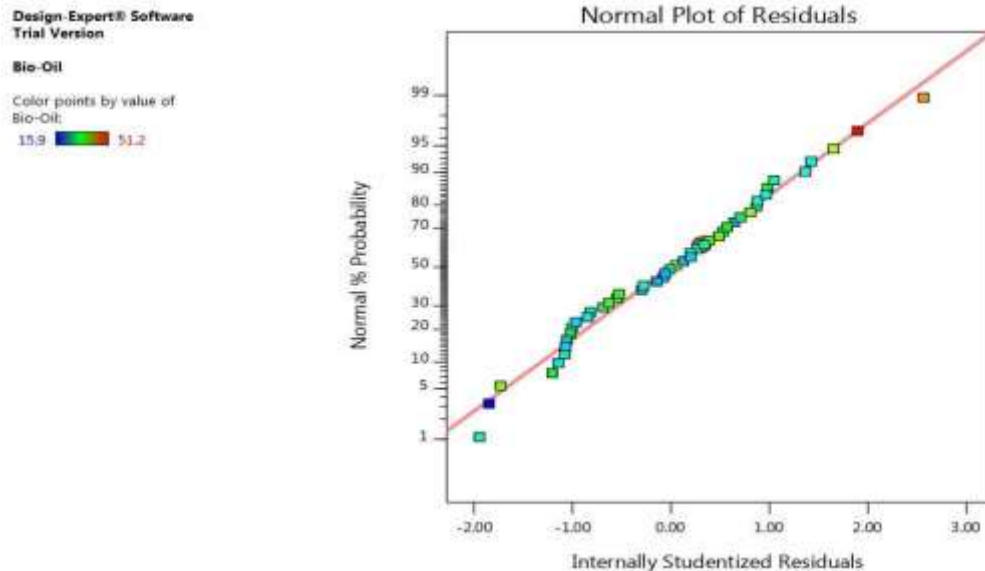


Figure 4.27: Normal Residual Plot for Bio-oil

## Contour and 3D Plots for Bio-oil

The three plots (Contour, 3D and Interaction) represented on Figure 4.28a, 4.28b and 4.28c (for temperature and particle size) were presented to visualize the response (biooil) yields as a function of two separate independent variables that are significant and had interactive effect on bio-oil production. For contour plot, the yields were represented on the contour line while temperature and particle sizes were represented on horizontal and vertical axis. For 3D plot, yields of bio-oil, temperature and particle sizes were represented on y, x and z planes. For Interaction, yields were show on Y axis, while temperature and particle size lie on horizontal axis

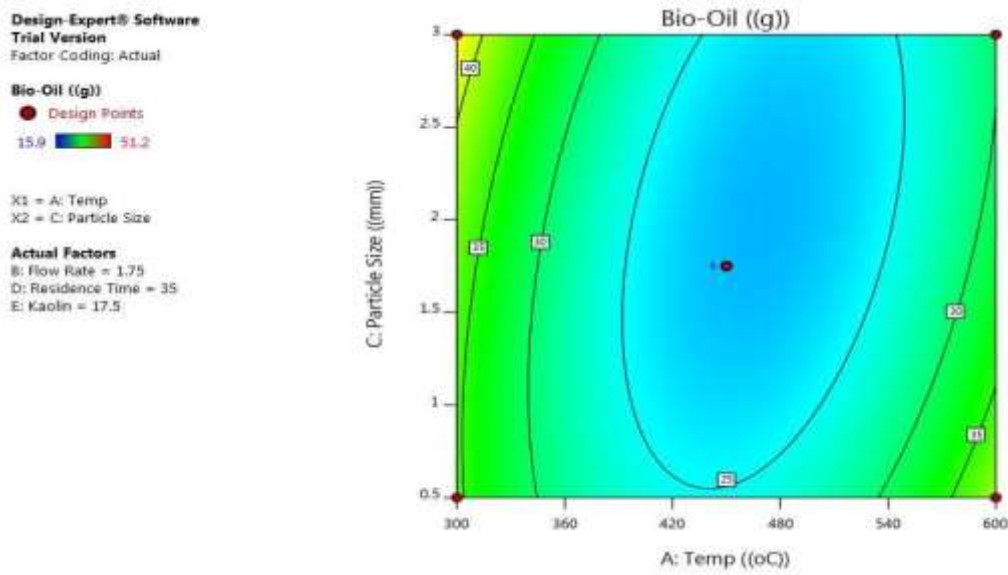


Figure 4.28a: Contour Plot for Temperature and Particle Sizes on Bio-oil yields

Design-Expert® Software  
Trial Version  
Factor Coding: Actual

Bio-Oil ((g))

● Design points above predicted value

○ Design points below predicted value

15.8  51.2

X1 = A: Temp

X2 = C: Particle Size

Actual Factors

B: Flow Rate = 1.75

D: Residence Time = 35

E: Kaolin = 17.5

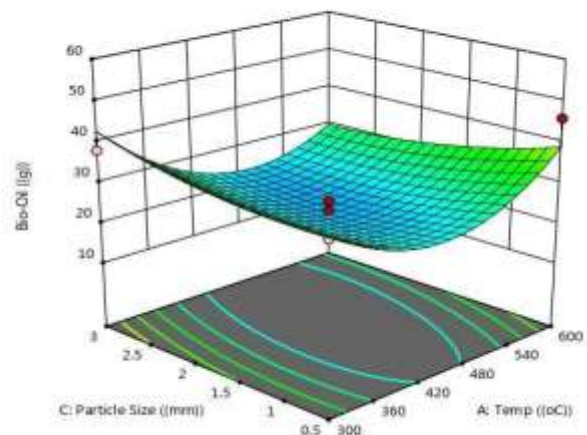


Figure 4.28b: 3D Plot for Temperature and Particle Sizes on Bio-oil yields

Design-Expert® Software  
Trial Version  
Factor coding: Actual

Bio-Oil ((g))

● Design Points

- - 95% CI Bands

X1 = A: Temp

X2 = C: Particle Size

Actual Factors

B: Flow Rate = 1.75

D: Residence Time = 35

E: Kaolin = 17.5

C = 0.5

C = 2

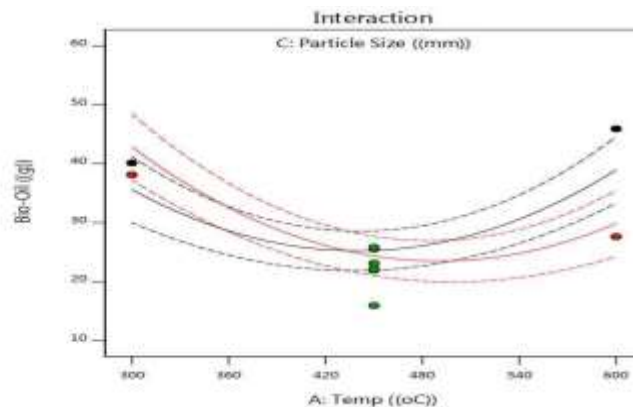


Figure 4.28c: Interaction Plot for Temperature and Particle Sizes on Bio-oil yields

#### 4.7.1.3 ANOVA for Quadratic Model of Response 3: Biogas

There is only a 1.32 % chance that an F-value may be large or could occur due to noise.

P-values less than 0.0500 indicate model terms are significant. In this case A, AD, A<sup>2</sup>,

D<sup>2</sup> are significant model terms. Conventionally, values greater than 0.1000 indicate the model terms are not significant. If there are many insignificant model terms (not counting those required to support hierarchy), model reduction was employed to improve the model. The Lack of Fit F-value of 1.04 implies the Lack of Fit is not significant relative to the pure error. There is a 53.52 % chance that a Lack of Fit F-value could occur due to noise. Non-significant lack of fit is good -- we want the model to fit.

Table 4.15: ANOVA for Biogas

Source	Sum of Squares	Df	Mean Square	F-value	p-value	
Model	560.46	20	28.02	2.58	0.0132	Significant
A-Temp	77.00	1	77.00	7.08	0.0134	
AD	104.04	1	104.04	9.56	0.0048	
A <sup>2</sup>	104.88	1	104.88	9.64	0.0047	
D <sup>2</sup>	67.61		67.61	6.22	0.0196	
Residual	271.95	<u>1</u> 25	10.88			
Lack of Fit	219.28	20	10.96	1.04	0.5352	Not significant
Pure Error	52.67	5	10.53			
Cor Total	832.41	45				

#### Final Equation in Terms of Actual Factors

$$\text{Bio-Gas} = +100.29383 - 0.218392\text{Temp} + 0.001360 * \text{Temp} * \text{Residence Time} - 0.000387 * \text{Temp} * \text{Kaolin} + 0.000154 * \text{Temp}^2 - 0.004453 * \text{Residence Time}^2 \quad (4.3)$$

The equation in terms of actual factors can be used to make predictions about the response for given levels of each factor. Here, the levels are specified in the original units for each factor. This equation cannot be used to determine the relative impact of each factor because the coefficients are scaled to accommodate the units of each factor.

#### Model Validation for Biogas

##### Normal Residual Plot

As one might expect for all responses, as the regression was run, the Design Expert automatically calculates and plots the residual plot for bio-oil (Figure 4.29) to validate the model. Since the points in the residual plot are randomly distributed on the vertical axis, a nonlinear (quadratic) is appropriate for the data and model prediction can be considered accurate.

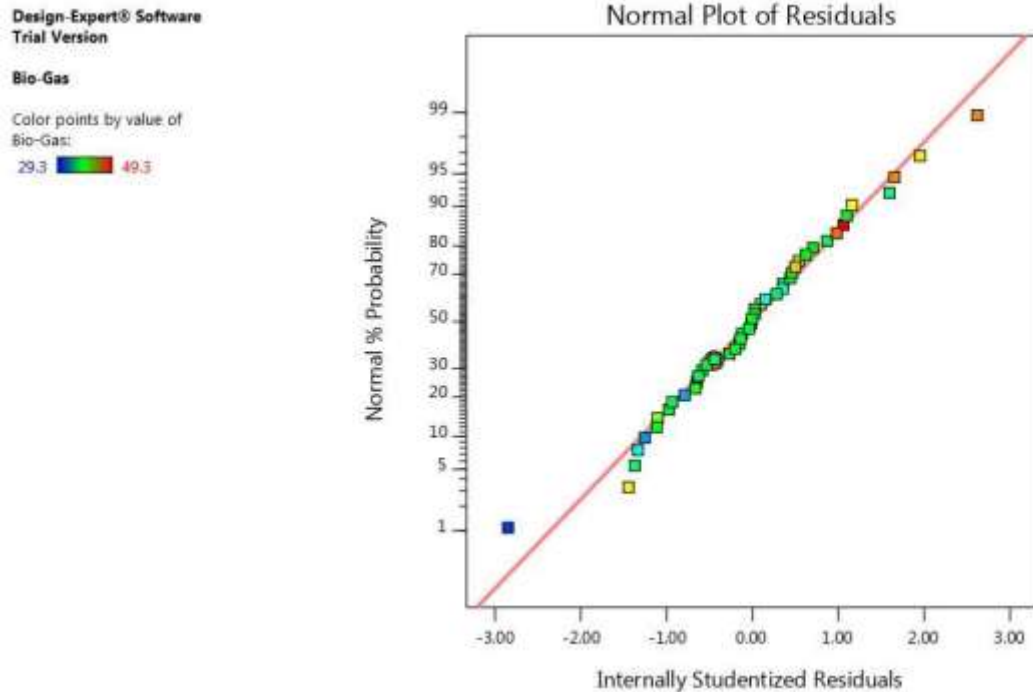


Figure 4.29: Normal Residual Plot for SD Biogas

#### Contour and 3D Plots for Biogas

The two plots (Contour and 3D) represented on Figure 4.30a and 4.30b (for temperature and residence time) were presented to visualize the response (biogas) yields as a function of two separate independent variables that are significant and had interactive effect on biogas production. For contour plot, the yields were represented on the contour line while temperature and particle sizes were represented on horizontal and vertical axis. For 3D plot, yields of biogas, temperature and particle sizes were represented on y, x and z planes.

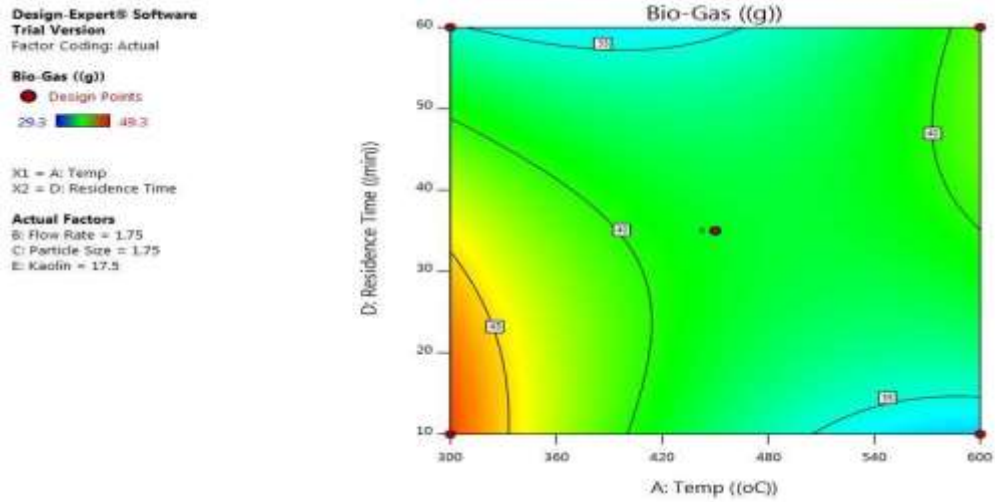


Figure 4.30a: Contour Plot for Temperature and Residence Time on Biogas yields

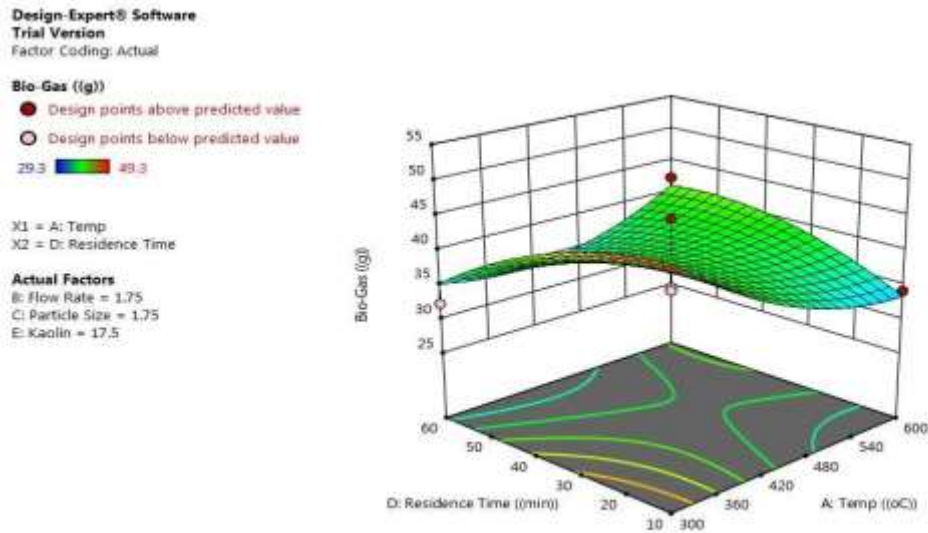


Figure 4.30b: 3D Plot for Temperature and Residence Time on Biogas yields 4.7.2

### Optimization of PW pyrolysis

This section depicted the optimization results of Poultry Waste as a function of some independent variables otherwise called process parameters (Temperature, Flow rate, Particle size, Residence Time and Kaolin ratio) to obtain various responses known as pyrolysis products (Biochar, Bio-oil and Biogas). As shown on the Table (available at appendix D), the

computational software (Design Expert version 12.0) adopted for the optimization purpose divided the coded factor into low, mid and upper points corresponding to -1, 0 and +1 languages understood by computer. In similar manner, the yields of responses 1 and 2 (Biochar and Bio-oil) attained high values around the midpoint of temperature, low value of residence and kaolin along with high residence time appeared to favour biochar production.

#### 4.7.2.1 ANOVA for quadratic model of response 1: biochar

The analysis of variance and fit statistics of biochar resulted from optimization of PW pyrolysis are shown on Table 4.16 and 4.17 respectively. The Model F-value of 1214.03 implies the model is significant. There is only a 0.01% chance that an F-value could occur due to noise-values of less than 0.0500 indicate that model terms are significant. In this case A, C, AE, A<sup>2</sup> are significant model terms. Basically, values greater than 0.1000 indicate the model terms are not significant. Many insignificant model terms are removed for the reduction of model

Table 4.16: ANOVA for Biochar

Source	Sum of Squares	df	Mean Square	F-value	p-value
Model	4032.60	20	201.63	1214.03	< 0.0001 Significant
A-Temperature	8.70	1	8.70	52.40	< 0.0001
C-Particle Size	0.9025	1	0.9025	5.43	0.0281
AE	1.0000	1	1.0000	6.02	0.0214
A <sup>2</sup>	3382.67	1	3382.67	20367.31	< 0.0001
Residual	4.15	25	0.1661		
Lack of Fit	4.15	20	0.2076		
Pure Error	0.0000	5	0.0000		
Cor Total	4036.75	45			

Table 4.17: Fit Statistics

Fit Statistics			
Std. Dev.	0.4075	R <sup>2</sup>	0.9990
Mean	42.61	Adjusted R <sup>2</sup>	0.9981
C.V. %	0.9564	Predicted R <sup>2</sup>	0.9959

PRESS	16.61	Adeq Precision	77.9825
-------	-------	-------------------	---------

---

The Predicted R<sup>2</sup> of 0.9959 is in reasonable agreement with the Adjusted R<sup>2</sup> of 0.9981; i.e., the difference is less than 0.2. Adequate Precision usually measures the signal to noise ratio. A ratio greater than 4 is desirable. Thus, the ratio of 77.983 indicates an adequate signal.

#### Final Equation in Terms of Actual Factors

$$\text{Biochar} = -124.29350 + 0.776517 * \text{Temperature} - 0.214000 * \text{Particle Size} + 0.000267 * \text{Temperature} * \text{Kaolin Ratio} - 0.000875 * \text{Temperature}^2 \quad (4.4)$$

The equation in terms of actual factors can be used to make predictions about the response for given levels of each factor. Here, the levels are specified in the original units for each factor. This equation cannot be used to determine the relative impact of each factor because the coefficients are scaled to accommodate the units of each factor.

#### Model Validation for PW Biochar

##### Normal Residual Plot

Stat Ease Design Expert version 12.0 automatically calculates and plots the residual plot (Figure 4.31) to validate the model. Since the points in the residual plot are randomly distributed on the vertical axis, a nonlinear (quadratic) is appropriate for the data and model prediction can be considered accurate.

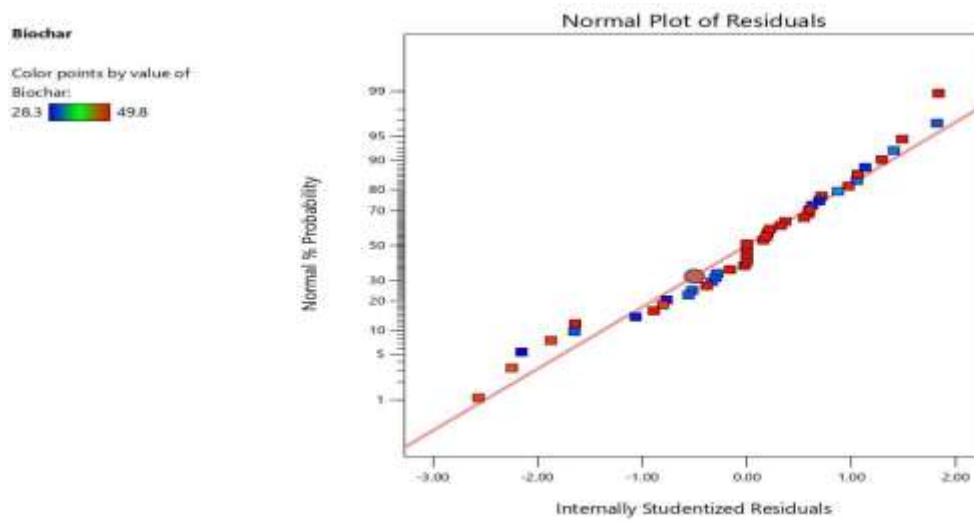


Figure 4.31: Normal Residual Plot for PW Biochar

#### Single Factor Effect on PW Biochar

The single effects of temperature and particle size on the optimization of PW for biochar production are shown in Figure 4.32a and 4.32b respectively. It could be observed that the yield of biochar initially increased up to approximately 450 °C and later decreases to the final temperature of 600 °C. The yields of biochar also increase with increasing particle size. This could be as a result of temperature gradient established between the biomass core and its outer surface.

Factor Coding: Actual

**Biochar ((g))**

● Design Points

--- 95% CI Bands

X1 = A

**Actual Factors**

B = 1.75

C = 1.75

D = 35

E = 17.5

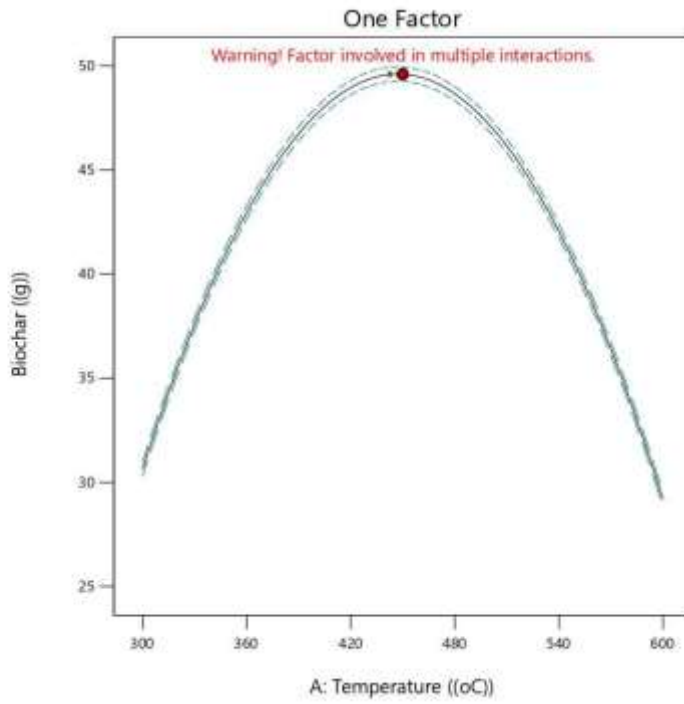


Figure 4.32a: Single Effect of Temperature on PW Biochar

Factor Coding: Actual

**Biochar ((g))**

● Design Points

--- 95% CI Bands

X1 = C

**Actual Factors**

A = 450

B = 1.75

D = 35

E = 17.5

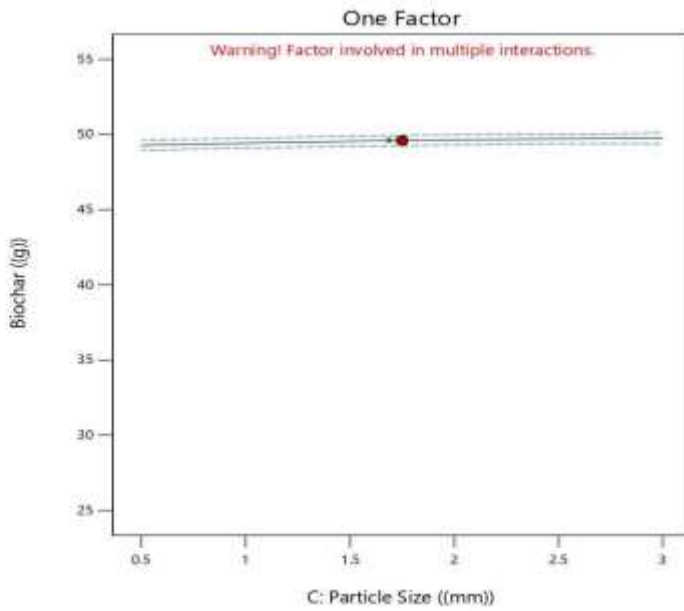


Figure 4.32b: Single Effect of Particle Size on PW Biochar

Contour and Interaction Plots for PW Biochar

The two plots (Contour and Interaction) represented on Figure 4.33a and 4.33b (for temperature and Kaolin ratio) were presented to visualize the response (biochar) yields as a function of two separate independent variables that are significant and had interactive effect on biochar production. For contour plot, the yields were represented on the contour line while temperature and Kaolin ratio were represented on horizontal and vertical axis. For Interaction plot, yields of biochar, temperature and kaolin ratio were represented on y, x and z planes.

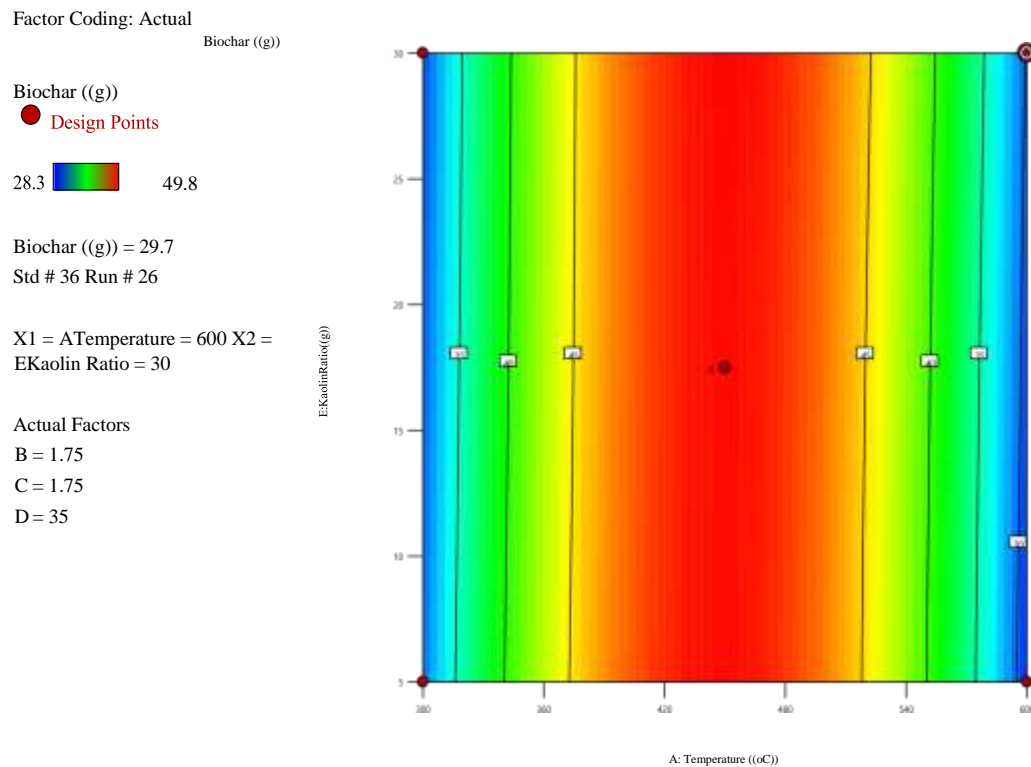


Figure 4.33a: Contour Plot for Temperature and Kaolin ratio on PW Biochar yields

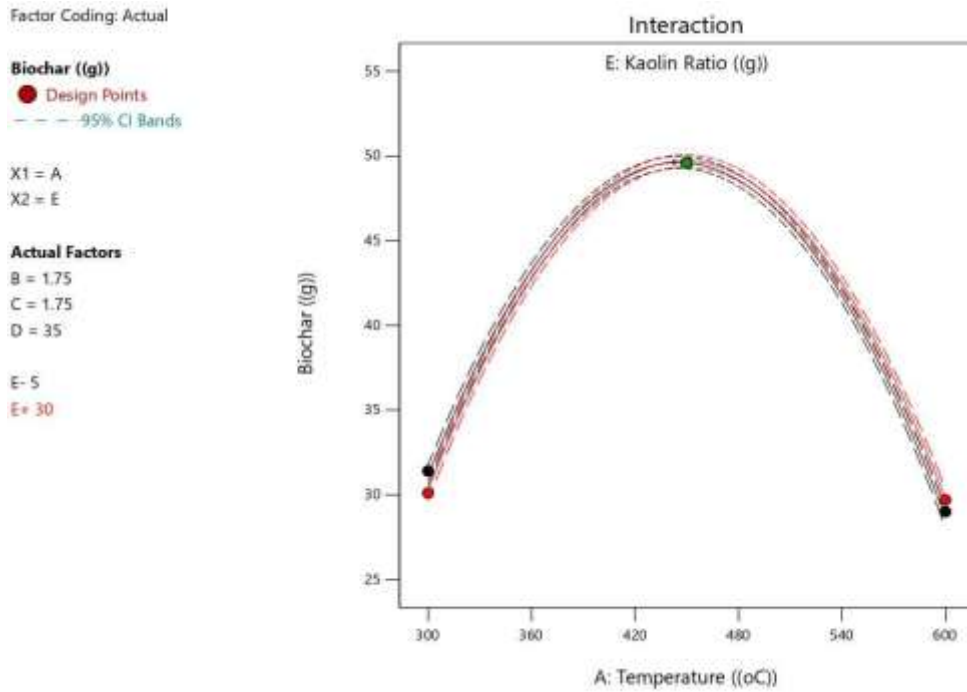


Figure 4.33b: Interaction Plot for Temperature and Kaolin on PW Biochar yields

#### 4.7.2.2 ANOVA for quadratic model of response 2: bio-oil

The Model F-value of 4.66 implies the model is significant. There is only a 0.02 % chance that an F-value this large could occur due to noise. With P-values less than 0.0500 shows model terms are significant. In this case A, C, AE, A<sup>2</sup> are significant model terms.

Values greater than 0.1000 indicate the model terms are not significant. The Lack of Fit F-value of 79.14 implies the Lack of Fit is significant. There is only a 0.01% chance that a Lack of Fit F-value could occur due to noise. Table 4.18 and 4.19 represent the ANOVA and Fit statistics for PW bio-oil

Table 4.18: ANOVA for PW Bio-oil

Source	Sum of Squares	df	Mean Square	F-value	p-value
Model	39.45	20	1.97	4.66	0.0002 Significant
A-Temperature	12.78	1	12.78	30.18	< 0.0001
C-Particle Size	1.89	1	1.89	4.46	0.0448
AE	2.72	1	2.72	6.43	0.0179
A <sup>2</sup>	13.28	1	13.28	31.35	< 0.0001
Residual	10.59	25	0.4234		
Lack of Fit	10.55	20	0.5276	79.14	< 0.0001 Significant
Pure Error	0.0333	5	0.0067		
Cor Total	50.03	45			

Table 4.19: Fit Statistics for PW Bio-oil

Fit Statistics			
Std. Dev.	0.6507	R <sup>2</sup>	0.7884
Mean	32.85	Adjusted R <sup>2</sup>	0.6192
C.V. %	1.98	Predicted R <sup>2</sup>	0.1554
PRESS	42.26	Adeq Precision	8.5624

The Predicted R<sup>2</sup> of 0.1554 is not as close to the Adjusted R<sup>2</sup> of 0.6192 as one might normally expect; i.e., the difference is more than 0.2. This indicates a large block effect or a possible problem with model and/or data. Adequate Precision measures the signal to noise ratio. A ratio greater than 4 is desirable. Thus, ratio of 8.562 indicates an adequate signal.

#### Final Equation in Terms of Actual Factors

$$\text{Bio-oil} = +40.88617 - 0.041525 * \text{Temperature} + 0.649000 * \text{Particle Size} - 0.000440 * \text{Temperature} * \text{Kaolin Ratio} + 0.000055 * \text{Temperature}^2 \quad (4.4)$$

The equation in terms of actual factors can be used to make predictions about the response for given levels of each factor. Here, the levels are specified in the original units for each factor. This equation cannot be used to determine the relative impact of

each factor because the coefficients are scaled to accommodate the units of each factor and the intercept is not at the center of the design space.

## Model Validation for PW Bio-oil

### Normal Residual Plot

Stat Ease Design Expert version 12.0 automatically calculates and plots the residual plot (Figure 4.34) to validate the model. Since the points in the residual plot are randomly distributed on the vertical axis, a nonlinear (quadratic) is appropriate for the data and model prediction can be considered accurate.

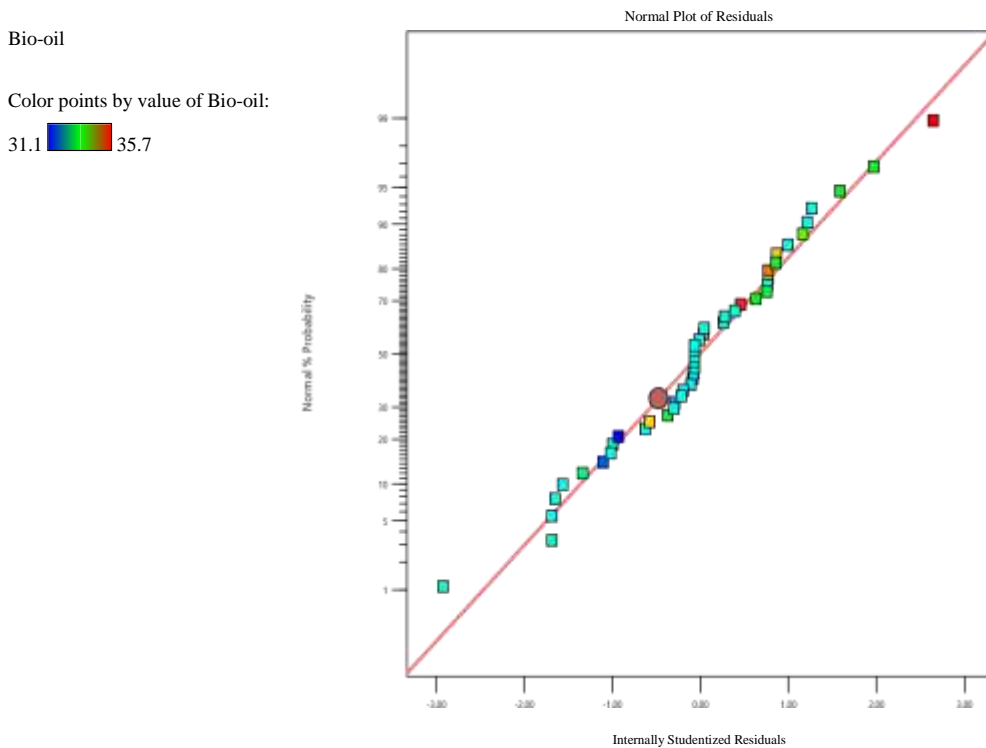


Figure 4.34: Normal Residual Plot for PW Bio-oil

### Single Factor Effect on PW Bio-oil

Figure 4.35a and 4.35b are representative of the single effect of temperature and particle size on bio-oil production from PW. It could be observed that the yield of bio-oil

increased up to approximately 450 °C and later decreases to the final temperature of 600 °C. The yields of bio-oil decrease with increasing particle size. Thus, small particle size favors bio-oil production.

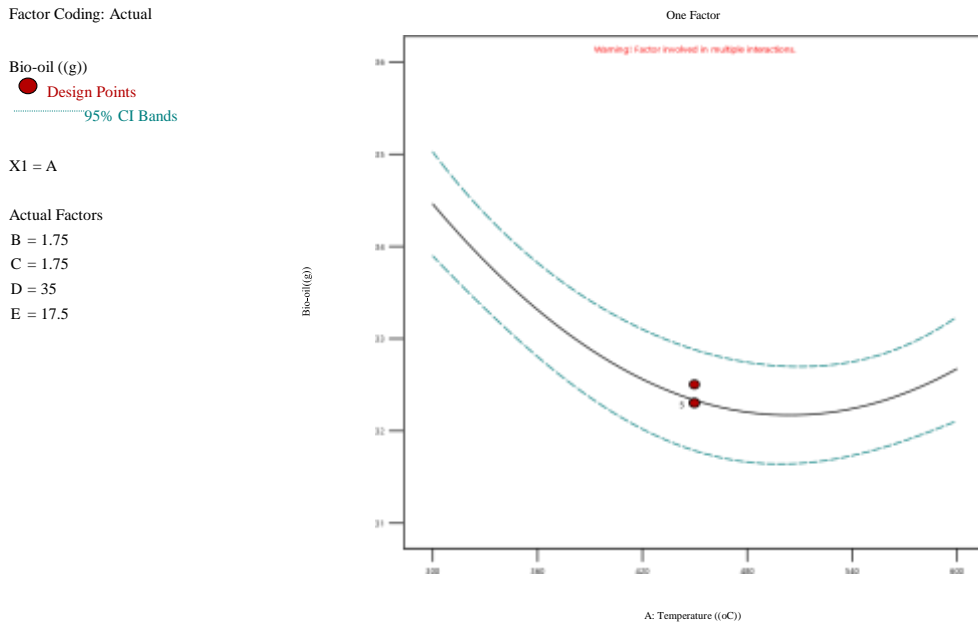


Figure 4.35a: Single Effect of Temperature on PW Bio-oil

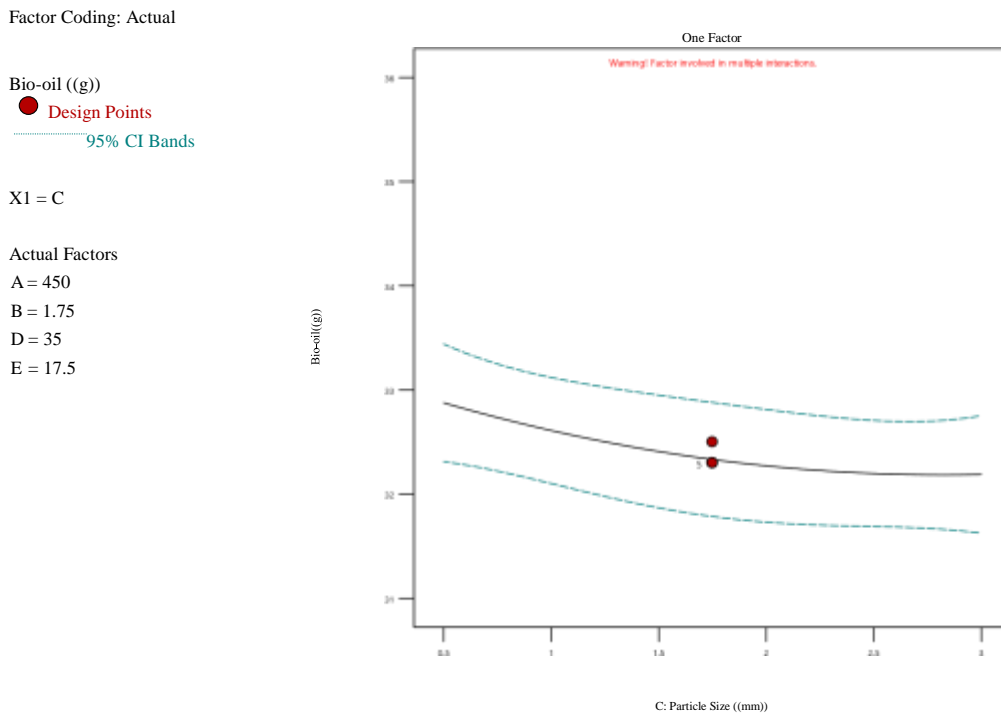


Figure 4.35b: Single Effect of Particle Size on PW Bio-oil

Contour and Interaction Plots for PW Bio-oil

The two plots (Contour and Interaction) represented on Figure 4.36a and 4.36b (for temperature and Kaolin ratio) were presented to visualize the response (bio-oil) yields as a function of two separate independent variables that are significant and had interactive effect on bio-oil production. For contour plot, the yields were represented on the contour line while temperature and Kaolin ratio were represented on horizontal and vertical axis. For Interaction plot, yields of biochar, temperature and kaolin ratio were represented on y, x and z planes.

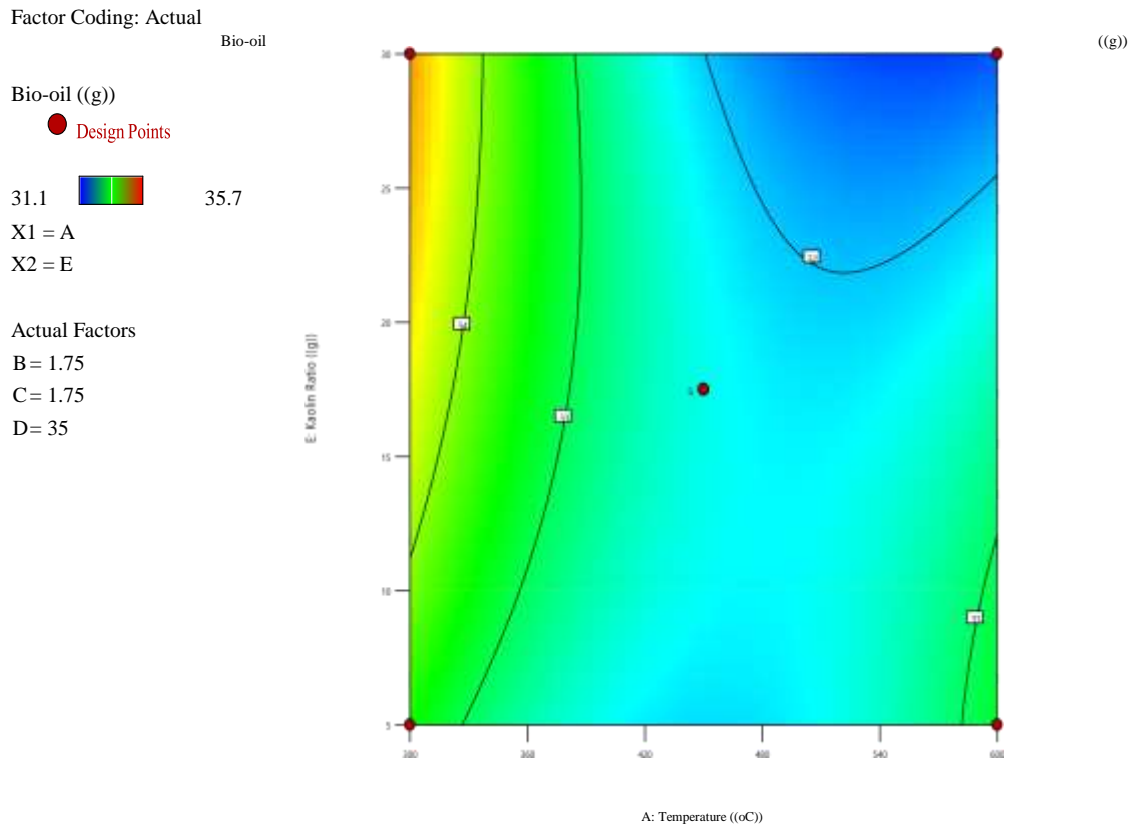


Figure 4.36a: Contour Plot for Temperature and Kaolin ratio on PW Bio-oil Production

Factor Coding: Actual

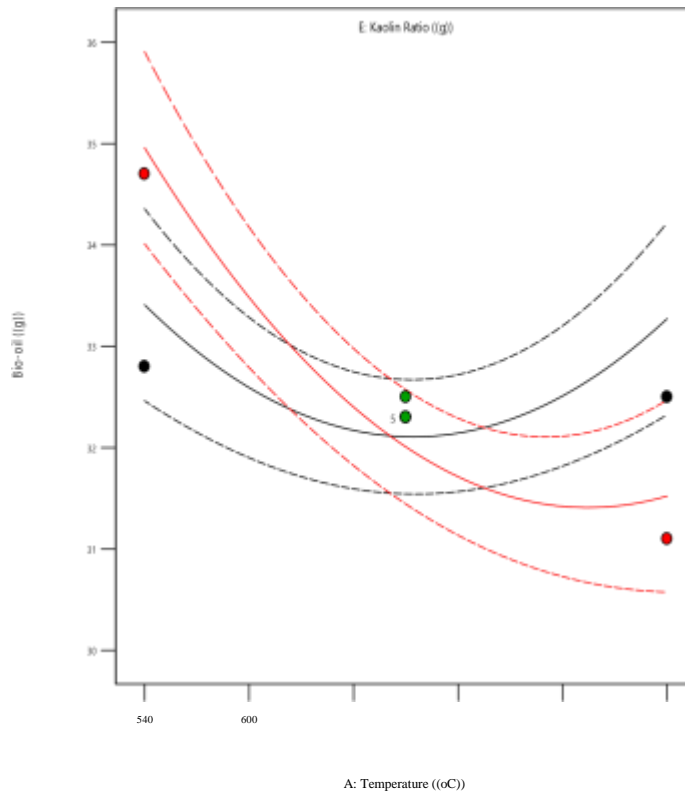
Interaction

Bio-oil ((g))  
 ● Design Points  
 — 95% CI Bands

X1 = A  
 X2 = E

Actual Factors  
 B = 1.75  
 C = 1.75  
 D = 35

E- 5  
 E+ 30



300  
420

360  
480

Figure 4.36b: Interaction Plot for Temperature and Kaolin ratio on PW Bio-oil

#### 4.7.2.3 ANOVA for quadratic model of response 3: biogas

Table 4.20 and 4,21 present the ANOVA and Fit statistics for biogas. The Model F-value of 155.11 implies the model is significant. There is only a 0.01 % chance that an F-value been large could occur due to noise. Since P-value is less than 0.0500, it implies the model terms are significant. In this case A, AD, CE, A<sup>2</sup> are significant model terms. Values greater than 0.1000 indicate the model terms are not significant. Many insignificant model terms are removed to improve the model. The Lack of Fit F-value of 0.97 implies the Lack of Fit is not significant relative to the pure error. There is a 57.53 % chance that a Lack of Fit F-value been large could occur due to noise. Non-significant lack of fit is good -- we want the model to fit.

Table 4.20: ANOVA for PW Biogas

Source	Sum of	df	Mean Square	F-value	p-value
--------	--------	----	-------------	---------	---------

### Squares

Model	4429.44 20	221.47 155.11	< Significant 0.0001
A-Temperature	191.13 1	191.13 133.86	< 0.0001
AD	6.25 1	6.25 4.38	0.0467
CE	7.02 1	7.02 4.92	0.0359
A <sup>2</sup>	3493.82 1	3493.82 2446.85	< 0.0001
Residual	35.70 25	1.43	
Lack of Fit	28.36 20	1.42 0.9669	0.5753 not significant
Pure Error	7.33 5	1.47	
Cor Total	4465.14 45		

Table 4.21: Fit Statistics for PW Biogas

Fit Statistics			
Std. Dev.	1.19	R <sup>2</sup>	0.9920
Mean	25.40	Adjusted R <sup>2</sup>	0.9856
C.V. %	4.70	Predicted R <sup>2</sup>	0.9722
PRESS	124.01	Adeq Precision	31.7979

The Predicted R<sup>2</sup> of 0.9722 is in reasonable agreement with the Adjusted R<sup>2</sup> of 0.9856; i.e. the difference is less than 0.2. Adequate Precision measures the signal to noise ratio. A ratio greater than 4 is desirable. A ratio of 31.798 indicates an adequate signal. This model can be used to navigate the design space.

#### Final Equation in Terms of Actual Factors

$$\text{Biogas} = +189.52317 - 0.771925 * \text{Temperature} - 0.000333 * \text{Temperature} * \text{Residence Time} + 0.084800 * \text{Particle Size} * \text{Kaolin Ratio} + 0.000889 * \text{Temperature}^2 \quad (4.5)$$

The equation in terms of actual factors can be used to make predictions about the response for given levels of each factor. Here, the levels are specified in the original units for each factor. This equation cannot be used to determine the relative impact of each factor because the coefficients are scaled to accommodate the units of each factor.

## Model Validation for PW Biogas

### Normal Residual Plot

Stat Ease Design Expert version 12.0 automatically calculates and plots the residual plot (Figure 4.37) to validate the model. Since the points in the residual plot are randomly distributed on the vertical axis, a nonlinear (quadratic) is appropriate for the data and model prediction can be considered accurate.

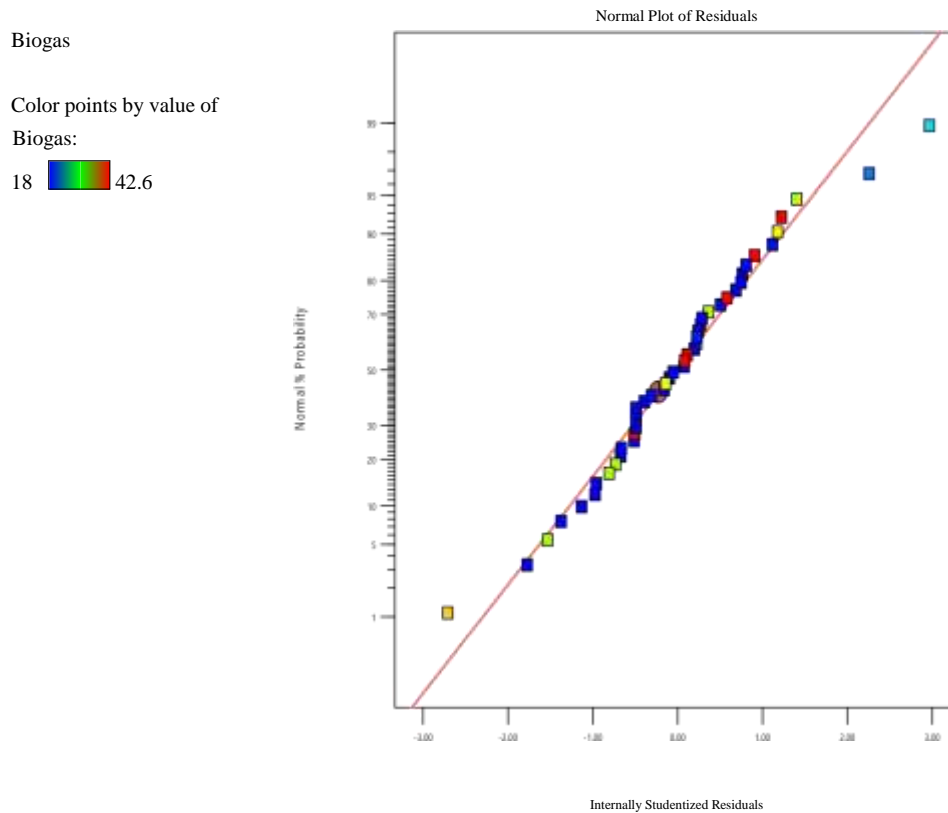


Figure 4.37: Normal Residual Plot for PW Biogas

### Contour and Interaction Plots for PW Biogas

The two plots (Contour and Interaction) represented on Figure 4.38a and 4.38b (for temperature and residence time) were presented to visualize the response (biogas) yields as a function of two separate independent variables that are significant and had

interactive effect on bio-oil production. For contour plot, the yields were represented on the contour line while temperature and residence time were represented on horizontal and vertical axis. For Interaction plot, yields of biogas, temperature and residence time were represented on y, x and z planes.

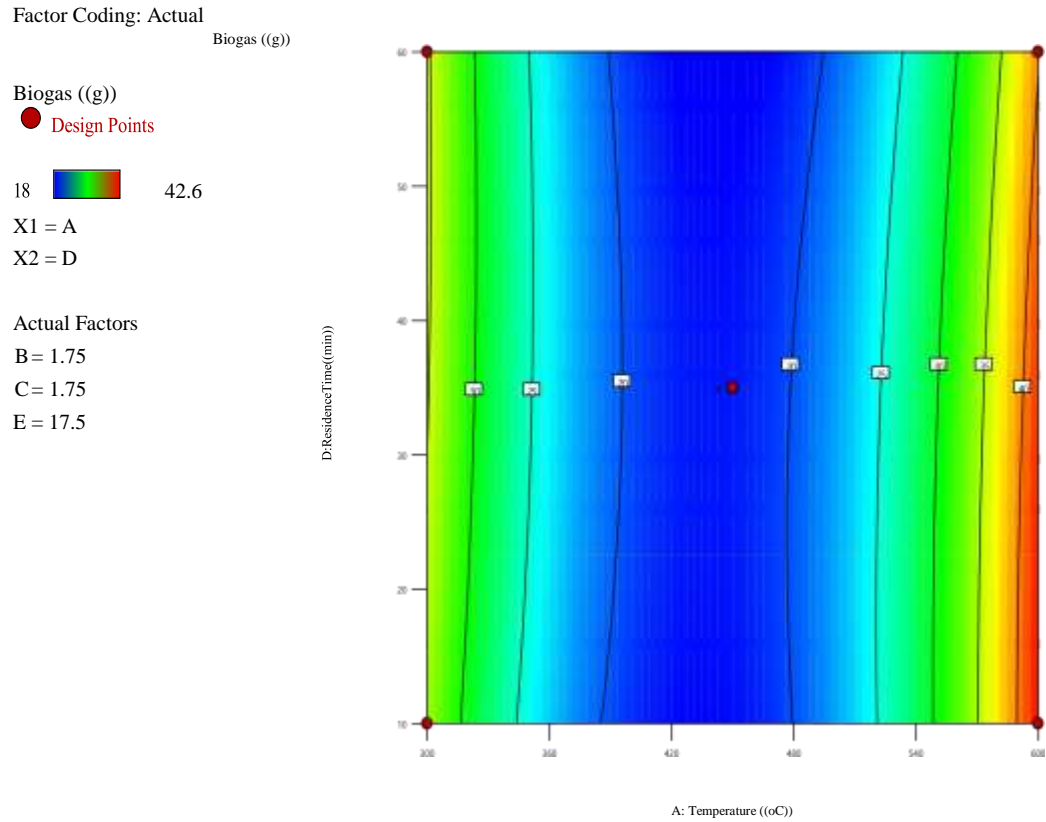


Figure 4.38a: Contour Plot for Temperature and residence time on PW Biogas

Factor Coding: Actual

Interaction

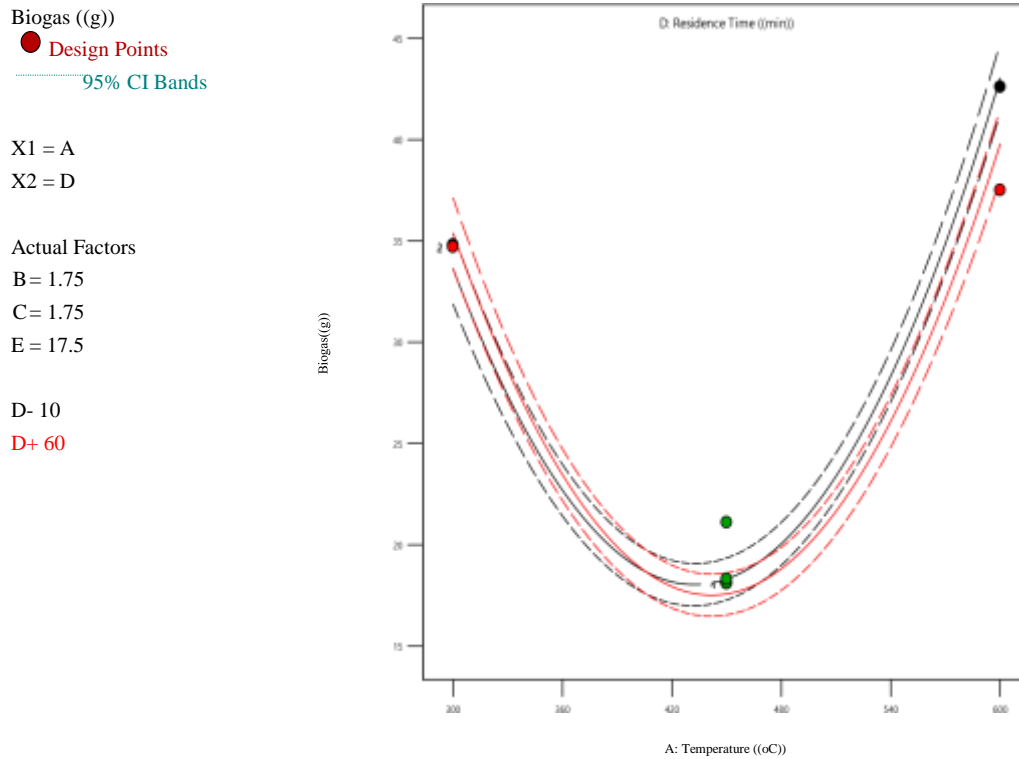


Figure 4.38b: Interaction Plot for Temperature and residence time on PW Biogas

#### Effect of Particle size and Kaolin ration on Biogas Formation

As can be seen in Figure 4.39, low values of kaolin ratio and particle size favoured the production of biogas. The yields appeared optimum when kaolin ratio was 5 g and particle was 0.5 mm while other conditions remained constant.

Factor Coding: Actual

Interaction

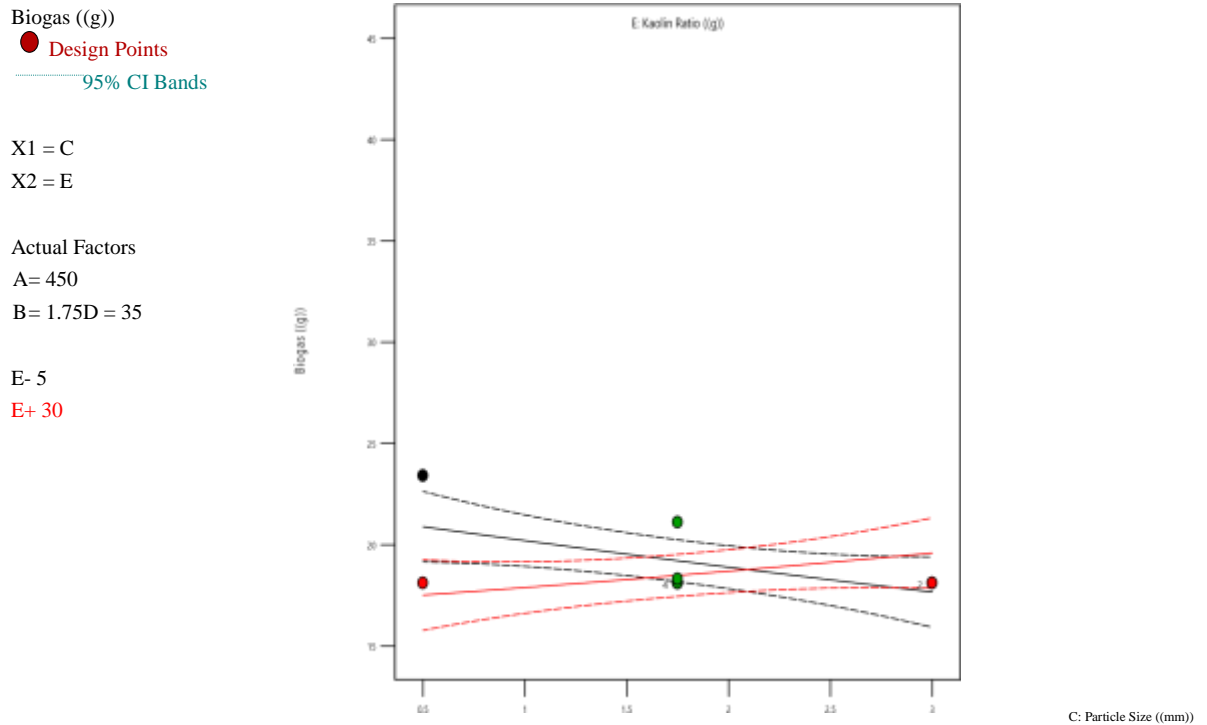


Figure 4.39: Effect of Particle size and Kaolin ratio on Biogas Formation 4.8.3

#### Experimental and predicted results

The predicted results obtained at the optimum conditions of the optimization process which include: temperature (468 °C), flow rate (1.6 L/min), particle size (3 mm), residence time (60 min) and kaolin ratio (5.6 g) for the sawdust and temperature (443 °C), flow rate (0.5 L/min), particle size (3mm), residence time (54 min) and kaolin ratio (5.0g) for the poultry waste were shown on Table 4.22. The experimental result of sawdust biochar was 36.2 % as against experimental value of 39.2 %. The variation could be due to high flow rate and longer residence time employed. Longer residence provides a greater chance for the re-polymerization of constituents of biomass thereby enhancing the yields of biochar (Krishna and Sheeja, 2018). The observed yields of bio-oil and biogas were 30.7 % and 33.1 % respectively. It could be reasonable to suggest that high flow rate of inert gas reduced the residence time of volatiles which contributed to their high yields. Similarly for poultry waste, observed value of biochar

yield had a close value to the predicted value by the model. The observed yield of bio-oil was less than the predicted value. This could be due to ineffectiveness of the condensing medium which gave rise to more yield of biogas. Also, longer-sized particles were found to be responsible for low yields of liquid product due to occurrence of secondary reaction at high temperature (Di Blasi et al., 2021).

Table 4.22: Experimental and Predicted Values

Responses	Experimental value		Predicted Value	
	SD	PW	SD	PW
Biochar	39.2	50.3	36.2	49.5
Bio-oil	28	31.3	30.7	24.1
Biogas	32.5	18.4	33.1	24.9

#### 4.8.4 Summary of optimization process

The use of Stat Ease Design Expert is indeed a powerful computer software tool for process optimization. The following response variables were evaluated: Biochar, Bio-oil and Biogas. While the independent variables include: temperature, flow rate, particle size, residence time and kaolin ratio. For each response, the program delivered a regression model which is quadratic in nature and validated through normal residual plot. Model reduction was embraced which involve elimination of model terms that are not significant. Each response had a model equation with variables that are significant in its production. As such, six model equations were developed for the three responses each from the selected biomass (sawdust and poultry waste).

At the instance of optimization process, the constraints were set which involve maximizing the yield of biochar and to minimize other two responses (bio-oil and biogas). The lower and upper limits of the variables were set: temperature (300 to 600 °C), flow rate (0.5 to 3L/min), particle size (0.5 to 3 mm), residence time (10 to 60 mm) and kaolin ratio (5 to 30 g). The system performed 46 runs for each biomass and generated over 100 solutions.

For sawdust, the optimum conditions suggested by the model are: temperature (468 °C), flow rate (1.6 L/min), particle size (3 mm), residence time (60 min) and kaolin ratio (5.6 g) while that of poultry waste are: temperature (443 °C), flow rate (0.5 L/min), particle size (3 mm), residence time (54 min) and kaolin ratio (5.0 g). On comparison, the observed yields of biochar in both scenarios were lesser than the predicted values.

## CHAPTER FIVE

### 5.0 CONCLUSION AND RECOMMENDATIONS

#### 5.1 Conclusion

The present study examined the effect of metakaolin and process parameters on the production of biochar for carbon dioxide sequestration. The effect of pyrolysis conditions on the production of biochar is becoming a frontier study. This study discussed comprehensively how metakaolin, biomass compositions and their physiochemical properties and pyrolysis operating conditions such as temperature, sweeping gas flow rate, residence time and feed stock particle sizes affect the yield of biochar. Temperature is widely studied in pyrolysis process because all other fundamental changes in the resulting products are temperature dependant. As such, the study found that:

The candidatures of sawdust and poultry waste with moisture contents of 3.56 and 1.4 % and fixed carbon contents of 28.32 and 51.6 % were reasonable to be used for biochar production as little energy would be expended during carbonization.

Moderate temperature of about 400 °C at optimum conditions of other riverine parameters produced 39.2 % and 50.3 % of biochar when sawdust and poultry waste biomass were pyrolyzed.

Shorter residence of volatiles in the reactor caused relatively minor decomposition of higher molecular weight compounds. Thus, shorter residence of 10 mins gives higher yield of biochar in both sawdust and poultry waste biomass.

High yield of biochar was achieved at 3.00 mm particle sizes. This was influenced by heat transfer mechanism between the biomass particles.

Different grades of biochar such SBC400, PBC400, SKBC400 and PKBC400 were produced at 400 °C under optimum conditions other parameters to deduced the effect of metakaolin on biochar production.

Relatively low metakaolin mixing ratio of 10 wt% for every 20 g of sawdust and poultry waste biomass pyrolyzed yielded reasonable amount of biochar at optimum operating condition.

The percentage increment when metakaolin was added at 10 % ratio shows 18.4 and 8.2 % increment for sawdust and poultry waste as compared to values obtained for SBC400 and PBC400.

SKBC and PKBC have 57.50 % and 60.78 % Carbons present in biochar and subsequently they have highest potential CO<sub>2</sub> sequestration.

To avoid energy expended on the carbonization, production and subsequent modification of activated carbon with high pore sizes, direct solid – solid mixing of biomass with metakaolin is desirable and cheaper to obtain the same activated carbon with adsorptive properties (that is, Sawdust Kaolin Modified Activated Carbon and Poultry Waste Kaolin Modified Activated Carbon represented as SUMAC and PUMAC).

Interest in biochar production from organic waste has been growing in recent time due to its broad applicability and availability. Biochar, as a carbon sequester, is based on the idea that biochar carbon can persist in the soil for hundreds of years or even longer. This study confirmed that metakaolin as an additive in pyrolysis process increased the biochar yield when added at optimum conditions. To combat world's major problems of global warming, scarcity of fuel and attaining efficient waste management strategy, biochar production and its characterization should be considered priority.

### 5.3 Recommendations

Continuous investigation on the influence of mineral additives such kaolin and production conditions on the yield of biochar is desirable due in part as a climate change mitigator and waste management strategy. Since strategies were proposed to promote

the utilization of biochar as climate change mitigation tool, research effort should be constantly tailored to enhance biochar yield. This study, therefore, offered the following recommendations:

Further research work should be conducted on the pyrolysis of sawdust and poultry waste with addition of metakaolin between 5 % and 10 % to ascertain the exact proportion of metakaolin for optimum biochar yield.

- i. Slow pyrolysis of biomass is already apparent for biochar production and high feedstock particle sizes was concluded to favoured biochar yield. However, additional effort should be tailored toward obtaining the limit level of particle size that gives high production of biochar.
- ii. The negative correlation between biochar yield and residence time is an indication that further research effort is required to determine the limit level of sweeping gas flow rate that favours biochar production.
- iii. Investigation on the use of other Kaolin is necessary to established the influence of geographical location and their inherent properties on the biochar production.

### 5.3 Contribution to Knowledge

The study on the effect of metakaolin and process conditions on the pyrolysis of sawdust and poultry waste biomass was carried out in a fixed bed reactor and the results show that metakaolin addition at 10 wt% to the selected biomass increases their biochar production at optimum operating conditions (Temperature 400 °C, Sweeping gas flowrate 1.0 L/min, particle size 3.00 mm and residence time of 10 min) with yield increased by 8.7% and 18.4% respectively while also increasing their carbon dioxide sequestration potentials by 32.2% and 10,1% for sawdust and poultry waste biomass. Thus, these results indicated that the climate change mitigation can be achieved through progressive production of biochar from biomass amended with metakaolin and its

subsequent utilization in CO<sub>2</sub> capture. The mechanism and the effect of metakaolin on biochar production was proposed.

#### References

- Agba, A.M., Ushie, M.E., Abam, F.I., Agba M.S. & Okoro, J. (2020). Developing the Biofuel Industry for Effective Rural Transformation, *European Journal of Scientific Research*, 40(3), 441-449.
- Ajueyitsi, O.N. (2018). Optimization of Biomass Briquette Utilisation as Fuel for Domestic Use, PhD Research Proposal, Department of Mechanical Engineering, FUTO.
- Akhtar, J., Amin, N., & Saidina, A. (2017). A Review on Operating Parameters for Optimum Liquid Oil Yield in Biomass Pyrolysis. *Renewable Sustainable Energy Reserve*, 16 (7), 5101–5109.

- Akwasi, A.B. (2020). Energy Crops – Biomass Resources and Traits. *Pyrolysis of Biomass for Fuels and Chemicals*, 23, 301 – 310.
- Alhassan, M., Andrew, I., Auta, M., Umaru, M., Garba, U. G., Isah, A. G. & Alhassan, B. (2017). Comparative studies of CO<sub>2</sub> Capture Using Acid and Base Modified Activated Carbon from Sugarcane Bagasse. *Biofuels*, DOI:10.1080/17597269.2017.1306680.
- Allyson, S. (2017). Biochar Production for Carbon Dioxide Sequestration. Qualifying Project for Award of Bachelor of Engineering, Worcester Polytechnic Institute.
- Anex, R.P., Aden, A., Kazi, F.K., Fortman, J., Swanson, R.M., Wright, M.M., Satrio, J., Brown, R.C., Daugaard, D.E., Platon, A., Kothandaraman, G., Hsu, D.D., & Dutta, A. (2020). Techno-economic Comparison of Biomass-To-Transportation Fuels via pyrolysis, Gasification, and Biochemical Pathways. *Fuel*, 89, 29 – 35.
- Angin, D. (2018). Effect of Pyrolysis Temperature and Heating Rate on Biochar Obtained from Pyrolysis of Safflower Seed Press Cake. *Bioresource Technology*, 128, 593 – 597.
- Antal, M.J. & Gronli, M. (2017). The Art, Science and Technology of Charcoal Production. *Industrial and Engineering Chemistry Research*, 42(8), 1619 - 1640.
- Antal, M.J., Allen, S.G., Dai, X., Shimizu, B., Tam, M.S., & Grønli, M. (2019). Attainment of the Theoretical Yield of Carbon from Biomass. *Industrial and Engineering Chemistry Research*, 39(11), 4024 – 4031.
- Arenillas, A., Rubiera, F., Parra J.B., Ania, C.O., & Pis, J.J., (2017). Surface Modification of Low-Cost Carbons for their application in the Environmental Protection, *Applied Surface Science*. 252, 619 – 624.
- Arsen, U., & Gregorio, F. (2019). A Waste Management Planning Based on Substance Flow Analysis. *Resource Conservation and Recycling*, 85, 54 – 66.
- Asai, H., Samson, B.K., Stephan, H.M., Songyikhangsuthor K., Homma, K., Kiyono Y., Inoue Y., Shiraiwa, T. & Horie, T. (2019). Biochar Amendment Techniques for Upland Rice Production in Northern Laos, *Field Crops Research*, 10(111), 8184.
- Ayllon, M., Aznar, M., Sanchez, J., Gea, G., & Arauzo J. (2019). Influence Of Temperature and Heating Rate on the Fixed Bed Pyrolysis of Meat and Bone Meal. *Chemical Engineering Journal.*, 121(2–3), 85 – 96.
- Aysu, T., & Kuck, M.M. (2021). Biomass Pyrolysis in a Fixed-Bed Reactor: Effects of Pyrolysis Parameters on Product Yields and Characterization of Products. *Energy*, 64, 1002 – 1025.

- Azevedo, S.G., Trago, S., Marcelo, S., & Luis, M. (2019). Biomass-Related Sustainability: A Review of the Literature and Interpretive Structural Modelling. *Energy*, 171, 1107 – 1125.
- Badejo, S. O. (2017). Preliminary Study on the Utilisation of Nigerian Sawmill Sawdust for the Production of Water Proof Cement Bonded Ceiling Boards, *FRIN Bulletin*. 58.
- Bardalai, M. & Mahanta, D.K. (2020). Study of some Catalyst in Biomass Pyrolysis, *International Journal of Chemistry Research* 5, 433- 439.
- Bates, A. (2017). The Biochar Solution. *Bioresources Technology*, 97(12), 22 - 25.
- Beaumont, O. & Schwob, Y. (2021). Influence of Physical and Chemical Parameters on Wood Pyrolysis. *Industrial & Engineering Chemistry Process Design and Development*, 23(4), 637-641.
- Bello, A., Mohammed, A., Habibu, U., Garba, M.U., Abubakar, I.G., & Aisha, F. (2017). Catalytic Effect of Kaolin on Pyrolysis of Sawdust and Poultry Waste to produce Biochar for CO<sub>2</sub> Sequestration. *Nigerian Journal of Engineering and Applied Sciences*, 4(1), 118 – 130
- Biedemann, P., Riley, R., & Ross, B. (2018). Catalytic Hydrothermal Processing of Microalgae: Decomposition and Upgrading of Lipids. *Bioresources. Technology*. 102(7), 4841 – 4848.
- Biederman, L. A., & Harpole, W. S. (2018). Biochar and its Effects on Plant Productivity and Nutrient Cycling: A Meta-Analysis. *GCB Bioenergy* 5(2), 202 - 214.
- Bilgen, S., Keleş, S., Kaygusuz, A., Sari, A., & Kaygusuz, K. (2018). Global Warming and Renewable Energy Sources for Sustainable Development: A Case Study in Turkey. *Renewable and Sustainable Energy Reserve*, 12(2), 372 – 396.
- Blackwell, P., Riethmuller G. & Collins, M. (2019). Biochar Application to improve Soil Values and Microbial activities, *Agricultural Centre Bulletin*, 4(11), 234 - 241.
- Bouraoui, Z., Jeguirim, M., Guizani, C., Limousy, L., Dupont, C., & Gadiou, R. (2017). Thermogravimetric Study on the Influence of Structural, Textural and Chemical Properties of Biomass Chars on CO<sub>2</sub> Gasification Reactivity. *Energy*, 88, 703 – 710.
- Brebu, M., & Vasile, C. (2020). Thermal Degradation of Lignin - A Review. *Journal of Cellulose Cell*, 2, 43 – 51.
- Bridgwater, A. (2017). Renewable Fuels and Chemicals by Thermal Processing of Biomass. *Chemical Engineering Journal*, 91(2–3), 87–102.

- Brownsort, A. (2019). Biomass Pyrolysis Process – Performance Parameters and their Influence on Biochar System Benefits, B.Sc. Project in Chemical Engineering, University of Edinburgh.
- Bryden, K.M., & Hagge, M.J. (2018). Modelling the Combined Impact of Moisture and Char Shrinkage on The Pyrolysis of a Biomass Particle. *Fuel*, 82(13), 1633 – 1644.
- Canabarro, N., Soares, J.F., Anchieta, C.G., Kelling, C.S., & Mazutti, M.A. (2021). Thermochemical Processes for Biofuels Production from Biomass. *Sustainable Chemistry*. 11(7), 211 – 217.
- Cantrell, K., Ro, K. & Mahajan, D. (2017). Role of Thermochemical Conversion in Livestock Waste-to-Energy Treatments, Obstacles and Opportunities. *Industrial & Engineering Chemistry Research*. 46(26), 8918 - 8927.
- Cao, Q., Xie, K.C. & Bao, W.R. (2018). Process Effects on Activated Carbon with Large Specific Surface Area from Corn Cob. *Bioresources Technology*, 32, 110 – 115.
- Carrier, M., Hardie, A.G., Uras, Ü. Görgens, J., & Knoetze, J. (2017). Production of Char from Vacuum Pyrolysis of South-African Sugar Cane Bagasse and Its Characterization as Activated Carbon and Biochar. *Journal of Analytical and Applied Pyrolysis*, 96, 24 – 32.
- Chan, K.Y. & Xu, Z.H. (2019). Biochar - Nutrient Properties and their Enhancement. *Chemistry Technology*, 44(9), 353 – 363.
- Chang, P.L., Wu, Y.C., Lai, S.J., & Yen, F.S. (2019). Size Effects on V- to A-Al<sub>2</sub>O<sub>3</sub> Phase Transformation. *Journal of European Society*, 29, 3341 – 3348.
- Chen, T., Zhang, Y., Wang, H., Lu, W., Zhou, Z., Zhang, Y., & Ren, L. (2021). Influence of Pyrolysis Temperature on Characteristics and Heavy Metal Adsorptive Performance of Biochar Derived from Municipal Sewage Sludge. *Bioresource Technology*, 164, 47-54.
- Cheng, J., Huang, R., Yu, T., Li, T., Zhou, J., & Cen, K. (2017). Biodiesel Production from Lipids in Wet Microalgae with Microwave Irradiation and Bio-Crude Production from Algal Residue Through Hydrothermal Liquefaction. *Bioresource Technology*, 151, 415 – 418.
- Choi, H.S., Choi, Y.S., & Park, H.C. (2021). Fast Pyrolysis Characteristics of Lignocellulosic Biomass with Varying Reaction Conditions. *Renewable Energy*, 42, 131 - 135
- Claoston N., Samsuri, A.W., & Husni M.H.A. (2017). Effects of Pyrolysis Temperature on the Physicochemical Properties of Empty Fruit Bunch and Rice Husk Biochars. *Waste Management and Research*, 32, 331–339.

- Das, D., & Veziroglu, T.N. (2018). Hydrogen Production by Biological Processes: A Survey of Literature. *International Journal of Hydrogen Energy*, 26, 13 – 28
- Day, D., Evans, R.J., Lee, J.W., & Reicosky, D. (2017). Economical CO<sub>2</sub>, SO<sub>x</sub>, and NO<sub>x</sub> Capture from Fossil-Fuel Utilization with Combined Renewable Hydrogen Production and Large-Scale Carbon Sequestration. *Energy*, 30(14), 2558 - 2579
- Dehkhoda, A. M., & Ellis, N. (2017). Biochar-Based Catalyst for Simultaneous Reactions of Esterification and Transesterification. *Catalysis Today*, 207, 86 - 92.
- Demirbas, A. & Balat, B. (2019). Effects of Temperature and Particle Size on Biochar Yield from Pyrolysis of Agricultural Residues. *Journal of Analytical and Applied Pyrolysis*, 6(3), 243 – 248.
- Demirbas, A. (2018a). Effects of Temperature and Particle Size on Biochar Yield from Pyrolysis of Corn Nob and Agricultural Residues. *Journal of Analytical and Applied Pyrolysis*, 72, 243 - 248.
- Demirbas, A. (2018b). Potential Applications of Renewable Energy Sources, Biomass Combustion Problems in Boiler Power Systems and Combustion Related Environmental Issues. *Programming Energy Combustion Science*, 31(2), 171 – 192.
- Demirbas, A. (2019). Bio-fuels from Agricultural Residues. *Energy Source, Part A Recovery and Utilization. Environmental Effluents*, 30(2), 101 – 109.
- Demirbas, A., & Arin, G. (2022). An Overview of Biomass Pyrolysis. *Energy Sources* 24(5), 471 – 482.
- Devi, P., & Saroha, A. K. (2019). Effect of Pyrolysis Temperature on Polycyclic Aromatic Hydrocarbons Toxicity and Sorption Behaviour of Biochar Prepared by Pyrolysis of Paper Mill Effluent Treatment Plant Sludge. *Bioresource Technology*, 192, 312 – 320.
- Di Blasi, C., Chimica, I., & Li, F. (2021). Modelling Intra and Extra Particle Processes of Wood Fast Pyrolysis, *American Institute of Chemical Engineers Journal*. 48, 2386 – 2397.
- Dominguez, A., Menendez, J. A., & Pis, J.J. (2017). Hydrogen Rich Fuel Gas Production from the Pyrolysis of Wet Sewage Sludge at High Temperature. *Journal of Analytical and Applied Pyrolysis*, 77(2), 127 – 132.
- Downie, A., Crosky, A., & Munroe, P. (2019). Physical Properties of Biochar. *Fuel*, 28, 106 – 112.
- Drag, T.C., Arenillas, A., Smith, K.M., Pevida, C., Piippo, S., & Snape C.E., (2017). Preparation of Carbon Dioxide Adsorbents from chemical activation of Ureaformaldehyde and Melanine-formaldehyde Resins. *Fuel*, 86, 22 – 31.

- El-Zahhar, A. A. & Al-Hazmi, G. A. (2019). Organically Modified Clay for Adsorption of Petroleum Hydrocarbon, *European Chemical Bulletin*, 4(2), 87 - 91.
- Emam, A. E. (2018). Modified activated carbon and bentonite used to adsorb petroleum hydrocarbons emulsified in aqueous solution, *American Journal of Environmental Protection*, 2(6), 161 – 169.
- Emrich, W. (2017). Handbook of Biochar Making on the Traditional and Industrial Methods, *Biochar Handbook*, 11, 537- 543.
- Encinar, J.M., Gonzalez, J.F. & Gonzalez, J. (2021). Fixed- Bed Pyrolysis of *Cynara Cardunculus* L Product Yields and Compositions. *Fuel Processing Technology*, 68, 209 – 222.
- Erta, M. & Alma, M.I. (2017). Pyrolysis of Laurel (*Laurus nobilis*) Extraction Residues in a Fixed Bed Reactor: Characterization of Bio-Oil and Biochar. *Journal of Analytical and Applied Pyrolysis*, 88, 22 – 29.
- Fagbemi, L., Khezami, L., & Capart, R. (2020). Pyrolysis Products from Different Biomasses: Application to the Thermal Cracking of Tar. *Energy*, 9, 293 – 306.
- Fang, J., Leavey, A., & Biswas, P. (2019). Controlled Studies on Aerosol Formation During Biomass Pyrolysis in a Flat Flame Reactor. *Fuel*, 116, 350 – 357.
- FAO, (2022). Food Resources. And their Potentials in Human Society. Retrieved from <http://www.fao.org/DOREP/004/x6519E/x6518E00.htm>.
- Fassinou, F.W., Laurent, V.S., & Siaka, T. (2020). Pyrolysis of *Pinus pinaster* in a TwoStage Gasifier: Influence of Processing Parameters and Thermal Cracking of Tar. *Fuel Processing Technology*, 90, 75 – 90.
- Foroutan, R., Zareipour, R. & Mohammadi, R. (2018). Fast Adsorption of Chromium (Vi) Ions from Synthetic Sewage Using Bentonite and Bentonite/Biocoal Composite: A Comparative Study. *Materials Research Express*, October: 1 – 26.
- Friedl, A.; Padouvas, E.; Rotter, H.; & Varmuza, K. (2017). Prediction of Heating Values of Biomass Fuel from Elemental Composition. *Analytical Chemistry Journal*, 544, 191 – 198.
- Funazukuri, T., Hudgins, R. & Silveston, P. (2021). Product Distribution in Pyrolysis of Cellulose in Micro Fluidized Bed. *Journal of Analytical Pyrolysis*, 9, 139 - 158.
- Gani, A., & Naruse, I. (2017). Effect of Cellulose and Lignin Content on Pyrolysis and Combustion Characteristics for Several Types of Biomasses. *Renewable Energy*, 32(4), 649 – 661.
- George, S. C. & Betzy, N.T. (2018). Production of Activated Carbon from Natural Sources. *Trend in Green Chemistry*, 1, 1-7.

- Gercel, H.F. (2017). The Production and Evaluation of Bio-Oils from Pyrolysis of Sunflower- Oil Cake. *Biomass and Bioenergy*, 307- 314.
- Glaser, B., Lehmann, J., & Zech, W. (2022). Ameliorating Physical and Chemical Properties of Highly Weathered Soils in the Tropics with Charcoal - A review. *Biology and Fertility of Soils*, 35, 219 - 230.
- Gonzalez, J.F., Roman, S., Gonzalez-Garcia, C.M., Nabais, J.M.V. & Ortiz, A.L. (2018a). Porosity Development in Activated Carbons Prepared from Walnut Shells by Carbon Dioxide or Steam Activation. *Industrial And Engineering Chemistry Research*, 48, 7474 – 7481.
- Gonzalez, M.E., Cea, M., Medina, J., Gonzalez, A., & Cartes, P. (2018b). Evaluation of Biodegradable Polymers as Encapsulating Agents for the Development of a Urea Controlled-Release Fertilizer Using Biochar as Support Materials. *Science of Total Environment*, 505, 446 – 453.
- Gonzalez, M.E., Luis, R., Gonzalez, A., Hildalgo, P., Meier, S., & Cea, M. (2020). Effects of Pyrolysis Conditions on Physicochemical Properties of Oat Hull Derived Biochar. *Bioresources* 12(1), 2040 – 2057.
- Goyal, H.B., Seal, D. & Saxena, R.C. (2018). Bio-fuels from Thermochemical Conversion of Renewable Resources. *Renewable and Sustainable. Energy*, 12, 504 – 517.
- Hall, D.O. (2018). Biomass for Energy Supply Prospects, *Renewable Energy*, 23(8), 567 - 5774.
- Hamdaoui, O. & Naffrechoux, E. (2017). Modelling of Adsorption Isotherms of Phenol and Chlorophenols onto Granular Activated Carbon. Part II. Models with More Than Two Parameters. *Journal of Hazardous Materials*, 147(1-2), 401 - 411.
- Haro, M., Ruiz, B., Andrade, M., Mestre, A.S., Parra, J.B., Carvalho, A.P. (2022). Dual Role of Copper on Reactivity of Activated Carbons from Coal and Lignocellulosic Precursors. *Microporous and Mesoporous Materials*. 154, 68- 73
- Heidari, A., Stahl, R., Younesi, H., Rashidi, A., Troeger, N., & Ghoreyshi, A.A. (2021). Effect of Process Conditions on Product Yield and Composition of Fast Pyrolysis of Eucalyptus Grandis in Fluidized Bed Reactor. *Journal Industrial and Engineering Chemistry*, 35(2), 123 – 127.
- Hileman, B. (2018). Climate Change Threatens Global Economy. *Chemical & Engineering News*, 84, 7- 8.
- Ho, Y. S., Ng, J. C. Y. & McKay, G. (2020). Kinetics of Pollutant Sorption by Biosorbents: Review. *Separation and Purification Methods*. 29 (2), 189 - 232.
- Hokkanen, S., Bhatnagar, A., Srivastava, V., Suorsa, V. & Sillanpää, M. (2018). Removal of  $Cd^{2+}$ ,  $Ni^{2+}$  and  $PO_4^{3-}$  from Aqueous Solution By HydroxyapatiteBentonite Clay Nanocellulose Composite. *International Journal of Biological Macromolecules*, 118, 903 - 912.

- Hossaini, M.K., Strezov, V., Chan, K.Y., Ziolkowski, A. & Nelson, P.F. (2018). Influence of Pyrolysis Temperature on Production and Nutrient Properties of Wastewater Sludge Biochar. *Journal of Environmental Management*, 92, 223 - 228.
- Hosseini, S., Bayesteh, J., Marahel, E., Babadi, F.F., Abdullah, L.C., & Choong, T.S.Y. (2019). Adsorption of Carbon Dioxide Using Activated Carbon Impregnated with Cu Promoted by Zn. *J. Taiwan Institute of Chemical Engineers*. 52, 109 - 117.
- Huang, H., Yuan, X., Zeng, G., Wang, J., Li, H., Zhou, C., Pei, X., You, Q., & Chen, L. (2020). Thermochemical Liquefaction Characteristics of Microalgae in Sub- and Super-Critical Ethanol. *Fuel Processing Technology*, 92(1), 147 - 153
- Huber, G.W. (2018). Breaking the Chemical and Engineering Barriers to Lignocellulosic Bio-fuels, Next Generation Hydrocarbon Biorefineries. *Journal of Chemical Engineering*, 21(5), 836 - 841.
- IBI, (2020). Prospect of Biochar. Retrieved from <http://www.biocharinternational.org/biochar>. Accessed on 4<sup>th</sup> August, 2020.
- Imam, T., & Capareda, S. (2019). Characterization of Bio-Oil, Syn-Gas and Biochar from Switchgrass Pyrolysis at Various Temperatures. *Journal of Analytical and Applied Pyrolysis*, 93, 170 - 177.
- Industries, P. (2018). Wood Based Lignin Reactions Important to the Biorefinery and Pulp and Paper Industries. *Energy*, 8(1), 1456 - 1477
- Intani, K., Latif, S., Kabir, A.K., & Müller, J. (2018). Effect of Self-Purging Pyrolysis on Yield of Biochar from Maize Cobs, Husks and Leaves. *Bioresources Technology*, 218, 541 - 551.
- Iron, R., Sekkapan, G., Panesar, R., Gibbins, J. & Lucquiaud, M. (2017). CO<sub>2</sub> Capture Ready Plants. IEA Greenhouse Gas Research and Development Programme. Retrieved from [www.ieagreen.org.uk](http://www.ieagreen.org.uk). Accessed on 3<sup>rd</sup> May, 2018.
- Janse, M.C., Westerhout, R.W.J., & Prins, W. (2019). Modelling of Flash Pyrolysis of a Single Wood particle. *Chemical Engineering Processing: Process Intensification*, 39(3), 239 - 252.
- Jia, Q. & Lua, A.C. (2018). Effect of Pyrolysis Conditions on the Physical Characteristics Oil Palm Shell Activated Carbon Used in Aqueous Phase Phenol Adsorption. *Journal of Analytical and Applied Pyrolysis*, 83(2), 175-179.
- Joan, J. (2020). Pyrolysis for Biochar Purposes: A Review to Establish Current Knowledge Gaps and Research Needs. *Environmental Science & Technology* 46, 7939 - 7954

- Joseph, S.D., Joseph, B.R., & William, A. (2020). An Investigation into the Realities of Biochar in Soil. *Australian Journal of Soil Research*, 48, 501 – 515.
- Jung, S. H., Kang, B. S., & Kim, J. S. (2020). Production of Bio-Oil from Rice Straw and Bamboo Sawdust Under Various Reaction Conditions in a Fast Pyrolysis Plant Equipped with a Fluidized Bed and a Char Separation System. *Journal of Analytical and Applied Pyrolysis* 82(2), 240 – 247.
- Kajjumba, G. W., Emik, S., Qngen, A., Qzcan, H. K. & Aydin, S. (2018). Modelling of Adsorption Kinetic Processes: Errors, Theory and Application. *Advanced Sorption Process Applications*, 4,1 – 19.
- Keiluweit, M., Nico, P.S., Johnson, M.G., & Kleber, M. (2019). Dynamic Molecular Structure of Plant Biomass-Derived Black Carbon (Biochar). *Environmental Science Technology*, 44, 1247 - 1253.
- Kerng, K., Hornung, A., Karsten, U., & Griffiths, G. (2018). Intermediate Pyrolysis and Product Identification by TGA and Py-Gc/Ms of Green Microalgae and Their Extracted Protein and Lipid Components. *Biomass and Bioenergy*, 49(10), 38 – 48.
- Kim, K.H., Eom, I.Y., Lee, S.M., Choi, D., Yeo, H., Choi, I-G., & Choi, J.W. (2017). Investigation of Physicochemical Properties of Biooils Produced from Yellow Poplar Wood (*Liriodendron tulipifera*) at Various Temperatures and Residence Times. *Journal of Analytical and Applied Pyrolysis*, 92(1), 2 – 9.
- Klark, M., & Rule, A. (2021). The Technology of Wood Distillation, *Bioresources Technology*, 34, 688 - 681.
- Krishna, J., & Sheeja J. (2018). Influence of Process Parameters on Synthesis of Biochar by Pyrolysis of Biomass: Alternative Source of Energy. *Fuel*, 88, 204 - 209
- Lathouwers, D., & Bellan, J. (2020). Yield Optimization and Scaling of Fluidized Beds for Tar Production from Biomass. *Energy Fuels*, 15(5), 1247 – 1262.
- Lee, S.J., Kim, H.S., Park, N., Lee, T.J. & Kang, M., (2020). Low Temperature Synthesis of Alpha Alumina from Aluminium Hydroxide Hydrothermally Synthesized Using  $[Al(C_2O_4)_x(OH)_y]$  Complexes. *Chemical Engineering Journal*, 230, 351 - 360.
- Lee, Y.W., Park, J.J., & Ryun, C. (2018). Comparison of Biochar Properties from Biomass Residues Produced by Slow Pyrolysis at 500 °C. *Bioresource Technology*, 148, 196 - 201.
- Lehmann, J. (2017). Sustainable Biochar to Mitigate Global Change. *Fuel*, 22, 1155 – 1160
- Lehmann, J & Joseph, S. (2019). *Biochar for Environmental Management: Science and Technology*. Earthscan Publishers Ltd. 317 – 340. London, UK.

- Li, F., Cao, X. & Zho, L. (2017). Effect of Mineral Additives on Biochar Formation: Carbon Retention, Stability and Properties. *Environmental Science Technology*, 48(19), 241- 255.
- Li, L., Rowbotham, J.S., Greenwell, C.H., & Dyer, P.W. (2018a). *An Introduction to Pyrolysis and Catalytic Pyrolysis: Versatile Techniques for Biomass Conversion*. Elsevier, 173 –208.
- Li, X., Shen, Q., Zhang, D., Mei, X., Ran,W., Xu, Y., & Yu, G. (2018b). Functional Groups Determine Biochar Properties (pH and EC) as Studied by TwoDimensional <sup>13</sup>C NMR Correlation Spectroscopy. *Journal of Environmental Science*, 8, 217 - 224.
- Liang, B., Lehmann, J., Solomon, D., Sohi, S., Thies, J.E., Skjemstad, J.O., Luizao, F.J., Engelhard, M.H., Neves, E.G. & Wirick, S. (2017). Stability of Biomass-Derived Black Carbon in Soils, *Geochemical* 72, 6069-6078.
- Liu, Z.G., Quek. A. & Hoekman, S.K. (2020). Production of Solid Biochar Fuel from Waste Biomass by Hydrothermal Carbonization. *Fuel*, 103, 943 - 949.
- Lv, D., Xu, M., Liu, X., Zhan, Z., Li, Z., & Yao, H. (2017). Effect of Cellulose, Lignin, Alkali and Alkaline Earth Metallic Species on Biomass Pyrolysis and Gasification. *Fuel Processing Technology*, 91(8), 903 – 909.
- Mahmood, A.S.N., Brammer, J.G., Hornung, A., Steele, A., & Poulston, S. (2017). The Intermediate Pyrolysis and Catalytic Steam Reforming of Brew Lingers Spent Grain. *Journal of Analytical and Applied Pyrolysis*, 103, 328 – 342.
- Mani, T., Murugan, P., Abedi J, & Mahinpey N. (2020). Pyrolysis of Wheat Straw in a Thermogravimetric Analyzer: Effect of Particle Size and Heating Rate on Devolatilization and Estimation of Global Kinetics. *Chemical Engineering and Research Design*, 88 (8), 952 – 958.
- Manya, J.J., Roca, F.X., & Perales, J.F. (2018). TGA Study Examining: The Effect of Pressure and Peak Temperature on Biochar Yield During Pyrolysis of Two-Phase Olive Mill Waste. *Journal of Analytical and Applied Pyrolysis*, 103, 86 – 95.
- Marketer, T.L., Felix, L.G., Linck, M.B., & Roberts, M.J. (2017). Integrated Hydro Pyrolysis and Hydro Conversion (IH2) for the Direct Production of Gasoline and Diesel Fuels or Blending Components from Biomass, Part 1: Proof of Principle Testing. *Environmental Progress Sustainable Energy*, 31(2), 1919 – 1923.
- Maschio, G., Koufopoulos, C., & Lucchesi, A. (2017). Pyrolysis, a Promising Route for Biomass Utilization. *Bioresources. Technology*. 42, 219 – 231.
- McHendry, P. (2020). Energy Production from Biomass: Overview of Biomass, *Bioresource Technology.*, 83, 37 – 46.

- McLaughlin, H., Anderson, P.S., Shields, F.E. & Reed, T.B. (2019). All Biochars are Not Created Equal, and How to Tell Them Apart. North American Biochar Conference, Boulder, CO.
- Meesuk, S., Cao, J.P., Sato, K., Ogawa, Y., & Takarada, T. (2019). The Effects of Temperature on Product Yields and Composition of Bio-Oils in Hydropyrolysis of Rice Husk Using Nickel-Loaded Brown Coal Char Catalyst. *Journal of Analytical and Applied Pyrolysis*, 94, 238 – 245.
- Melliga, F., Hayes, M.H.B., Kwapinski, W., & Leahy, J.J. (2020). A Study of Hydrogen Pressure During Hydropyrolysis of *Miscanthus X Giganteus* and Online Catalytic Vapour Upgrading with Ni On ZSM-5. *Journal of Analytical and Applied Pyrolysis* 103, 369 – 377.
- Mohamed, A.R., Hamzah, Z., Daud, M.Z.M., & Zakaria, Z. (2018). The Effects of Holding Time and the Sweeping Nitrogen Gas Flowrates on the Pyrolysis of EFB Using a Fixed-Bed Reactor. *Procedia Engineering*, 53, 185 – 191.
- Mohammed, I.Y., Kazi, F.K., Abakr, Y.A. & Alshareef, I.M. (2019). Pyrolysis of Napier Grass in Fixed Bed Reactor: Effect of Operating Conditions on Product Yields and Characterization. *Bioresource*, 10(14), 6457 – 6478.
- Mohan, D., Pittman, C.U., & Steele, P.H. (2021). Pyrolysis of Wood/Biomass for Biooil – A Critical Review. *Energy Fuels*, 20(3), 848 – 889.
- Mokwunye, U., (2021). Meeting the Phosphorus Needs of the Soils and Crops Of West Africa: The Role Of Indigenous Phosphate Rocks: Paper Presented on Balanced Nutrition Management Systems for the Moist Savanna and Humid Forest Zones of Africa At A Symposium Organized By IITA At Kulleuva At Cotonun, Benin Republic, October 9 -12.
- Momina, M., Mohammad S & Suzylawati, I. (2018). A Review on Regeneration Performance of Clay-Based Adsorbents for the Removal of Industrial Dyes. *Journal of Royal Society of Chemistry*, 24571 – 24587.
- Moradi, M., Dehpahlavan, A., Kalantary, R. R., Ameri, A., Farzadkia, M. & Izanloo, H. (2019). Application of Modified Bentonite Using Sulfuric Acid for the Removal of Hexavalent Chromium from Aqueous Solutions. *Environmental Health Engineering and Management Journal*, 2(3), 99 – 106.
- Morrin, S., Lettieri, P., Chapman, C., & Mazzei, L. (2020). Two Stage Fluid Bed-Plasma Gasification Process for Solid Waste Valorisation - Technical Review and Preliminary Thermodynamic Modelling of Sulphur Emissions. *Waste Management*, 32(4), 676 - 684.
- Motasemi, F., & Afzal, M.T. (2021). A Review on the Microwave-Assisted Pyrolysis Technique. *Renew and Sustainable Energy Review*, 28, 317 – 330.
- Mubarak, N.M., Kundu, A., Sahu, J.N., Abdullah, E.C., & Jayakumar, N.S. (2017). Synthesis of Palm Oil Empty Fruit Bunch Magnetic Pyrolytic Char

- Impregnating with FeCl<sub>3</sub> by Microwave Heating Technique. *Biomass Bioenergy*, 61, 265 - 275.
- Mullen, C. A, Boateng, A.A., Goldberg, N.M., Lima, I.M., Laird, D. A., & Hicks, K.B. (2017). Bio-oil and Biochar Production from Corn Cobs and Stover by Fast Pyrolysis. *Biomass Bioenergy*, 34(1), 67 – 74.
- Nassar, M., Bilgesu, A. & MacKeay, G. (2021). Effects of Inorganic Salts on Product Composition During Pyrolysis of Black Spruce and Rice Straw. *Wood Fiber Science*, 18 (1), 3 – 10.
- Nethaji, S., Sivasamy, A. & Mandal, A. B. (2018). Adsorption Isotherms, Kinetics and Mechanism for the Adsorption of Cationic and Anionic Dyes onto Carbonaceous Particles Prepared from Juglans Regia Shell Biomass. *International Journal of Environmental Science and Technology*, 10, 231 - 242.
- Neves, D., Thunman, H., Matos, A., Tarelho, L. & Gomez-Barea, A. (2018) Characterization and Prediction of Biomass Pyrolysis Products. *Progress in Energy and Combustion Science*, 37(5), 611 – 630.
- Nunn, T.R., Howard, J.B., Longwell, J.P. & Peters W.A. (2020). Pyrolysis of Lignocellulosic Material. *Industrial Engineering Processing Chemistry Description Development*, 24, 844 - 849.
- Nurrokhmah, L., Mezher, T. & Abu-Zahra, M.R.M. (2018). Evaluation of Handling and Reuse Approaches for the Waste Generated from Mea-Based CO<sub>2</sub> Capture with the Consideration of Regulations in the UAE. *Environmental Science Technology*, 47 (23), 13644 - 13651.
- Oasmaa, A., & Czernik, S. (2018). Fuel Oil Quality of Biomass Pyrolysis Oils and State of the Art for the End Users. *Energy*, 4, 914 – 921.
- Ogi, T. (2022). *Biomass Handbook*. *Japan Journal of Chemical Engineers*, 3 (23), 197199.
- Ojo, G.P., Igbokwe, U.G., Egbuachor, C.J., and Nwozor, K.K. (2017). Geotechnical Properties and Geochemical Composition of Kaolin Deposits in Parts of Ifon, Southwestern Nigeria. *American Journal of Engineering Research*, 6(3), 15 - 24
- Olajire, A.A., (2017). CO<sub>2</sub> Capture and Separation Technologies for End-of-Pipe Applications – A Review. *Energy*, 35, 2610 – 2628.
- Onay, O., & Kockar, O.M. (2018). Slow, Fast and Flash Pyrolysis of Rapeseed. *Renewable Energy*, 28(15), 2417 – 2433.
- Onay, O. (2018). Effects of catalyst on pyrolysis of Laure seed in a Fixed Bed Tubular Reactor. *Chemical engineering Transaction*.37, 45-49 published by AIDIC.
- Paenpong, C., Inthidech S, & Pattiya, A. (2018). Effect of Filter Media Size, Mass Flow Rate and Filtration Stage Number in a Moving-Bed Granular Filter on the Yield

- and Properties of Bio-Oil from Fast Pyrolysis of Biomass. *Bioresource Technology*, 139, 34 – 42.
- Panda, A. K., Mishra, B. G., Mishra, D. K. & Singh, R. K. (2020). Effect of Sulphuric Acid Treatment on the Physico-Chemical Characteristics of Kaolin Clay. *Colloids Surfaces A*, 363, 98 - 104.
- Panda, A. K., Singh, R.K, & King, T. (2018). Co-pyrolysis of Propylene with Kaolin Clay. *Bioresources*, 125(61), 1156 – 1162.
- Park, H. J. (2018). Pyrolysis Characteristics of Oriental White Oak: Kinetic Study and Fast Pyrolysis in a Fluidized Bed with an Improved Reaction System. *Fuel Processing Technology*, 90 (2), 186 – 195.
- Park, J., Hung, I., Rojas, O.J., & Park, S. (2018). Activated Carbon from Biochar: Influence of its Physicochemical Properties on the Sorption Characteristics of Phenanthrene. *Bioresources Technology*, 149, 383 – 389.
- Parolo, M. E., Pettinari, G. R., Mussoa, T. B., Sánchez-Izquierdo, M. P. & Fernández, L. G. (2021). Characterization of Organo-Modified Bentonite Sorbents: The Effect of Modification Conditions on Adsorption Performance, *Applied Surface Science*, 320, 356 - 363.
- Pevida, C., Plaza, M.G., Aias, B., Feroso, J., Rubiera, F., Pis, J.J., (2018). Surface Modification of Activated Carbon for CO<sub>2</sub> Capture. *Applied Surface Science*, 254 (22), 7165 – 7172.
- Plaza, M. (2019). Different Approaches for the Development of Low-Cost Adsorbents. *Journal of Environmental Engineering*, 135, 426 – 432.
- Plaza, M.G., Pevida, C., Martin, C.F., Feroso, J., Rubiera, F., & Pis J.J. (2020). Developing Almond Shell Derived-Activated Carbons as CO<sub>2</sub> Adsorbents. *Separation and Purification Technology*, 71, 102 – 109.
- Przepiorski, J., Czyzewski, A., Pietrzak, R., Toyoda, M., & Morawski, A.W. (2018). Porous Carbon Material Containing Cao for Acidic Gas Capture: Preparation and Properties. *Journal of Hazardous Materials*, 263, 353 – 360.
- Putun, A.E., Apaydin, E., & Putun, E. (2020). Bio-oil Production from Pyrolysis and Steam Pyrolysis of Soybean-Cake: Product Yields and Composition. *Energy*, 27, 703 – 713.
- Putun, E. (2022). Catalytic Pyrolysis of Biomass: Effects of Pyrolysis Temperature, Sweeping Gas Flow Rate and Mgo Catalyst. *Energy* 35(7), 2761 - 2766.
- Qiu, G., Gong, D., & Fan, M. (2020). Bioremediation of Petroleum-Contaminated Soil by Bio-stimulation Amended with Biochar. *International Biodeterioration and Biodegradation*, 85, 150 – 155.

- Rashidi, N.A. & Yusup, S., (2016). An Overview of Activated Carbon Utilization for Post-combustion Carbon Dioxide Capture. *Journal of CO<sub>2</sub> Utilization*, 13, 1 – 16.
- Romero, J. R. G., Moreno-Piraján, J. C. & Gutierrez, L. G. (2018). Kinetic and Equilibrium Study of the Adsorption of CO<sub>2</sub> in Ultra-micropores of Resorcinol-Formaldehyde Aerogels Obtained in Acidic and Basic Medium. *Journal of Carbon Research*, 4 (52), 1 – 17.
- Ronsse, F., Hecke, S.V., Dickinson, D., & Prins, W. (2021). Production and Characterization of Slow Pyrolysis Biochar: Influence of Feedstock Type and Pyrolysis Conditions. *Global Change Biology and Bioenergy*, 5, 104 - 115.
- Roy, C., Hébert, M., Kalkreuth, W., & Schwerdtfeger, A.E. (2021). Conversion Characteristics of Canadian Coals Subjected to Vacuum Pyrolysis Treatment. *Fuel*, 77(3), 197 - 208.
- Ruiz, J., Juárez, M.C., Morales, M.P., Muñoz, P., & Mendivil, M. (2018). Biomass Gasification for Electricity Generation: Review of Current Technology Barriers. *Renewable and Sustainable Energy Review*, 18, 174 - 183
- Salahudeen, A., Ahmed, A.S., Al-Muhtaseb, A.H., Dauda, M., Waziri, S.M. & Jibril, B.Y. (2019). Synthesis of Gamma Alumina from Kankara Kaolin Using a Novel Technique. *Applied Clay Science* 3 (2), 63 - 71.
- Savova, D., Apak, E., Ekinici, E., Yardim, F., Petrov, N., Budinova, T., Razvigorova, M., & Minkova, V. (2021). Biomass Conversion to Carbon Adsorbents and Gas. *Biomass and Bioenergy*, 21(2), 13 – 42.
- Saxena, R.C., Seal, D., Kumar, S., & Goyal, H.B. (2018). Thermochemical Routes for Hydrogen Rich Gas from Biomass: A Review. *Renewable and Sustainable Energy Review* 12 (7), 1909 - 1927.
- Schmidt, H. P., Abiven, S.K., Kammann, C.H., Glaser, B. N., Bucheli, G. L., Kuvar, H. V., Thomas, H.C. & Leifeld, J. (2021). Biochar-Based Fertilization with Liquid Nutrient Enrichment: 21 field Trials Covering 13 Crop Species in Nepal. *Land Degradation and Development*, 3(4), 213 - 224
- Scott, D.S., Piskorz, J. & Radlein, D. (2020). The Effect of Wood Species on Composition of Products Obtained by the Waterloo Fast Pyrolysis Process. *Journal of Chemical Engineering*, 33, 413 – 418.
- Senoz, S., & Angin, D. (2018). Pyrolysis of Safflower (*Charthamus tinctorius* L.) seed. The Effects of Pyrolysis Parameters on the Product Yields. *Bioresource Technology*, 99(13), 5492 – 5497.
- Shafeeyan, M.S., Daud, W.M.A.W., Houshmand, A., Arami-Niya, A. (2022). The Application of Response Surface Methodology to Optimize the Animation of

- Activated Carbon for the Preparation of Carbon Dioxide Adsorbents. *Fuel*, 94, 465 – 472.
- Shafizadeh F. (2019). Catalytic Pyrolysis of Poultry Material and Waste in a Fixed Bed Reactor. *Journal of Analytical and Applied Pyrolysis*, 3, 283 - 305.
- Shariff, A., Noor, N.M., Lau, A. & Ali, M.A. (2017). Comparative Study on Biochar from Slow Pyrolysis of Corn Cob and Cassava Wastes. *International Journal of Biotechnology and Bioengineering*, 10(12), 768 – 771.
- Sharma, R.K., Wooten, J.B., & Chan, W. (2017). Characterization of Char from Pyrolysis of Lignin. *Fuel*, 83, 1469 – 1482.
- Simeon, S., Saran, S., Stuart, H., David, M., & Ondrej, M. (2019). Biochar for removing CO<sub>2</sub> while improving soils: Evidence submitted to royal society geo-engineering climate enquiry. *Material Energies*, 10, 1293 – 1308.
- Skoulou, V. & Zabaniotou, A. (2017). Investigation of agricultural and animal wastes in Greece and their allocation to potential application for energy production. *Renew and Sustainable Energy Review*, 11(8), 1698–719
- Soltes, E. & Elder, T. (2020). Pyrolysis of Selected Biomass in a Slow Heating Condition to produce biochar. *Journal of Analytical and Applied Pyrolysis*, 7, 771- 779.
- Sombroek, W. (2017) Amazon Soil: A Reconnaissance of the Soils of the Brazilian Amazon Region Centre for Agricultural Publications and Documentation Wageningen. *Soil*, 4(17), 222 – 234.
- Stefanidis, S.D., Kalogiannis, K.G., Iliopoulou, E.F., Lappas, A.A., & Pilavachi, P. (2017). In-Situ Upgrading of Biomass Pyrolysis Vapours: Catalyst Screening on a Fixed Bed Reactor. *Bioresource Technology*, 102(17), 8261 - 8267
- Suleiman, W., Ray, P., & Matin, Z. (2018). Influence of Feedstock and Pyrolysis Temperature on Biochar Bulk and Surface Properties. *Biomass and Bioenergy*, 83, 37 – 48.
- Sun, J., Yinghua, P., & Fuhung, H. (2019). Effect of Pyrolysis Temperature and Residence Time on Physicochemical Properties of Different Biochar Types. *Acta agricultural Scandinavica*, 67(1), 12 – 22.
- Sun, N., Tang, Z., Wei, W., Snape, C.E. & Sun, Y. (2021). Solid Adsorbent for Low Temperature CO<sub>2</sub> Capture with Low-Energy Penalties Leading to More Effective Integrated Solutions for Power Generation and Industrial Processes. *Frontier in Energy Research*, 3, 1-16.
- Suttibak, S, Sriprateep K, & Pattiya, A. (2017). Production of Bio-Oil Via Fast Pyrolysis of Cassava Rhizome in a Fluidised-Bed Reactor. *Energy Procedia*, 14, 668 - 673.

- Taylor, P. & Mason, J. (2021). Biochar Production Fundamentals, in: P. Taylor (Ed.), the Biochar Revolution: Transforming Agriculture and Environment, Global Publishing Group, Victoria, Australia. 113 - 131.
- Tillman, D.A. (2021). Biomass Cofiring: The Technology, The Experience, The Combustion Consequences. *Biomass and Bioenergy*, 19, 65 – 84.
- Tripathi, M., Sahu JN, Ganesan, P., & Dey, T.K. (2019). Effect of Temperature on Dielectric Properties and Penetration Depth of Oil Palm Shell (OPS). *Biomass Bioenergy* 153, 257 – 266.
- Tsai, W.T., Chang, C.V., & Lee, S. (2017). Preparation and Characterization of Activated Carbons from Corn Cob. *Carbon*, 35, 1198 - 2000
- Tsai, W.T., Lee, M.K., & Chang, Y.M. (2019). Fast Pyrolysis of Rice Husk: Product Yields and Compositions. *Bioresource Technology*, 98(1), 22 – 28.
- Uduakobong, A. E. & Augustine, O. I. (2020). Kinetics, Isotherms, and Thermodynamic Modeling of the Adsorption of Phosphates from Model Wastewater Using Recycled Brick Waste. *Processes*, 8 (665), 1 – 15.
- Uras, Ü, Carrier, M., Hardie, A.G., & Knoetze, J.H. (2017). Physico-chemical Characterization of Biochars from Vacuum Pyrolysis of South African Agricultural Wastes for Application as Soil Amendments. *Journal of Analytical and Applied Pyrolysis*, 98, 207 – 213.
- Utioh, A.C., Bakshi, N.N. & MacDonald, V. G. (2019). Pyrolysis of Grain Screening in a Batch Reactor. *Canadian Journal of Chemical Engineering*, 67, 439 - 442.
- Uzun, B.B., Putun, A.E., & Putun, E. (2017). Fast Pyrolysis of Soybean Cake: Product Yields and Compositions. *Bioresource Technology*, 97 (4), 569 - 576.
- Vamvuka, D., & Zografos, D. (2021). Predicting The Behaviour of Ash from Agricultural Wastes During Combustion. *Fuel*, 83(14–15), 2051 – 2057.
- Van Wambeke, A. (2018). Soils of the Tropics: Properties and Appraisal. *Soil*, 34(45), 604 – 609.
- Vardon, D.R., Sharma, B.K., Blazina, G.V., Rajagopalan, K., & Strathmann, T.J. (2021).  
Thermochemical Conversion of Raw and Defatted Algal Biomass Via Hydrothermal (Liriodendron Tulipifera) at Various Temperatures and Residence Times. *Journal of Analytical and Applied Pyrolysis*, 92(1), 2 – 9.
- Vassilev, S.V., Baxter, D., Andersen, L.K., & Vassileva, C.G., & Morgan, T.J. (2020). An Overview of the Organic and Inorganic Phase Composition of Biomass. *Fuel*, 94, 1 – 33.

- Velez, J.F., Chejne, F., Valdes, C.F., Emery, E.J., & Londono, C.A. (2019). CoGasification of Colombian Coal and Biomass in Fluidized Bed: An Experimental Study. *Fuel*, 88(3), 424 - 430
- Wang, J., Zhang, M., Chen, M., Min, F., Zhang, S., Ren, Z., & Yan, Y. (2018). Catalytic Effects of Six Inorganic Compounds on Pyrolysis of Three Kinds of Biomass. *Thermochim Acta*, 444(1), 110 – 114.
- Wang, Y., He, T., Z, K., Wu, J., & Fang, Y. (2020). From Biomass to Advanced BioFuel by Catalytic Pyrolysis/Hydro-Processing: Hydrodeoxygenation of Bio-Oil Derived from Biomass Catalytic Pyrolysis. *Bioresource. Technology*, 108, 280 – 284.
- Waqas, M., Khan, S., Qing, H. & Chao, C. (2021). The Effect of Sewage Sludge Biochar on PAHS and Potentially Toxic Element Bioaccumulation in Cucumis Sativa L. *Chemosphere*. 105, 53 – 61.
- Woolf, D., Amonette, J., Street-Perrot, A., Lehmann, J., & Joseph, S. (2017). Sustainable Biochar to Mitigate Global Change. *Fuel*, 22, 1155 – 1160.
- Xiao, R., Chen, X., Wang, F., & Yu, G. (2020). Pyrolysis Pretreatment of Biomass for Entrained Flow Gasification. *Applied Energy*, 87(1), 149 - 155.
- Xiong, S., Zhuo, J., Zhang, B., & Yao, Q. (2018). Effect of Moisture Content on the Characterization of Products from the Pyrolysis of Sewage Sludge. *Journal of Analytical and Applied Pyrolysis*, 104, 632 – 639.
- Yaman, S. (2017). Pyrolysis of Biomass to Produce Fuels and Chemical Feedstocks. *Energy Conversion Management*, 45, 651 - 671.
- Yang, H., Yan, R., Chen, H., Zheng, C., Lee, D.H., & Liang, D.T. (2019). In-depth Investigation of Biomass Pyrolysis Based on Three Major Constituents: Hemicellulose, Cellulose and Lignin. *Energy & Fuels*; 20(1), 388 - 393
- Yeasmin, H., Mathews, J.F., & Ouyang, S. (2017). Rapid Devolatilization of Yallourn Brown Coal at High Pressures and Temperatures. *Fuel*; 78(1), 11 – 24.
- Yong, Z., Mata, V.G., & Rodrigues, A.E. (2019). Adsorption of Carbon Dioxide on Chemically Modified High Surface Area Carbon-Based Adsorbents at High Temperature. *Adsorption*, 7, 41-50.
- Yu, Y., Yu, J., Sun, B., & Yan, Z. (2020). Influence of Catalyst Types on the Microwave Induced Pyrolysis of Sewage Sludge. *Journal of Analytical and Applied Pyrolysis*, 106, 86 – 91.
- Zanzi, R., Sjoström, K. & Bjornbom, E. (2021). Rapid Pyrolysis of Agricultural Residues at High Temperature. *Biomass Bioenergy* 23(5), 357- 366.

- Zhang, H., Xiao, R., Huang, H., & Xiao, G. (2019). Comparison of Non-Catalytic and Catalytic Fast Pyrolysis of Corncob in a Fluidized Bed Reactor. *Bioresource Technology*, 100(3), 1428 – 1434.
- Zhang, R., Li, C., Xie, Z., & Wang, Q. (2021). The Influence of Particle Size and Feed Stock on Biochar Production. *Environmental Science Pollution Research International*, 24(28), 2240 – 2252.
- Zhao, B., Zhang, J., David, C. & Peng, T. (2017). Effect of Pyrolysis Temperature, Heating Rate and Residence Time on Rapeseed Stem Derived Biochar. *Journal of Cleaner Production* 174, 23 – 39.
- Zornoza, R., Moreno-Barriga, F., Acosta, J.A., Muñoz, M.A. & Faz, A. (2019). Stability, Nutrient Availability and Hydrophobicity of Biochars Derived from Manure, Crop Residues, and Municipal Solid Waste for their Use as Soil Amendments. *Chemosphere*, 144, 122–130.

## APPENDICES

### Appendix A

#### Materials and Methods of Construction

Pyrolysis is the thermal degradation of biomass under the absence of oxygen. Pyrolysis results in three products: biochar, non-condensable gases and condensate (tars and water). The proportion of each is a strong function of the feedstock and the operating conditions of the pyrolyser. Some systems (slow pyrolysers) focus on biochar production with syngas as the major co-product, while other systems (fast pyrolysers) focus on biooil (condensate) production with biochar as the major co-product. These guidelines focus on slow pyrolysers.

The main parts of this section are to design, construct and assemble the parts of the fixed bed reactor and condenser for pyrolysis reaction. The pyrolysis system is designed based on the following assumptions:

- Low vapour residence time in the reactor (slow pyrolysis)
- Rapid condensation of the vapour product
- Reliable heat supply for efficient conversion
- Rapid heat transfer in the wall of the reactor so that less heating material would be required for cost effectiveness
- Adequate gas flow rate to dispose-off the vapour mixture (condensable & noncondensable vapours)
- Proper mass flow rate of feedstock
- Size of the reactor system is such that sufficient amount of pyrolysis action can take place for a considerable amounts of char products to be collected

### Equipment

The equipment and materials used in this project are listed below:

- Laser thermometer
- Electronic balance
- Hammer and chisel
- Automatic sieve shaker

## Materials Used

1. Sawdust
2. Filler
3. Stainless steel
4. Mild steel
5. Heating filaments
6. Thermocouple
7. Fiber glass wool
8. Refractory clay
9. Ceramics
10. Wires
11. Threaded valves
12. Connecting pipes
13. Switch

## Design Consideration

To construct a unit that will be used by locals to convert biomass into biochar, the following design considerations were employed:

- Availability
- Affordability
- Workability
- Strength
- Suitability

The equipment that was selected is a horizontal fixed-bed reactor which could be operated in an enclosed but clear area. Its user-friendliness enables it to be operated by anybody.

## Design Objectives Specification

- Simple to manufacture, assemble and operate
- Easy for two people to transport
- Achieve a yield of 30kg biochar or more per day

#### Theoretical Design and Performance Parameters

##### Design concept development

Two designs were considered for the construction of the unit. The following gives the description of the designs considered.

##### Design A

The initial design that was selected had features similar to the final design. The only difference was the reduction in size as the final design only represents the prototype of the initial design. So also, the number of heating filament used at the upper layer was lesser than those used at the bottom layer (which sits directly on top of the furnace). During the testing of this design, it was realized that it took a considerably longer time for the burning process to complete. This was due to the lack of very low oxygen content in the reactor.

##### Design B

The final design was obtained through a combination of trial-and-error testing, comparative study with existing reactors. The guiding objective during this process was to successfully convert almost all of the sawdust inserted into the reactor body into biochar. Design B was able to accomplish this objective.

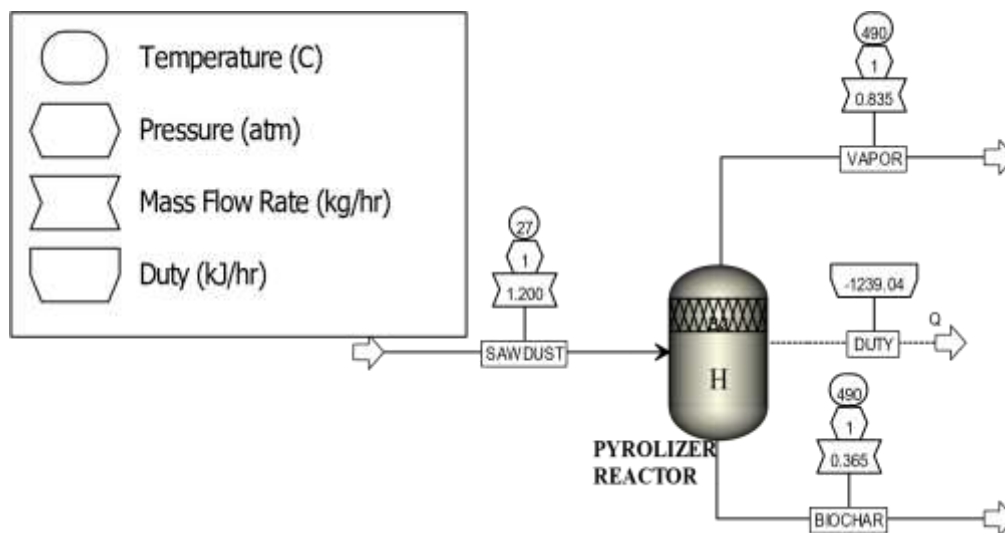


Figure A<sub>1</sub>: Process Flow Diagram for Biochar Production from Biomass

### Mass and Material Balance

In chemical processing we deal with the transformation of raw materials of lower value into products of higher value and, in many, cases unwanted by-products that must be disposed of. In addition, many of these chemical compounds may be hazardous. The material balance is the chemical engineer's tool for keeping track of what is entering and leaving the process as well as what goes on internally. Without accurate material balances, it is impossible to design or operate a chemical plant safely and economically. Material quantities, as they pass through processing operations, can be described by material balances. Material balances are the basis of process design. A material balance taken over the complete process will determine the quantities of raw materials required and products produced. Balances over individual process units set the process stream flows and compositions. Such balances are statements on the conservation of mass. If there is no accumulation, what goes into a process must come out. This is true for batch operation. It is equally true for continuous operation over any chosen time interval.

Material balances are fundamental to the control of processing, particularly in the control of yields of the products. The first material balances is determined in the

exploratory stage of a new process, and improved during pilot plant or when the process is being planned and tested, checked out when the plant is commissioned and then refined and maintained as a control instrument as production continues. When any changes occur in the process the material balances need to be determined again. Material balances are also useful tools for the study of plant operation and troubleshooting. They can be used to check performance against design, to extend the often-limited data available from the plant instrumentation, to check instrument calibrations; and to locate sources of material loss.

Material balance design Basis: 1.2 kg/hr of sawdust waste General

Mass Balance Equation:

$$\text{Mass Output} = \text{Mass Input} + \text{Generation} - \text{Consumption} - \text{Accumulation}$$

- At Steady State and no chemical reaction:

$$\text{Generation} = 0; \text{Consumption} = 0; \text{Accumulation} = 0$$

- Thus, Mass output = Mass Input

Table A<sub>1</sub>: Sawdust waste and their respective composition (Oasmaa et al.,2018)

Component	Composition(%wt)
Cellulose	43.50
Hemicellulose	20.60
Lignin	28.40

Ash	4.80
Moisture	2.00
Volatiles	0.70
<b>Σ</b>	100.00

Table A<sub>2</sub>: Pyrolysis product and their elemental constituents (Neves et al., 2018)

Component (% wt)	Bio char	Bio oil	Bio gas
Carbon	97.10	49.50	-
Hydrogen	1.00	6.40	-
Oxygen	1.60	42.50	0.80
Nitrogen	0.30	1.60	-
Methane	-	-	80.00
Carbondioxide	-	-	19.20
<b>Σ</b>	100.00	100.00	100.00

Table A<sub>3</sub>: Mass Balance across the Pyrolyser

Stream Name	Units	Material		
		SAWDUST	VAPOR	BIOCHAR
Temperature	C	27	490	490
Pressure	Atm	1	1	1
Mass Vapor Fraction		0	1	0
Mass Liquid Fraction		0	0	0
Mass Solid Fraction		1	0	1
Mass Enthalpy	kJ/kg	-3428.79000	-3717.56109	623.57046
Mass Density	kg/cum	1256.05190	0.69167	2250.02063

Enthalpy Flow	kJ/hr	-4114.54800	-3103.25968	227.75465
Mass Flows	kg/hr	1.20000	0.83476	0.36524
CO	kg/hr	0.00000	0.06152	0.00000
CO2	kg/hr	0.00000	0.07212	0.00000
H2	kg/hr	0.00000	0.00174	0.00000
N2	kg/hr	0.00000	0.00109	0.00000
NH3	kg/hr	0.00000	0.00011	0.00000
H2S	kg/hr	0.00000	0.00057	0.00000
CH4	kg/hr	0.00000	0.02394	0.00000
C2H4	kg/hr	0.00000	0.00983	0.00000
C2H6	kg/hr	0.00000	0.00535	0.00000
C3H8	kg/hr	0.00000	0.00308	0.00000
BIO-OIL	kg/hr	0.00000	0.49284	0.00000
H2O	kg/hr	0.00000	0.16256	0.00000
S-BIOMAS	kg/hr	1.20000	0.00000	0.00000
BIOCHAR	kg/hr	0.00000	0.00000	0.36524
		0.00000	0.07370	0.00000
Mass Fractions		0.00000	0.08639	0.00000
CO		0.00000	0.00208	0.00000
CO2		0.00000	0.00130	0.00000
H2		0.00000	0.00014	0.00000
N2		0.00000	0.00068	0.00000
NH3		0.00000	0.02868	0.00000
H2S		0.00000	0.01177	0.00000
CH4		0.00000	0.00641	0.00000
C2H4		0.00000	0.00369	0.00000
C2H6		0.00000	0.59040	0.00000
C3H8		0.00000	0.19474	0.00000
BIO-OIL		1.00000	0.00000	0.00000
H2O		0.00000	0.00000	1.00000
S-BIOMAS				
BIOCHAR				
Volume Flow	liter/min	0.01592	20.11457	0.00271

## Energy Balance

Energy can exist in several forms; heat, mechanical energy, electrical energy, chemical energy etc. In process design, energy balances are made to determine the energy requirement of the process; the heating, cooling, and powering required. Furthermore, in plant operation, an energy balance (energy audit) on the plant will show the pattern of energy usage, and suggest areas for conservation and savings. As with mass balance, materials can change form, new molecular species can be formed by chemical reaction,

but the total mass flow into a process unit must be equal to the flow out at the steady state. The same is not true of energy. The total enthalpy of the outlet streams will not equal that of the inlet streams if energy is generated or consumed in the process; such as that due to heat of reaction.

In this design, the energy balance of the entire plant is carried out by determining the enthalpies of all the streams present in the process using the specific heat capacity and the mole fraction of each component in any particular streams. The heat capacity being a function of temperature, were determined using the heat capacity coefficients of the components.

A general equation can be written for the conservation of energy:

Energy input + Energy generated = Energy Output + Energy Accumulated + Energy Consumed

Formation of energy balance equation

The equation to be used for the energy balance is given as:

$$\Delta H = n \int C_p . dT$$

Where:

H	Enthalpy
C <sub>p</sub>	Heat Capacity
T	Temperature
N	Amount
T <sub>r</sub>	Reference Temperature
T <sub>s</sub>	System Temperature.

If a reaction is involved, the equation becomes:

$$\Delta H = z \int C_p . dT + h_f$$

Where h<sub>f</sub> = heat of formation.

It should be noted that heat capacity is given in terms of heat capacity coefficient as;

$$C_p = a + b.T + c.T^2 + d.T^3$$

Where a, b, c, are heat capacity coefficients (constants) So,

the enthalpy balance equation will then become:

$$\Delta H = z \int (a + bT + c.T^2 + d.T^3) dT + h$$

The energy Balance formulae then becomes:

$$H_{p,s} = h + Z_{p,s} [ \int (a + bT + c.T^2 + d.T^3) dT ]$$

Where:

$H_{p,s}$  = Enthalpy of component P in stream S

$Z_{p,s}$  = Molar flow rate of component P in stream S in kmol/hr

But if no reaction is involved,  $h_f = 0$  and the equation become:

$$H_{p,s} = Z_{p,s} [ \int (a + bT + c.T^2 + d.T^3) dT ]$$

Table A4: Heat capacity coefficients of compound

Component	A	B	C	D
Cellulose	8.24522	$1.90634 \times 10^{-3}$	$9.14687 \times 10^{-4}$	$-8.41228 \times 10^{-8}$
Hemi cellulose	0	$0.80633 \times 10^{-3}$	$5.30010 \times 10^{-6}$	$0.46115 \times 10^{-9}$

Lignin	36.11	$7.02032 \times 10^{-3}$	$2.00040 \times 10^{-5}$	$1.61391 \times 10^{-7}$
Ash	45.44	$0.50080 \times 10^{-2}$	$-8.73200 \times 10^{-5}$	0
Air	$0.29 \times 10^{-5}$	$0.09390 \times 10^{-5}$	$3.01200 \times 10^{-3}$	$0.00756 \times 10^{-5}$
Water	32.243	$19.23800 \times 10^{-4}$	$10.55500 \times 10^{-6}$	$3.59600 \times 10^{-9}$
Carbon	1.771	$0.77100 \times 10^{-3}$	0	$-0.86700 \times 10^{-5}$
Hydrogen	29.088	$-0.19200 \times 10^{-2}$	$0.40000 \times 10^{-5}$	$-0.87000 \times 10^{-9}$
Oxygen	25.460	$1.51900 \times 10^{-2}$	$-0.71500 \times 10^{-5}$	$1.31100 \times 10^{-9}$
Nitrogen	28.883	$-0.15700 \times 10^{-2}$	$0.80800 \times 10^{-5}$	$-2.87100 \times 10^{-9}$
CH <sub>4</sub>	19.875	$5.02100 \times 10^{-2}$	$1.26800 \times 10^{-5}$	$-11.00400 \times 10^{-9}$
CO <sub>2</sub>	22.243	$5.97700 \times 10^{-2}$	$-3.49900 \times 10^{-5}$	$7.46400 \times 10^{-9}$

Table A<sub>5</sub>: Energy Balance across the Pyrolyser

	Heat	Stream Name
		DUTY
QCALC (kJ/hr)		-1239.04203
TBEGIN C		27
TEND C		490

### Appendix B

The yield of biochar and bio-oil were measured in gram with the aid of weighing machine while that of biogas was obtained by mass difference:

$$\text{Weight of biogas (g)} = 20 - (\text{Weight of biochar} + \text{biooil})$$

$$\text{At } 400\text{ }^{\circ}\text{C, Biogas yield (g) for Sawdust} = 20 - (7.84 + 8.42) = 3.74\text{g}$$

$$\text{Biogas yield (g) for Poultry waste} = 20 - (10.06 + 5.16) = 4.78\text{g At}$$

$$500\text{ }^{\circ}\text{C, Biogas yield (g) for Sawdust} = 20 - (4.52 + 9.16) = 6.32\text{g}$$

$$\text{Biogas yield (g) for Poultry waste} = 20 - (8.38 + 5.76) = 7.42\text{g}$$

The yields for all temperatures under consideration is shown below

#### Appendix B<sub>1</sub>: Effect of Temperature on Pyrolysis Product Yields

Biomass (g)	Temperature ( $^{\circ}\text{C}$ )	Pyrolysis products (g)					
		Sawdust			Poultry waste		
		Biochar -SD	Bio- oil-SD	Bio- gas-SD	Biochar -PW	Bio- oil- PW	Bio- gas- PW
20	SBC400	7.84	8.42	3.74	10.06	5.16	4.78
20	SBC500	4.52	9.16	6.32	8.38	5.76	5.86
20	SBC600	4.02	7.32	8.66	7.92	4.12	7.96
20	SKBC400	9.28	7.72	3.00	10.88	3.98	5.14

#### Percent Weight Yield and Conversion of Products

$$\text{weight yield} = \frac{\text{Percentage}}{\text{Percentage}} \times 100\%$$

$$\text{Percentage weight conversion} = \frac{\text{Percentage}}{\text{Percentage}} \times 100\%$$

$$\text{At } 400\text{ }^{\circ}\text{C, For Sawdust, \% wt yield of biochar} = \frac{7.84}{20} \times 100\% = 39.2\%$$

$$\% \text{ wt conversion of biochar} = \frac{7.84}{12.72} \times 100\% = 60.8\%$$

$$\text{At } 400\text{ }^{\circ}\text{C, For Poultry waste, \% wt yield of biochar} = \frac{10.06}{20} \times 100\% = 50.3\%$$

$$\% \text{ wt conversion} = \frac{10.06}{20.54} \times 100\% = 49.7\%$$

Appendix B<sub>2</sub>: Percentage weight yield and conversion of sawdust

Sawdust (g)	Biochar Grades	Biochar (g)	Wt % yield	Wt % conversion
20	SBC400	7.84	39.2	60.8
20	SBC500	4.52	22.6	77.4
20	SBC600	4.02	20.1	79.9
20	SKBC400	9.28	46.4	53.6

Similarly for Poultry waste, the result is shown below

Appendix B<sub>3</sub>: Percentage weight yield and conversion of poultry waste

Sawdust (g)	Biochar Grades	Biochar (g)	Wt % yield	Wt % conversion
20	PBC400	10.06	50.3	49.7
20	PBC500	8.38	41.9	58.1
20	PBC600	7.92	39.6	60.4
20	PKBC400	10.88	54.4	45.6

## Appendix C Carbon Sequestration

### Calculation

100 million tone of biomass was used as basis:

At 500°C the amount of biochar obtained from SD was 65.2wt% of the total biomass and the total C content from SD was 76.32wt%. Similarly, for SDK25 the amount of biochar obtained and its carbon content are 66.5wt% and 78.10wt%

Table C<sub>1</sub>: Data Used in Calculating Carbon Sequestration

Parameters	SBC400	SBC500	SBC600	SKBC400
------------	--------	--------	--------	---------

Biochar Yield (wt %)	39.2	22.6	20.1	46.4
Carbon Content(wt%)	51.2	52.62	56.06	57.50

Assumption: 100 million tons of SD to be pyrolysed.

- For every 100 million tons of SD pyrolysed at 400 °C, about 39.2% of it is converted into biochar (SBC400).
- Therefore, biochar produced from SD at 400 °C =  $100 \times 39.2 / 100 = 39.2$  million tones.
- For every ton of biochar produced from SD at 400 °C 51.2% of it is C. This implies that carbon sequestration potentials of biochar production from 100 million tons of SD at 400 °C =  $(51.2/100) \times 39.2 = 20.07$  million tones
- Now, assuming 80% of carbon sequestered is stable, then carbon dioxide removed by biohar is  $20.07 \times 80 / 100 = 16.06$  million tones

Similarly, the same assumptions and procedures go for poultry waste pyrolysis

Parameters	PBC400	PBC500	PBC600	PKBC400
Biochar Yield (wt %)	50.3	41.9	39.6	54.4
Carbon Content (wt %)	59.7	61.86	60.77	60.78

- For every 100 million tons of PW pyrolysed at 400 °C, about 50.3% of it is converted into biochar (PBC400).
- Therefore, biochar produced from PW at 400 °C =  $100 \times 50.3 / 100 = 50.3$  million tones.

- For every ton of biochar produced from SD at 400 °C 59.7.2% of it is C. This implies that carbon sequestration potentials of biochar production from 100 million tones of PW at 400 °C =  $(59.7/100)*50.3 = 30.03$  million tones
- Now, assuming 80% of carbon sequestered is stable, then carbon dioxide removed by PBC400 is  $30.03*80/100= 20.02$  million tones

## Appendix D

### Adsorption Study

#### Intra-Particle Diffusion Model

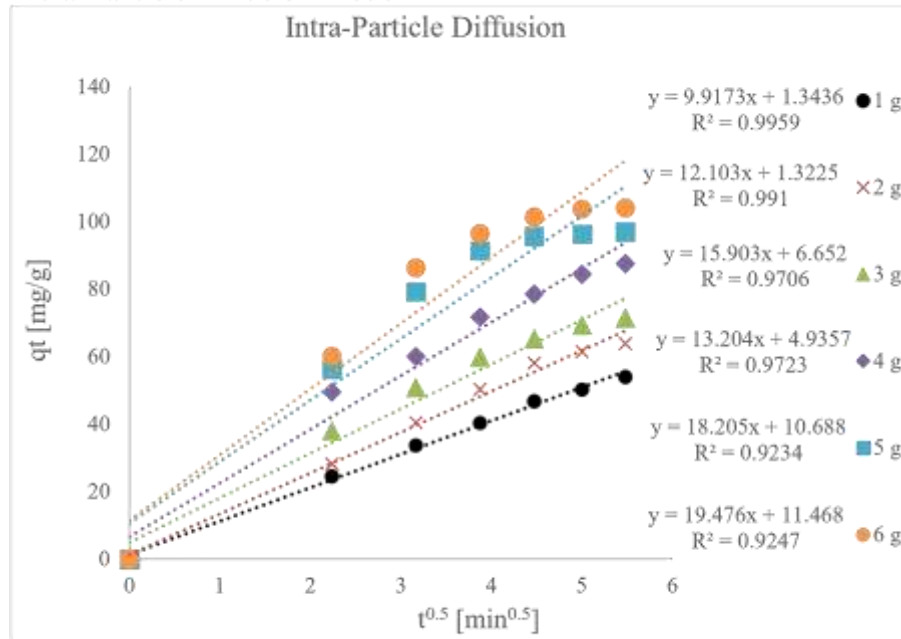


**Figure D<sub>1</sub>: SUMAC with Kaolin**

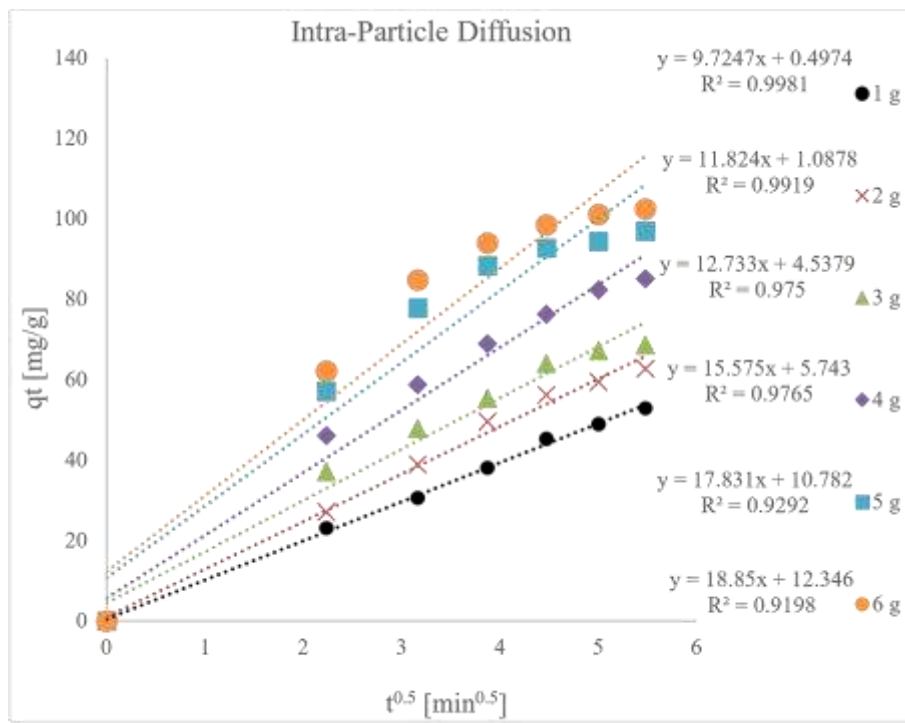


**Figure D<sub>2</sub>: SUMAC with Kaolin**

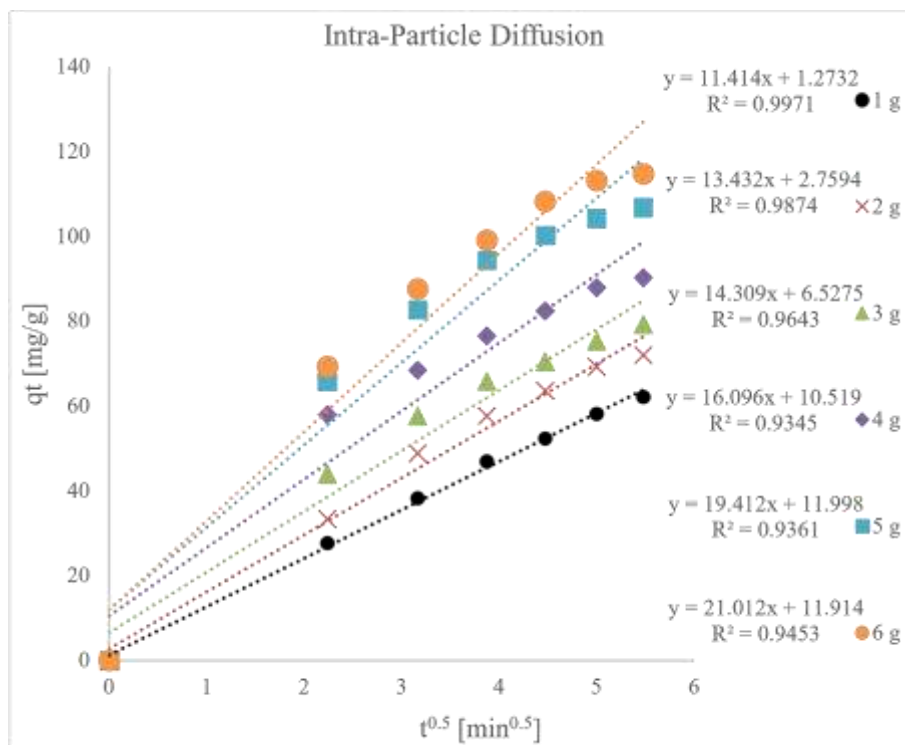


**Figure D<sub>3</sub>: SBMAC with NaOH**

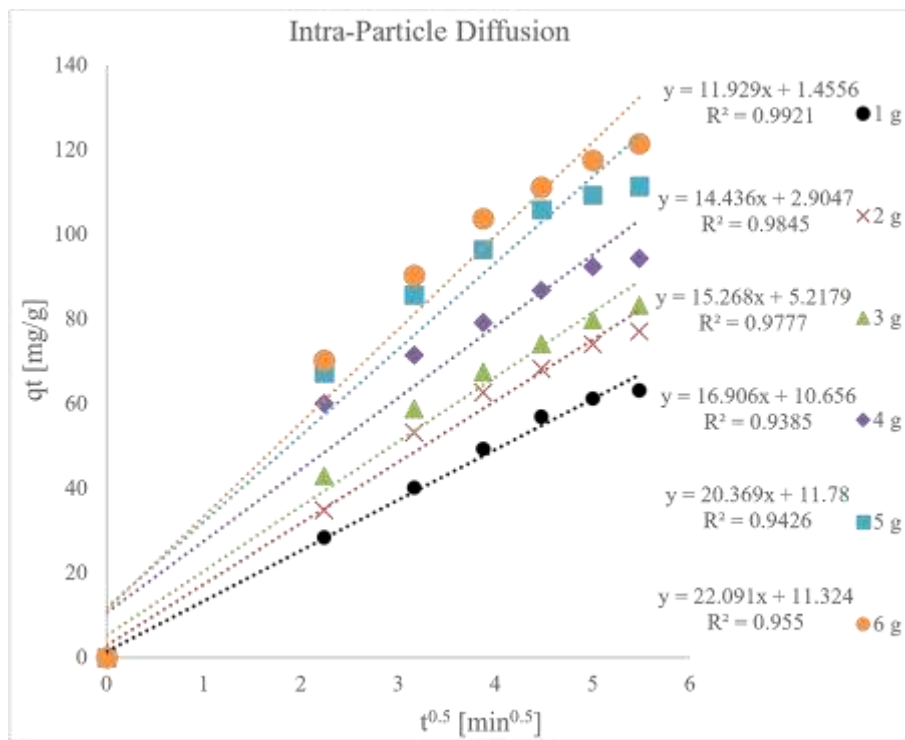


**Figure D4:** PBMAC with NaOH

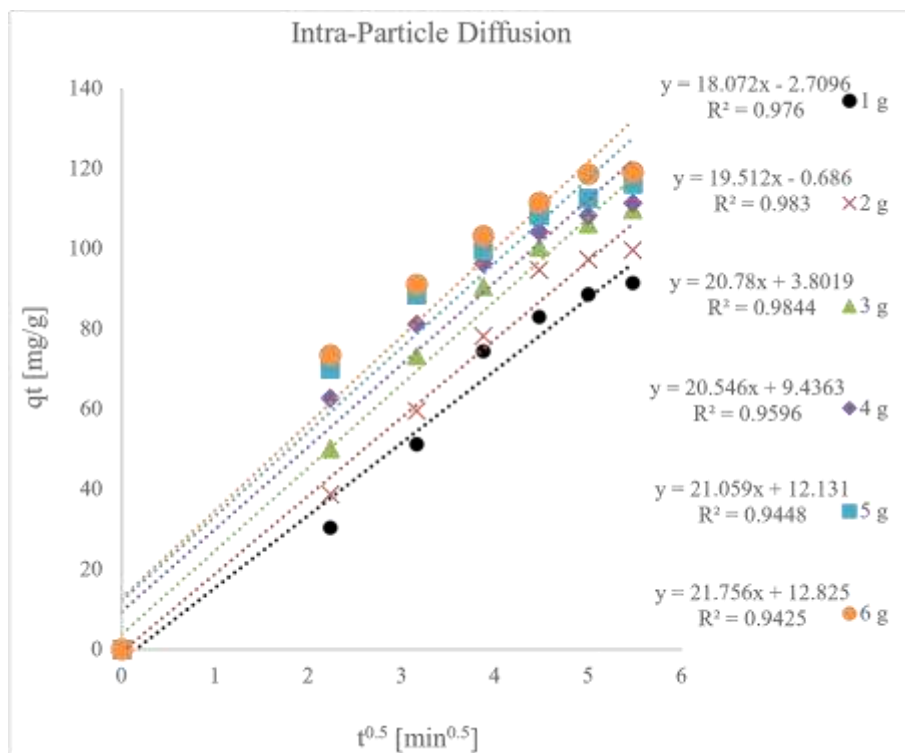


**Figure D5:** SAMAC with H<sub>3</sub>PO<sub>4</sub>.

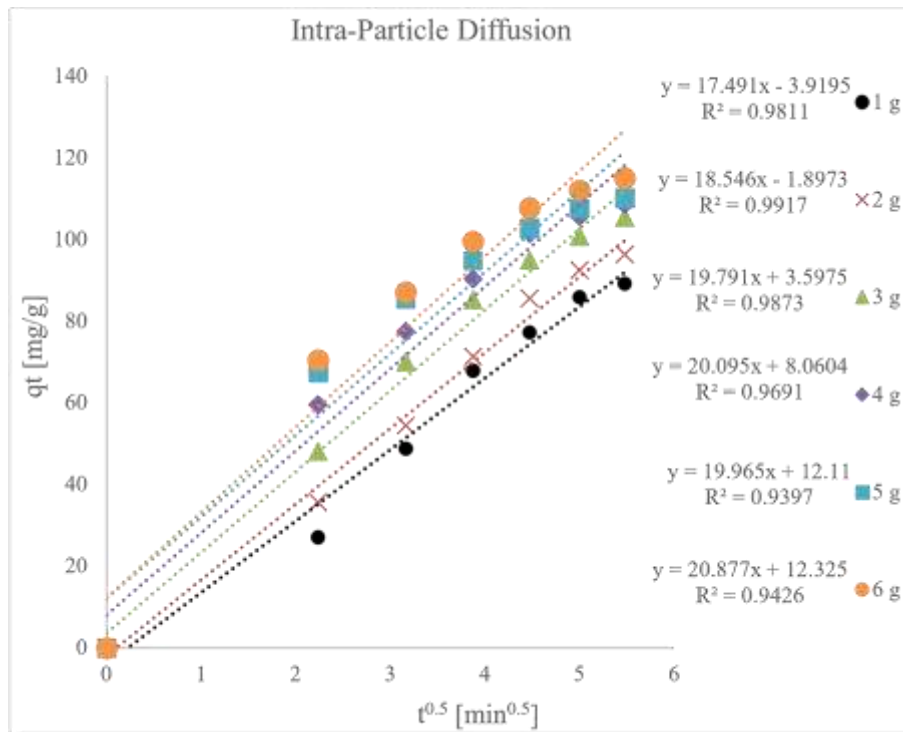


**Figure D6:** PAMAC with H<sub>3</sub>PO<sub>4</sub>.

**Elovich Model**

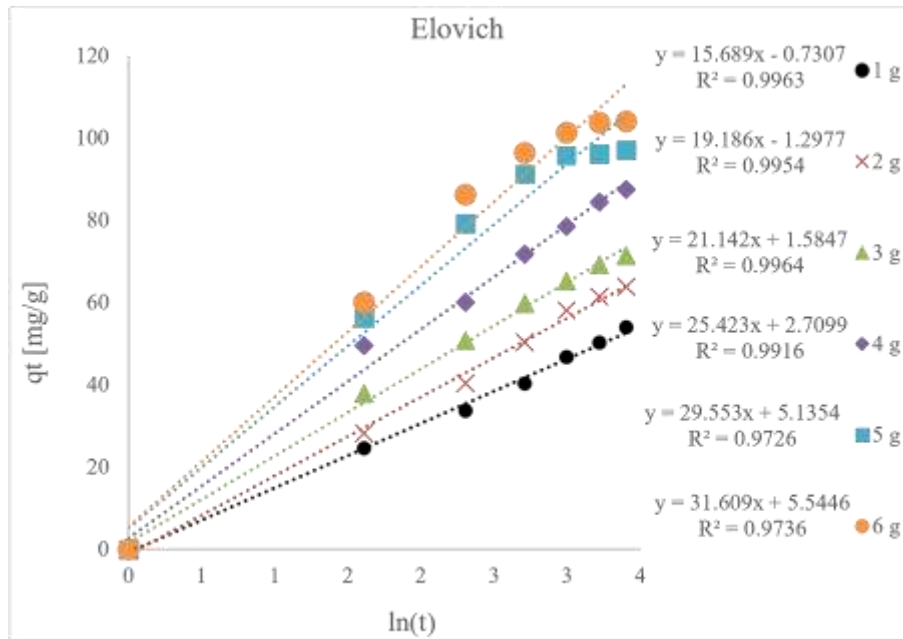


**Figure D7:** SUMAC with Kaolin

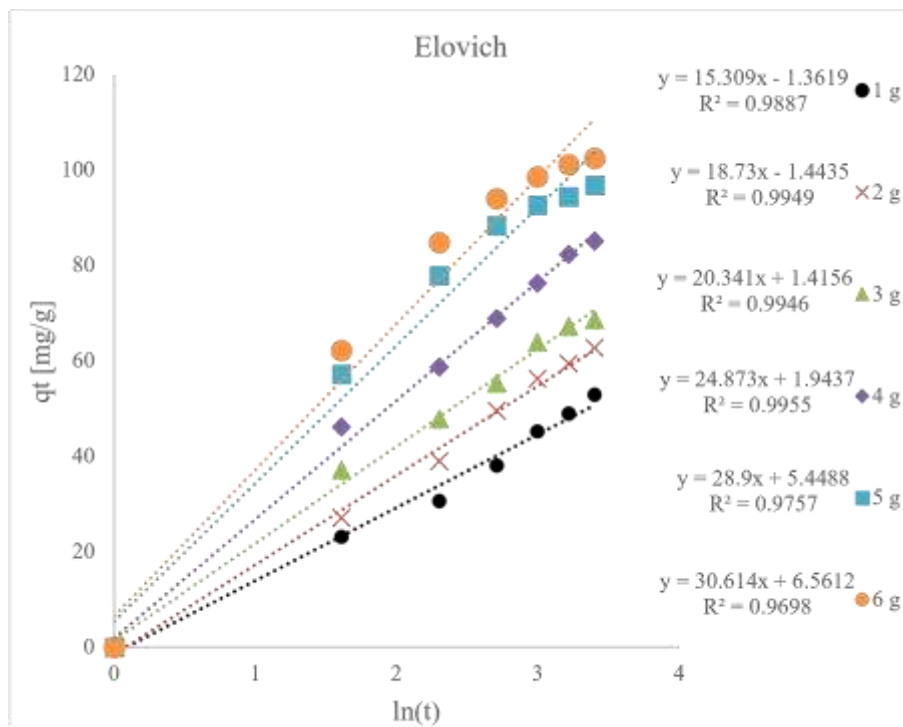


**Figure D<sub>8</sub>: PUMAC with Kaolin**

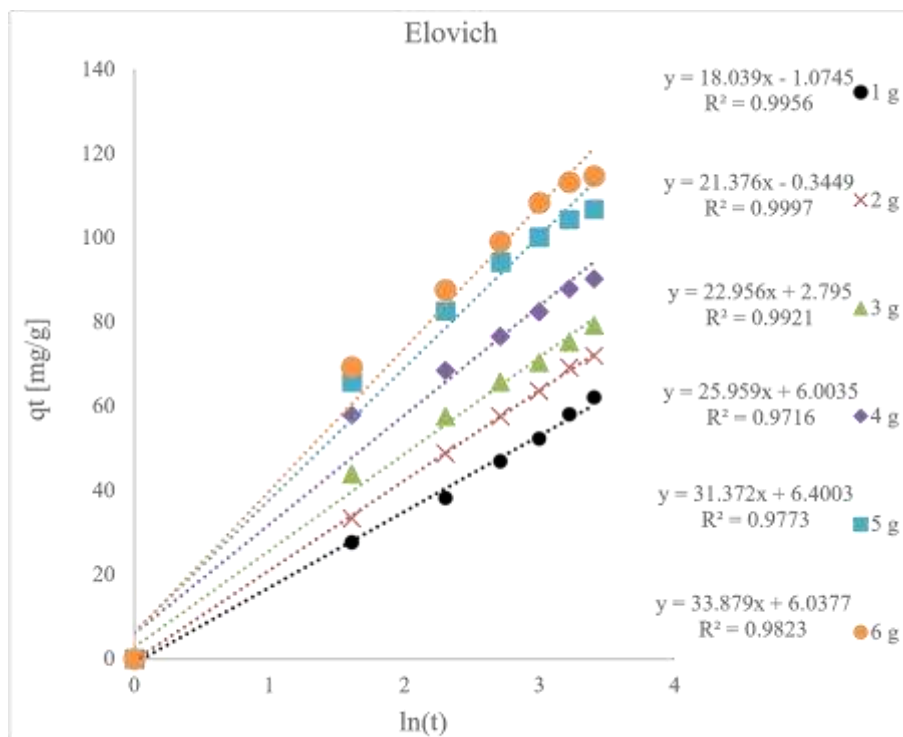


**Figure D<sub>9</sub>: SBMAC with NaOH**

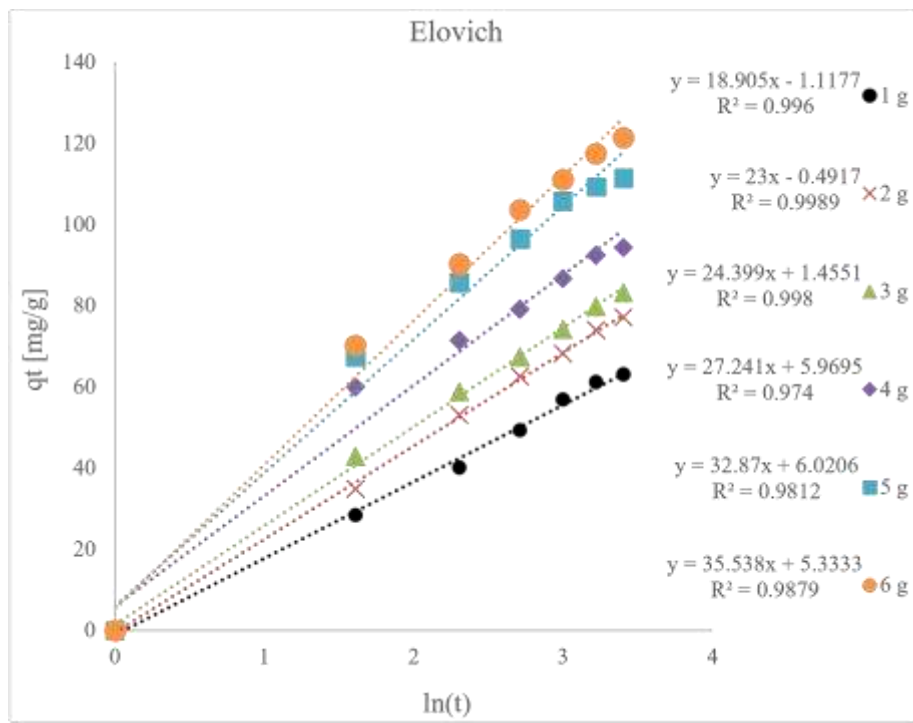


Figure D<sub>10</sub>: PBMAC with NaOH

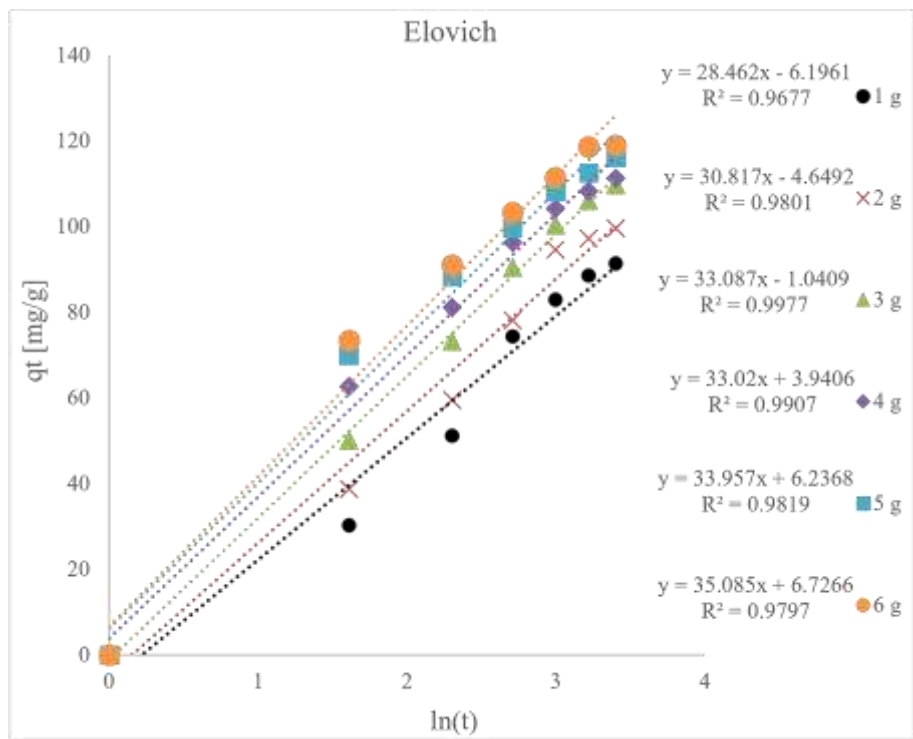
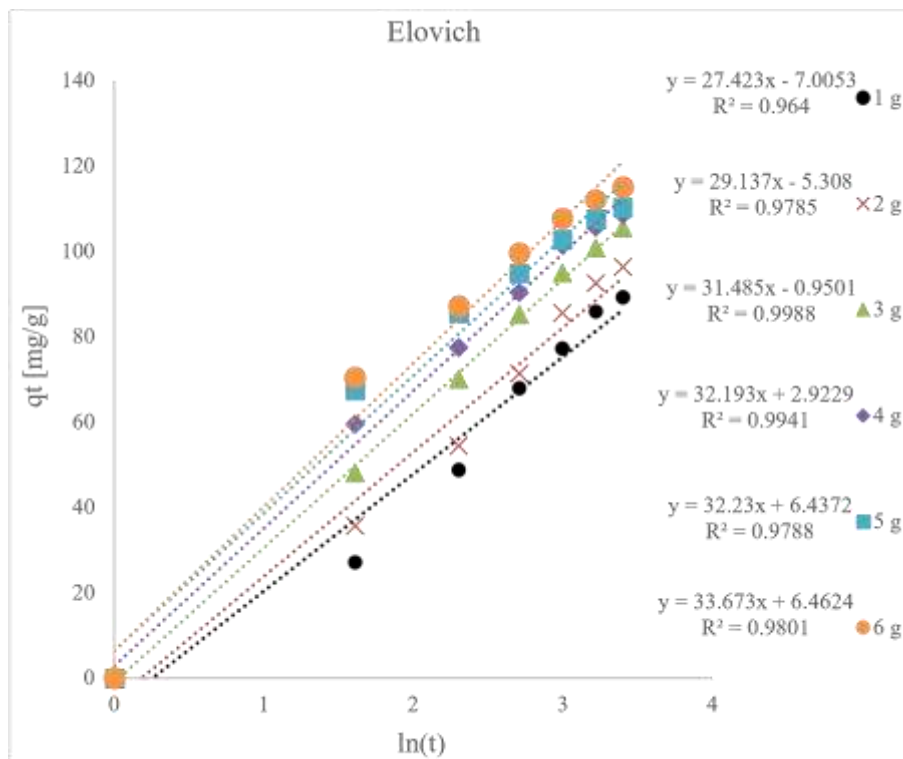


Figure D<sub>11</sub>: SAMAC with H<sub>3</sub>PO<sub>4</sub>.



**Figure D12: PAMAC with H<sub>3</sub>PO<sub>4</sub>.**

## Appendix E

### Optimization Outcomes

**Table E1: Effect of Low, Mid and Upper points on SD Pyrolysis**

Std Run	Factor 1 Temp (°C)	Factor 2		Factor 3		Factor 4 Residence Time (min)	Factor 5 Kaolin (g)	Biochar (g)	BioOil (g)	BioGas (g)
		Flow Rate (L/min)		Particle Size (mm)						
27	1	300	1.75	1.75	60	17.5	16.5	51.2	32.3	
16	2	600	1.75	3	35	17.5	33.2	27.6	39.2	
26	3	600	1.75	1.75	10	17.5	31.7	34.1	34.2	
44	4	450	1.75	1.75	35	17.5	39.5	23.1	37.4	
8	5	450	1.75	3	60	17.5	36.5	34.2	29.3	
39	6	450	0.5	1.75	60	17.5	34.6	32.8	32.6	
42	7	450	1.75	1.75	35	17.5	39.5	25.8	34.7	
24	8	450	3	3	35	17.5	33.7	27.9	38.4	
7	9	450	1.75	0.5	60	17.5	32.3	29.1	38.6	
32	10	450	1.75	3	35	30	33.4	28.7	37.9	

33	11	300	1.75	1.75	35	5	18.2	36.2	45.6
12	12	450	3	1.75	35	30	33.6	26.8	39.6
6	13	450	1.75	3	10	17.5	34.7	26.8	38.5
46	14	450	1.75	1.75	35	17.5	39.5	15.9	44.6
35	15	300	1.75	1.75	35	30	17.2	35.5	47.3
1	16	300	0.5	1.75	35	17.5	18.6	32.1	49.3
11	17	450	0.5	1.75	35	30	35.5	26.3	38.2
20	18	450	1.75	1.75	60	30	36.8	28.6	34.6
10	19	450	3	1.75	35	5	37.6	22.2	40.2
18	20	450	1.75	1.75	60	5	38.3	23.9	37.8

Effect of Low, Mid and Upper points on SD Pyrolysis - Continuation

---

28	21	600	1.75	1.75	60	17.5	21.3	36.4	42.3
4	22	600	3	1.75	35	17.5	24.2	29.1	46.7
43	23	450	1.75	1.75	35	17.5	39.5	21.9	38.6
3	24	300	3	1.75	35	17.5	15.9	38.5	45.6
23	25	450	0.5	3	35	17.5	38.5	22.4	39.1
45	26	450	1.75	1.75	35	17.5	39.5	22.2	38.3
14	27	600	1.75	0.5	35	17.5	23.8	45.9	30.3
5	28	450	1.75	0.5	10	17.5	37.8	25.4	36.8
34	29	600	1.75	1.75	35	5	30.5	30.6	38.9
2	30	600	0.5	1.75	35	17.5	25.5	27.8	46.7
40	31	450	3	1.75	60	17.5	38.3	23.3	38.4
30	32	450	1.75	3	35	5	37.9	22.4	39.7
15	33	300	1.75	3	35	17.5	17.6	38.1	44.3
31	34	450	1.75	0.5	35	30	37.3	24.1	38.6

21 35	450	0.5	0.5	35	17.5	36.8	23.4	39.8
19 36	450	1.75	1.75	10	30	36.5	26.1	37.4
41 37	450	1.75	1.75	35	17.5	35.8	25.5	38.7
38 38	450	3	1.75	10	17.5	36.3	26.6	37.1
37 39	450	0.5	1.75	10	17.5	36.5	25.2	38.3
17 40	450	1.75	1.75	10	5	37.1	23.6	39.3
25 41	300	1.75	1.75	10	17.5	18.2	37.2	44.6

---

Table E2: Effect of Low, Mid and Upper points on PW Pyrolysis

STD	Runs	Temp (°C)	Flow (L/min)	Particle Rate Size (mm)	Time (min)	Kaolin Ratio (g)	Biochar (g)	Bio-Oil (g)	Biogas (g)
15	1	300	1.75	3	35	17.5	30.4	35.2	34.4
45	2	450	1.75	1.75	35	17.5	49.6	32.5	18.1
6	3	450	1.75	3	10	17.5	49.4	32.3	18.3
18	4	450	1.75	1.75	60	5	49.8	32.2	18
8	5	450	1.75	3	60	17.5	49.7	32	18.3
17	6	450	1.75	1.75	10	5	49.2	32.7	18.1
44	7	450	1.75	1.75	35	17.5	49.6	32.3	21.1
7	8	450	1.75	0.5	60	17.5	48.6	33.3	18.1
46	9	450	1.75	1.75	35	17.5	49.6	32.3	18.3
37	10	450	0.5	1.75	10	17.5	48.4	33.3	18.7

3	11	300	3	1.75	35	17.5	30.4	35.1	34.5
41	12	450	1.75	1.75	35	17.5	49.6	32.3	18.1
29	13	450	1.75	0.5	35	5	48.3	33.3	23.4
22	14	450	3	0.5	35	17.5	49.6	32.3	18.1
2	15	600	0.5	1.75	35	17.5	28.9	32.4	42.6
19	16	450	1.75	1.75	10	30	49.6	32.3	18.1
24	17	450	3	3	35	17.5	49.6	32.2	18.2
26	18	600	1.75	1.75	10	17.5	29.1	33.2	42.6
28	19	600	1.75	1.75	60	17.5	28.7	33.8	37.5
40	20	450	3	1.75	60	17.5	49.6	32.3	18.1
35	21	300	1.75	1.75	35	30	30.1	34.7	35.2
31	22	450	1.75	0.5	35	30	49.6	32.3	18.1
16	23	600	1.75	3	35	17.5	30.1	31.5	42.6
38	24	450	3	1.75	10	17.5	48.6	33.3	18.1

Effect of Low, Mid and Upper points on PD Pyrolysis - Continuation

20	25	450	1.75	1.75	60	30	49.6	32.3	18.1
36	26	600	1.75	1.75	35	30	29.7	31.1	42.6
9	27	450	0.5	1.75	35	5	49.6	32.3	18.1
33	28	300	1.75	1.75	35	5	31.4	32.8	35.8
1	29	300	0.5	1.75	35	17.5	30.8	32.4	36.8
5	30	450	1.75	0.5	10	17.5	49.6	32.3	18.1
10	31	450	3	1.75	35	5	49.6	32.3	18.1
25	32	300	1.75	1.75	10	17.5	30.7	35.5	34.8
21	33	450	0.5	0.5	35	17.5	49.6	32.3	18.1
4	34	600	3	1.75	35	17.5	28.3	33.3	42.6
34	35	600	1.75	1.75	35	5	29	32.5	42.6
43	36	450	1.75	1.75	35	17.5	49.6	32.3	18.1

32	37	450	1.75	3	35	30	49.6	32.3	18.1
14	38	600	1.75	0.5	35	17.5	28.8	34.1	42.6
27	39	300	1.75	1.75	60	17.5	30.5	34.8	34.7
12	40	450	3	1.75	35	30	49.6	32.3	18.1
42	41	450	1.75	1.75	35	17.5	49.6	32.3	18.1
13	42	300	1.75	0.5	35	17.5	30.1	35.7	34.2
23	43	450	0.5	3	35	17.5	49.6	32.3	18.1
11	44	450	0.5	1.75	35	30	49.6	32.3	18.1
39	45	450	0.5	1.75	60	17.5	49.6	32.3	18.1
30	46	450	1.75	3	35	5	49.6	32.3	18.1

---

## Appendix F

### Publications

1. Bello, A., Mohammed, A., Manase, A & Abdulsalam, A. (2021). Ascertainning Optimum Pyrolysis Conditions for Biochar Production from Maple Sawdust. *Current Journal of Applied Science and Technology*, 40(40): 1 – 6
2. Bello, A., Mohammed, A., Abdullahi, A., & Onipede, E.A. (2022). Optimization of Pyrolysis Process to Produce Biochar from Poultry Waste. *International Journal of Innovative Science and Research Technology*. 7(8): 1869 – 1877
3. Bello, A., Mohammed, A., & Garuba, M.U. (2023). Potential of Biochar for Activated Carbon Production and Energy Utilization. 4<sup>th</sup> International Engineering Conference by SIPET, FUT, Minna.